

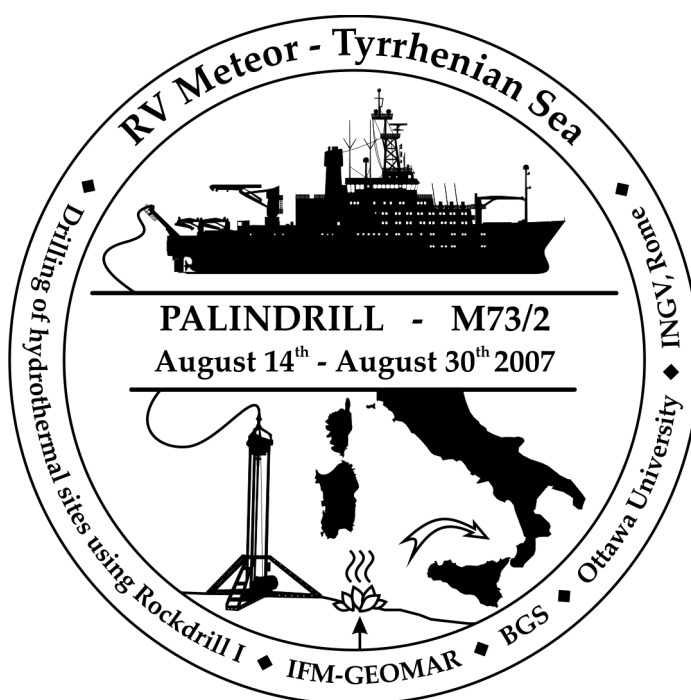


IFM-GEOMAR

Leibniz-Institut für Meereswissenschaften
an der Universität Kiel

FS METEOR
Fahrtbericht / Cruise Report M73/2
Shallow drilling of
hydrothermal sites in the Tyrrhenian Sea (PALINDRILL)

Genoa – Heraklion
14.08.2007 – 30.08.2007



Berichte aus dem Leibniz-Institut
für Meereswissenschaften an der
Christian-Albrechts-Universität zu Kiel

Nr. 30
June 2009

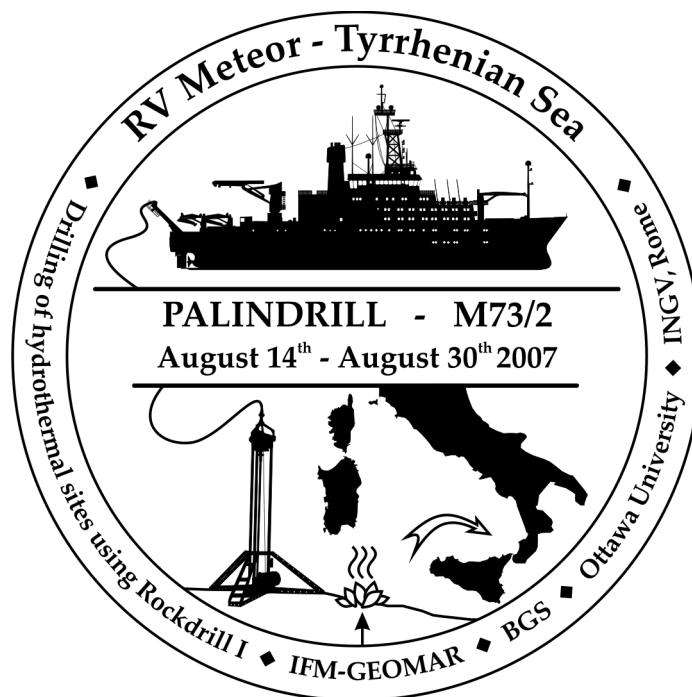


IFM-GEOMAR

Leibniz-Institut für Meereswissenschaften
an der Universität Kiel

FS METEOR
Fahrtbericht / Cruise Report M73/2
Shallow drilling of
hydrothermal sites in the Tyrrhenian Sea (PALINDRILL)

Genoa – Heraklion
14.08.2007 – 30.08.2007



Berichte aus dem Leibniz-Institut
für Meereswissenschaften an der
Christian-Albrechts-Universität zu Kiel

Nr. 30, June 2009

ISSN Nr.: 1614-6298



Das Leibniz-Institut für Meereswissenschaften
ist ein Institut der Wissenschaftsgemeinschaft
Gottfried Wilhelm Leibniz (WGL)

The Leibniz-Institute of Marine Sciences is a
member of the Leibniz Association
(Wissenschaftsgemeinschaft Gottfried
Wilhelm Leibniz).

Herausgeber / Editor:

Sven Petersen and Thomas Monecke

IFM-GEOMAR Report

ISSN Nr.: 1614-6298

Leibniz-Institut für Meereswissenschaften / Leibniz Institute of Marine Sciences

IFM-GEOMAR
Dienstgebäude Westufer / West Shore Building
Düsternbrooker Weg 20
D-24105 Kiel
Germany

Leibniz-Institut für Meereswissenschaften / Leibniz Institute of Marine Sciences

IFM-GEOMAR
Dienstgebäude Ostufer / East Shore Building
Wischhofstr. 1-3
D-24148 Kiel
Germany

Tel.: ++49 431 600-0
Fax: ++49 431 600-2805
www.ifm-geomar.de

1. Cruise Participants

1.1. Shipboard Scientific Party

1. Sven Petersen	Chief scientist	IFM-GEOMAR
2. Thomas Monecke	Co-chief scientist	Ottawa U
3. Klas Lackschewitz	Alteration	IFM-GEOMAR
4. Nico Augustin	Bathymetry	IFM-GEOMAR
5. Anke Gardeler	Bathymetry	IFM-GEOMAR
6. Alexander Kayser	Bathymetry	IFM-GEOMAR
7. Michael Hügler	Microbiology	IFM-GEOMAR
8. Andrea Gärtner	Microbiology	IFM-GEOMAR
9. Frank Lappe	Microbiology	IFM-GEOMAR
10. Jan Küver	Microbiology	MPA Bremen
11. Marc Peters	Sulfur geochemistry	U Münster
12. Reinhard Kleeberg	Alteration	TUBAF
13. Nicolai Kummer	Pore water chemistry	TUBAF
14. Alessandra Esposito	Petrology	INGV Roma
15. Arnaldo A. De Benedetti	Petrology	U Roma
16. Harold Gibson	Volcanology	Laurentian U
17. Kirstie Simpson	Volcanology	CODES
18. Bruce Gemmell	Economic geology	CODES
19. Gaowen He	Economic geology	COMRA
20. Buyan Wan	Economic geology	COMRA
21. Katie Perrin	Economic geology	Neptune
22. Robina Sharpe	Economic geology	Neptune
23. Thorsten Schott	Technician	OKTOPUS
24. Dave Smith	Rockdrill team	BGS
25. Dave Baxter	Rockdrill team	BGS
26. Neil Campbell	Rockdrill team	BGS
27. Dave Wallis	Rockdrill team	BGS
28. Eileen Gillespie	Rockdrill team	BGS
29. Heather Stewart	Rockdrill team	BGS

1.2. Participating Institutions

IFM-GEOMAR

Leibniz-Institut für
Meereswissenschaften
Wischhofstraße 1-3
24148 Kiel, Germany
www.ifm-geomar.de

BGS

British Geological Survey,
Marine Operations & Engineering
2a Nivensknowe Road
Loanhead, EH20 9AU, UK

CODES

ARC Centre of Excellence in
Ore Deposits
University of Tasmania
Private Bag 126
Hobart, TAS 7001, Australia

COMRA

China Ocean Mineral Resources R&D
Association
Fuxingmenwai Avenue 1
Beijing, 100860, PR China

INGV Roma

Istituto Nazionale di Geofisica e
Vulcanologia
Via di Vigna Murata 605
00143 Roma, Italia

Laurentian U

Department of Earth Sciences
Laurentian University
935 Ramsey Lake Road
Sudbury, ON, P3E 2C6, Canada

MPA Bremen

Amtliche Materialprüfungsanstalt der
Freien Hansestadt Bremen
Paul-Feller-Straße 1
28199 Bremen, Germany

Neptune

Neptune Minerals
56 Alfred Street
Milsons Point, NSW 2061, Australia

OKTOPUS

OKTOPUS GmbH
Kieler Straße 51
24594 Hohenwestedt, Germany

Ottawa U

University of Ottawa
Department of Earth Sciences
Marion Hall, 140 Louis Pasteur
Ottawa, ON, K1N 6N5, Canada

TUBAF

TU Bergakademie Freiberg
Institut für Mineralogie
Brennhausgasse 14
09596 Freiberg, Germany

U Münster

Universität Münster
Geologisch-Paläontologisches
Institut
Corrensstraße 24
48149 Münster, Germany

U Roma

Università degli Studi Roma Tre
Dipartimento di Scienze Geologiche
Largo San Leonardo Murialdo 1
00146 Roma, Italy

1.3. Crew

1. Walter Baschek	Master
2. Torsten Kowitz	Chief Mate
3. Nico Szepanski	RFL
4. Peter Neumann	Chief Engineer
5. Tilo Becker	Second Mate
6. Tilo Birnbaum	Second Mate
7. Uwe Kapiéske	Surgeon
8. Uwe Schade	Second Engineer
9. Sascha Schnick	Second Engineer
10. Rudolf Freitag	Electrician
11. Jörg Walter	Chief Electronic Engineer
12. Olaf Willms	Electronic Engineer
13. Katja Pfeiffer	System Administrator
14. Werner Sosnowski	Fitter
15. Manfred Gudera	Boatswain
16. Günther Ventz	Able Seaman
17. Pjotr Bussmann	Able Seaman
18. Günther Stängl	Able Seaman
19. Matthias Pomplun	Able Seaman
20. Erdmann Wegner	Able Seaman
21. Bernd Neitzsch	Able Seaman
22. Thomas Dohrn	Motorman
23. Rudolf Groß	Motorman
24. Heinrich Riedler	Motorman
25. Klaus Hermann	Cook
26. Franciszek Pytlik	Cook's Mate
27. Michael Both	First Steward
28. Irina Wartenberg	Second Steward
29. Jan Hoppe/Ulrike Parlow	Second Steward
30. Na Sng Lee	Laundry man
31. Sven Anders	Technical Assistant
32. Rene Schroeter	Apprentice Seaman
33. Nikolas Woeckner	Apprentice Seaman
34. Christian Meyer	Nautical Assistant
35. Wolf-Thilo Ochsenhirt	FW Technician

2. Executive Summary

S. Petersen and T. Monecke

R/V Meteor cruise M73/2 departing Genoa, Italy, on August 14 and arriving at Heraklion, Greece, on August 30 was the second of two consecutive research cruises exploring the Tyrrhenian Sea for submarine hydrothermal systems. This multinational expedition aimed to conduct shallow drilling at three previously identified hydrothermal vent sites using a lander-type drilling device of the British Geological Survey. Research focused on two main areas, namely a massive sulfide occurrence at the Palinuro volcanic complex and shallow marine sulfate deposits forming offshore Panarea Island. In addition to these sites located in the submerged portion of the Aeolian arc, a low-temperature hydrothermal vent site at the spreading axis of the Marsili back-arc basin was investigated. Drilling to a maximum depth of 5 m allowed, for the first time, a detailed documentation of the third dimension of the three submarine hydrothermal systems. Research on the recovered core material will constrain the origin and evolution of mineralizing fluids forming polymetallic metal deposits at comparably shallow water depth and unravel the nature and diversity of life thriving under these conditions.

Drilling in a small topographic depression (603 to 633 m water depth) at the summit of a volcanic cone in the western part of the Palinuro volcanic complex commenced on August 15. Already the first hole intersected massive sulfide and sulfate mineralization. Eleven successful instrument deployments yielded a total of 13.59 m of core including one hole that intersected 485 cm of sulfide and sulfate mineralization. Shallow drilling was conducted at a closely spaced grid in a 70 by 50 m large area. In this area, sulfide mineralization was encountered at depths from a few centimeters up to several meters below a thick cover of mud and sand, with unconsolidated monomictic and polymictic breccia being locally present. The thickness of the mineralized zone remained unknown because all drill holes ended in sulfide and sulfate mineralization. Textural evidence suggests that the massive sulfides may have largely formed by subseafloor replacement processes. The recovered ore samples are of unusual mineralogical composition when compared to mid-ocean ridge massive sulfide deposits. In addition to pyrite and barite, abundant sphalerite, enargite, and sulfosalts were recognized. The mineralization is crosscut by a network of late veins lined by pyrite and containing abundant native sulfur.

Successful gravity coring and vibrocoring was conducted at several locations at the Palinuro volcanic complex. The gravity coring yielded 11.42 m of core that were used to sample pore water for geochemical and isotopic investigations and to obtain sediments permitting microbiological experiments. In addition, three successful TV-guided grab stations were conducted at Palinuro. One station retrieved warm unconsolidated mud (maximum temperature of 60°C measured on board) and banded silica-sulfide-sulfate crusts along with vent-specific macro fauna. The observed in-situ temperatures indicate that hydrothermal activity at Palinuro is still ongoing, despite the fact that noticeable surface manifestations for venting such as black smoker activity has not been observed during ROV diving in the previous year.

Extensive drilling has also been carried out in the working area off Panarea Island. Initially, drilling focused on a near-shore (<70 m water depth) area typified by the occurrence of numerous circular depressions ranging from 20 to over 100 m in diameter that were identified in a previous high-resolution bathymetric survey (Anzidei et al.,

2005; Esposito et al., 2006). ROV operations onboard R/V Poseidon conducted in 2006 revealed that the emission of gas and thermal waters is common in these depressions, interpreted to represent hydrothermal explosion craters. Eight holes drilled within these depressions encountered massive anhydrite and gypsum, totaling 784 cm of core. One drill hole yielded 289 cm of continuous massive sulfates. These sulfates are interpreted to represent a cap forming at the interface between an underlying geothermal system and the seafloor. The presence of minor pyrite, marcasite, and sphalerite infilling vugs and fractures within the massive anhydrite and gypsum indicates that the deep fluids are enriched in metals.

Drilling at the submerged portion of the Panarea platform also yielded variably altered coherent volcanic rocks, allowing comparison to the lava units exposed on land. A flow-banded rhyolite dome recognized during ROV diving in 2006 was drilled during three stations yielding 621.5 cm of core. The recovered feldspar-amphibole porphyritic rhyolite contained abundant amphibole-biotite-feldspar porphyritic andesite xenoliths. Textural observations suggested that both lavas formed contemporaneously and that mingling of the two compositionally distinct melts must have occurred in the magma chamber or in the volcanic conduit. Several successful vibrocoring stations were conducted to sample unconsolidated to poorly consolidated sedimentary and volcanoclastic facies covering the seafloor at the Panarea platform. The retrieved core was also used to obtain samples for pore water analysis and the microbiological investigations.

Four drilling stations and two TV-guided grab operations were conducted at the Marsili volcanic complex. The Rockdrill operations yielded intersections of feldspar-olivine porphyritic andesite that showed only weak hydrothermal alteration along fractures, whereas TV-guided grabbing returned Fe-oxide crusts as well as comparably fresh andesite.

During R/V Meteor cruise M73/2, a total of 17 seafloor mapping stations covering an area of approximately 2,600 km² were conducted using the Kongsberg Simrad EM120 multibeam system. Detailed bathymetric mapping showed that the Palinuro volcanic complex consists of several coalesced eruption centers located along an E-W trending fault system. Mapping at the Marsili volcanic complex provided a high-resolution survey of this superinflated back-arc spreading ridge. The seafloor survey at Panarea explored the deeper portion of the platform and the northern slope of the volcanic complex, adding to the existing shallow water (<70 m) dataset of Anzidei et al. (2005) and Esposito et al. (2006).

3. Scientific Background

S. Petersen and T. Monecke

Volcanic arcs are one of the principal active volcanic environments on Earth, accounting for approximately 26% of the global magmatic budget (Perfit and Davidson, 2000). About half of the volcanic arcs (ca. 22,000 km) are predominantly submarine or completely submerged (de Ronde et al., 2003). In contrast to mid-ocean ridges, submerged volcanic arcs have only been the focus of intensive mapping and seafloor sampling in recent years, with most research being carried out in the Mariana arc (Embley et al., 2004; Resing et al., 2007) and the Tonga-Kermadec arcs (de Ronde et al., 2001, 2007; Stoffers et al., 2006). Surveying of these arcs revealed a volcanic environment that is unexpectedly rich in hydrothermal vent sites, some of which are associated with polymetallic sulfide formation.

Submarine hydrothermal systems in volcanic arcs have a number of characteristics that differ from those at mid-ocean ridges (de Ronde et al., 2005; Hannington et al., 2005). They are commonly typified by comparably acidic hydrothermal fluids that are notably enriched in CO₂. In addition, hydrothermal vents in volcanic arcs are located in shallow to moderately-deep water (<1,600 m), whereas mid-ocean ridge hydrothermal systems occur at water depth in excess of 2,000 m, with some being located as deep as 4,000 m. The lower ambient hydrostatic pressure in arc hydrothermal systems permits the widespread occurrence of boiling during fluid ascent and venting at the seafloor (Hannington et al., 2005).

Current genetic concepts for the formation of polymetallic seafloor sulfides suggest that partial removal of metals from the footwall volcanic rocks by evolved seawater convecting above synvolcanic intrusions is the principal mechanism leading to the enrichment of metals in submarine hydrothermal systems. A more active role of the intrusions at depth such as direct magma degassing and related magmatic contributions of volatiles and metals to seafloor hydrothermal systems is commonly ruled out, largely because these genetic models were initially developed for mid-ocean ridge hydrothermal systems where magmatic volatiles are not widely recognized in the hydrothermal fluids.

However, fumarolic discharges associated with subaerial arc volcanoes are widely accepted to contain volatiles of magmatic origin (Giggenbach et al., 1992). In this context, it is not surprising that volatiles in hydrothermal systems associated with submarine arc volcanoes may also be of magmatic derivation. The recent discovery of liquid sulfur lakes at submarine hydrothermal vent sites provides strong evidence for a magmatic contribution to arc hydrothermal systems (Embley et al., 2004; Stoffers et al., 2006; de Ronde et al., 2007). In addition, the anomalous acidity of some submarine hydrothermal systems may be best explained by the presence of magmatic SO₂, which disproportionates to H₂S and H₂SO₄ upon fluid cooling (Fouquet et al., 1993; Gamo et al., 1997; Herzig et al., 1998; Embley et al., 2004). Magmatic contributions to seafloor hydrothermal systems may result in anomalous enrichments of certain metals. Some ancient polymetallic sulfide deposits that formed in volcanic arcs or related extensional settings indeed show an anomalous enrichment of gold. Similarly high precious metal grades have also been encountered in sulfides from modern seafloor hydrothermal vent sites (Hannington et al., 1999, 2005).

Anomalous precious metal enrichment in shallow marine hydrothermal systems may, however, also be related to the occurrence of boiling during fluid evolution. Boiling is known to be accompanied by a dramatic cooling of the hydrothermal fluids which, in turn, influences the capability of the fluids to transport metals (Drummond and Ohmoto, 1985; Butterfield et al., 1990). Theoretical considerations suggest that fluid cooling accompanying boiling prevents hydrothermal fluids from transporting significant amounts of Cu to a vent site located in shallow water. The temperature-dependent stability of dissolved metal complexes is, however, different for the precious metals and the epithermal-suite of elements (e.g., As, Bi, Hg, and Sb). These elements can be transported under lower temperature conditions and are likely to become selectively enriched in boiling fluids. Sulfide deposits forming in the shallow marine environment may, therefore, show anomalous enrichment of these metals. In many respects, deposition of metals in the shallow water environment can be compared to the formation of epithermal deposits on land (Hannington et al., 1999). Consequently, a continuum of deposit types ranging from submarine massive sulfides to subaerial epithermal deposits may form in volcanic arcs (Fig. 1).

The above discussion illustrates the need for a new genetic model explaining the characteristics of sulfide deposits forming in both, the submarine and subaerial portions of volcanic arcs. Models describing the anomalous metal enrichment in shallow marine massive sulfide deposits need to distinguish between the origin of the mineralizing fluids (i.e., degassing of magma and host rock composition) and processes related to the depositional environment (i.e., boiling of hydrothermal fluids). The study of polymetallic sulfide deposits hosted by ancient volcanic successions does not provide sufficient evidence to make this distinction. Reconstruction of the fluid origin and the evolution of the fluids during their ascent to the seafloor are typically hampered by the effects of metamorphism and deformation, which obscure the primary mineralogical and geochemical characteristics of the deposits and associated hydrothermal alteration halos. In addition, it is difficult or even impossible to constrain water depth of sulfide formation in ancient volcanic successions as few unequivocal volcanic facies criteria allow field observations to be linked to water depth. Significant advances in this research area can, therefore, only be made by the study of modern seafloor hydrothermal systems where spatial and temporal relationships between submarine volcanism and deposit formation can be readily established and where water depth can be directly measured.

R/V Meteor cruise M73/2 provided a unique opportunity to study the formation of polymetallic sulfides associated with shallow marine magmatic-hydrothermal systems in the Tyrrhenian Sea through the use of a lander-type drilling device permitting drilling to a maximum penetration of 5 m. Together with seafloor observations obtained by ROV diving onboard R/V Poseidon cruise POS340 in 2006 (Petersen and Monecke, 2008), drilling allowed the first comprehensive three-dimensional description of these shallow marine hydrothermal systems.

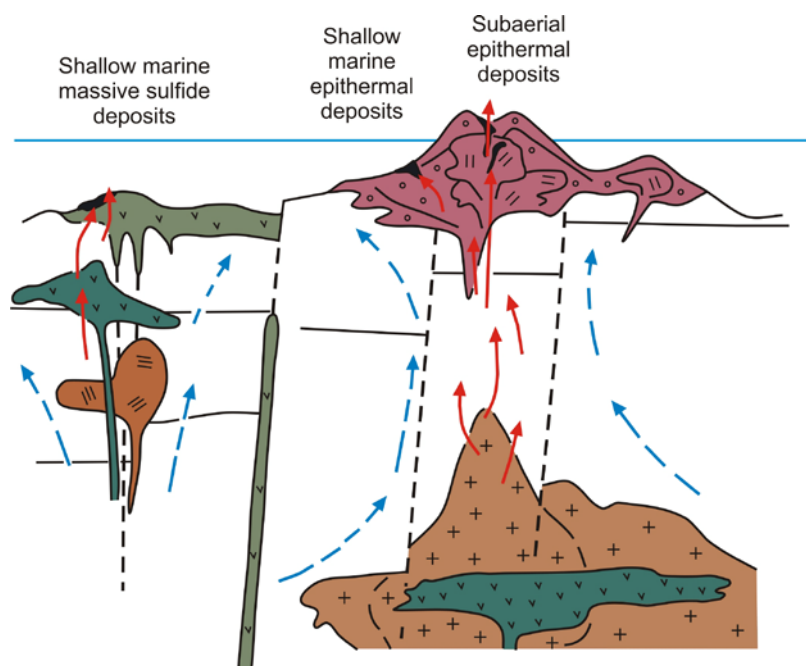


Fig. 1: Model for the formation of different deposit types in volcanic arcs. Magmatic input (red arrows) and heated seawater (blue) may both contribute to the metal enrichment.

3.1. Regional Geology

T. Monecke, S. Petersen, A.A. De Benedetti, and A. Esposito

The southeastern Tyrrhenian Sea comprises the Marsili abyssal plain and the volcanoes of the Aeolian arc (Fig. 2). The Marsili abyssal plain represents a small oceanic back-arc basin that formed as a consequence of roll-back of the northwestward-dipping Ionian subduction zone and migration of arc volcanism from the island of Sardinia towards the east-southeast (Savelli, 2001). Opening of the Marsili back-arc basin was initiated close to the Pliocene-Pleistocene boundary at approximately 1.9 Ma (Savelli, 1988; Savelli and Schreider, 1991).

The central part of the Marsili abyssal plain is occupied by the Marsili volcanic complex, which represents the superinflated spreading ridge of the back-arc basin (Marañi and Trua, 2002). Lava sampled from the summit region of the Marsili volcanic complex yielded K/Ar ages of <0.2 Ma (Selli et al., 1977), which is consistent with magnetostratigraphic data suggesting that the bulk of the volcanic complex is <0.8 Ma in age (Brusilovskiy and Gorodnitskiy, 1990; Faggioni et al., 1995).

The Marsili back-arc basin is surrounded by the tightly arcuate chain of Aeolian arc volcanoes that rest on an up to 20 km thick continental basement (Morelli et al., 1975). The volcanic chain comprises seven major islands and several submerged volcanoes extending for approximately 200 km parallel to the continental slope of northern Sicily and western Calabria (Fig. 2). Volcanism in the Aeolian arc commenced ca. 1.5 Ma ago in the western part of the volcanic chain (Beccaluva et al., 1985). Subaerial volcanic activity was restricted to the past 500 ka. Volcanic eruptions occurred during historical times at Stromboli, Lipari, and Vulcano. Today, only Stromboli exhibits ongoing eruptive volcanism, but fumarolic activities also occur on Salina, Lipari, and Vulcano.

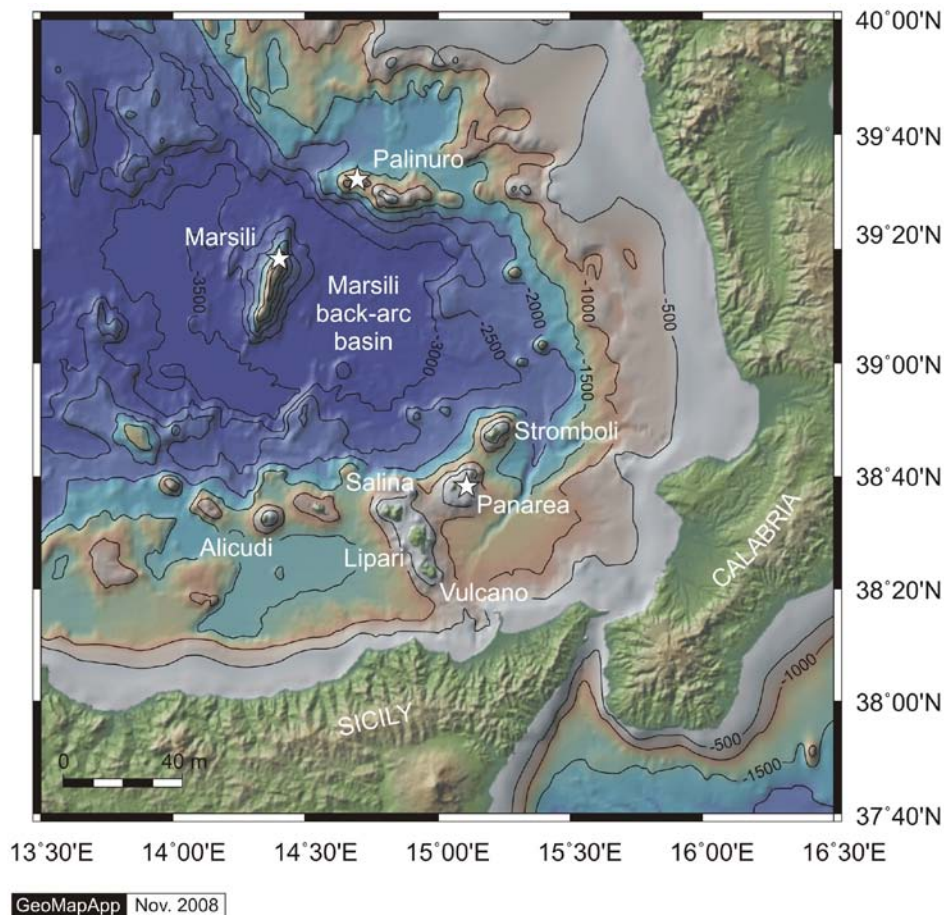


Fig. 2: Map of the southeastern Tyrrhenian Sea showing the Marsili back-arc basin and the volcanoes of the Aeolian arc. Locations of polymetallic sulfide occurrences are highlighted.

3.2. High-temperature hydrothermal sites

T. Monecke and S. Petersen

Submarine hydrothermal precipitates have been recorded at several localities in the southeastern Tyrrhenian Sea. Hitherto, research in the area has mainly focused on low-temperature hydrothermal precipitates (Dekov and Savelli, 2004). Three sites of polymetallic sulfide formation are known to be present in this region, namely the Palinuro volcanic complex, the Marsili volcanic complex, and the Panarea hydrothermal field located between the islands of Panarea and Basiluzzo.

Palinuro volcanic complex

The Palinuro volcanic complex consists of several coalesced volcanic edifices lying along an E-W trending fault system. This elongated complex extends about 50 km in an E-W direction, with a maximum width of about 25 km at its base (Fig. 2). The western sector of the volcanic complex has a minimum water depth of 570 m, whereas the eastern sector shoals to a water depth of 70 m. The peaks of the Palinuro volcanic complex are regularly shaped and probably represent former centers of eruption (Fabbri et al., 1973; Colantoni et al., 1981; Minniti and Bonavia, 1984; Stüben et al., 1993; Yevsyukov, 1994). The shallow peak in the eastern portion of Palinuro is built on a plateau that is about 2 km in diameter, and probably formed as

a result of erosion during the last glacial lowering of the sea level (Fabbri et al., 1973).

Seafloor observations have shown that large parts of Palinuro are covered with sediments. Outcrops of volcanic rocks are scarce in the upper portion of the coalesced volcanic edifices. The occurrence of massive sulfides and, more extensive, Mn-Fe-oxide deposits has been established by seafloor sampling, TV-guided camera surveys, and ROV operations (Kidd and Ármannson, 1979; Minniti and Bonavia, 1984; Puchelt and Laschek, 1986; Tufar, 1991; Eckhardt et al., 1997; Marani et al., 1999; Dekov and Savelli, 2004; Petersen and Monecke, 2008).

Massive sulfide fragments have been recovered from the western portion of the volcanic complex at a water depth of approximately 600 m by gravity coring (Minniti and Bonavia, 1984; Marani et al., 1999), dredging (Marani et al., 1999; Petersen and Monecke, 2008), and TV-guided grab sampling (Puchelt and Laschek, 1986; Tufar, 1991). So far, at least two areas of sulfide mineralization have been identified that are located approximately 5 km apart from each other. The sulfide mineralization appears to be buried by sediments and no sulfide chimneys have been reported to occur at Palinuro (Puchelt and Laschek, 1986; Marani et al., 1999). However, abundant flocculent white and yellow bacterial mats as well as yellow, brown, and green staining of sediments and outcrops have been recognized suggesting relatively recent hydrothermal activity (Minniti and Bonavia, 1984; Puchelt and Laschek, 1986; Stüben et al., 1993; Eckhardt et al., 1997; Petersen and Monecke, 2008). ROV diving conducted in 2006 revealed the presence of tube worm colonies in an area characterized by the venting of shimmering water, demonstrating that the hydrothermal activity at Palinuro is still ongoing (Petersen and Monecke, 2008).

In addition to the local occurrence of massive sulfides, a variety of hydrothermal Fe-Mn-oxide deposits have been recovered at water depths between 90 m and 900 m (Kidd and Ármannson, 1979; Minniti et al., 1986; Eckhardt et al., 1997; Dekov and Savelli, 2004). Mn-rich crusts commonly form thin films on calcareous sediment and fossil fragments such as shells and corals (Eckhardt et al., 1997). Besides these crusts, Mn-rich micromnodules appear to be relatively abundant on the upper slopes and summits of the Palinuro volcanic complex (Kidd and Ármannson, 1979; Eckhardt et al., 1997).

Marsili volcanic complex

Marsili represents a prominent NNE-SSW trending volcanic edifice located in the central part of the ocean crust-floored Marsili basin (Fig. 2). It is the largest submarine volcano in the Tyrrhenian Sea and has an overall length of 55 km, a maximum width of 30 km, and a height of approximately 3,000 m. Marsili possesses a long and narrow summit region that stretches approximately 20 km along the main axis of the volcano and rises to a water depth of less than 500 m. The summit region, which occurs mainly above the 1,000 m isobath, is generated by the linear alignment of elongated approximately 200 m high volcanic cones and the occurrence of contiguous cones forming narrow cone ridges (Marani and Trua, 2002; Trua et al., 2002). Video surveys showed that the summit region is dominated by young lavas. The eruptive products of the summit area consist of viscous and scoraceous lava flows and associated breccia, whereas pillow lavas and elongate tube flows form the deeper portions of the volcanic edifice at water depth greater than 1,000 m. Linear fault scarps

and several meter-wide open fissures are abundant in the summit area, but also occur along the slopes of the volcanic complex (Sborshchikov et al., 1989; Savelli, 1992; Sborshchikov and Al'mukhamedov, 1992). Sediments are scarce or absent in the summit area. The volcano flanks are overlain by a sediment cover that thickens considerably with depth (Sborshchikov et al., 1989).

Fe-oxide deposits, forming numerous mounds, stacks, and chimney-like structures, occur in the central part of the summit region (Uchupi and Ballard, 1989; Savelli, 1992; Sborshchikov and Al'mukhamedov, 1992; Petersen and Monecke, 2008). The occurrence of shimmering water in the area suggests that low-temperature hydrothermal activity is still ongoing (Uchupi and Ballard, 1989; Savelli, 1992; Petersen and Monecke, 2008). In addition to Fe-oxides, one massive sulfide fragment with abundant barite was discovered during dredging at the volcano (Marani et al., 1999).

Panarea hydrothermal field

Panarea is the smallest island of the Aeolian archipelago (Fig. 2). It represents a small emerged volcanic complex set on a large, near circular platform that has a size of approximately 55 km². The platform is bounded by a shelf break at a water depth of 120 to 130 m. The submerged platform has steep slopes and a height of about 1,050 m above the surrounding seafloor. Including the subaerial portion of the volcano, the total height of Panarea is approximately 1,600 m (Favalli et al., 2005). Subaerial parts of the volcanic complex comprise the main island of Panarea in the west, the island of Basiluzzo in the northeast, and the central islets and reefs in the east (Gabbianelli et al., 1990; Calanchi et al., 1999).

Shallow-water gas venting is widespread in the submerged portion of the Panarea volcanic complex. Hydrothermal discharge is most pronounced in a 2.3 km² large area between the islets of Dattilo, Panarelli, Lisca Bianca, Bottaro, and Lisca Nera, where numerous shallow marine (<30 m) vents occur (Gabbianelli et al., 1990; Calanchi et al., 1999; Esposito et al., 2006). Hydrothermal alteration is frequently observed around the vent sites with alunite veins being particularly abundant to the west of Lisca Bianca and Bottaro (Esposito et al., 2006).

Since historical times, continuous gas venting in the area has been repeatedly interrupted by short periods of vigorous gas discharge, presumably due to new magmatic inputs into the geothermal reservoir (Caliro et al., 2004; Caracausi et al., 2005). The most recent hydrothermal crisis occurred between Lisca Bianca and Bottaro in November 2002. The submarine explosion resulted in the formation of an ellipsoidal crater near Bottaro that has a dimension of 35 x 20 m and a depth of 8 m (Caliro et al., 2004; Caracausi et al., 2005; Esposito et al., 2006). A whitish plume of suspended sediment was caused by the submarine explosion, extending for several hectares to the SSE due to dispersal by the currents. The hydrothermal crisis was accompanied by a seismic swarm of low intensity (<1.8 M) and triggered gas venting in five other areas around Panarea (Caliro et al., 2004; Caracausi et al., 2005; Esposito et al., 2006). After a few days, the degassing activity decreased, but clearly remained higher than prior to the crises.

A highly unusual, shallow marine sulfide mineralization has been discovered at a water depth of only 80 m to the north of the central islets (Marani et al., 1997). Box coring in this area yielded two massive sulfide fragments of decimeter size, consisting

mainly of pyrite, sphalerite, galena, and barite (Marani et al., 1997; Savelli et al., 1999). In addition to the massive sulfide mineralization, disseminated sulfides and sulfates, veinlets of pyrite, and siliceous concretions occur in the strongly altered seafloor sediments (Marani et al., 1997, 1999; Gamberi et al., 1999). Montmorillonite, kaolinite, cristobalite, and quartz are common alteration products (Marani et al., 1997). Sediment samples possessed a notable H₂S smell, suggesting that sulfide precipitation is currently taking place at this locality (Marani et al., 1997; Savelli et al., 1999).

4. Daily Narrative

S. Petersen and T. Monecke

R/V Meteor cruise M73/2 started at 07:00 UTC on August 14, 2007, when the vessel left the harbor of Genoa to test the Gyro navigation system. Following these trials, the vessel returned to the port to drop off the Kongsberg system personnel before sailing to the first study site at the Palinuro volcanic complex. An equipment deployment meeting was held at 13:20 UTC, followed by a successful test deployment of the Rockdrill at 14:50 UTC. The regional geology of the Tyrrhenian Sea was discussed during a first meeting of the shipboard scientific party. At 08:30 UTC on August 15, a meeting was held to discuss core handling procedures. The geology of the working areas was discussed at a third meeting starting at 16:30 UTC. R/V Meteor reached Palinuro shortly before midnight on August 15.

Following acquisition of the sound velocity profile 849SP (23:23-00:34 UTC), seafloor mapping was carried out using the Kongsberg EM120 multibeam system. Surveying was continued during the remainder of the night (station 850SB; 01:14-06:28 UTC). In the morning of August 16, the first Rockdrill station (851RD; 07:17-09:59 UTC) was conducted in the general area where living tube worm colonies have been observed in 2006 (Petersen and Monecke, 2008). This first drill hole of the cruise returned 135 cm of sulfide and sulfate mineralization, causing considerable excitement amongst the scientific party. Five distinct hydrothermal facies were recognized, namely dark vuggy sulfate with black inclusions, vuggy sulfate-sulfide, vuggy sulfide-sulfate, massive sulfate, and massive sulfide.

During the remainder of the day, four additional Rockdrill stations were carried out in the same area. Following some difficulties with the transponder, station 852RD (10:53-13:46 UTC) was targeted ca. 20 m to the north of the discovery hole. In total, 96 cm of core were recovered. The upper 39 cm of core consisted of sulfur-cemented sandstone-siltstone, polymictic breccia with pumice clasts, and polymictic breccia with white and black clasts, while the lower part of the core consisted of massive sulfate and vuggy sulfate-sulfide. Subsequent drilling (station 853RD; 14:23-16:16 UTC) to the east yielded 34 cm of dark vuggy sulfate with black inclusions. Station 854RD (16:32-19:37 UTC) had no recovery, presumably due to a thick sediment cover at the site or the soft nature of the underlying mineralization. The last Rockdrill station of the day (855RD; 19:48-21:11 UTC) yielded altered sandstone-siltstone and minor polymictic breccia with pumice clasts.

Scientific work at the Palinuro volcanic complex had to be terminated in the evening because one scientist needed immediate medical attention, which was arranged for the morning of the following day at the harbor of Salerno. Because of the short transit time, it was decided to conduct two hours of seafloor mapping prior to sailing (station 856SB; 21:13-23:06 UTC). On the morning of August 17, Nico Augustin left the vessel and returned to Germany from Napoli airport. After returning to the work area, four Rockdrill stations were conducted. The first hole (station 857RD; 11:50-13:27 UTC) was targeted to the east of the discovery hole 851RD in an area of thick sediment cover. In total, 47 cm of core were recovered that consisted of a thin layer of polymictic breccia with pumice clasts overlying vuggy sulfate-sulfide. Rockdrill station 858RD (14:13-15:39 UTC) yielded 2 cm of massive sulfide. Fast penetration (less than 30 min for a total of 5 m) suggests that the sediment cover in the drilled area was very thick. The next two drill holes were placed in the northwestern (station

859RD; 16:20-17:48 UTC) and southwestern (station 860RD; 18:13-20:21 UTC) part of the inferred mineralization trend to test its lateral continuity. Only the first hole was successful yielding 50 cm of vuggy sulfate-sulfide and sandstone-siltstone.

During the night of August 17-18, three gravity corer stations were conducted to obtain samples for pore water geochemical investigations, sulfur geochemical research, and microbiological studies. Station 861GC (20:36-21:08 UTC) conducted to the southeast of the discovery hole 851RD yielded 295 cm of unconsolidated mud and sand. The upper portion of the core was strongly oxidized and light brown in color, whereas the lower portion of the core was greenish. A small interval of banded silica-sulfide-sulfate was encountered in the lower reduced portion of the core. The second gravity corer (station 862GC; 22:25-23:00 UTC), targeted to the northwest of the area of mineralization, yielded 40 cm of brown unconsolidated mud containing some shell fragments. The last gravity corer station (863GC; 23:43-00:33 UTC) of the day was targeted to sample unconsolidated mud and sand within the large crater to the east of the topographic high hosting the sulfide mineralization. The upper portion of the 298 cm long core was again oxidized, whereas the lower part was reduced and greenish-gray.

The early morning of August 18 was used to collect additional bathymetric data at Palinuro (station 864SB; 00:53-05:26 UTC). Seafloor mapping was followed by Rockdrill station 865RD (06:02-08:21 UTC), yielded a full barrel of sulfide mineralization. The recovered core consisted of 12 cm of sandstone-siltstone and polymictic breccia with white and black clasts overlying 473 cm of vuggy sulfate-sulfide, vuggy sulfide-sulfate, and massive sulfide. During station work, a problem with the umbilical birdcaging was noticed at a cable length of approximately 600 m. To inspect the problem, a test deployment of the drilling device (no station number; 09:32-10:44 UTC) was conducted to a water depth of 610 m. Because the outer armor of the umbilical began to unravel, the cable was provisionally taped further up the umbilical. Following a meeting at 10:45 UTC, it was decided to deploy the TV-guided grab for the remainder of the day. After initial difficulties with the telemetry, TV-guided grab station 866TVG (14:30-16:18 UTC) recovered mud, banded silica-sulfide-sulfate, and vuggy sulfide-sulfate. The second TV-guided grab station (867TVG; 18:29-20:07 UTC) was targeted on a summit to the east of the mineralized area. Unconsolidated mud, bioclastic sandstone-breccia, and Mn-oxides were recovered. The night was used for the seafloor mapping station 868SB (21:35-05:27 UTC).

August 19 started with station 869TVG (06:35-11:06 UTC), but an electrical failure prevented successful deployment of the TV-grab. The problem persisted during two additional test deployments. Due to the lack of functional instrumentation, a short seafloor survey was conducted (station 870SB; 12:00-13:00 UTC). As the problem with the TV-guided grab could not be resolved, it was decided to conduct additional gravity coring. Station 871GC (14:03-14:44 UTC) yielded 210 cm of core from the area of sulfide mineralization. Only the upper 5 cm of the core were oxidized, whereas the remaining part consisted of grayish-green unconsolidated sand and mud containing several intervals of unconsolidated monomictic breccia of sulfide and sulfate clasts and unconsolidated polymictic breccia of mud and volcanic clasts. Station 872GC (16:00-16:40 UTC), also targeted within the area of sulfide mineralization, returned 299 cm of dark gray unconsolidated mud and minor sand, containing several intervals of unconsolidated monomictic breccia of sulfide and sulfate clasts, unconsolidated polymictic breccia of mud and volcanic clasts, and unconsolidated monolith-

ic volcanic sandstone clast breccia. Both cores were extensively sampled for pore water analysis, sulfur geochemical studies, and microbiological investigations. Seafloor mapping at Palinuro was continued during stations 873SB (17:25-03:44 UTC) and 874SB (04:09-06:06 UTC).

Since permission to use the mobile winch and the umbilical in shallow water had already been obtained at 14:00 UTC on August 19, the ship transited to the second working area near Panarea following completion of the bathymetric survey 874SB in the morning of August 20. The volcanic active island of Stromboli was passed at 09:30 UTC. During the following four days, an extensive work program was carried out in the shallow marine (<100 m) portion of the Panarea platform.

During the second part of August 20, six Rockdrill and one Rockdrill vibrocorer stations were conducted. Initial drilling took place in one of the seafloor depressions to the north of Lisca Bianca. The first core recovered (station 875RD; 11:21-12:35 UTC) was 89.5 cm long and consisted of crystal-lithic and pumice-rich sandstone to pebble conglomerate and feldspar-olivine porphyritic andesite. The second hole (station 876RD; 12:56-14:09 UTC) returned 12 cm of intensely altered, coherent volcanic rocks, possibly feldspar-olivine porphyritic andesite. To obtain samples for pore water analysis, it was attempted to conduct a Rockdrill vibrocorer station in the same area. Station 877RDV (14:44-15:28 UTC) recovered 66 cm of sulfur-bearing sandy sediment slurry that was discarded because vibrocoring had already destroyed the original stratigraphy of the sediment. Subsequent drilling (station 878RD; 16:12-17:44 UTC) within the same seafloor depression drilled earlier in the day yielded 35 cm of sulfur cemented crystal-lithic and pumice-rich sandstone to pebble conglomerate overlying feldspar-olivine porphyritic andesite. The last three Rockdrill stations of the day were targeted at a channel-like depression in the north of the Secca dei Panarelli that was recognized in the bathymetric data set of Anzidei et al. (2005) and Esposito et al. (2006). All three stations recovered massive anhydrite and gypsum containing minor pyrite and sphalerite as well as white clay. Station 879RD (18:06-19:07 UTC) yielded 70 cm of this sulfate rock, whereas 89 cm and 289 cm of this material were recovered during the stations 880RD (19:29-21:36 UTC) and 881RD (22:00-00:13 UTC), respectively. Station 881RD was completed in the early morning of August 21.

The intense drilling program continued on August 21. In total, 13 sites were cored during the day. The first station 882RD (00:46-02:06 UTC) did not yield any material. The following two Rockdrill stations 883RD (02:23-03:45 UTC) and 884RD (04:13-05:50 UTC) were targeted in a circular seafloor depression in the north of the Secca dei Panarelli. Drilling was successful yielding 69 and 84 cm of massive sulfate and minor unconsolidated mud, respectively. Although station 885RD (06:18-08:38 UTC) did not return any core, a large sample of white clay was wedged in the drilling platform. Following Rockdrill station 886RD (08:49-09:47 UTC) in the channel-like depression located to the north of the Secca dei Panarelli, which resulted in 21.5 cm of massive anhydrite and gypsum, a vibrocorer station (887RDV; 10:07-10:49 UTC) was conducted to sample unconsolidated sediments in the same area. In total, 179 cm of pumice-rich sand to pebble breccia and unconsolidated mud and sand were recovered. Because of illegal fishing activities by local fishermen after nightfall of the previous day, it was decided to conduct a bathymetric survey of the area during daylight and to use the night to continue the drilling program. The area between Basiluzzo and the central islets was mapped for four and a half hours (station 888SB; 11:00-15:39 UTC). Following this seafloor survey, station 889RD (15:58-16:45 UTC)

was conducted in the channel-like depression to the north of the Secca dei Panarelli, which yielded 30 cm of dark gray mudstone. After this station, vibrocoring (station 890RDV; 17:46-18:07 UTC) was carried out at the same location. Unfortunately, the core shot out of the liner when the bolts were removed. Although the upper portion of the core was lost, 410 cm of gray-brown unconsolidated sand containing traces of pyrite were recovered. The next station (891RD; 18:41-19:18 UTC) in the channel-like depression returned 126 cm of intensely clay-altered feldspar porphyritic andesite. Stations 892RD (19:37-20:26 UTC) and 893RD (20:46-21:53 UTC) were not successful. The last operation of the day was the vibrocorer station 894RDV (22:13-22:52 UTC) that was targeted to the southwest of the channel in an area where Fe-oxide chimneys were observed during the ROV dives in 2006. In total, 375 cm of unconsolidated sand with some Fe-oxide encrustations were recovered. The following station was marked by some initial problems with the Posidonia sub-positioning system. Subsequent to the initial deployment of the drilling device at the incorrect location, the system was recovered and the ship moved.

Drilling continued on August 22 with station 895RD (00:16-02:47 UTC), which was targeted at the felsic lava dome located to the northwest of Panarelli. Initial deployment failed because the chosen site was unsuitable for landing of the drilling device. The second attempt yielded 81 cm of feldspar-amphibole porphyritic rhyolite and amphibole-biotite-feldspar porphyritic andesite. Following another unsuccessful attempt to land the drilling device on the felsic lava dome, drilling during station 896RD (03:14-06:25 UTC) recovered 492 cm of feldspar-amphibole porphyritic rhyolite and feldspar porphyritic andesite. A Rockdrill station (897RD; 06:54-08:54 UTC) on the northeastern flank of the lava dome yielded 48.5 cm of feldspar-amphibole porphyritic rhyolite and feldspar porphyritic andesite. During daylight, several hours of seafloor survey (station 898SB; 09:19-11:25 UTC) were conducted to add information to the growing bathymetric data set. Mapping focused on an area between Panarea and Basiluzzo. Following this survey, one successful drilling operation (899RD; 11:50-12:39 UTC) returned 68.5 cm of unconsolidated dark gray sand overlying feldspar porphyritic andesite from the channel-like seafloor depression to the north of the Secca dei Panarelli. A nearby Rockdrill vibrocorer station (900RDV; 13:00-13:29 UTC) yielded 396 cm of unconsolidated sand and mud. No recovery was obtained from Rockdrill station 901RD (13:51-14:42 UTC). Subsequent drilling has been performed in a boulder field in the most westerly portion of the working area where Fe-oxide chimneys have been observed during ROV dives onboard R/V Poseidon cruise POS340. Drilling at this location was found to be very challenging because the drilling device could not be readily landed on the Fe-oxide structures. Station 902RD (15:48-16:59 UTC) recovered 38 cm of coarse conglomerate forming the substrate to the delicate chimneys. Subsequent drilling at the same location (903RD; 17:13-18:20 UTC) yielded only 5.5 cm of conglomerate. The third drill hole in the area of the boulder field (904RD; 18:30-21:13 UTC) returned 85 cm of coarse conglomerate. The last two stations of the day (905RD; 21:52-23:04 UTC and 906RD; 23:15-00:00 UTC) had no recovery.

August 23 was the final day of drilling at Panarea. During the early morning, vibrocoring was conducted (907RDV; 00:13-00:57 UTC) in a large seafloor depression located to the north of Lisca Bianca. The vibrocoring yielded 193 cm of unconsolidated sand. Subsequent drilling (station 908RD; 01:25-03:09 UTC) in the same seafloor depression drilled at the start of the station work at Panarea resulted in the recovery of 12 cm core consisting of crystal-lithic and pumice-rich sandstone to pebble con-

glomerate overlying feldspar-olivine porphyritic andesite. The next two Rockdrill stations were unsuccessful and no material was recovered (909RD; 03:35-04:15 UTC and 910RD; 04:31-05:20 UTC). Following a third station without recovery (911RD; 06:09-06:54 UTC), two hours of seafloor survey were conducted to the south of Basiluzzo (912SB; 07:05-08:54 UTC). Three more Rockdrill stations targeted in the channel-like seafloor depression to the north of the Secca dei Panarelli were carried out during the remainder of the day. The first station (913RD; 10:00-10:49 UTC) yielded 21 cm of massive anhydrite and gypsum with some minor unconsolidated mud. The second station (914RD; 11:06-13:14 UTC) was highly successful and 140.5 cm of sulfate mineralization was recovered. The vibrocorer station 915RDV (13:34-14:00 UTC) yielded 417 cm of polymictic breccia with crystal-rich sandstone clasts, as well as unconsolidated sand and mud. During an extended seafloor survey (916SB-1; 14:32-01:20 UTM), the eastern slope of the Panarea platform and the area to the north of Basiluzzo were mapped.

Since clearance to use the Rockdrill in deeper water was obtained, the ship transited to the working area at the Marsili volcanic complex in the morning of August 24. A short seafloor survey (916SB-2; 05:21-07:11 UTC) was conducted prior to drilling. During the first set of Rockdrill stations, it was attempted to recover the substrate of the delicate Fe-oxide chimneys observed onboard R/V Poseidon cruise POS340 (Petersen and Monecke, 2008). Rockdrill station 917RD (07:21-09:59 UTC) had no recovery, but a large sample of Fe-oxides was wedged in the drill platform. Subsequent drilling (station 918RD; 10:06-12:38 UTC) yielded 32 cm of feldspar-olivine porphyritic andesite. Due to the poor recovery, it was decided to conduct a TV-guided grab station (919TVG; 13:10-13:48 UTC). The station successfully recovered Fe-oxide crusts and feldspar-olivine porphyritic andesite. Drilling during the next station (920RD; 15:49-18:14 UTC) yielded 48.5 cm of feldspar-olivine porphyritic andesite. No material was recovered during the last Rockdrill station (921RD; 18:51-20:59 UTC) that was targeted to recover basalt from one of volcanic cones to the south of the low-temperature hydrothermal field. TV-guided grabbing (922TVG; 21:16-21:53 UTC) at this location was also unsuccessful as the grab was not able to penetrate into the subsurface and no outcrop was found that would have been suitable for biting off a rock sample. The entire night and the morning of August 25 were used for an extensive seafloor mapping survey that continued into the afternoon of the same day (923SB; 22:28-14:20 UTC). After a brief transit, seafloor mapping was continued at the Palinuro volcanic complex (station 924SB; 14:39-07:44 UTC). Since little work could be carried out while conducting the extensive bathymetric survey at Palinuro, a BBQ was organized to keep the moral of the scientific party and the crew high.

Seafloor mapping was followed by several Rockdrill stations starting in the morning of August 26. Station 925RD (10:25-13:25 UTC) was conducted on the most westerly topographic high of the Palinuro volcanic complex, in an area where low-temperature Fe-oxides have been observed during ROV diving onboard R/V Poseidon in 2006. The station yielded 29 cm of feldspar-olivine porphyritic andesite, the first lava encountered at the intensely sedimented volcanic complex during the cruise. Following some difficulties with the Posidonia sub-positioning system, an attempt to drill on the flank of this topographic high (station 926RD; 13:52-16:21 UTC) failed due to the steep topography causing the drill rig to slide down-slope. Drilling during station 927RD (16:46-19:20 UTC) was initially hampered by a problem with the echosounder. After exchange of the subsea computer, drilling was successfully conducted on top of the ridge to the north of this topographic high. The station returned 15 cm of

bioclastic sandstone-breccia. Vibrocoring (station 928RDV; 19:45-20:42 UTC) at the same location yielded 68 cm of brown unconsolidated mud and sand. During drilling, an electric fault had occurred, which burnt out the connector of the vibrocorer motor on the subsea computer. During repair, an additional TV-guided grab station was attempted to sample the tube worm colonies observed in 2006. Due to the old telemetric system of the TV-guided grab and the poor quality of the online-images, the tube worm colonies could not be identified with confidence and a grab was attempted within the general vent area (station 929TVG; 22:15-23:33 UTC). Although sampling of the tube worm colonies was unsuccessful, 30 kg of unconsolidated mud, banded silica-sulfide-sulfate, massive sulfate, and sandstone-siltstone were recovered. Two more drill holes (station 930RD; 23:52-02:13 UTC and 931RD; 02:38-05:43 UTC) were conducted in the morning of August 27. The first hole yielded 118 cm of mudstone-sandstone, crystal-rich sandstone, and massive sulfide. The second drill hole recovered 45 cm of vuggy sulfide-sulfate, vuggy sulfate-sulfide, and minor massive sulfides. Station 932RD (06:03-07:57 UTC) was conducted within the area of known mineralization, returning 291 cm of polymictic breccia with white and black clasts overlaying vuggy sulfide-sulfate, vuggy sulfate-sulfide, and massive sulfide. Demobilization of the Rockdrill commenced at 08:00 UTC.



Fig. 3: Group photo of R/V Meteor cruise M73/2 shipboard scientific and technical party.

To complete the bathymetric survey of the Palinuro volcanic complex, one additional mapping station was conducted in the morning of August 27 (933SB; 08:46-09:44 UTC). Following transit to Panarea, seafloor mapping was continued in this working area (934SB; 14:12-19:10 UTC). A group photo (Fig. 3) was taken before the two Italian colleagues left board at 15:30 UTC. They were picked up by a small motor boat that transferred them to Panarea Island. The research program at the Panarea volcanic complex ended with an additional mapping station (935SB; 22:00-02:41 UTC). R/V Meteor left the working area in the early morning of August 28 and headed for Heraklion, Greece. The remainder of the day as well as August 29 was used for demobilization of the equipment and packing of the recovered sample material. The preliminary scientific findings of the cruise were discussed in a series of talks by all

working groups. The very successful research cruise ended at 06:00 UTC on August 30. A complete list of stations conducted during R/V Meteor cruise M73/2 is given in Appendix A1.

5. Cruise Statistics

T. Monecke and S. Petersen

R/V Meteor cruise 73/2 included a total of 207:57 hours of instrument deployments during 88 stations (Fig. 4). The Rockdrill was successfully deployed 36 times yielding 31.91 m of drill core during 66:26 hours of operation. An additional 15 Rockdrill stations did not yield any core. The vibrocorer function of the Rockdrill was used seven times retrieving 20.38 m of core during 4:18 hours of operation. One additional vibro-coring station was unsuccessful. Five stations of gravity coring yielded 11.42 m of core. The TV-guided grab was successfully deployed four times for a total of 5:22 hours of operation. Two TV-guided grab station had to be abandoned due to technical difficulties. Collection of a sound velocity profile at the Palinuro volcanic complex was performed for 1:11 hours. Bathymetric surveying in the three working areas was conducted during 17 multibeam stations, totaling 97:34 hours of data collection. The dead time between instrument deployments accumulated to 56:34 hours and the transit time totaled 4 days and 22:29 hours.

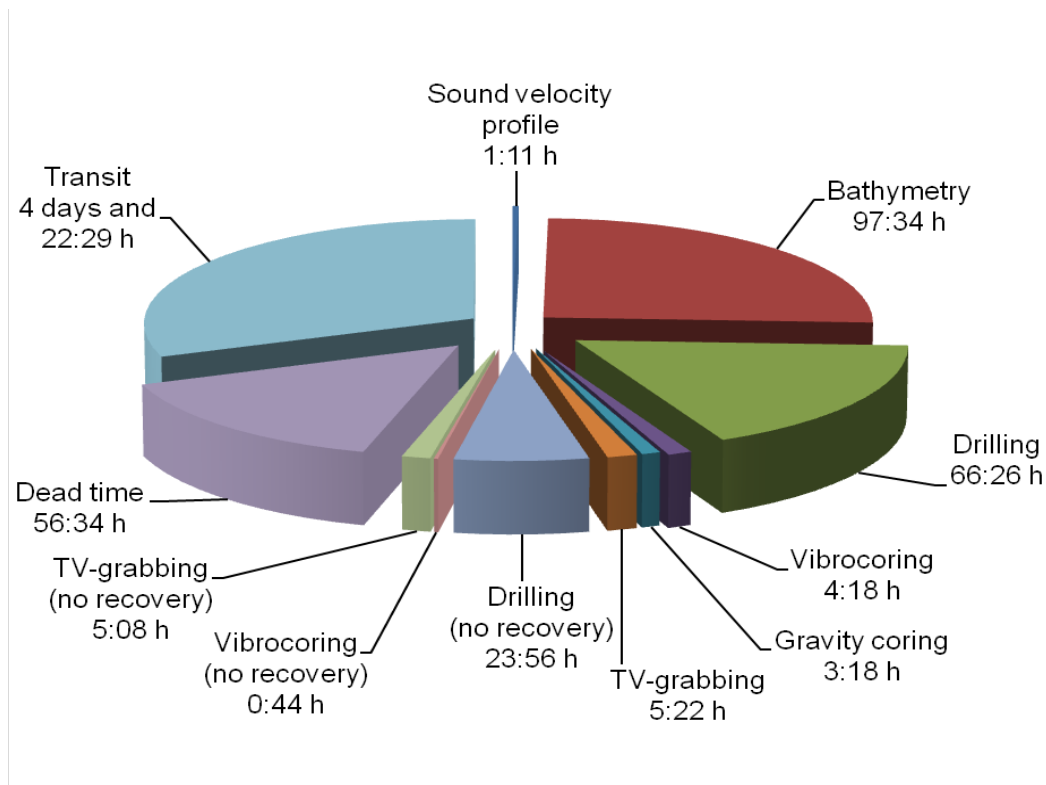


Fig. 4: Time utilization chart illustrating the usage of the different instruments onboard R/V Meteor cruise M73/2.

6. Preliminary Results

6.1. Bathymetry

N. Augustin, A. Gardeler, A. Kayser, T. Monecke, and S. Petersen

Extensive seafloor mapping was conducted using the Kongsberg Simrad EM120 multibeam system onboard R/V Meteor to obtain high-resolution bathymetric maps of the Palinuro and Marsili volcanic complexes. In addition, the seafloor surrounding Panarea Island was surveyed to add to the existing shallow water (<70 m) dataset of Anzidei et al. (2005) and Esposito et al. (2006). In total, 17 multibeam mapping stations were conducted covering an area of ca. 2,600 km² (Figs. 5-7).

The Kongsberg Simrad EM120 multibeam system consisted of 2 transmitter/receiver units coupled with a motion reference unit. The system was set at an operating frequency of 12 kHz, with a 2 x 30° opening angle and 191 simultaneous beams per ping. These settings resulted in a swath width of about 1,400 m at a water depth of 2,500 m, yielding a theoretical resolution of about 10 m at this water depth. The echo sounding system was operated using the Seafloor Information Software (SIS) by Kongsberg. The software Neptune was employed for data editing and post processing. Final data processing, gridding and map production were conducted using the software packages Fledermaus by IVS and Surfer by Golden Software. The final grid files were obtained by kriging (Isaaks and Srivastava, 1989; Cressie, 1991) and filtering using a 3 x 3 low-pass filter in up to two passes, depending on the quality of the grid file.

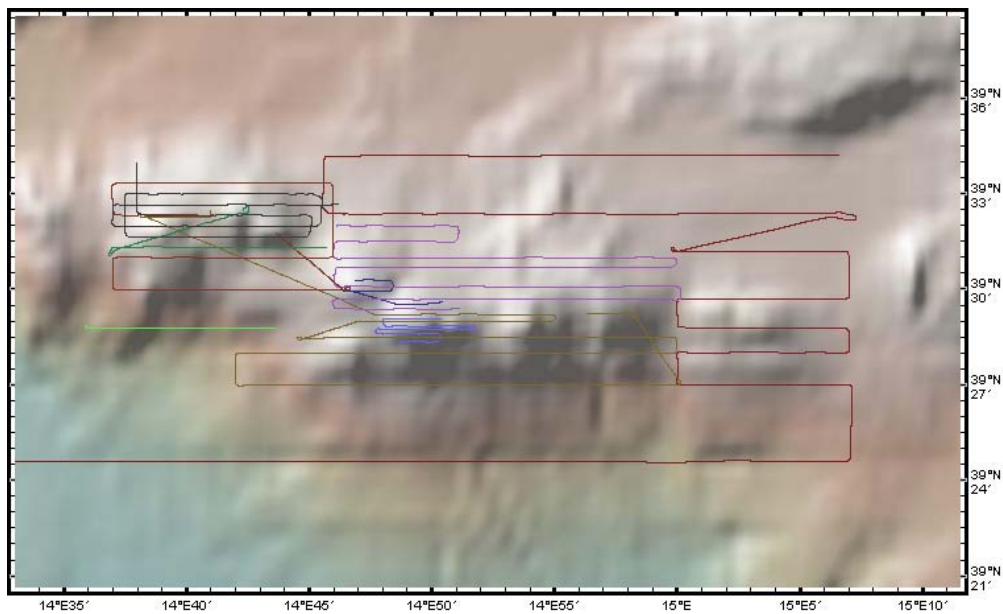


Fig. 5: Track lines of the bathymetric surveys conducted during R/V Meteor cruise M73/2 at the Palinuro volcanic complex (background bathymetry from GeoMapApp).

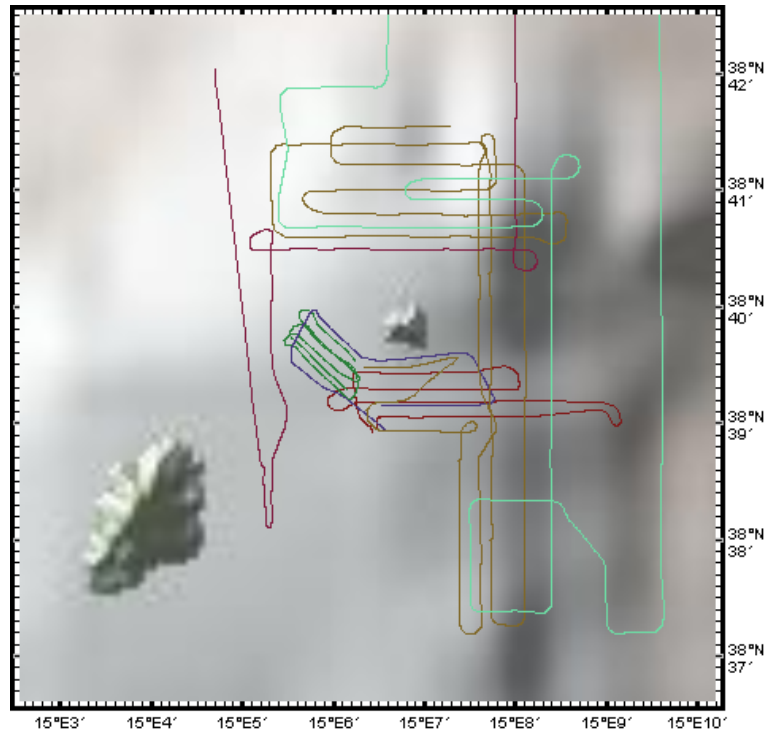


Fig. 6: Track lines of the bathymetric surveys conducted during R/V Meteor cruise M73/2 at the Panarea volcanic complex (background bathymetry from GeoMapApp).

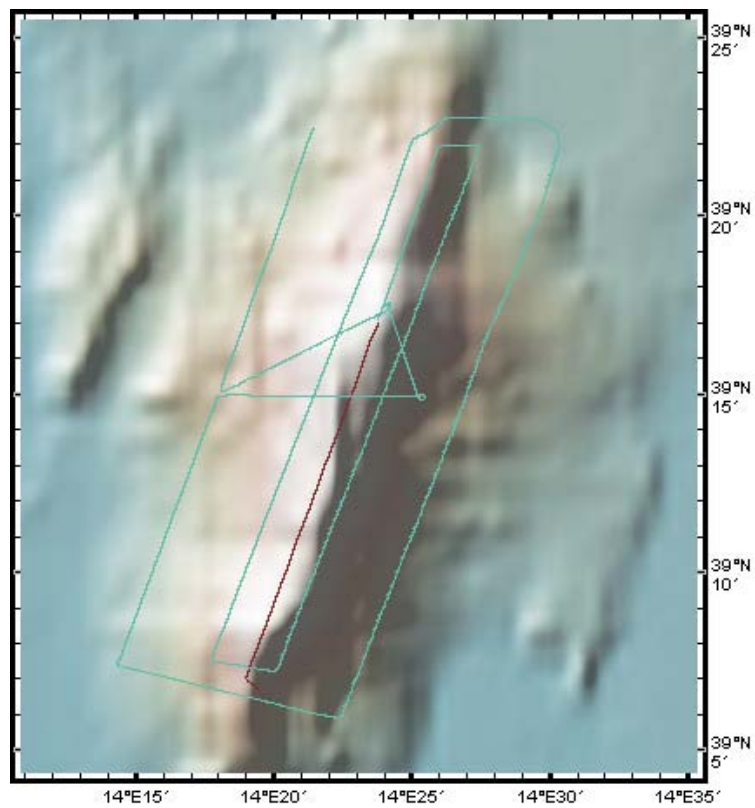


Fig. 7: Track lines of the bathymetric surveys conducted during R/V Meteor cruise M73/2 at the Marsili volcanic complex (background bathymetry from GeoMapApp).

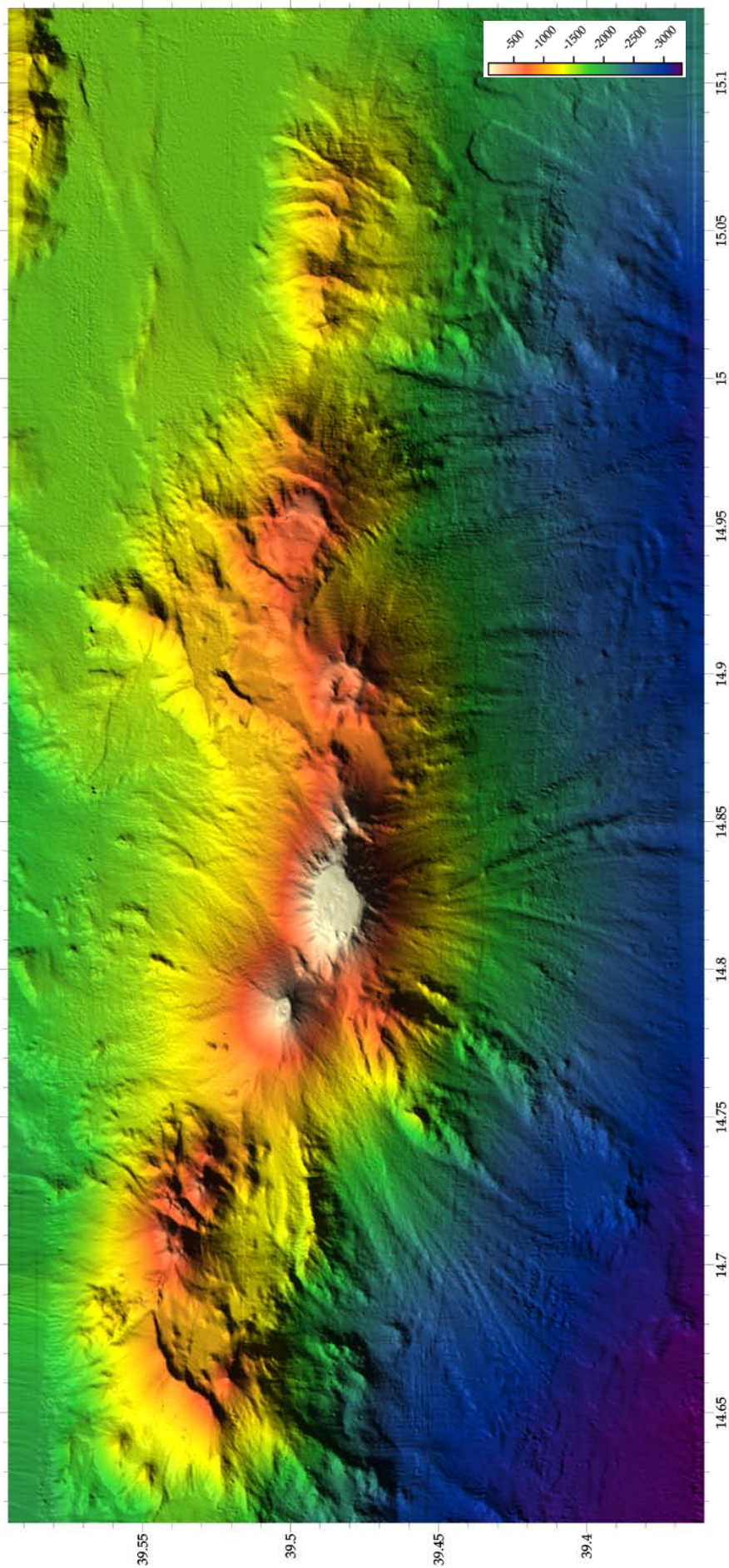


Fig. 8: Bathymetric map of the Palinuro volcanic complex generate from processed multibeam data collected during R/V Meteor cruise M73/2.

Cruise M73/2 provided the first detailed bathymetric survey of the Palinuro volcanic complex, which consists of several coalesced eruptive centers that appear to be aligned along an E-trending fault system (Fig. 8). The mapped part of the volcanic complex has an E-W extend of 42 km and is up to 17 km wide at its base. The survey showed that at least three distinct sectors can be distinguished. The easternmost sector extends from 15.000°E to 15.103°E. The shallowest peak of this sector (minimum water depth of 895 m) is located at 39.488°N and 15.034°E. The southern flank of this sector is typified by several large debris-flow scars. During mapping of the eastern sector of Palinuro, a pronounced smell of H₂S was noted onboard R/V Meteor, possibly suggesting ongoing volcanic or hydrothermal activity in the area.

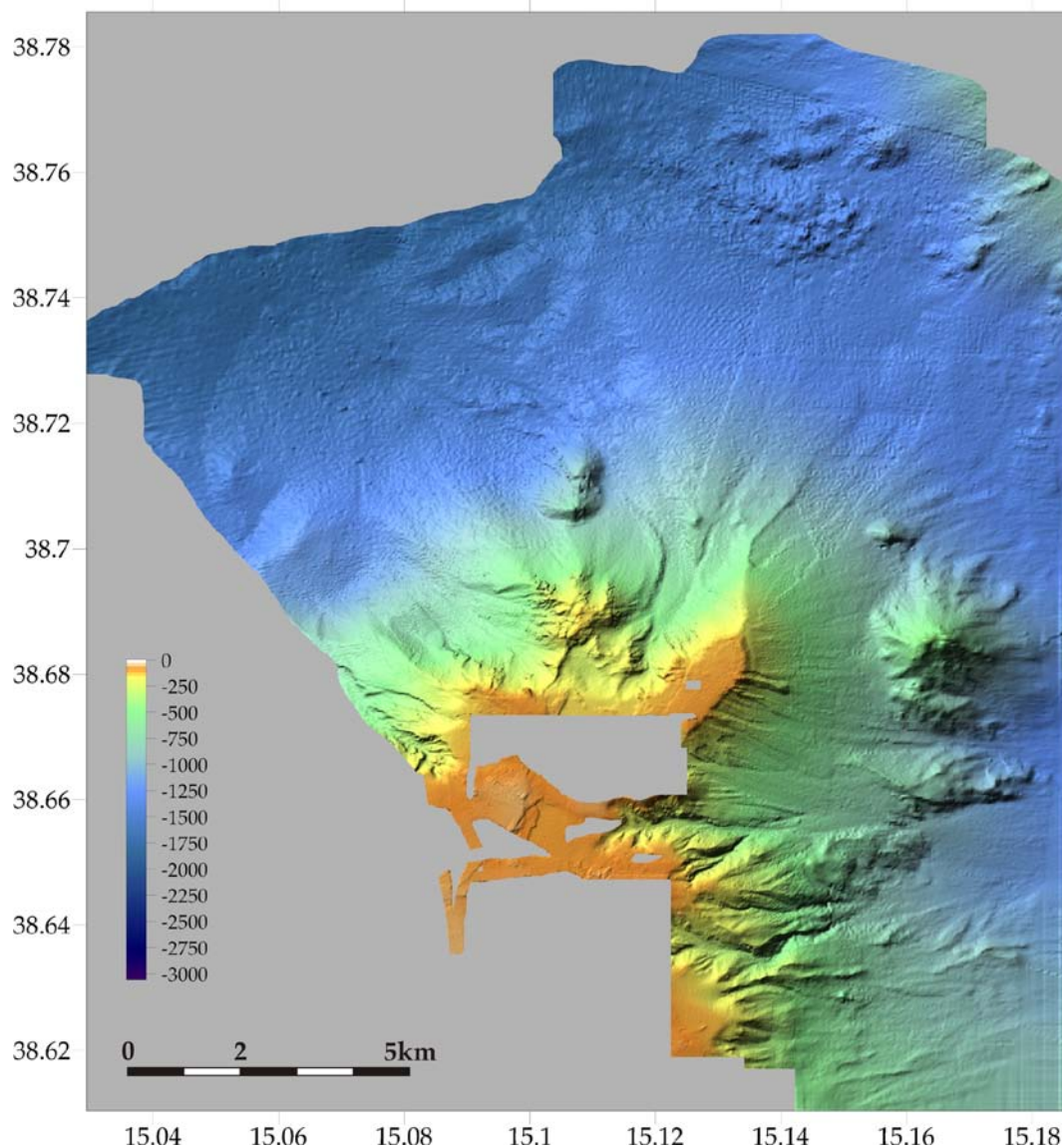


Fig. 9: Bathymetric map of Panarea generated from processed multibeam data collected during R/V Meteor cruise M73/2.

The central sector of the Palinuro volcanic complex consists of four large volcanic centers located between 14.754°E and 15.000°E (Fig. 8). The two easternmost edifices shoal to water depths of 510 m and 550 m, respectively. The volcanic peak at

14.894°E is typified by a pronounced summit crater, whereas the peak at 14.946°E may represent a resurgent dome within an older crater structure. The two westerly peaks have cone-like shapes and relatively flat tops, occurring at water depths between 80 and 150 m. The cone at 14.787°E appears to be located on a NW-striking lineament that separates the central sector from the western extension of the Palinuro volcanic complex. The western sector of Palinuro is morphologically complex and includes a cluster of volcanic cones at 14.719°E that shoal to a minimum water depth of 500 m. The known sulfide occurrences are located in this sector of the volcanic complex (Minniti and Bonavia, 1984; Puchelt and Laschek, 1986; Tufar, 1991; Marani et al., 1999; Petersen and Monecke, 2008).

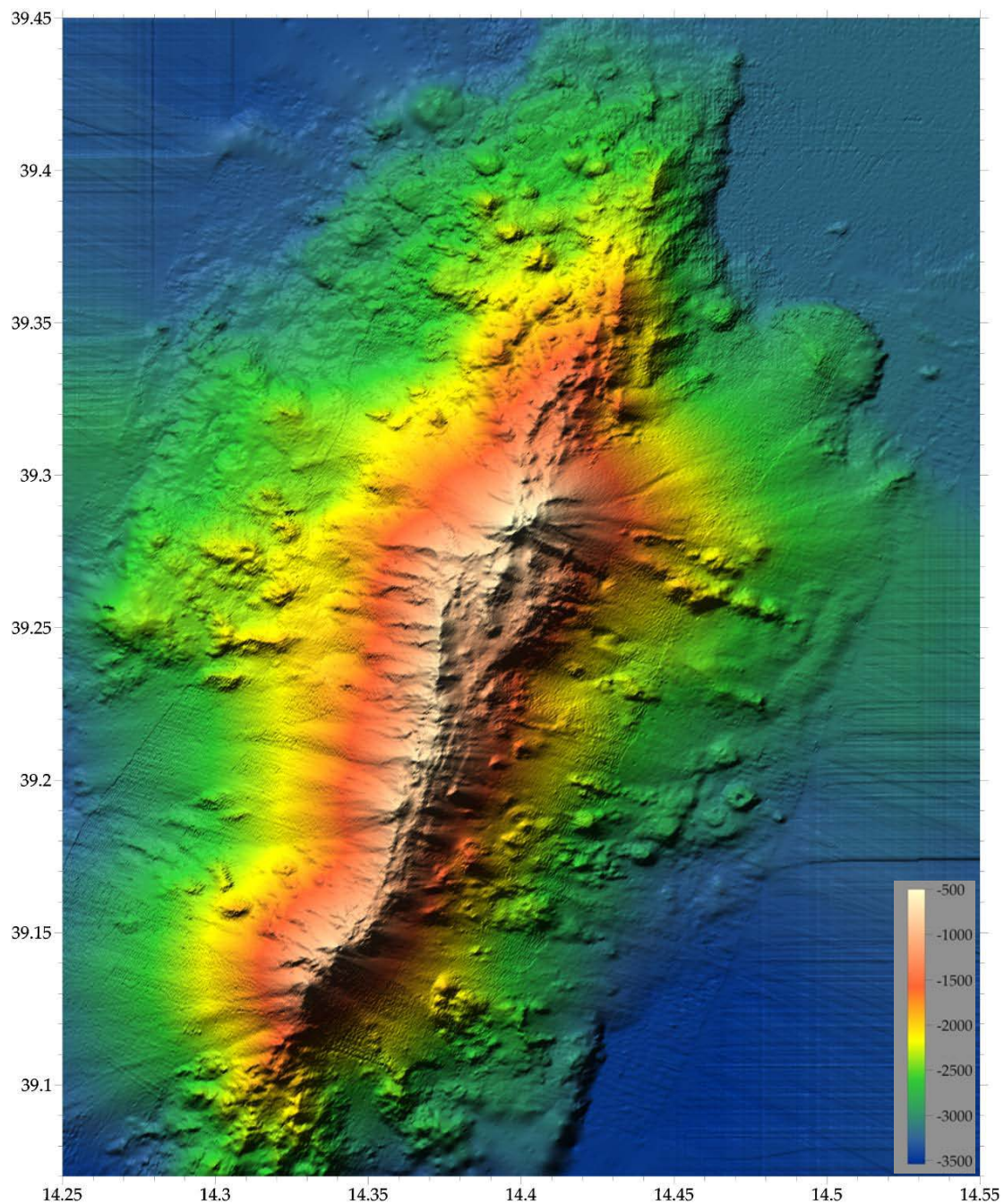


Fig. 10: Bathymetric map of the Marsili volcanic complex generated from processed multi-beam data collected during R/V Meteor cruise M73/2.

The survey of the working area at Panarea revealed the presence of complex morphological features (Fig. 9). The area immediately to the north of Basiluzzo is typified by a NE-trending ridge that has a comparably flat plateau. The slope of the ridge dips gentle to the east and is apparently covered by volcanoclastic deposits. To the west, the ridge is bounded by a major NW-striking lineament that dissects the Panarea platform. One large and two smaller volcanic centers are located to the north of Basiluzzo and one large volcanic cone can be recognized to the east. The southern portion of the mapped area is characterized by an E-trending carved valley and several large submarine fans.

The multibeam surveying at Marsili revealed that this volcanic complex is characterized by a linear summit region that is roughly defined by the 1,000 m isobath. The summit region stretches along the main axis of the volcano and can be subdivided into four distinct segments (Fig. 10). The southernmost segment of the summit region extends from 39.120°N to 39.160°N, where an abrupt change in the orientation of the ridge axis occurs. The topographic high of the 5 km long southern segment is located half way between its northern and southern limits. The second segment stretches northward to 39.206°N, where another change in the orientation of the ridge axis occurs. Water depths decrease from the southern to the northern tip of this 5 km long segment. The third segment of the summit region has a length of 6 km and is located between 39.206°N and 39.258°N. The morphology of the offset between this segment and the northernmost segment closely resembles that of overlapping spreading centers identified along mid-ocean ridges. The northernmost segment is located between 39.250°N and 39.290°N. The northern tip of this segment is characterized by the occurrence of the two shallowest peaks of the Marsili volcanic complex.

Extensive fields of volcanic cones and cone ridges to the north and south of the main edifice stretch approximately parallel to the summit region of Marsili (Fig. 10). The northern cone field is delimited to the east by a very steep slope, whereas a lower gradient prevails to the west. Another extensive cone field occurs on the western flank of Marsili. It is delimited to the north and south by NW-trending lineaments. Several clusters and trails of circular satellite cones can be observed at the eastern flank of the main edifice. Most noticeable is a trail of NW-aligned small volcanic cones that runs towards the shallowest peak of the ridge axis in the northernmost segment. The eastern and western flanks of the Marsili volcanic complex are limited by two large lineaments that are approximately parallel to the ridge axis (Fig. 10). Sedimentation across the lineament to the east of the main edifice is pronounced, especially along the northeastern flank of the volcanic complex.

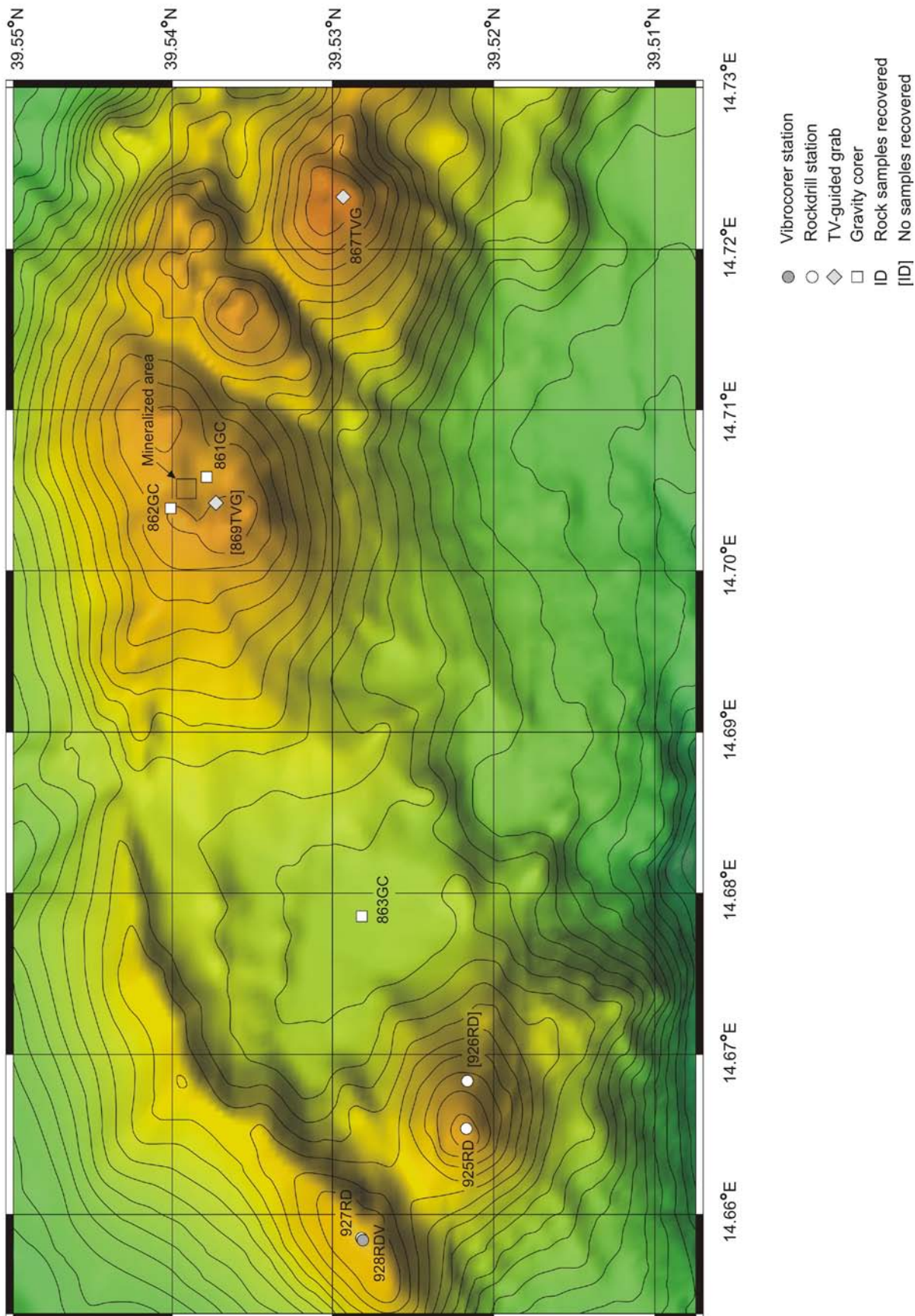


Fig. 11: Location map of station work conducted at the western sector of the Palinuro volcanic complex. A detailed map of the mineralized area is given in Fig. 12.

6.2. Sampling at the Palinuro volcanic complex

S. Petersen, T. Monecke, A. A. De Benedetti, A. Esposito, A. Gardeler, B. Gemmell, H. Gibson, G. He, A. Kayser, R. Kleeberg, K. Lackschewitz, K. Perrin, R. Sharpe, K. Simpson, and B. Wan

Station work at Palinuro focused on the western sector of the volcanic complex (Fig. 11). Most instrument deployments were conducted in a small area encompassing a seafloor depression (603 to 633 m water depth) in the summit region of one of the volcanic edifices, where massive sulfide mineralization and shimmering water were discovered during previous research cruises (Puchelt and Laschek, 1986; Tufar, 1991; Petersen and Monecke, 2008). Additional station work was conducted at the summit of a volcanic edifice to the west where widespread Fe-oxide precipitates were discovered in 2006 (Petersen and Monecke, 2008), at a volcanic ridge in the north-west of the working area, at the bottom of the crater-like structure, and at the summit of the easternmost volcanic edifice (Fig. 11).

Sampling at Palinuro involved thirteen successful Rockdrill deployments, one station using the vibrocorer function of the lander-type drilling device, and five deployments of the gravity corer. Additional three deployments of the Rockdrill did not yield any core (Appendix A1-A3). The TV-guided grab was deployed during four stations, but one station had to be aborted due to technical difficulties (Appendix A1, A4). Sampling at the western sector of the Palinuro volcanic complex yielded a wide range of hydrothermal and volcanic facies (Table 1). Representative samples were taken for clay mineral analysis and whole-rock geochemical investigations (Appendix A5, A6).

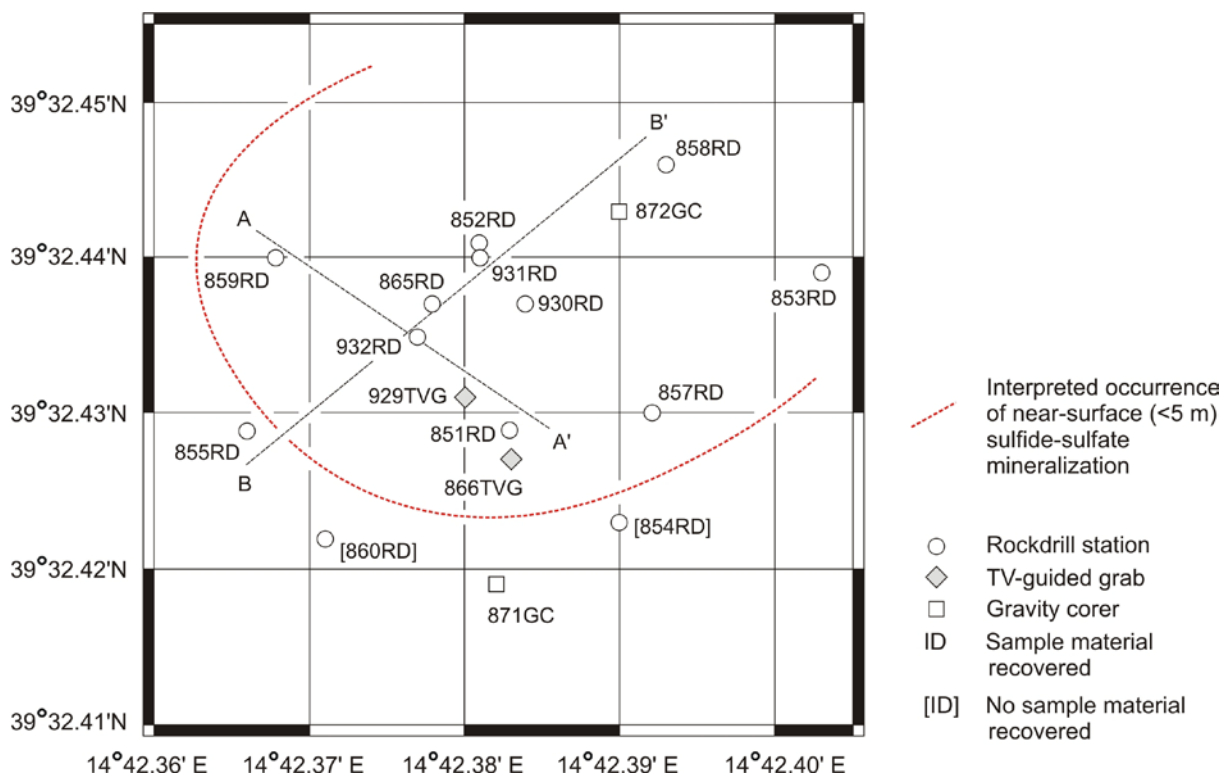


Fig. 12: Location map of station work conducted in the mineralized area in the western sector of the Palinuro volcanic complex. Schematic cross-sections along the profile lines A-A' and B-B' are given in Figs. 13 and 14.

Eleven holes were successfully drilled within the mineralized area at the Palinuro volcanic complex (Fig. 12). Drilling to a maximum depth of 5 m was conducted at a closely spaced grid covering an area of approximately 70 by 50 m. In total 13.59 m of core were recovered, including one hole that intersected 485 cm of sulfide and sulfate mineralization (station 865RD). Seafloor observations during landing of the drill rig showed that the seafloor in the target area is largely covered by unconsolidated fine-grained sediments, which explains the rapid drilling progress in the upper portion of most drill holes. These observations, combined with the results of the drilling and gravity coring (Appendix A4), suggest that the sulfide and sulfate mineralization at Palinuro occurs below a centimeter to several meters thick cover of unconsolidated mud and sand, with locally occurring breccia intervals. All drill holes in the northeastern portion of the mineralized area intersected sulfide and sulfate mineralization (Fig. 12). The sediment cover appears to rapidly increase in thickness to the south, southwest, and northwest. The mineralized zone has not been drilled off in any direction and appears to be open towards depth as all holes ended in sulfide and sulfate mineralization.

Based on the drill core logging, schematic sections through the mineralized area were constructed (Figs. 13 and 14). These sections illustrate that recovery of drill core was only possible below the unconsolidated mud and sand. The upper portion of the cored intervals typically consisted of variably altered volcanoclastic rocks including mudstone-sandstone, sandstone-siltstone, polymictic breccia with pumice clasts, polymictic breccia with white and black clasts, and crystal-rich sandstone. TV-guided grabbing (stations 866TVG and 929TVG) also yielded abundant banded silica-sulfide-sulfate samples from close to surface, which may represent intensely altered and mineralized equivalents of fine-grained and formerly bedded sediments (Fig. 15). Some volcanoclastic rocks showed extensive yellow staining interpreted to be orpiment. In most drill holes, the variably altered volcanoclastic rocks were in sharp contact with vuggy sulfate with black inclusions, vuggy sulfate-sulfide, and vuggy sulfide-sulfate. These different facies were found to be typified by polymetallic sulfides. Massive sulfates and locally massive barite were also encountered in this stratigraphic position (Fig. 15). Towards depth, these sulfate-rich hydrothermal facies are replaced by massive sulfides, with pyrite being the most abundant sulfide mineral. Late veins of pyrite and marcasite with an infill of native sulfur crosscut all hydrothermal facies encountered. The 4.85 m long drill core recovered during station 865RD represents an excellent example of the overall stratigraphy in the mineralized area (Fig. 16).

TV-grab guided sampling in the mineralized area provided evidence for ongoing hydrothermal activity in the study area. Unconsolidated mud recovered during station 866TVG was still warm when brought on deck (maximum temperature of 60°C and a minimum pH of 6.12). In addition, vent-specific macrofauna was recovered. Gravity coring (871GC and 872GC) in the mineralized area yielded unconsolidated sediments that were almost entirely reduced. Only unconsolidated mud in the upper <5 cm of core 871GC was orange brown in color suggesting that reduced conditions close to the seafloor are maintained by diffuse hydrothermal fluid flow.

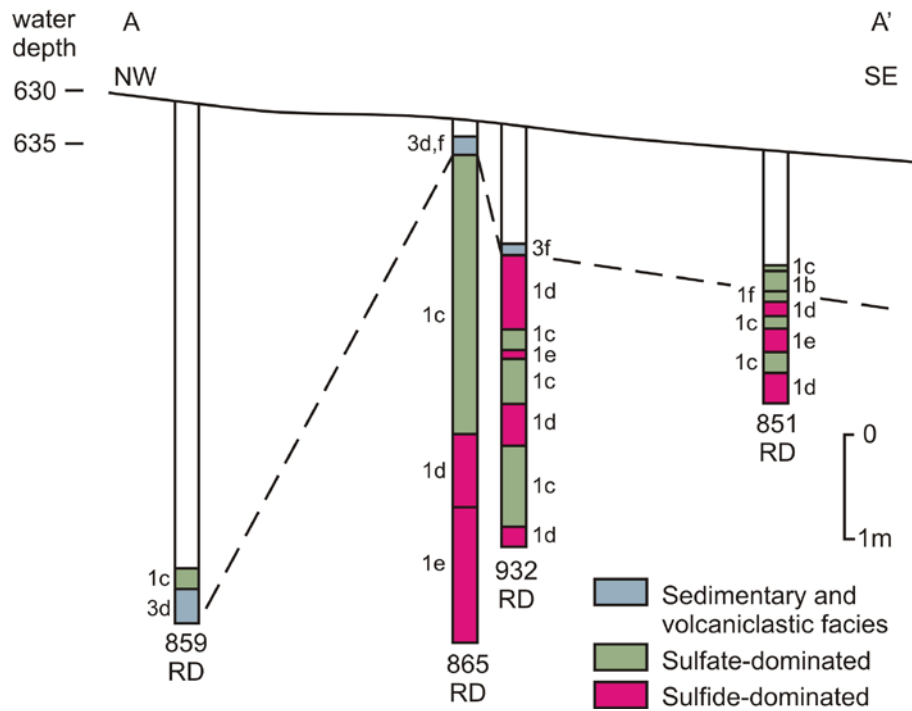


Fig. 13: Schematic cross section through the mineralized area showing the distribution of hydrothermal and volcanic facies along the profile line A-A' as shown in Fig. 12.

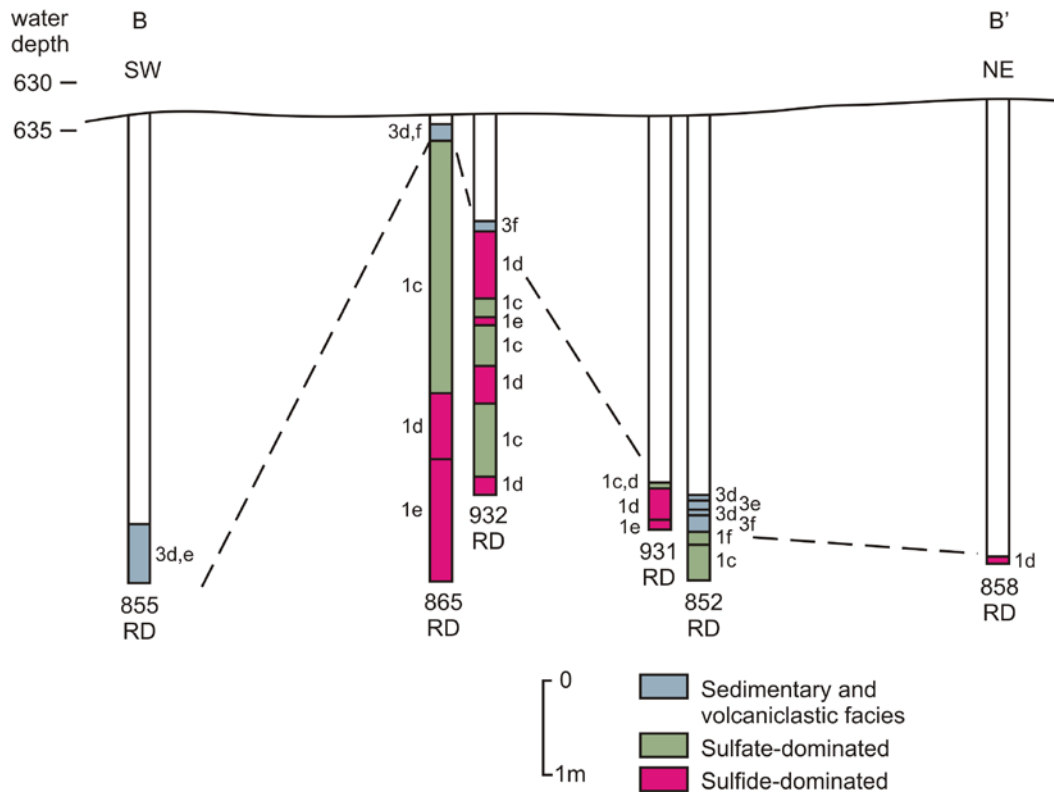


Fig. 14: Schematic cross section through the mineralized area showing the distribution of hydrothermal and volcanic facies along the profile line B-B' as shown in Fig. 12.



Fig. 15: Representative hand specimens recovered from the Palinuro volcanic complex: a. Banded silica-sulfide-sulfate consisting of alternating 1-5 mm thick layers of variable compositions (866TVG). b. Banded silica-sulfide-sulfate (866TVG). c. Vuggy sulfide-sulfate sample with native sulfur veining and encrustations (866TVG). d. Vuggy sulfide-sulfate with abundant native sulfur crystals lining fractures and cavities (866TVG). e. Banded silica-sulfide-sulfate (929TVG). Yellow staining is likely orpiment. f. Massive barite consisting of large bladed crystals (929TVG). g. Bioclastic sandstone-breccia with siliceous carbonate matrix (867TVG). h. Botryoidal Mn-oxide aggregates (867TVG).



Fig. 16: Drill core obtained by station 865RD (total length of core 485 cm; stratigraphic top is at the upper right and stratigraphic bottom is at the lower left corner of the image). The uppermost portion of the drill core consists of volcanoclastic sediments that are in sharp contact with the underlying polymetallic sulfide-sulfate mineralization. The lower part of the core is dominated by massive pyrite. Late veins of native sulfur crosscut the sulfide and sulfate mineralization.

Gravity coring was also conducted to the southeast and northwest of the mineralized area (stations 861GC and 862GC). The core recovered during station 861GC showed extensive oxidation to a depth of 90 cm. Minor banded silica-sulfide-sulfates was encountered between 252 and 255 cm depth. The entire 40 cm of core recovered during station 862GC was found to be oxidized. Station 863GC aimed to sample background sediments within the large crater to the southwest of the volcanic edifice hosting the sulfide and sulfate mineralization. The retrieved core consisted of unconsolidated mud and minor sand with the depth of oxidation being located at 46 cm.

Sampling of the volcanic edifice in the western part of the working area at the Palinuro volcanic complex (station 925RD) yielded 29 cm of feldspar-olivine porphyritic andesite, the only coherent volcanic rocks recovered from the volcanic complex during R/V Meteor cruise M73/2. Fe-oxide mineralization observed during ROV diving in 2006 was not recovered. Sampling at the volcanic ridge in the northwest of the working area yielded bioclastic sandstone as well as unconsolidated mud and sand (stations 927RD and 928RDV). TV-guided grabbing at the easternmost volcanic edifice in the working area also showed no evidence for hydrothermal activity (station 867TVG). Recovered material included unconsolidated brown to light brown mud, bioclastic sandstone-breccia, and Mn-oxide (Fig. 15). The samples of the bioclastic sandstone-breccia were coated with Mn-oxide suggesting that this facies represents older material being exposed at the seafloor.

Table 1: Description of hydrothermal and volcanic facies recovered from the Palinuro volcanic complex.

Facies	Facies description	Interpretation
1. Hydrothermal facies		
1a. Banded silica-sulfide-sulfate	<p>Characteristics: Dark brown, black and white banded or brecciated appearance</p> <p>Description: Intact dark brown, black to white banded appearance, or a polymictic breccia containing clasts of sulfide, black and red-brown sediment, and banded amorphous silica in a matrix of sulfide-sulfate and late native sulfur; coloration of beds and clasts represents Fe-, Mn- and Si-enrichment; locally overprinted by native sulfur contained within vugs and fractures</p> <p>Contact relations: Not observed but occurs at or below seafloor above or in proximity to a massive sulfate-sulfide deposit</p> <p>Distribution: 861GC, 866TVG, and 929TVG</p>	Thought to represent Fe-, Mn-, Si-, sulfide-, and sulfate-enrichment of seafloor sediments by ascending hydrothermal fluids and down-drawn seawater (sulfate) above an actively forming sub-seafloor sulfate-sulfide lens; oval-shaped structures of banded silica or limonite may represent fluid channel ways or chimneys
1b. Dark vuggy sulfate with black inclusions	<p>Characteristics: Black, vuggy, earthy black inclusions</p> <p>Description: Vuggy-textured dark sulfate containing black earthy-textured inclusions; bladed sulfate-barite (?) with fine pyrite; marcasite and silica forms a network of veins that contains the black inclusions; local cavities (vugs) mantled by 3-5 mm thick rims of pyrite-marcasite may be fluid channels; late veins and vugs commonly contain amorphous or crystalline sulfur with pyrite-marcasite</p> <p>Contact relations: Contact with overlying polymictic breccia with white and black clasts is sharp; however, the sulfide content of the polymictic breccia with white and black clasts increases towards its lower contact; grades downwards into more massive sulfate containing fewer inclusions; gradational contacts with other hydrothermal facies</p> <p>Distribution: 851RD and 853RD</p>	This facies is interpreted as a hydrothermal deposit and the earthy inclusions may represent remnants of host sediments that are rich in Mn-oxides
1c. Vuggy sulfate-sulfide	<p>Characteristics: Vuggy, variably textured sulfate, >35% Fe-sulfides, native sulfur in veins and vugs</p> <p>Description: This facies is characterized by: 1) a network of barite and possibly other sulfate minerals locally containing fine black clots; 2) fine disseminated, patchy, and fracture controlled pyrite or marcasite along with numerous vugs that contain sulfur crystals and are often lined by a thin silica crust that overgrows the barite and pyrite, but not the sulfur crystals; 3) a pseudoclastic texture where pseudoclasts of intergrown barite crystals are surrounded by a pseudomatrix of fine barite containing 10 to 35% fine pyrite; and/or 4) coarse, bladed, honeycomb textured sulfate</p> <p>Contact relations: Contacts with banded silica-sulfide-sulfate, vuggy sulfide-sulfate, massive sulfide, and massive sulfate facies are gradational; units contain 5-35% pyrite and marcasite</p> <p>Distribution: 851RD, 852RD, 857RD, 859RD, 865RD, 931RD, and 932RD</p>	This facies is a primary hydrothermal deposit that may have formed at and/or below the seafloor; black earthy inclusions may be remnants of preexisting sediments indicating sub-seafloor formation; the sulfate is dominantly barite with minor anhydrite; the honeycomb and pseudoclastic textures indicate several generations of sulfate; pyrite, marcasite, and various Ag-sulfosalts fill voids between sulfate crystals, fill fractures and line vugs indicating that they formed later and represent a hydrothermal overprint on the massive sulfate; vugs with botryoidal to crys-

Facies	Facies description	Interpretation
		talline pyrite/marcasite (sphalerite, Ag-sulfosalts ?) and amorphous to crystalline sulfur mark fluid conduits; native sulfur is a product of the youngest hydrothermal event
1d. Vuggy sulfide-sulfate	<p>Characteristics: >50% sulfides, pseudoclastic texture, vuggy, native sulfur</p> <p>Description: Facies contains >50% pyrite (marcasite) and is characterized by a pseudoclastic textures where highly pitted and vuggy pseudoclasts or irregular, web-like, stringers veins of fine- to coarse-bladed sulfate with pyrite occur within a finer, more dense pseudomatrix of massive pyrite that contains finer, irregular inclusions of coarse barite crystals; amorphous to crystalline sulfur occurs within fractures and vugs</p> <p>Contact relations: Contacts with other hydrothermal facies, particularly with the vuggy sulfate-sulfide and massive sulfide facies are gradational over a centimeter to decimeter interval</p> <p>Distribution: 851RD, 865RD, 866TVG, 931RD, and 932RD</p>	This facies is a hydrothermal deposit where Fe-sulfides are interpreted to have progressively replaced a preexisting sulfate deposit; the pseudoclasts, irregular veins, and inclusions of sulfate are interpreted to be remnants of the original sulfate deposit; Ag-sulfosalts (?), sphalerite, and chalcopyrite occur with native sulfur (amorphous and crystalline) in fractures and vugs; some vugs and fractures are lined by fine marcasite
1e. Massive sulfide	<p>Characteristics: Massive, dense pyrite, <10% sulfate inclusions and/or veins, native sulfur in vugs and fractures</p> <p>Description: Occurs as massive, dense pyrite but more commonly as massive vuggy-textured pyrite where the irregular vugs contain barite crystals imparting a pseudoclastic texture to the massive sulfide; native sulfur and native sulfur intergrown with barite occurs as veins that crosscut massive pyrite; locally subangular to rounded pseudoclasts of massive pyrite are present in an open-space pseudomatrix of amorphous silica and sulfur</p> <p>Contact relations: Contacts are gradational with other hydrothermal facies, particularly with vuggy sulfide-sulfate facies</p> <p>Distribution: 851RD, 858RD, 865RD, 930RD, 931RD, and 932RD</p>	This facies is interpreted to represent the near complete replacement of an original sulfate deposit by pyrite; the open-space fractures and vugs may represent the total dissolution of a preexisting sulfate; late fractures (and vugs) within the massive pyrite are filled by amorphous and crystalline sulfur; the occurrence of intergrown, crystalline sulfur and sulfate veins that crosscut massive pyrite indicate a late, post Fe-sulfide overprint
1f. Massive sulfate	<p>Characteristics: Vuggy sulfate, 5% sulfides, native sulfur in veins and vugs</p> <p>Description: Gray to black sulfate with numerous, irregular pits or vugs, some of which contain amorphous to crystalline sulfur; unit is massive to in situ brecciated and commonly displays distinct bladed crystals of barite; fine pyrite and clay minerals (?) are a minor constituents and typically occur between the sulfate crystals</p> <p>Contact relations: Gradational contacts with the vuggy sulfide-sulfate and vuggy sulfate-sulfide facies</p> <p>Distribution: 851RD, 852RD, and 929TVG</p>	Primary hydrothermal deposit that formed at or below the seafloor
1g. Mn-oxide	<p>Characteristics: Black, botryoidal</p> <p>Description: Irregularly shaped to nodular aggregates; greasy, dull black surfaces with variable coating by Fe-</p>	Primary hydrothermal deposit that formed at or immediately below the

Facies	Facies description	Interpretation
	oxides Contact relations: Not observed Distribution: 867TVG	seafloor
2. Coherent volcanic facies		
2a. Feldspar-olivine porphyritic andesite	Characteristics: Massive, black and feldspar-olivine porphyritic Description: Massive andesite with phenocrysts of subhedral feldspar (<5 mm, 8-10%) and lesser anhedral olivine (<2.5 mm, 1%) in an aphanitic, black to gray groundmass containing 3-5%, round to elongate vesicles that are <7 mm in size (intersection also includes clay containing granule size grains of basalt/andesite, olivine, clay-altered clasts and an intermediate amphibole porphyritic granule) Contact relations: Contacts not observed Distribution: 925RD	As contacts with enclosing units were not observed, this facies could be a flow or sill
3. Sedimentary and volcanoclastic facies		
3a. Unconsolidated sand	Characteristics: Unconsolidated, poorly stratified and well sorted sand Description: Yellowish, brown to cream-colored, very fine sand; massive, thickly to thinly bedded, occasionally laminated; some sand-sized mica crystals, shells and shell fragments; diffuse black bands may be Mn-oxides or organic; some distinct black beds contain grains of quartz, pyroxene (?), amphibole (?), black volcanic grains and plate-like grains of sulfate Contact relations: Intercalated with mud where contacts are either abrupt and sharp or gradational over decimeter intervals; where the upper contact represents the seafloor, the sand facies is characterized by red oxidation and finer stratification Distribution: 861GC, 863GC, 871GC, 872GC, and 928RDV	The lack of obvious volcanic detritus (pumice clasts) except for some crystal-rich beds suggests that this is a terrigenous epiclastic facies; the lack of bedding is not characteristic of this facies type
3b. Unconsolidated mud	Characteristics: Unconsolidated, mottled coloration, diffuse black bedding/banding and fine grain size Description: Brown, yellow-brown to green-gray and cream colored fine mud that is typically massive and diffusely stratified (devoid of bedding) with occasional worm burrows and vugs; brown patches may represent more oxidized areas and also tend to be more indurated; wispy, diffuse black bands are common and may represent Mn-oxide or organic material; shells (gastropods ?) and rock fragments distributed through some sections; occasional gray pumice lapilli occur (0.5-3 cm in 872GC) Contact relations: Intercalated with sand where contacts are either abrupt and sharp or gradational over decimeter intervals Distribution: 861GC, 862GC, 863GC, 866TVG, 867TVG, 871GC, 872GC, 928RDV, and 929TVG	The lack of obvious volcanic detritus suggests this is a terrigenous epiclastic facies
3c. Bioclastic sandstone-breccia	Characteristics: Numerous shells and shell fragments, well stratified Description: Thinly laminated, yellowish brown, very fine sand with numerous shell fragments and complete shells up to 3 mm in size (this facies is indurated and, therefore, distinct from the unconsolidated sand facies) Contact relations: Not in contact with other lithofacies Distribution: 867TVG and 927RC	Terrigenous epiclastic sediment; bioclastic component suggests reworking and redeposition
3d. Sandstone-	Characteristics: Fine grain size, crystal content, local siliceous appearance and interbedded nature	Fragments of quartz, biotite and feldspar indi-

Facies	Facies description	Interpretation
siltstone	<p>Description: Green to cream-buff colored, poorly stratified, fine-grained sandstone containing fragments of quartz, biotite, feldspar and locally barite crystals; mm-scale bioturbation structures; distinctly red-brown in color (oxidized) over a 5 cm interval where exposed at (or near) the seafloor; diffuse bands of black Mn-oxide recognized in 859RD; sandstone and siltstone are commonly interbedded (e.g., 865RD)</p> <p>Contact relations: Contacts not always observed but appear to be conformable with intercalated facies; conformably (?) overlies a vuggy-textured barite lens in 865RD</p> <p>Distribution: 852RD, 855RD, 859RD, 865RD, and 929TVG</p>	cate a volcanic provenance (pyroclastic), whereas barite crystals suggest a hydrothermal component; possibly a reworked and redeposited volcanoclastic deposit with some hydrothermal input; siltstone is a finer-grained, well-bedded equivalent that locally resembles an exhalite, possibly due to silicification
3e. Polymictic breccia with pumice clasts	<p>Characteristics: Framework supported mixture of sedimentary and volcanic clasts including pumice</p> <p>Description: Facies is characterized by subangular to angular clasts of black, mudstone enriched in Mn-oxide, felsic quartz porphyry, black obsidian, and pumice; matrix in 852RD is fine-grained and siliceous (20 -25% matrix); matrix in 855RD is vuggy, with minor siliceous (quartz) cement; pumice clasts are more common towards the top of depositional units</p> <p>Contact relations: Conformable with intercalated sandstone-siltstone and mudstone facies</p> <p>Distribution: 852RD, 855RD, and 857RD</p>	The obsidian, felsic and pumice clasts indicate a volcanic provenance, the presence of pumice suggests pyroclastic fragmentation; the black siltstone clasts indicate a “sedimentary” provenance; the facies is interpreted to represent a reworked and resedimented deposit with the pumice being a pyroclastic component
3f. Polymictic breccia with white and black clasts	<p>Characteristics: Framework supported mixture of volcanic and sedimentary clasts</p> <p>Description: Facies dominated by black, banded Mn-rich mudstone clasts (?), and white felsic clasts that resemble a volcanic siltstone; framework supported breccia with a vuggy matrix that contains “blue quartz” and native sulfur; pyrite occurs in the matrix where near the contact with an underlying sulfate lens in 852RD</p> <p>Contact relations: Conformable with intercalated sandstone-siltstone and mudstone facies</p> <p>Distribution: 852RD, 865RD, and 932RD</p>	The mixture of volcanic clasts and mudstone clasts suggests that this facies was derived through reworking and resedimentation of sedimentary and volcanic facies
3g. Crystal-rich sandstone	<p>Characteristics: Crystal-rich sand</p> <p>Description: Massive crystal-rich sandstone containing crystals of quartz, feldspar and mafic minerals with a few green, clay-altered lithic (vitric ?) clasts (<2 mm)</p> <p>Contact relations: Contacts not observed but appear to be conformable with mudstone-sandstone lithofacies</p> <p>Distribution: 930RD</p>	Terrigenous epiclastic deposit perhaps with direct or indirect volcanic input (crystal and lithic components) during reworking and resedimentation
3h. Mudstone-sandstone	<p>Characteristics: Silicified and banded</p> <p>Description: An intensely altered (silicified) and banded lithofacies; the original lithofacies may have been a fine mudstone-sandstone; bands (mm-cm scale) are irregular, wavy, discontinuous and range in color from gray to black</p> <p>Contact relations: Contacts not observed but facies appears to be conformable (banding may not be primary but an alteration feature ?)</p> <p>Distribution: 930RD</p>	Altered terrigenous epiclastic sediment; alteration suggests proximity to a hydrothermal vent as does: 1) overprinting by native sulfur which occurs in vugs throughout the unit and 2) the occurrence of a massive sulfide lens/layer (?) in the underlying crystal-rich sandstone facies
3i. Unconsolidated mo-	<p>Characteristics: Sulfate/sulfide clasts, sand to mud matrix, matrix supported, sharp contacts</p>	The sulfate, sulfide, and silica clasts indicate

Facies	Facies description	Interpretation
nomictic breccia of sulfide and sulfate clasts	<p>Description: Poorly sorted, matrix supported breccia containing subangular to angular clasts (2-7 cm) of black sulfate-sulfide (pyrite)-silica in a gray, fine sand/silt to black mud matrix</p> <p>Contact relations: Conformable and sharp contacts with enclosing sand and mud facies</p> <p>Distribution: 861GC, 871GC, and 872GC</p>	derivation from a sulfate-sulfide lens, the sand to mud matrix is representative of the enclosing sedimentary lithofacies; may be a product of mass wasting (hydrothermal eruption or earthquake triggered ?) of a sub-seafloor to seafloor sulfate deposit and mass flow transport/deposition
3j. Unconsolidated polymictic breccia of mud and volcanic clasts	<p>Characteristics: Volcanic and mudstone clasts, sand to mud matrix, matrix supported, sharp contacts</p> <p>Description: Poorly sorted, matrix supported breccia containing subangular clasts (2-7 cm) of green, indurated mudstone, dark green-black volcanic clasts and clasts of obsidian in a fine sand to mud matrix</p> <p>Contact relations: Conformable and sharp contacts with enclosing sand and mud facies</p> <p>Distribution: 871GC and 872GC</p>	The mudstone and volcanic clasts indicate sedimentary and volcanic derivation; may be a product of mass wasting (eruption or earthquake triggered ?) with transport and deposition of clasts and matrix by mass flows
3k. Unconsolidated monolithic volcanic sandstone clast breccia	<p>Characteristics: Poor sorting, crystal and lithic-rich sandstone clasts, matrix supported, sand matrix</p> <p>Description: Poorly sorted, matrix supported breccia containing angular clasts (<4 cm) of crystal-lithic-rich sandstone in a sand matrix; crystals include biotite and quartz; clasts also contain disseminated sulfate, Fe-sulfide and amorphous silica</p> <p>Contact relations: Conformable and sharp contacts with enclosing sand and mud facies</p> <p>Distribution: 872GC</p>	The crystal (and lithic ?) component of the sandstone may indicate a volcanic provenance (pyroclastic component ?); the occurrence of Fe-sulfides, sulfate and silica in the clasts and not the matrix indicates hydrothermal input to the sandstone prior to brecciation and transport; may be a product of mass wasting (eruption or earthquake triggered ?) of volcanic sandstones in proximity to or hosting a sulfate-sulfide lens with subsequent transport and deposition by mass flows

6.3. Sampling at the Panarea hydrothermal field

T. Monecke, S. Petersen, A. A. De Benedetti, A. Esposito, A. Gardeler, B. Gemmell, H. Gibson, G. He, A. Kayser, R. Kleeberg, K. Lackschewitz, K. Perrin, R. Sharpe, K. Simpson, and B. Wan

Sampling at the deeper portion of the Panarea platform involved 21 successful Rockdrill stations and 6 stations using the vibrocorer function of the Rockdrill. An additional 10 Rockdrill deployments as well as one vibrocorer station did not yield any core (Appendix A1-A3). The TV-guided grab and the gravity corer were not used at Panarea. Sampling was performed to the north of the Secca dei Panarelli, north of Lisca Bianca, and northwest of Panarelli. Drilling targets in these areas were defined on the basis of the high-resolution bathymetric survey of Esposito et al. (2006) and the seafloor observations conducted onboard R/V Poseidon cruise POS340 in 2006 (Petersen and Monecke, 2008).

A wide range of different facies were encountered in the recovered core from the Panarea platform (Table 2). In addition to detailed description, the obtained core was cut onboard R/V Meteor and representative samples were taken for clay mineral analysis, whole-rock geochemical investigations, and sample petrography (Appendix A5-A7).

Most of the drilling was conducted to the north of the Secca dei Panarelli in the area where massive sulfides were previously discovered (Marani et al., 1997). This area is typified by a number of circular craters, some of which coalesced to form an NW-trending channel (Fig. 17). A total of eight Rockdrill stations in this area yielded massive anhydrite and gypsum, with the longest continuous core being 289 cm (Fig. 18). The massive anhydrite-gypsum facies is interpreted to represent a cap forming at the interface between rising geothermal waters and seawater-saturated sediments. Seafloor observations conducted during drilling suggest that the hydrothermal facies occurs at or very close to the seafloor. In many cases, the drilling device was landed on a hard substrate with an irregular and pitted surface that may represent outcrops of this facies. However, in several cases unconsolidated mud overlying the massive anhydrite-gypsum facies was recovered by drilling. Careful drill core inspection revealed that the hydrothermal sulfates locally contain green and white clay-altered clasts that may represent intensely altered volcanic rocks. This suggests that the massive anhydrite-gypsum facies may, at least in part, have formed below the seafloor by replacement of a volcanic host rock. The presence of trace amounts of sulfides including pyrite and sphalerite suggests that the upwelling geothermal fluids at Panarea are enriched in metals. The sulfides typically occur between the anhydrite and/or gypsum crystals, or are located in vugs and fractures.

Feldspar porphyritic andesite was recognized in three holes drilled to the north of the Secca dei Panarelli (Fig. 17) suggesting that the basement is composed of coherent volcanic rocks, possibly forming lavas or high-level intrusions. One drill hole (891RD) returned intensely clay-altered, apparently coherent volcanic rocks that showed only faint plagioclase phenocrysts. Similar material was wedged into the drilling platform during station 885RD that had no recovery. A third drill hole in the area (899RD) returned several centimeters of feldspar porphyritic andesite that was overlain by unconsolidated sand.

One additional Rockdrill station (889RD) and five stations using the vibrocorer (887RDV, 890RDV, 894RDV, 900RDV, and 915RDV) recovered sedimentary and volcanoclastic facies from the working area to the north of the Secca dei Panarelli (Fig. 17). Drilling during station 889RD yielded pale to dark gray mudstone that is possibly tuffaceous. The mudstone contained minor amounts of disseminated pyrite. Vibrocoring during station 887RDV returned pumice-rich sand to pebble breccia overlying unconsolidated mud and sand. The pumiceous pyroclastic deposit is interpreted to correlate with the Pianoforte Formation of Esposito et al. (2006). Vibrocoring of station 890RDV yielded unconsolidated sand that contained abundant disseminated pyrite. Locally, pyrite-rich zones with 3-5% pyrite were observed. Subsequent vibrocoring during stations 894RDV and 900RDV returned unconsolidated sand and mud. The final vibrocoring station (915RDV) yielded 417 cm of core. A polymictic breccia with crystal-rich sandstone clasts and possibly pumice fragments occurred in the uppermost part of the core. The lower portion of the core consisted of unconsolidated sand and mud. The results of the drilling were used to construct schematic sections through the channel-like depression to the north of the Secca dei Panarelli (Figs. 19 and 20).

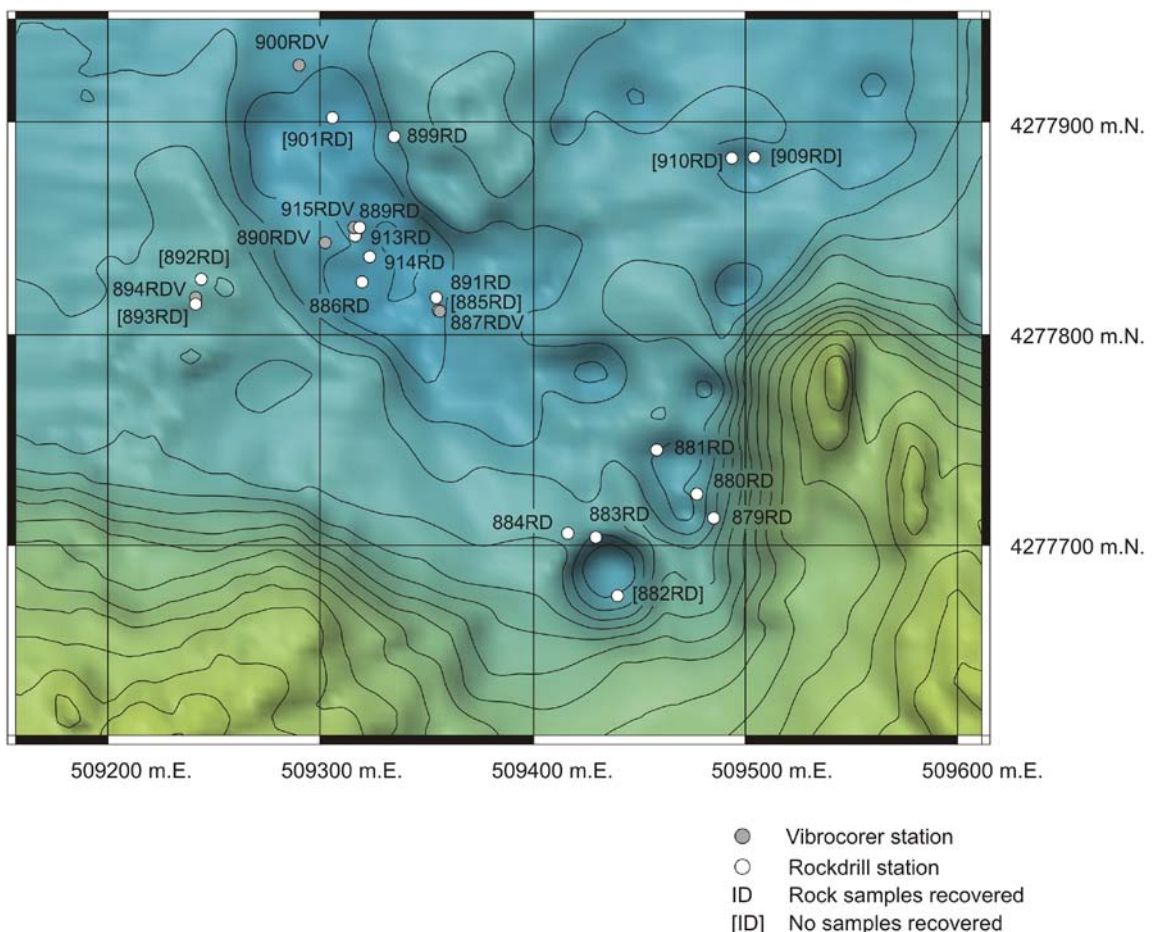


Fig. 17: Location map of station work conducted in the working area north of the Secca dei Panarelli (UTM coordinates, WGS84).



Fig. 18: Drill core 881RD consisting of massive anhydrite and gypsum. Top of the hole is located in the lower right hand corner.

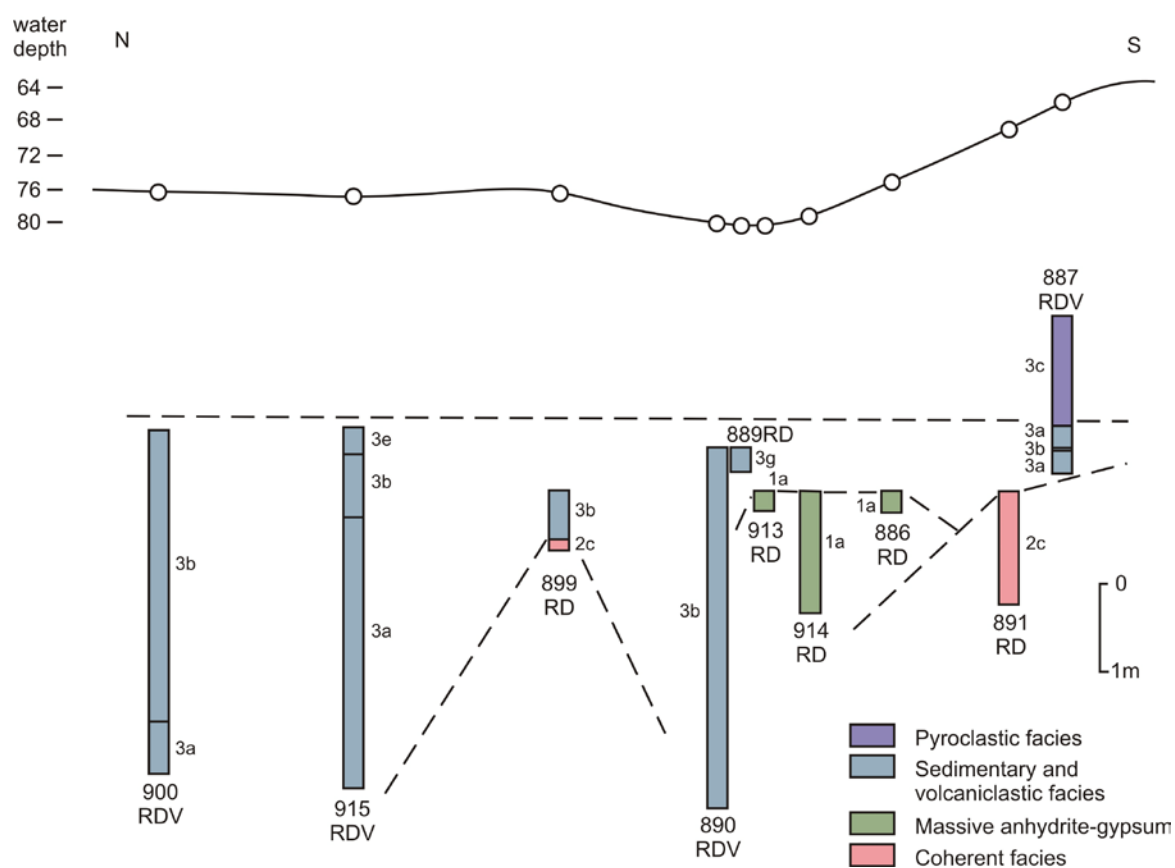


Fig. 19: Schematic N-S section through the channel-like depression to the north of the Secca dei Panarelli.

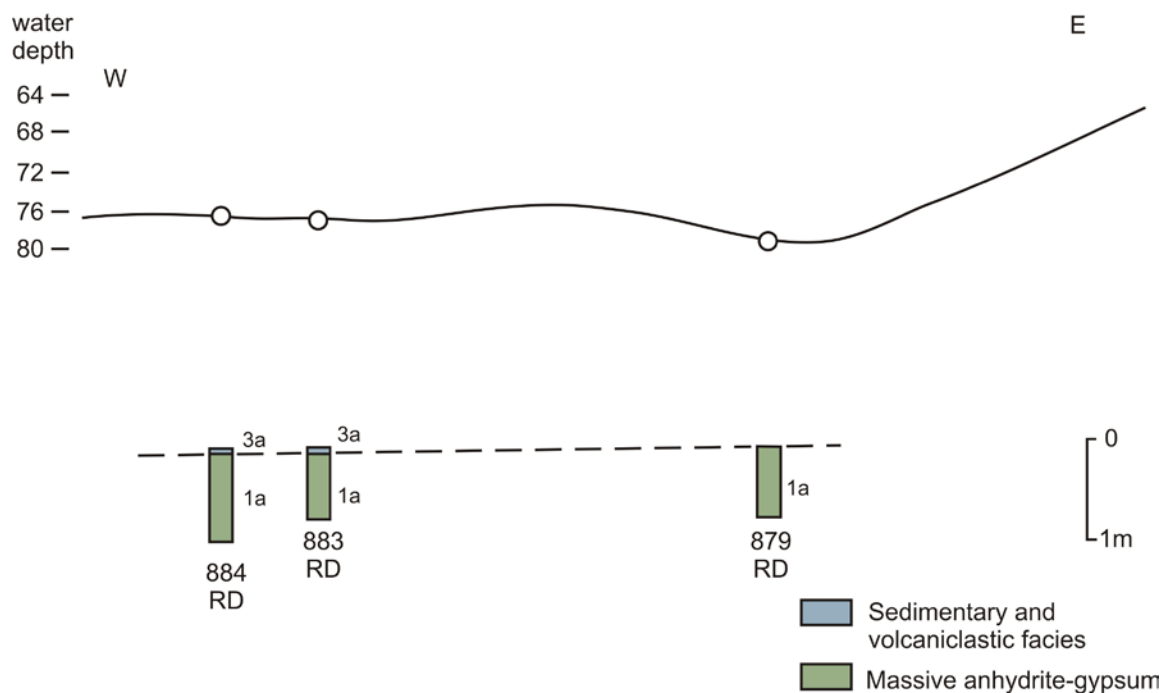


Fig. 20: Schematic W-E section through the seafloor depression north of the Secca dei Panarelli, where massive anhydrite-gypsum was recovered by shallow drilling.

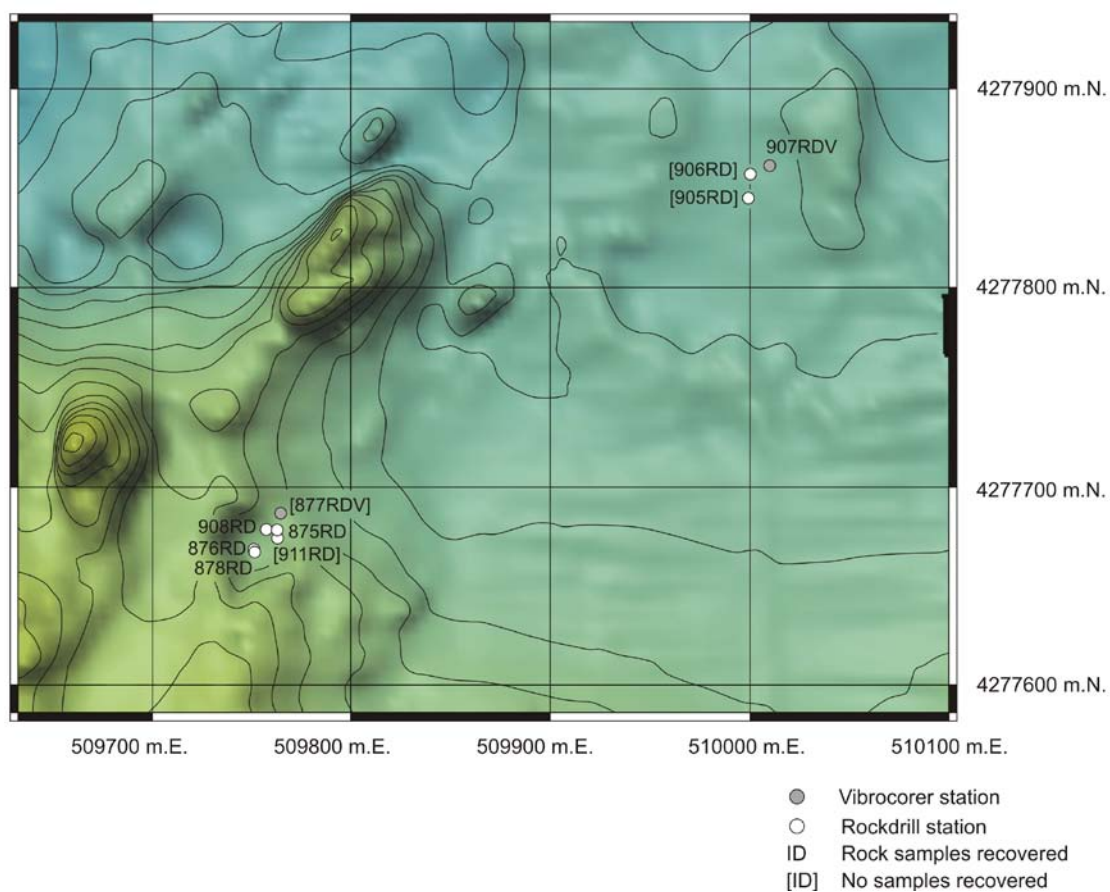


Fig. 21: Location map of station work conducted in the working area north of Lisca Bianca (UTM coordinates, WGS84).

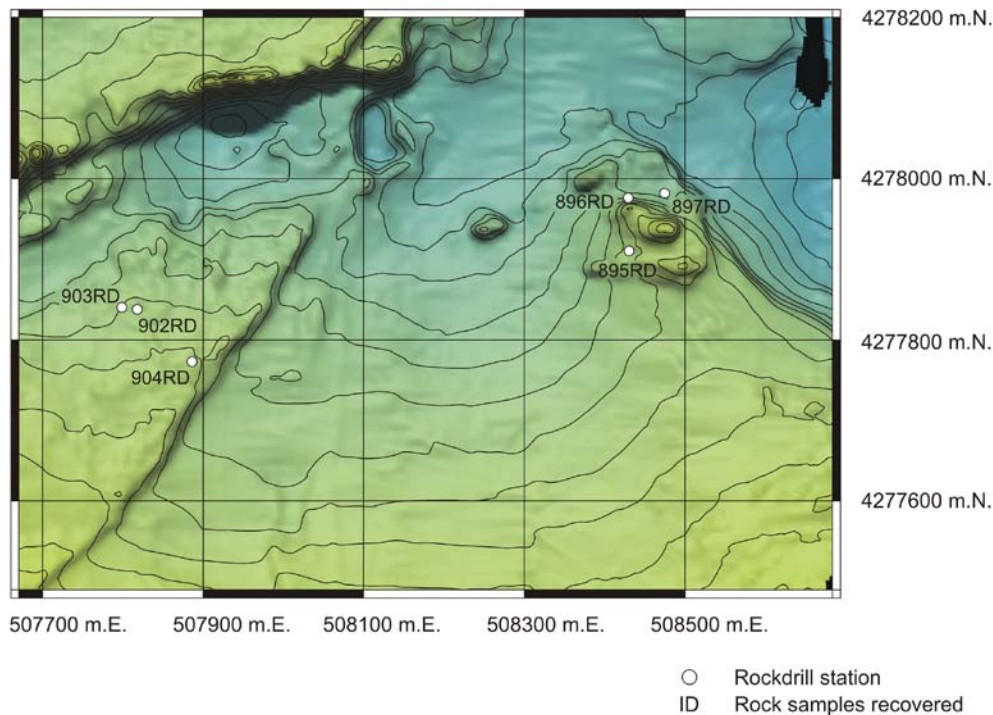


Fig. 22: Location map of station work conducted in the working area northwest of Panarelli (UTM coordinates, WGS84).

Drilling in one of the craters to the north of Lisca Bianca (Fig. 21) yielded three intersections of feldspar-olivine porphyritic andesite (875RD, 878RD, and 908RD). One additional drill hole (876RD) recovered intensely altered and silicified coherent material that may represent an altered equivalent of the same volcanic facies. In the drill core recovered from the crater, the feldspar-olivine porphyritic andesite was found to be overlain by crystal-lithic and pumice-rich sandstone to pebble conglomerate that contained abundant sulfur cementing the clastic material. The volcanic sandstone to pebble conglomerate was normally graded and contained abundant tube pumice clasts in addition to subrounded to rounded grains of quartz, feldspar, and rock fragments. No visible sulfide mineralization was found to be associated with the sulfur impregnation. Vibrocoring 907RDV in another crater located to the northeast (Fig. 21) returned unconsolidated sand with some Fe encrustations in the upper oxidized part of the core.

The flow-banded rhyolite complex to the northwest of Panarelli represented an additional target for drilling (Fig. 22). All three drilling stations (895RD, 896RD, and 897RD) were successful in recovering feldspar-amphibole porphyritic rhyolite, with the longest continuous intersection being 492 cm (896RD). The feldspar-amphibole porphyritic rhyolite was spherulitic and flow-banded. Two of the cored rhyolite intersections (895RD and 896RD) included short intervals of amphibole-biotite-feldspar porphyritic andesite. Due to the presence of chilled margins, these intersections are interpreted to represent high-level dikes or sills. However, amphibole-biotite-feldspar porphyritic andesite also forms abundant xenoliths within the coherent feldspar-amphibole porphyritic rhyolite. The observed textural relationships suggest that both lavas formed contemporaneously and that mingling of the two compositionally distinct melts may have occurred in the magma chamber or the volcanic conduit. In the third

drill core (897RD), the feldspar-amphibole porphyritic rhyolite overlies coherent feldspar porphyritic andesite that may have been emplaced as a high-level sill, dike, or flow.

Three holes (902RD, 903RD, and 904RD) were drilled to sample the Fe-oxide chimneys and mounds located on a large boulder fan to the northwest of Panarelli (Fig. 22). Positioning of the drill rig on top of the Fe-oxide structures was found to be excessively difficult and, therefore, only the underlying substrate was cored. Drilling showed that the coarse conglomerate facies is dominated by feldspar-amphibole-pyroxene porphyritic andesite boulders. The andesite commonly showed evidence for hydrothermal alteration and most boulders displayed rinds of Fe-oxides.

Table 2: Description of hydrothermal and volcanic facies recovered from the Panarea volcanic complex.

Facies	Facies description	Interpretation
1. Hydrothermal facies		
1a. Massive anhydrite-gypsum	<p>Characteristics: Anhydrite and/or gypsum, which constitute 80 to 100% of the facies</p> <p>Description: White to gray, massive, crystalline anhydrite; some intersections are brecciated or in situ brecciate; may contain distinct bladed crystals that are variably recrystallized to coarser gypsum; some intersections consist almost entirely of gypsum; fine white clay is typically a minor component (<5%) and occurs between the anhydrite and/or gypsum crystals, or in vugs; pyrite/marcasite (trace to 5%) and sphalerite (<1%) are commonly associated with the fine clay component, but also occur within vugs or within fractures; green and white clay altered “clasts”, some preserving pseudomorphs of primary amphibole (?) phenocrysts indicate that they were originally volcanic and constitute up to 20% of some intersections</p> <p>Contact relations: The upper contact between the sulfate facies and enclosing strata is not observed; however, in holes 883RD and 884RD, 2 cm and 1.5 cm of clay occurs above, but not in contact with, the sulfate facies; the lower contact is not observed, however in hole 913RD, 1 cm of pyritic clay occurs below, but not in contact with the overlying sulfate facies</p> <p>Distribution: 879RD, 880RD, 881RD, 883RD, 884RD, 886RD, 913RD, and 914RD</p>	The massive anhydrite-gypsum facies is a primary hydrothermal deposit that likely formed at and below the seafloor; where it contains abundant clay and clay-altered volcanic fragments it may have formed below the seafloor; fine clay interstitial to the anhydrite and gypsum crystals may represent fine, suspension sediment trapped during growth of a seafloor sulfate mound that was subsequently altered to clay, perhaps during the later hydrothermal event(s) responsible for the pyrite (sphalerite) mineralization
2. Coherent volcanic facies		
2a. Amphibole-biotite-feldspar porphyritic andesite	<p>Characteristics: Skeletal biotite-amphibole-feldspar porphyritic andesite</p> <p>Description: Characterized by acicular crystals of amphibole (up to 1 cm) and biotite (7 mm) forming a skeletal network for interstitial skeletal feldspar crystals that are oriented approximately perpendicular to the amphibole and biotite; minor (<1%) subhedral primary magnetite (<1 mm); vuggy texture and vesicles common; the groundmass is highly porous (vesicular ?) in 895RD and may contain miarolitic cavities; distinct chilled margins to enclosing feldspar-amphibole porphyritic rhyolite; chilled mar-</p>	Interpreted to be high-level synvolcanic dikes or sills; also occurs as xenoliths in the feldspar-amphibole porphyritic rhyolite facies; resembles Unit C of Espósito et al. (2006)

Facies	Facies description	Interpretation
	<p>gins are defined by a progressive decrease in the abundance of feldspar and a decrease in crystal size, but the skeletal forms of amphibole and biotite are maintained</p> <p>Contact relations: Sharp contacts and chilled margins with the enclosing feldspar-amphibole porphyritic rhyolite; also occurs as xenoliths in the feldspar-amphibole porphyritic rhyolite facies</p> <p>Distribution: 895RD and 896RD</p>	
2b. Feldspar-olivine porphyritic andesite	<p>Characteristics: Massive, gray to black, feldspar-olivine porphyritic andesite</p> <p>Description: Massive andesite with phenocrysts of subhedral feldspar (<3 mm, 8-10%) and lesser anhedral olivine (<2 mm, <1%) in an aphanitic, black to gray groundmass with minor crystallites; poorly vesicular (1-2 mm); rare pyrite along fractures and as disseminations</p> <p>Contact relations: Overlain by crystal-lithic and pumice-rich sandstone to pebble conglomerate pumice-rich sandstone, but actual contact not observed</p> <p>Distribution: 875RD, (876RD ?), 878RD, and 908RD</p>	Because contact relationships with enclosing units are not observed, this facies could be a flow or sill
2c. Feldspar porphyritic andesite	<p>Characteristics: Light to dark gray, feldspar porphyritic andesite</p> <p>Description: Massive andesite with subhedral to euhedral feldspar phenocrysts (<4 mm, 5-8%); may contain rare biotite and amphibole (<2 mm, <1%) phenocrysts; groundmass is aphanitic; sparsely vesicular (up to 2%)</p> <p>Contact relations: Contacts not observed but this facies is overlain by feldspar-amphibole porphyritic rhyolite in 897RD and unconsolidated sand in 899RD</p> <p>Distribution: 885RD, 891RD, 897RD, and 899RD</p>	As contacts with enclosing units are not preserved, this facies may be a lava flow or high-level intrusion
2d. Feldspar-amphibole porphyritic rhyolite	<p>Characteristics: Coherent, spherulitic, feldspar-amphibole porphyritic rhyolite that is flow banded</p> <p>Description: Characterized by feldspar (<4 mm, 10-15%) and amphibole (<5 mm, 5-8%) phenocrysts that are randomly oriented or, less commonly, aligned in an aphanitic, gray, felsic, spherulitic, massive to flow banded groundmass; may contain traces of magnetite (<1 mm); vugs and vesicles common; contains short intersections and xenoliths of amphibole-biotite-feldspar porphyritic andesite</p> <p>Contact relations: Contacts not observed, but in drill hole 897RD this facies is underlain by feldspar porphyritic andesite</p> <p>Distribution: 895RD, 896RD, and 897RD</p>	Without constraints provided by the examination of contacts with enclosing units, this facies could be a lava dome, cryptodome or high-level sill; resembles Unit B of Esposito et al. (2006), which is interpreted to be a lava dome
3. Sedimentary and volcanoclastic facies		
3a. Unconsolidated mud	<p>Characteristics: Diffusely bedded and fine-grained; in places indurated</p> <p>Description: Massive, diffusely stratified, gray-brown mud composed predominately of feldspar and quartz grains with a lesser mafic component (biotite and magnetite?), vugs and cavities common</p> <p>Contact relations: Contacts not observed</p> <p>Distribution: 883RD, 884RD, 887RDV, 900RDV, 913RD, and 915RDV</p>	Terrigenous epiclastic deposit (absence of bedding uncharacteristic of this deposit type)

Facies	Facies description	Interpretation
3b. Unconsolidated sand	<p>Characteristics: Unconsolidated, poorly stratified, and well sorted</p> <p>Description: Gray to brown, unconsolidated sand containing rounded to well-rounded grains of quartz, feldspar, and biotite; well sorted with respect to grain size; bedding not observed but occasional white clasts of pumice (<3 mm) and gray aphanitic dacite or andesite present</p> <p>Contact relations: Basal contact not observed; upper 20 cm of unit characterized by red oxidation and oxide encrustation, presumably a product of seafloor weathering</p> <p>Distribution: 887RDV, 890RDV, 894RDV, 899RD, 900RDV, 907RDV, and 915RDV</p>	Terrigenous epiclastic deposit (absence of bedding uncharacteristic of this deposit type)
3c. Pumice-rich sand to pebble breccia	<p>Characteristics: Homogeneous, white colored, and pumice-rich</p> <p>Description: Consists of white, clay altered, pumice-rich, normally graded depositional units; pumice ranges in size from 2 mm to 3 cm and occurs in a white, clay altered (ash ?) matrix; abundance and size of pumice clasts are difficult to estimate as clumps that developed in the white clay matrix during drying resemble pumice</p> <p>Contact relations: Sharp contact with overlying, gray to brown colored unconsolidated sand that also contains white pumice clasts (typically <3 mm, possible 4 cm pumice clast at the base of the overlying unconsolidated sand facies); sharp contact with underlying gray unconsolidated sand that contains a possible 3 cm thick pumice-bearing bed</p> <p>Distribution: 887RDV</p>	Homogeneous, and pumice (ash ?)-rich character suggests that this is a primary pyroclastic deposit; correlates with the Piano-forte Formation of Esposito et al. (2006)
3d. Crystal-lithic and pumice-rich sandstone to pebble conglomerate	<p>Characteristics: Yellow, sulfur- and clay-cemented, well stratified, crystal and lithic-rich, locally pumice-rich</p> <p>Description: Well stratified, yellow, sulfur and clay cemented, intercalated, normally graded, volcanic sandstone to fine pebble conglomerate; sandstone in places contains up to 20-30% fine, white to clear clasts of tube pumice, and subrounded to rounded grains of quartz, feldspar and rock fragments; pebble conglomerate contains 1 to 2.5 cm, tube pumice clasts and rock fragments; 5-10% of matrix is clay and sulfur with another 5-10% being open void space. Sulfur lined vugs and cavities are common; no visible sulfide mineralization</p> <p>Contact relations: Upper contact not observed; actual lower contact not observed, but facies overlies coherent feldspar-olivine porphyritic andesite in all drill holes recovered</p> <p>Distribution: 875RD, 878RD, and 908RD</p>	The tube pumice is indicative of pyroclastic fragmentation and its occurrence with detrital feldspar, quartz and rock fragments suggests that this facies is a reworked and redeposited volcanoclastic deposit
3e. Polymictic breccia with crystal-rich sandstone clasts	<p>Characteristics: Polymictic clasts in a sand matrix</p> <p>Description: Polymictic breccia with subangular to subrounded clasts that are up to 10 cm in size; clasts of the crystal-lithic and pumice-rich sandstone to pebble conglomerate facies, possibly some pumice clasts, and other unidentified clast types; clasts are commonly sulfur cemented; matrix consists of sand</p> <p>Contact relations: Diffuse lower contacts with unconsolidated sand facies</p>	The presence of crystal-rich sandstone clasts and pumice clasts suggests that this facies was derived through reworking and resedimentation of sedimentary and volcanoclastic facies

Facies	Facies description	Interpretation
	Distribution: 915RDV	
3f. Coarse conglomerate	<p>Characteristics: Dominantly monolithic, boulder conglomerate, and clasts of gray, feldspar-amphibole-pyroxene porphyritic andesite</p> <p>Description: Dominantly monolithic, boulder conglomerate containing rounded clasts of feldspar-amphibole-pyroxene porphyritic andesite with lesser clasts of a feldspar-amphibole-biotite porphyritic andesite, and a feldspar-amphibole-quartz porphyritic volcanic rock; clasts range in size from 5-30 cm; feldspar-amphibole-pyroxene porphyritic andesite contains euhedral feldspar phenocrysts (1-7 mm, 2-10%), euhedral amphibole phenocrysts (1-4 mm, <5%), and euhedral pyroxene phenocrysts (1-2 mm, 1%) in a gray, aphanitic matrix with patchy limonite/hematite alteration; irregular vugs and round to angular 0.5-1 mm large vesicles in feldspar-amphibole-pyroxene porphyritic andesite are commonly lined with Fe-oxides or greenish clay; feldspars are partially altered to clay; Fe-oxide crusts on some boulders</p> <p>Contact relations: Contacts not observed</p> <p>Distribution: 902RD, 903RD, and 904RD</p>	The monolithic character suggests derivation from a single provenance, perhaps through mass wasting and collapse of an andesitic edifice; clast rounding suggests considerable transport and/or reworking in the marine environment; Fe-oxide crusts are consistent with seafloor weathering; resembles Unit Ab of Esposito et al. (2006)
3g. Mudstone	<p>Characteristics: Pale to dark gray mudstone</p> <p>Description: Massive, diffusely stratified, pale to dark gray mudstone composed of quartz and feldspar grains, possibly tuffaceous; contains traces of pyrite</p> <p>Contact relations: No contacts observed</p> <p>Distribution: 889RD</p>	Terrigenous epiclastic deposit (absence of bedding uncharacteristic of this deposit type)

6.4. Sampling at the Marsili volcanic complex

T. Monecke, S. Petersen, A. A. De Benedetti, A. Esposito, A. Gardeler, B. Gemmell, H. Gibson, G. He, A. Kayser, R. Kleeberg, K. Lackschewitz, K. Perrin, R. Sharpe, K. Simpson, and B. Wan

The sampling program at the Marsili volcanic complex included four Rockdrill stations and two TV-guided grab stations (Appendix A1). Drilling in the northern target area at the Marsili volcanic complex (Fig. 23) was comparably difficult due to the steep terrain. The first station (917RD) did not yield any core, although some Fe-oxide material was wedged into the drilling platform. Two additional Rockdrill stations (918RD and 920RD) and a subsequent TV-guided grab station (919TVG) in the same target area were successful. No sample material was recovered during two stations (921RD and 922TVG) targeted to sample volcanic rocks in the southern working area (Fig. 23).

Material recovered from the volcanic edifice in the north included Fe-oxide crusts and coherent feldspar-olivine porphyritic andesite (Fig. 24). Seafloor observations conducted during drilling (Appendix A2) suggest that the recovered Fe-oxide crusts form part of the chimney-like structures noted during previous ROV diving (Petersen and Monecke, 2008). The coherent feldspar-olivine porphyritic andesite forms the substrate below these delicate Fe-oxide structures and locally shows evidence for low-temperature hydrothermal alteration. The facies characteristics of the recovered

hydrothermal precipitates and the coherent volcanic rocks are summarized in Table 3. Representative samples were selected for geochemical analysis (Appendix A6).

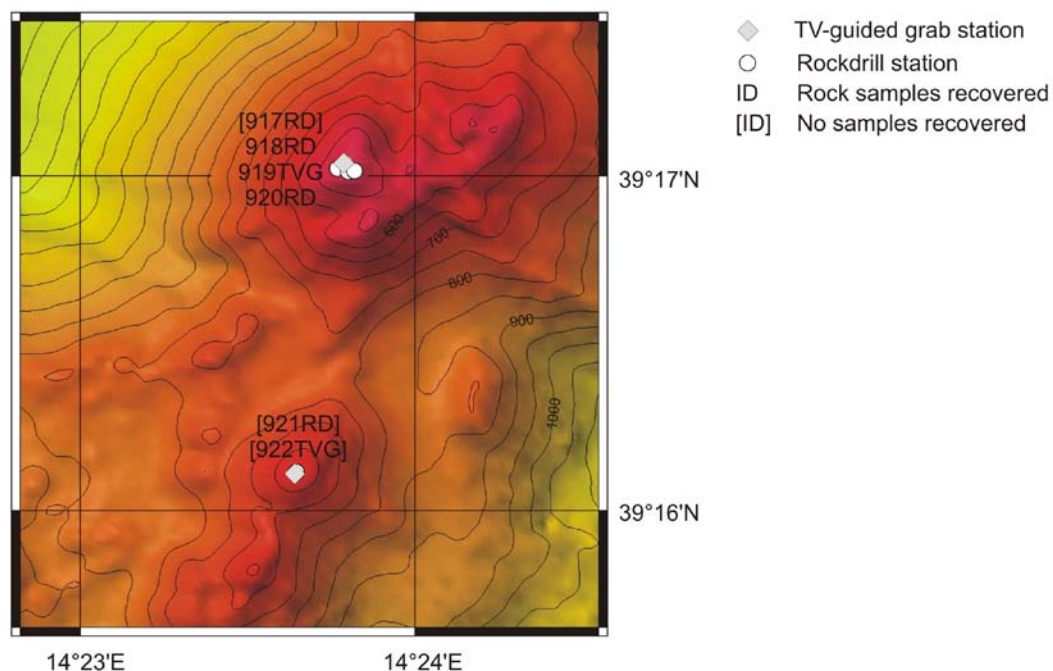


Fig. 23: Location map of station work conducted at the Marsili volcanic complex.

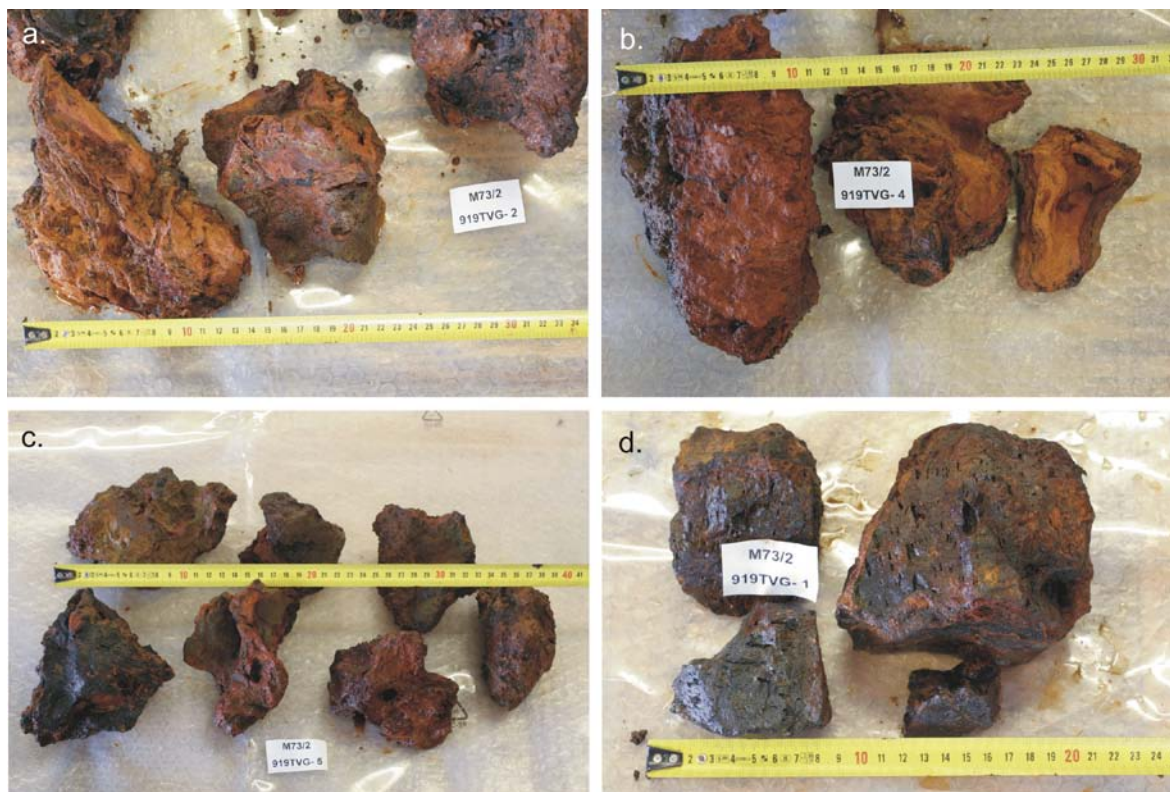


Fig. 24: Representative hand specimens recovered from the Marsili volcanic complex (919TVG): a-c. Fe-oxide crusts. d. Vesicular feldspar-olivine porphyritic andesite.

Table 3: Description of hydrothermal and volcanic facies recovered from the Marsili volcanic complex.

Facies	Facies description	Interpretation
1. Hydrothermal facies		
1a. Fe-oxide crust	<p>Characteristics: Earthy, reddish brown and black color, layered, and poorly consolidated Fe crust</p> <p>Description: Consists of predominately red to reddish brown layers (Fe-rich) with subordinate black layers (Mn-rich); consist predominately of mud-sized material; sand- and granule-sized clasts of volcanic rock fragments and crystals occur; crumbles to the touch; extremely friable</p> <p>Contact relations: Forms at the seafloor</p> <p>Distribution: 917RD and 919TVG</p>	Low-temperature hydrothermal deposit on the seafloor
2. Coherent volcanic facies		
2a. Feldspar-olivine porphyritic andesite	<p>Characteristics: Feldspar-olivine porphyritic and vesicular andesite</p> <p>Description: Black, sparsely feldspar (<5%, <2.5 mm) and olivine (<1%, <1 mm) porphyritic, vesicular (<10%) andesite; microlites in groundmass and magnetic; black groundmass; vesicle elongation defines a flow foliation; thin silica lining to some vesicles</p> <p>Contact relations: Not observed</p> <p>Distribution: 918RD, 919TVG, and 920RD</p>	Occurrence in the near surface environment suggests that unit is a flow; but could also be a high level sill or dike

6.5. Pore water chemistry

N. Kummer and M. Peters

Extraction of pore water from sediment cores obtained by gravity coring and vibrocoring was conducted immediately following retrieval. A sampling interval of 20 cm was used. Initially, small holes were drilled in the core liner to extract pore water from each hole using Rhizon soil moisture samplers (Fig. 25). These samplers consisted of a small microporous polymer tube (0.1 μm pore size) that was supported by a stabilizing glass fiber wire and connected to a PVC tube. The pore water was recovered using negative pressure produced by the attached 10 ml syringes (Luer-Lock connection). Because of the low dead volume (<0.5 ml), even small volumes of pore water could be sampled. The applied method permitted extraction of the pore water without disturbance of the sediment. Contact of the pore water samples with oxygen in the ambient air was minimized by connecting the Rhizon soil moisture samplers with the syringes.

Subsequently, the pore water samples were analyzed for their pH, redox potential, and electrical conductivity (Appendix A8). In addition, aliquots of pore water were filled in 2 ml vials to determine the concentration of cations (Na, K, Mg, and Ca), anions (F, Cl, Br, NO_3 , PO_4 , and SO_4) and trace elements on-shore and to allow future speciation experiments (As, S, B, and P). The samples taken for ICP-MS analysis and ion chromatography were acidified with HNO_3 , whereas aliquots collected for speciation analysis were frozen with liquid nitrogen immediately after sampling. To avoid contact with the ambient air and the oxidation of reduced species, all vials were flushed with nitrogen prior to the filling with pore water. In total, 11 cores (5 gravity cores and 6 vibrocores) from Palinuro and Panarea were sampled, totaling about 120 pore water samples (Appendix A8).

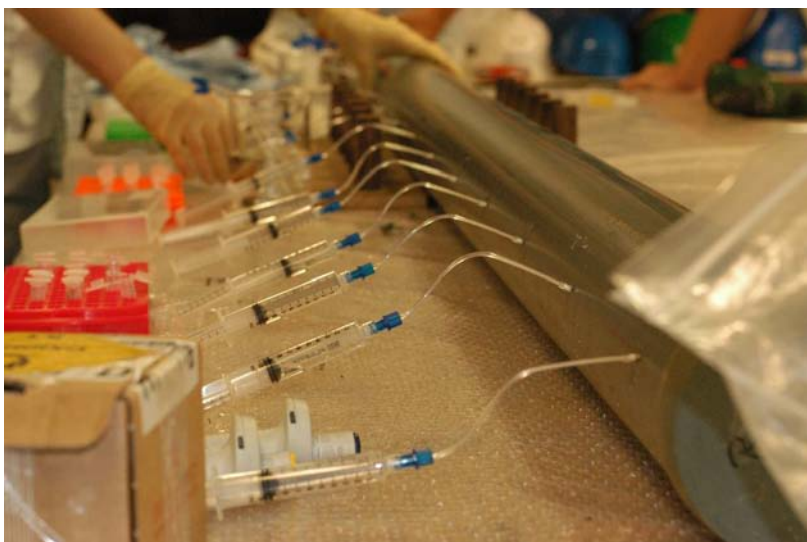


Fig. 25: Sampling of pore water from a gravity core.

6.6. Sulfur geochemistry

M. Peters

Laboratory work conducted during the cruise concentrated on two different aspects, namely the measurement of the dissolved sulfide concentrations in pore water sampled from sediment cores (gravity corer and vibrocorer) and the fixation of liquid and solid samples for on-shore analysis to prevent oxidation of reduced sulfur species during sample handling and transport (Appendix A9).

The pore water samples collected for sulfur geochemical investigations were obtained using the method described above. The concentration of dissolved sulfide was determined in aliquots of 1 ml. A zinc acetate gelatin solution was added to the sample, resulting in the precipitation of zinc sulfide in a colloidal state. Subsequently, the color agent N,N-dimethyl-1,4-phenylenediamine-dihydrochloride and an iron chloride solution were added, the latter being a catalyst for the formation of methylene blue. After one hour, the solutions were measured photometrically at a wavelength of 660 nm. A calibration curve was constructed using calibration solutions of different sulfide concentration. These calibration solutions were obtained from a fresh stock solution with a sulfide concentration of 5.8 mmol/L. The exact sulfide concentration of the stock solution was determined by titration with a 0.02 N thiosulfate solution.

The monobromobimane method (Fahey and Newton, 1987) was used to stabilize dissolved sulfide and thiols (i.e., intermediate sulfur species like sulfite or thiosulfate) in 50 µl aliquots of the pore water samples. This procedure will permit on-shore quantification of the different sulfur-bearing compounds dissolved in the hydrothermal fluids, including metastable phases that are of metabolic relevance for certain microorganisms. These stabilized solutions will also be used to separate the different sulfur compounds for sulfur isotopic measurements (development of method currently in progress). On-shore analysis of the stabilized solutions will be performed in cooperation with Dr. Christian Ostertag-Henning at BGR, Hannover.

Following the pore water sampling, the core liners were cut open to collect sediment samples from each core. All samples were frozen for further on-shore analysis. Isotopic analysis of the sediment samples will be conducted at the University of Münster.

6.7. Microbiology

M. Hügler, J. Küver, A. Gärtner, and F. Lappe

Microbiological investigations on sample material recovered from the three study sites visited during R/V Meteor cruise M73/2 will allow, for the first time, a comprehensive characterization of the microbiological communities associated with submarine hydrothermal venting in the Tyrrhenian Sea. The research aims to analyze the community structures of archaea and bacteria and will determine the metabolic potential of the microorganisms, with special emphasis on the sulfur and carbon metabolism. The work program will involve culturing of microorganisms adapted to the hydrothermal environments and the isolation of bacteria producing possible new biologically active compounds that have antibacterial, antiviral, antifungal, or other properties.

Samples collected for the microbiological investigations included surface seawater as well as sediment recovered by gravity coring, vibrocoring, and TV-guided grab sampling. In addition to sediments, several rock samples were collected (Appendix A10). Following sampling, the seawater was filtered (0.2 µm pore size) and the filters were then stored for analysis of the microorganisms. The sediment cores were initially cut in half, and samples were taken at different depths (Appendix A10). Samples collected from the sediment cores and taken from the material recovered by TV-guided grabbing were prepared for DNA and FISH analyses. The samples (up to 40 ml) collected for DNA analysis were stored at -80°C. The preparation of samples for FISH analysis involved the fixation of ca. 1-2 ml of sediment with 3 ml 1:10 solution of 37% formaldehyde. After a fixation time of 24 hours, the samples were centrifuged and washed with 3 ml of phosphate buffered saline (PBS). The material was then stored in a 1:1 mixture of ethanol and PBS at -20°C. In addition to onboard cultivation efforts, subsamples were preserved in 20% DMSO as well as in 20% glycerol for on-shore cultivation experiments.

The most promising material was recovered by TV-grab station 866TVG at the Palinuro volcanic complex. After retrieving, a maximum temperature of 60°C was measured in the sediment that emanated a strong H₂S smell. The grab contained several shrimps (Fig. 26). Since grab sampling was conducted in proximity to the tube worm colony observed in 2006 (Petersen and Monecke, 2008), it is likely that the shrimps and the tube worms form part of a specialized vent fauna. This would be the first vent fauna reported in the Mediterranean and the first occurrence of vent-specific tube worms outside the Pacific. The onboard culturing experiments for thermophilic sulfur oxidizing bacteria in the material from Palinuro were promising (Fig. 27). These bacteria were also enriched in the samples from Panarea.



Fig. 26: Image of a shrimp recovered from the Palinuro volcanic complex.

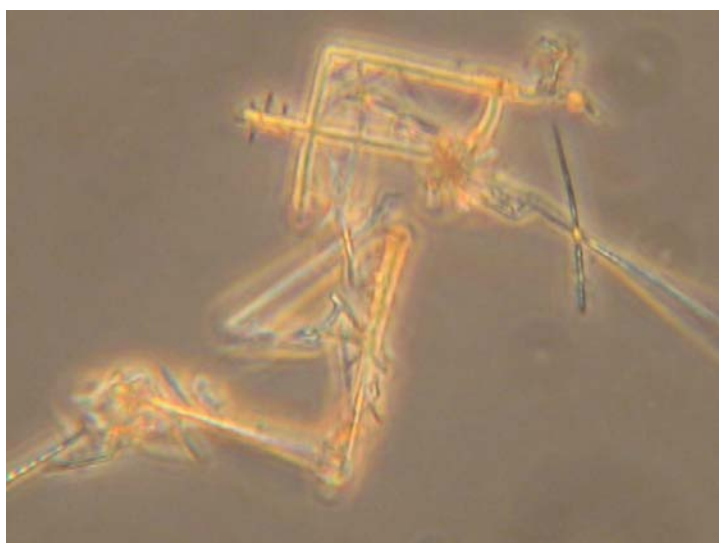


Fig. 27: Microscopic picture of an enrichment culture of sulfur oxidizing bacteria from the Palinuro volcanic complex showing crystals and bacterial filaments.

7. References

- Anzidei M, Esposito A, Bortoluzzi G, De Giosa F (2005) The high resolution bathymetric map of the exhalative area of Panarea. *Annals Geophys* 48: 899-921.
- Beccaluva L, Gabbianelli G, Lucchini F, Rossi PL, Savelli C (1985) Petrology and K/Ar ages of volcanics dredged from the Eolian seamounts: implications for geodynamic evolution of the southern Tyrrhenian basin. *Earth Planet Sci Lett* 74: 187-208.
- Brusilovskiy YV, Gorodnitskiy AM (1990) Evolution of basaltic volcanic activity and development of seamounts in the Tyrrhenian Basin as indicated by geomagnetic data. *Geotectonics* 24: 350-358.
- Butterfield DA, Massoth GJ, McDuff RE, Lupton JE, Lilley MD (1990) Geochemistry of hydrothermal fluids from Axial Seamount hydrothermal emission study vent field, Juan de Fuca Ridge: seafloor boiling and subsequent fluid-rock interaction. *J Geophys Res* 95: 12895-12921.
- Caliro S, Caracausi A, Chiodini G, Ditta M, Italiano F, Longo M, Minopoli C, Nuccio PM, Paonita A, Rizzo A (2004) Evidence of a recent input of magmatic gases into the quiescent volcanic edifice of Panarea, Aeolian islands, Italy. *Geophys Res Lett* 31: L07619.
- Calanchi N, Tranne CA, Lucchini F, Rossi PL, Villa IM (1999) Explanatory notes to the geological map (1:10,000) of Panarea and Basiluzzo islands (Aeolian arc, Italy). *Acta Vulcanol* 11: 223-243.
- Caracausi A, Ditta M, Italiano F, Longo M, Nuccio PM, Paonita A, Rizzo A (2005) Changes in fluid geochemistry and physico-chemical conditions of geothermal systems caused by magmatic input: The recent abrupt outgassing off the island of Panarea (Aeolian islands, Italy). *Geochim Cosmochim Acta* 69: 3045-3059.
- Colantoni P, Lucchini F, Rossi PL, Sartori R, Savelli C (1981) The Palinuro volcano and magmatism of the southeastern Tyrrhenian Sea (Mediterranean). *Marine Geol* 39: 1-12.
- Cressie NAC (1991) *Statistics for spatial data*. Wiley, New York, 900 p.
- Dekov VM, Savelli C (2004) Hydrothermal activity in the SE Tyrrhenian Sea: An overview of 30 years of research. *Marine Geol* 204: 161-185.
- de Ronde CEJ, Baker ET, Massoth GJ, Lupton JE, Wright IC, Feely RA, Greene RR (2001) Intra-oceanic subduction-related hydrothermal venting, Kermadec volcanic arc, New Zealand. *Earth Planet Sci Lett* 193: 359-369.
- de Ronde CEJ, Faure K, Bray CJ, Chappell DA, Wright IC (2003) Hydrothermal fluids associated with seafloor mineralization at two southern Kermadec arc volcanoes, offshore New Zealand. *Mineral Deposita* 38: 217-233.
- de Ronde CEJ, Hannington MD, Stoffers P, Wright IC, Ditchburn RG, Reyes AG, Baker ET, Massoth GJ, Lupton JE, Walker SL, Greene RR, Soong CWR, Ishibashi J, Lebon GT, Bray CJ, Resing JA (2005) Evolution of a submarine magmatic-hydrothermal system: Brothers Volcano, southern Kermadec arc, New Zealand. *Econ Geol* 100: 1097-1133.
- de Ronde CEJ, Baker ET, Massoth GJ, Lupton JE, Wright IC, Sparks RJ, Bannister SC, Reyners ME, Walker SL, Greene RR, Ishibashi J, Faure K, Resing JA, Lebon GT (2007) Submarine hydrothermal activity along the mid-Kermadec Arc, New Zealand: Large-scale effects on venting. *Geochem Geophys Geosys* 8: Q07007.
- Drummond SE, Ohmoto H (1985) Chemical evolution and mineral deposition in boiling hydrothermal systems. *Econ Geol* 80: 126-147.

- Eckhardt JD, Glasby GP, Puchelt H, Berner Z (1997) Hydrothermal manganese crusts from Enarete and Palinuro Seamounts in the Tyrrhenian Sea. *Marine Georesour Geotechnol* 15: 175-208.
- Embley RW, Baker ET, Chadwick WW, Jr., Lupton JE, Resing JA, Massoth GL, Nakamura K (2004) Explorations of Mariana arc volcanoes reveal new hydrothermal systems. *EOS Trans Amer Geophys Union* 85: 37-44.
- Esposito A, Giordano G, Anzidei M (2006) The 2002-2003 submarine gas eruption at Panarea volcano (Aeolian islands, Italy): Volcanology of the seafloor and implications for the hazard scenario. *Marine Geol* 227: 119-134.
- Fabbri A, Marabini F, Rossi S (1973) Lineamenti geomorfologici del Monte Palinuro e del Monte delle Baronie. *Giorn Geol* 29: 133-156.
- Faggioni O, Pinna E, Savelli C, Schreider AA (1995) Geomagnetism and age study of Tyrrhenian seamounts. *Geophys J Int* 123: 915-930.
- Fahey RC, Newton GL (1987) Determination of low-molecular-weight thiols using monobromobimane fluorescent labeling and high-performance liquid chromatography. *Methods Enzymol* 143: 85-96.
- Favalli M, Karátson D, Mazzuoli R, Pareschi MT, Ventura G (2005) Volcanic geomorphology and tectonics of the Aeolian archipelago (Southern Italy) based on integrated DEM data. *Bull Volcanol* 68: 157-170.
- Fouquet Y, von Stackelberg U, Charlou JL, Erzinger J, Herzig PM, Mühle R, Wiedicke M (1993) Metallogenesis in back-arc environments: The Lau basin example. *Econ Geol* 88: 2154-2181.
- Gabbianelli G, Gillot PY, Lanzafame G, Romagnoli C, Rossi PL (1990) Tectonic and volcanic evolution of Panarea (Aeolian islands, Italy). *Marine Geol* 92: 313-326.
- Gamberi F, Marani MP, Parr JM, Binns RA (1999) Sub-seafloor mineralisation at the Panarea shallow-water platform, Aeolian volcanic arc, Italy. In: CJ Stanley et al. (eds) *Mineral deposits: processes to processing*. Balkema, Rotterdam, pp 499-502.
- Gamo T, Okamura K, Charlou JL, Urabe T, Auzende JM, Ishibashi J, Shitashima K, Chiba H, Binns R, Gena K, Henry K, Matsubayashi O, Matsumoto T, Moss R, Nagaya Y, Naka J, Ruellan E (1997) Acid and sulfate-rich hydrothermal fluids from the Manus back-arc basin, Papua New Guinea. *Geology* 25: 139-142.
- Giggenbach WF (1992) Magma degassing and mineral deposition in hydrothermal systems along convergent plate boundaries. *Econ Geol* 87: 1927-1944.
- Hannington MD, Poulsen KH, Thompson JFH, Sillitoe RH (1999) Volcanogenic gold in the massive sulfide environment. *Rev Econ Geol* 8: 325-356.
- Hannington MD, de Ronde CEJ, Petersen S (2005) Sea-floor tectonics and submarine hydrothermal systems In: JW Hedenquist et al. (eds) *Economic geology 100th anniversary volume*. Society of Economic Geologists, Littleton, pp 111-141.
- Herzig PM, Hannington MD, Arribas A (1998) Sulfur isotopic composition of hydrothermal precipitates from the Lau back-arc: Implications for magmatic contributions to seafloor hydrothermal systems. *Mineral Deposita* 33: 226-237.
- Isaaks EH, Srivastava RM (1989) *Applied geostatistics*. Oxford University Press, New York, 561 p.
- Kidd RB, Ármannson H (1979) Manganese and iron micronodules from a volcanic seamount in the Tyrrhenian Sea. *J Geol Soc London* 136: 71-76.
- Marani MP, Trua T (2002) Thermal constriction and slab tearing at the origin of a superinflated spreading ridge: Marsili volcano (Tyrrhenian Sea). *J Geophys Res* 107: 2188.
- Marani MP, Gamberi F, Savelli C (1997) Shallow-water polymetallic sulfide deposits in the Aeolian island arc. *Geology* 25: 815-818.

- Marani MP, Gamberi F, Casoni L, Carrara G, Landuzzi V, Musacchio M, Penitenti D, Rossi L, Trua T (1999) New rock and hydrothermal samples from the southern Tyrrhenian Sea: The MAR-98 research cruise. *Giorn Geol* 61: 3-24.
- Minniti M, Bonavia FF (1984) Copper-ore grade hydrothermal mineralization discovered in a seamount in the Tyrrhenian Sea (Mediterranean): Is the mineralization related to porphyry-coppers or base metal lodes? *Marine Geol* 59: 271-282.
- Minniti M, Bonavia FF, Dacquino C, Raspa G (1986) Distribution of Mn, Fe, Ni, Co, and Cu in young sediments on the Palinuro Seamount in the southeast Tyrrhenian Sea (Mediterranean). *Marine Mining* 5: 277-305.
- Morelli C, Giese P, Cassinis R, Colombi B, Guerra I, Luongo G, Scarascia S, Schutte KG (1975) Crustal structure of Southern Italy. A seismic refraction profile between Puglia, Calabria, Sicily. *Boll Geofis Teor Appl* 17: 183-210.
- Petersen S, Monecke T (2008) R/V Poseidon Cruise Report P340. Report of the Leibniz-Institute of Marine Sciences at the Christian Albrechts University Kiel 21, 77 p.
- Perfit MR, Davidson JP (2000) Plate tectonics and volcanism In: H Sigurdsson et al. (eds) *Encyclopedia of volcanoes*. Academic Press, San Diego, pp. 89-113.
- Puchelt H, Laschek D (1986) *Fahrtbericht der Forschungsfahrt Sonne 41 HYMAS I (18.1.1986-28.4.1986)*. Universität Karlsruhe, 331 p.
- Resing JA, Lebon G, Baker ET, Lupton JE, Embley RW, Massoth GJ, Chadwick WW, Jr., de Ronde CEJ (2007) Venting of acid-sulfate fluids in a high-sulfidation setting at NW Rota-1 submarine volcano on the Mariana arc. *Econ Geol* 102: 1047-1061.
- Savelli C (1988) Late Oligocene to recent episodes of magmatism in and around the Tyrrhenian Sea: implications for the processes of opening in a young inter-arc basin of intra-orogenic (Mediterranean) type. *Tectonophysics* 146: 163-181.
- Savelli C (1992) Il rifting del vulcano Marsili (Mar Tirreno): Aspetti morfo-tettonici osservati da bordo del sottomarino "MIR 2". *Giorn Geol* 54: 215-227.
- Savelli C (2001) Two-stage progression of volcanism (8–0 Ma) in the central Mediterranean (southern Italy). *J Geodynamics* 31: 393–410.
- Savelli C, Schreider AA (1991) The opening processes in the deep Tyrrhenian basins of Marsili and Vavilov, as deduced from magnetic and chronological evidence of their igneous crusts. *Tectonophysics* 190: 119-131.
- Savelli C, Marani M, Gamberi F (1999) Geochemistry of metalliferous, hydrothermal deposits in the Aeolian arc (Tyrrhenian Sea). *J Volcanol Geotherm Res* 88: 305-323.
- Sborshchikov IM, Savelli C, Dukov N (1989) Side-scan sonar survey on the summit of Marsili volcano: rifting morphology of an active axial zone in the Tyrrhenian Sea. *Giorn Geol* 51: 109-116.
- Sborshchikov IM, Al'mukhamedov AI (1992) Submarine volcanoes of the Tyrrhenian Sea - Testaments to the opening of a backarc basin. *Int Geol Rev* 34: 166-177.
- Selli R, Lucchini F, Rossi PL, Savelli C, Del Monte M (1977) Dati geologici, petrochimici e radiometrici sui vulcani centro-tirrenici. *Giorn Geol* 42: 221-246.
- Stoffers P, Worthington TJ, Schwarz-Schampera U, Hannington MD, Massoth GJ, Hekinian R, Schmidt M, Lundsten LJ, Evans LJ, Vaiomo'unga R, Kerby T (2006) Submarine volcanoes and high-temperature hydrothermal venting on the Tonga arc, southwest Pacific. *Geology* 34: 453-456.
- Stüben D, Sedwick P, Savelli C, Ferretti E, Shipboard Scientific Party (1993) Cruise report Poseidon 200-4 MIPAMEHR-MAST 1 - Investigations on hydrothermalism in the Tyrrhenian and Aeolian Sea. *Berichte - Geologisch-Paläontologisches Institut der Universität Kiel* 69, 91 p.

- Trua T, Serri G, Marani M, Renzulli A, Gamberi F (2002) Volcanological and petrological evolution of Marsili Seamount (southern Tyrrhenian Sea). *J Volcanol Geotherm Res* 114: 441-464.
- Tufar W (1991) Paragenesis of complex massive sulfide ores from the Tyrrhenian Sea. *Mitt Österr Geol Ges* 84: 265-300.
- Uchupi E, Ballard RD (1989) Evidence of hydrothermal activity on Marsili Seamount, Tyrrhenian Basin. *Deep-Sea Res* 36: 1443-1448.
- Yevsyukov YD (1994) Morphology of Palinuro and Poseidon Seamounts (southeastern Tyrrhenian Sea). *Oceanology* 34: 415-420.

Appendices

A1. Station list

All coordinates, unless stated otherwise, are those of the Posidonia subpositioning system mounted on the instrument (Rockdrill) or on the cable (50 m above the instrument for gravity corer and TV-guided grab). Water depth is measured by the Kongsberg EM120 system. All data refer to the position and water depth of the respective station measured between bottom contact of the instrument and the start of the final heaving. Abbreviations: SP = Sound velocity profile. SB = Multibeam survey. RD = Rockdrill. RDV = Rockdrill vibrocorer. TVG = TV-guided grab. GC = Gravity corer.

Station	Date and Time (UTC)	Latitude	Longitude	Water depth (m)	Description
Palinuro					
849SP	15.08.07-16.08.07 (23:23-00:34)	39°34.00'N	14°38.00'E	1732	Sound velocity profile Cable length: 1600 m
850SB	16.08.07 (01:14-06:28)	39°33.97'N 39°32.39'N 39°32.28'N 39°31.63'N 39°31.66'N 39°33.00'N 39°32.93'N 39°32.00'N 39°31.99'N 39°32.60'N 39°32.66'N	14°38.01'E 14°38.10'E 14°45.08'E 14°44.83'E 14°37.66'E 14°37.58'E 14°45.39'E 14°45.37'E 14°37.13'E 14°37.01'E 14°46.18'E	1715 1390 1223 1004 1511 1463 1396 1211 1624 1636 1387	Multibeam survey
851RD	16.08.07 (07:17-09:59)	39°32.429'N	14°42.383'E	627	Cable length: 641 m Inclination: 19.7° Penetration: 230 cm Recovery: 135 cm Dark vuggy sulfate with black inclusions; vuggy sulfate-sulfide; vuggy sulfide-sulfate; massive sulfate; massive sulfide
852RD	16.08.07 (10:53-13:46)	39°32.441'N	14°42.381'E	626	Cable length: 632 m Inclination: 7.1° Penetration: 502 cm Recovery: 96 cm Sandstone-siltstone, polymictic breccia with pumice clasts; polymictic breccia with white and black clasts; massive sulfate; vuggy sulfate-sulfide
853RD	16.08.07 (14:23-16:16)	39°32.439'N	14°42.403'E	623	Cable length: 635 m Inclination: 8.0° Penetration: 502 cm Recovery: 34 cm Dark vuggy sulfate with black inclusions
854RD	16.08.07 (16:32-19:37)	39°32.423'N	14°42.390'E	626	Cable length: 644 m Inclination: 14.3° Penetration: 451 cm Recovery: no recovery

Station	Date and Time (UTC)	Latitude	Longitude	Water depth (m)	Description
855RD	16.08.07 (19:48-21:11)	39°32.429'N	14°42.366'E	620	Cable length: 636 m Inclination: 11.9° Penetration: 502 cm Recovery: 56 cm Sandstone-siltstone; polymictic breccia with pumice clasts
856SB	16.08.07 (21:13-23:06)	39°32.46'N 39°31.24'N 39°31.32'N 39°31.33'N	14°42.35'E 14°37.14'E 14°37.84'E 14°45.73'E	614 1650 1331 1029	Multibeam survey
857RD	17.08.07 (11:50-13:27)	39°32.430'N	14°42.392'E	615	Cable length: 641 m Inclination: 12.6° Penetration: 502 cm Recovery: 47 cm Polymictic breccia with pumice clasts; vuggy sulfate-sulfide
858RD	17.08.07 (14:13-15:39)	39°32.446'N	14°42.393'E	611	Cable length: 643 m Inclination: 11.5° Penetration: 502 cm Recovery: 2 cm Massive sulfide
859RD	17.08.07 (16:20-17:48)	39°32.440'N	14°42.368'E	603	Cable length: 631 m Inclination: 11.7° Penetration: 497 cm Recovery: 50 cm Vuggy sulfate-sulfide; sandstone-siltstone
860RD	17.08.07 (18:13-20:21)	39°32.422'N	14°42.371'E	612	Cable length: 638 m Inclination: 11.0° Penetration: 502 cm Recovery: no recovery
861GC	17.08.07 (20:36-21:08)	39°32.354'N	14°42.444'E	640	Ship position - no Posidonia data Cable length: 640 m Recovery: 295 cm Unconsolidated mud; unconsolidated sand; banded silica-sulfide-sulfate
862GC	17.08.07 (22:25-23:00)	39°32.504'N	14°42.300'E	594	Ship position - no Posidonia data Cable length: 596 m Recovery: 40 cm Unconsolidated mud
863GC	17.08.07-18.08.07 (23:43-00:33)	39°31.704'N	14°40.503'E	1071	Ship position - no Posidonia data Cable length: 1077 m Recovery: 298 cm Unconsolidated mud; unconsolidated sand
864SB	18.08.07 (00:53-05:26)	39°32.33'N 39°32.47'N 39°33.32'N 39°33.20'N 39°31.08'N 39°31.00'N 39°30.09'N 39°29.99'N 39°31.77'N	14°41.08'E 14°37.01'E 14°37.11'E 14°45.99'E 14°46.00'E 14°37.09'E 14°37.00'E 14°46.43'E 14°43.67'E	980 1622 1751 1508 902 1666 2016 606 554	Multibeam survey

Station	Date and Time (UTC)	Latitude	Longitude	Water depth (m)	Description
865RD	18.08.07 (06:02-08:21)	39°32.437'N	14°42.378'E	612	Cable length: 633 m Inclination: 11.0° Penetration: 502 cm Recovery: 485 cm Sandstone-siltstone; polymictic breccia with white and black clasts; vuggy sulfate-sulfide; vuggy sulfide-sulfate; massive sulfide
866TVG	18.08.07 (14:30-16:18)	39°32.427'N	14°42.383'E	622	Cable length: 639 m Recovery: ~500 kg Maximum temperature of recovered mud: 60°C; minimum pH in sediment: 6.12 Unconsolidated mud; banded silica-sulfide-sulfate; vuggy sulfide-sulfate
867TVG	18.08.07 (18:29-20:07)	39°31.783'N	14°43.567'E	500	Cable length: 513 m Recovery: ~5 kg Unconsolidated mud, bioclastic sandstone-breccia, and Mn-oxides
868SB	18.08.07-19.08.07 (21:35-05:27)	39°32.00'N 39°31.99'N 39°31.97'N 39°31.48'N 39°31.28'N 39°30.70'N 39°30.70'N 39°30.08'N 39°30.10'N 39°29.86'N 39°29.64'N 39°29.41'N 39°29.39'N	14°46.13'E 14°46.95'E 14°51.05'E 14°50.84'E 14°46.01'E 14°59.73'E 14°46.62'E 14°46.39'E 14°59.94'E 15°00.16'E 14°46.02'E 14°46.10'E 14°51.11'E	1203 1142 1401 1299 976 1377 627 599 1293 1328 879 962 613	Multibeam survey
869TVG	19.08.07 (06:35-11:06)	39°32.308'N	14°42.324'N	590	Ship position - no Posidonia data Cable length: 432 m Recovery: no recovery Terminated due to technical problems
870SB	19.08.07 (12:00-13:00)	39°30.29'N 39°29.95'N 39°30.05'N 39°29.54'N 39°29.61'N	14°46.88'E 14°48.33'E 14°46.34'E 14°48.80'E 14°50.46'E	314 570 634 217 497	Multibeam survey
871GC	19.08.07 (14:03-14:44)	39°32.419'N	14°42.382'E	633	Ship position - no Posidonia data Cable length: 646 m Recovery: 210 cm Unconsolidated sand; unconsolidated mud; unconsolidated monomictic breccia of sulfide and sulfate clasts; unconsolidated polymictic breccia of mud and volcanic clasts

Station	Date and Time (UTC)	Latitude	Longitude	Water depth (m)	Description
872GC	19.08.07 (16:00-16:40)	39°32.443'N	14°42.390'E	628	Ship position - no Posidonia data Cable length: 643 m Recovery: 299 cm Unconsolidated sand; unconsolidated mud; unconsolidated monomictic breccia of sulfide and sulfate clasts; unconsolidated polymictic breccia of mud and volcanic clasts; unconsolidated monolithic volcanic sandstone clast breccia
873SB	19.08.07-20.08.07 (17:25-03:44)	39°32.46'N 39°32.28'N 39°29.21'N 39°28.99'N 39°29.00'N 39°28.53'N 39°28.50'N 39°28.03'N 39°27.99'N 39°26.99'N 39°27.00'N 39°28.69'N 39°29.25'N	14°40.97'E 14°38.19'E 14°47.70'E 14°54.91'E 14°47.09'E 14°45.10'E 14°59.86'E 14°59.94'E 14°42.20'E 14°42.09'E 15°00.00'E 14°58.71'E 14°56.35'E	987 1316 598 828 792 1470 1467 1574 2185 2381 1977 1214 879	Multibeam survey
874SB	20.08.07 (04:09-6:06)	39°29.10'N 39°29.10'N 39°28.99'N 39°28.83'N 39°28.72'N 39°28.74'N 39°28.60'N 39°28.52'N 39°28.40'N 39°28.37'N	14°50.37'E 14°48.14'E 14°48.01'E 14°51.75'E 14°51.74'E 14°48.03'E 14°48.01'E 14°50.40'E 14°50.34'E 14°48.69'E	158 373 514 604 605 545 601 521 585 451	Multibeam survey
Panarea					
875RD	20.08.07 (11:21-12:35)	38°38.854'N	15°06.728'E	56	Cable length: 68 m Inclination: 3.9° Penetration: 502 cm Recovery: 89.5 cm Crystal-lithic and pumice-rich sandstone to pebble conglomerate; feldspar-olivine porphyritic andesite
876RD	20.08.07 (12:56-14:09)	38°38.848'N	15°06.719'E	52	No Posidonia data - coordinates of station 878RD are the best approximation (the drill hole of station 876RD was observed during station 878RD) Cable length: 64 m Inclination: 2.6° Penetration: 502 cm Recovery: 12 cm Intensely altered coherent volcanic rock, possibly feldspar-olivine porphyritic andesite

Station	Date and Time (UTC)	Latitude	Longitude	Water depth (m)	Description
877RDV	20.08.07 (14:44-15:28)	38°38.859'N	15°06.729'E	62	Ship position - no Posidonia data Cable length: 60 m Inclination: 2.6° Penetration: 62 cm Recovery: no recovery Unconsolidated sulfur-bearing sediment slurry (66 cm) was discarded because original stratigraphy was destroyed during coring
878RD	20.08.07 (16:12-17:44)	38°38.848'N	15°06.719'E	63	Cable length: 69 m Inclination: 0.9° Penetration: 502 cm Recovery: 35 cm Crystal-lithic and pumice-rich sandstone to pebble conglomerate; feldspar-olivine porphyritic andesite
879RD	20.08.07 (18:06-19:07)	38°38.876'N	15°06.540'E	54	Cable length: 84 m Inclination: 6.0° Penetration: 502 cm Recovery: 70 cm Massive anhydrite-gypsum
880RD	20.08.07 (19:29-21:36)	38°38.882'N	15°06.535'E	55	Cable length: 85 m Inclination: 5.8° Penetration: 434 cm Recovery: 89 cm Massive anhydrite-gypsum
881RD	20.08.07 (22:00-00:13)	38°38.893'N	15°06.522'E	61	Cable length: 82 m Inclination: 4.8° Penetration: 502 cm Recovery: 289 cm Massive anhydrite-gypsum
882RD	21.08.07 (00:46-02:06)	38°38.856'N	15°06.509'E	73	Cable length: 85 m Inclination: 4.4° Penetration: 502 cm Recovery: no recovery
883RD	21.08.07 (02:23-03:45)	38°38.871'N	15°06.502'E	74	Cable length: 80 m Inclination: 5.5° Penetration: 502 cm Recovery: 69 cm Unconsolidated mud; massive anhydrite-gypsum
884RD	21.08.07 (04:13-05:50)	38°38.872'N	15°06.493'E	75	Cable length: 80 m Inclination: 4.9° Penetration: 464 cm Recovery: 84 cm Unconsolidated mud; massive anhydrite-gypsum
885RD	21.08.07 (06:18-08:28)	38°38.930'N	15°06.448'E	75	Cable length: 87 m Inclination: 21.5° Penetration: 452 cm Recovery: no recovery Several kg of white clay were wedged in drill platform

Station	Date and Time (UTC)	Latitude	Longitude	Water depth (m)	Description
886RD	21.08.07 (08:49-09:47)	38°38.938'N	15°06.421'E	81	Cable length: 82 m Inclination: 2.5° Penetration: 502 cm Recovery: 21.5 cm Massive anhydrite-gypsum
887RDV	21.08.07 (10:07-10:49)	38°38.930'N	15°06.448'E	82	Cable length: 87 m Inclination: 7.7° Penetration: 502 cm Recovery: 179 cm Pumice-rich sand to pebble breccia; unconsolidated sand; unconsolidated mud
888SB	21.08.07 (11:00-15:39)	38°38.95'N 38°39.06'N 38°39.20'N 38°39.30'N 38°39.29'N 38°39.40'N 38°38.93'N	15°6.48'E 15°6.55'E 15°8.21'E 15°6.31'E 15°7.99'E 15°8.03'E 15°6.42'E	81 81 428 82 465 454 82	Multibeam survey
889RD	21.08.07 (15:58-16:45)	38°38.953'N	15°06.419'E	84	Cable length: 86 m Inclination: 10.7° Penetration: 502 cm Recovery: 30 cm Mudstone
890RDV	21.08.07 (17:46-18:07)	38°38.949'N	15°06.407'E	79	Cable length: 85 m Inclination: 6.0° Penetration: 502 cm Recovery: 410 cm Unconsolidated sand
891RD	21.08.07 (18:41-19:18)	38°38.934'N	15°06.447'E	80	Cable length: 86 m Inclination: 7.0° Penetration: 502 cm Recovery: 126 cm Intensely altered feldspar porphyritic andesite
892RD	21.08.07 (19:37-20:26)	38°38.939'N	15°06.363'E	79	Cable length: 80 m Inclination: 1.9° Penetration: 502 cm Recovery: no recovery
893RD	21.08.07 (20:46-21:53)	38°38.933'N	15°06.361'E	78	Cable length: 80 m Inclination: 4.7° Penetration: 446 cm Recovery: no recovery
894RDV	21.08.07 (22:13-22:52)	38°38.934'N	15°06.361'E	78	Cable length: 80 m Inclination: 4.2° Penetration: 500 cm Recovery: 375 cm Unconsolidated sand
895RD	22.08.07 (00:16-02:47)	38°38.984'N	15°05.818'E	61	Ship position - no Posidonia data Cable length: 57 m Inclination: 17.3° Penetration: 200 cm Recovery: 81 cm Feldspar-amphibole porphyritic rhyolite; amphibole-biotite-feldspar porphyritic andesite

Station	Date and Time (UTC)	Latitude	Longitude	Water depth (m)	Description
896RD	22.08.07 (03:14-06:25)	38°39.020'N	15°05.820'E	66	Ship position - no Posidonia data Cable length: 57 m Inclination: 12.2° Penetration: 500 cm Recovery: 492 cm Feldspar-amphibole porphyritic rhyolite; amphibole-biotite-feldspar porphyritic andesite
897RD	22.08.07 (06:54-08:54)	38°39.024'N	15°05.852'E	76	Cable length: 72 m Inclination: 12.6° Penetration: 167 cm Recovery: 48.5 cm Feldspar-amphibole porphyritic rhyolite; feldspar porphyritic andesite
898SB	22.08.07 (09:19-11:25)	38°39.56'N 38°39.96'N 38°39.36'N 38°39.68'N 38°39.24'N 38°39.74'N 38°39.29'N	15°06.22'E 15°05.75'E 15°06.24'E 15°05.50'E 15°06.23'E 15°05.54'E 15°06.15'E	75 81 83 57 83 64 84	Multibeam survey
899RD	22.08.07 (11:50-12:39)	38°38.979'N	15°06.432'E	80	Ship position - no Posidonia data Cable length: 84 m Inclination: 1.8° Penetration: 501 cm Recovery: 68.5 cm Unconsolidated sand; feldspar porphyritic andesite
900RDV	22.08.07 (13:00-13:29)	38°38.999'N	15°06.398'E	81	Cable length: 84 m Inclination: 3.1° Penetration: 445 cm Recovery: 396 cm Unconsolidated sand; unconsolidated mud
901RD	22.08.07 (13:51-14:42)	38°38.984'N	15°06.410'E	84	Cable length: 86 m Inclination: 0.8° Penetration: 500 cm Recovery: no recovery
902RD	22.08.07 (15:48-16:59)	38°38.944'N	15°05.388'E	59	Cable length: 66 m Inclination: 6.3° Penetration: 141 cm Recovery: 38.0 cm Coarse conglomerate
903RD	22.08.07 (17:13-18:20)	38°38.945'N	15°05.374'E	60	Cable length: 65 m Inclination: 2.6° Penetration: 93 cm Recovery: 5.5 cm Coarse conglomerate
904RD	22.08.07 (18:30-21:13)	38°38.908'N	15°05.436'E	59	Ship position - no Posidonia data Cable length: 65 m Inclination: 6.2° Penetration: 296 cm Recovery: 85 cm Coarse conglomerate

Station	Date and Time (UTC)	Latitude	Longitude	Water depth (m)	Description
905RD	22.08.07 (21:52-23:04)	38°38.948'N	15°06.898'E	73	Cable length: 76 m Inclination: 1.6° Penetration: 502 cm Recovery: no recovery
906RD	22.08.07-23.08.07 (23:15-00:00)	38°38.958'N	15°06.904'E	73	Cable length: 76 m Inclination: 3.2° Penetration: 502 cm Recovery: no recovery
907RDV	23.08.07 (00:13-00:57)	38°38.960'N	15°06.911'E	72	Cable length: 76 m Inclination: 2.8° Penetration: 296 cm Recovery: 193 cm Unconsolidated sand
908RD	23.08.07 (01:25-03:09)	38°38.852'N	15°06.728'E	63	Cable length: 69 m Inclination: 5.9° Penetration: 409 cm Recovery: 12 cm Crystal-lithic and pumice-rich sandstone to pebble conglomerate; feldspar-olivine porphyritic andesite
909RD	23.08.07 (03:35-04:15)	38°38.972'N	15°06.560'E	79	Cable length: 85 m Inclination: 5.7° Penetration: 321 cm Recovery: no recovery
910RD	23.08.07 (04:31-05:20)	38°38.973'N	15°06.553'E	82	Cable length: 84 m Inclination: 12.7° Penetration: 322 cm Recovery: no recovery
911RD	23.08.07 (06:09-6:54)	38°38.854'N	15°06.723'E	64	Cable length: 69 m Inclination: 6.7° Penetration: 436 cm Recovery: no recovery
912SB	23.08.07 (07:05-08:54)	38°38.95'N 38°39.69'N 38°39.98'N 38°39.58'N 38°39.61'N 38°39.18'N	15°06.56'E 15°05.57'E 15°05.78'E 15°06.29'E 15°07.42'E 15°07.74'E	80 59 79 69 120 232	Multibeam survey
913RD	23.08.07 (10:00-10:49)	38°38.951'N	15°06.418'E	82	Cable length: 85 m Inclination: 6.0° Penetration: 502 cm Recovery: 21 cm Massive anhydrite-gypsum; unconsolidated mud
914RD	23.08.07 (11:06-13:14)	38°38.946'N	15°06.422'E	84	Cable length: 86 m Inclination: 5.2° Penetration: 501 cm Recovery: 140.5 cm Massive anhydrite-gypsum
915RDV	23.08.07 (13:34-14:00)	38°38.953'N	15°06.418'E	82	Cable length: 85 m Inclination: 0.7° Penetration: 502 cm Recovery: 417 cm Polymictic breccia with crystal-rich sandstone clasts, unconsolidated sand, unconsolidated mud

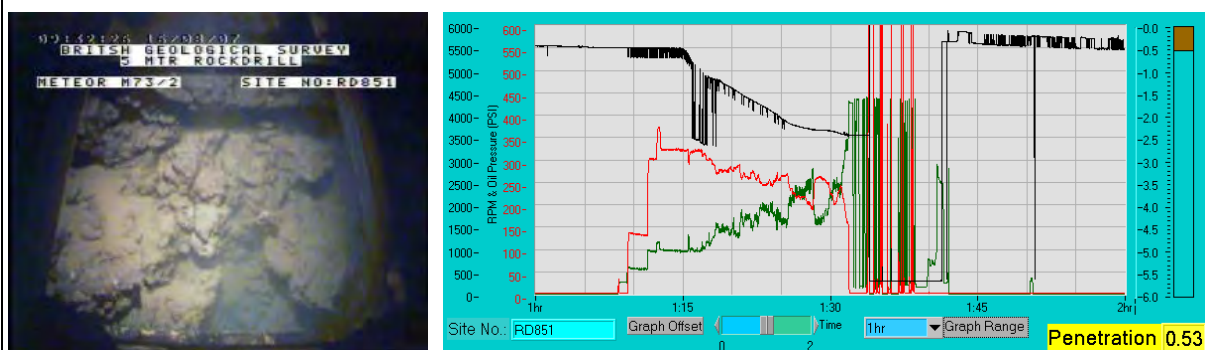
Station	Date and Time (UTC)	Latitude	Longitude	Water depth (m)	Description
916SB-1	23.08.07-24.08.07 (14:32-01:20)	38°39.49'N	15°06.34'E	76	Multibeam survey
		38°39.48'N	15°06.82'E	101	
		38°39.55'N	15°07.24'E	137	
		38°38.96'N	15°06.47'E	80	
		38°38.93'N	15°07.38'E	84	
		38°37.48'N	15°07.39'E	77	
		38°40.92'N	15°07.60'E	213	
		38°40.87'N	15°05.72'E	326	
		38°40.81'N	15°08.51'E	395	
		38°41.38'N	15°05.38'E	693	
		38°41.39'N	15°07.66'E	390	
		38°37.30'N	15°07.77'E	131	
		38°37.37'N	15°08.10'E	237	
		38°41.23'N	15°06.08'E	372	
		38°41.48'N	15°06.00'E	449	
		38°41.56'N	15°07.37'E	558	
Marsili					
916SB-2	24.08.07 (05:21-07:11)	39°06.73'N 39°17.00'N	14°19.50'E 14°23.80'E	1684 493	Multibeam survey
917RD	24.08.07 (07:21-09:59)	39°17.022'N	14°23.767'E	500	Ship position - no Posidonia data Cable length: 497 m Inclination: too steep Penetration: no drilling Recovery: no recovery Fe-oxide crust wedged in drill platform
918RD	24.08.07 (10:06-12:38)	39°17.014'N	14°23.798'E	508	Cable length: 494 m Inclination: 23.7° Penetration: 354 cm Recovery: 32 cm Feldspar-olivine porphyritic andesite
919TVG	24.08.07 (13:10-13:48)	39°17.038'N	14°23.788'E	501	Ship position - no Posidonia data Cable length: 506 m Fe-oxide crust; feldspar-olivine porphyritic andesite
920RD	24.08.07 (15:49-18:14)	39°17.016'N	14°23.816'E	513	Cable length: 494 m Inclination: 18.3° Penetration: 413 cm Recovery: 48.5 cm Feldspar-olivine porphyritic andesite
921RD	24.08.07 (18:51-20:59)	39°16.115'N	14°23.641'E	630	Cable length: 635 m Inclination: 11.1° Penetration: 502 cm Recovery: no recovery
922TVG	24.08.07 (21:16-21:53)	39°16.114'N	14°23.638'E	629	Cable length: 601 m Recovery: no recovery Terminated due to technical problems

Station	Date and Time (UTC)	Latitude	Longitude	Water depth (m)	Description
923SB	24.08.07- 25.08.07 (22:28- 14:20)	39°17.07'N 39°21.75'N 39°21.86'N 39°07.24'N 39°07.61'N 39°21.91'N 39°22.51'N 39°05.95'N 39°07.37'N 39°14.93'N 39°14.98'N 39°17.39'N 39°15.11'N 39°22.47'N	14°23.77'E 14°25.89'E 14°27.44'E 14°19.90'E 14°17.78'E 14°24.93'E 14°30.04'E 14°22.45'E 14°14.44'E 14°18.00'E 14°25.37'E 14°24.18'E 14°18.28'E 14°21.45'E	514 1813 2801 1538 2217 2185 3197 2867 3266 2346 1942 743 2327 2889	Multibeam survey
Palinuro					
924SB	25.08.07- 26.08.07 (14:39- 07:44)	39°24.59'N 39°24.60'N 39°26.96'N 39°27.00'N 39°28.01'N 39°28.01'N 39°28.74'N 39°28.81'N 39°29.49'N 39°29.70'N 39°31.20'N 39°31.22'N 39°32.37'N 39°34.18'N 39°34.20'N	14°22.71'E 15°06.94'E 15°07.12'E 15°00.46'E 15°00.03'E 15°06.84'E 15°06.98'E 15°00.17'E 15°00.01'E 15°06.67'E 15°06.90'E 14°59.92'E 14°46.18'E 14°45.75'E 15°06.62'E	2988 2042 1715 1776 1572 1640 1601 1436 1312 1600 1596 1489 1326 1691 1581	Multibeam survey
925RD	26.08.07 (10:25- 13:25)	39°31.261'N	14°39.707'E	635	Cable length: 601 m Inclination: 13.6° Penetration: 307 cm Recovery: 29 cm Feldspar-olivine porphyritic andesite
926RD	26.08.07 (13:52- 16:21)	39°31.252'N	14°39.879'E	705	Cable length: 726 m Inclination: too steep Penetration: no drilling Recovery: no recovery
927RD	26.08.07 (16:46- 19:20)	39°31.702'N	14°39.208'E	709	Cable length: 707 m Inclination: 3.3° Penetration: 406 cm Recovery: 15 cm Bioclastic sandstone-breccia
928RDV	26.08.07 (19:45- 20:42)	39°31.695'N	14°39.201'E	708	Cable length: 707 m Inclination: 4.0° Penetration: 120 cm Recovery: 68 cm Unconsolidated mud; unconso- lidated sand
929TVG	26.08.07 (22:15- 23:33)	39°32.431'N	14°42.380'E	631	Cable length: 635 m Recovery: 30 kg Unconsolidated mud; banded silica-sulfide-sulfate; massive sulfate; sandstone-siltstone

Station	Date and Time (UTC)	Latitude	Longitude	Water depth (m)	Description
930RD	26.08.07-27.08.07 (23:52-02:13)	39°32.437'N	14°42.384'E	627	Cable length: 636 m Inclination: 16.8° Penetration: 403 cm Recovery: 118 cm Mudstone-sandstone; crystal-rich sandstone; massive sulfide
931RD	27.08.07 (02:38-05:43)	39°32.440'N	14°42.381'E	626	Cable length: 637 m Inclination: 7.3° Penetration: 443 cm Recovery: 45 cm Vuggy sulfide-sulfate, vuggy sulfate-sulfide, massive sulfide
932RD	27.08.07 (06:03-07:57)	39°32.435'N	14°42.377'E	626	Cable length: 633 m Inclination: 3.6° Penetration: 406 cm Recovery: 291 cm Polymictic breccia with white and black clasts; vuggy sulfate-sulfide; vuggy sulfide-sulfate; massive sulfide
933SB	27.08.07 (08:46-09:44)	39°28.84'N 39°28.80'N	14°35.91'E 14°43.70'E	2360 1763	Multibeam survey
Panarea					
934SB	27.08.07 (14:12-19:10)	38°42.05'N 38°38.61'N 38°38.57'N 38°38.11'N 38°40.63'N 38°40.47'N 38°42.62'N 38°48.03'N 38°48.71'N	15°04.70'E 15°05.24'E 15°05.25'E 15°05.29'E 15°05.33'E 15°08.20'E 15°08.00'E 15°10.02'E 15°11.30'E	1149 53 51 38 155 318 935 861 670	Multibeam survey
935SB	27.08.07-28.08.07 (22:00-02:41)	38°44.99'N 38°41.89'N 38°41.85'N 38°40.71'N 38°40.69'N 38°40.92'N 38°41.11'N 38°37.39'N 38°38.34'N 38°38.34'N 38°37.74'N 38°37.27'N 38°37.21'N 38°44.03'N	15°06.34'E 15°06.27'E 15°05.47'E 15°05.44'E 15°07.88'E 15°07.14'E 15°08.61'E 15°07.71'E 15°07.55'E 15°08.30'E 15°08.99'E 15°09.02'E 15°09.49'E 15°09.64'E	1642 593 774 146 79 305 446 100 229 331 649 596 712 1337	Multibeam survey

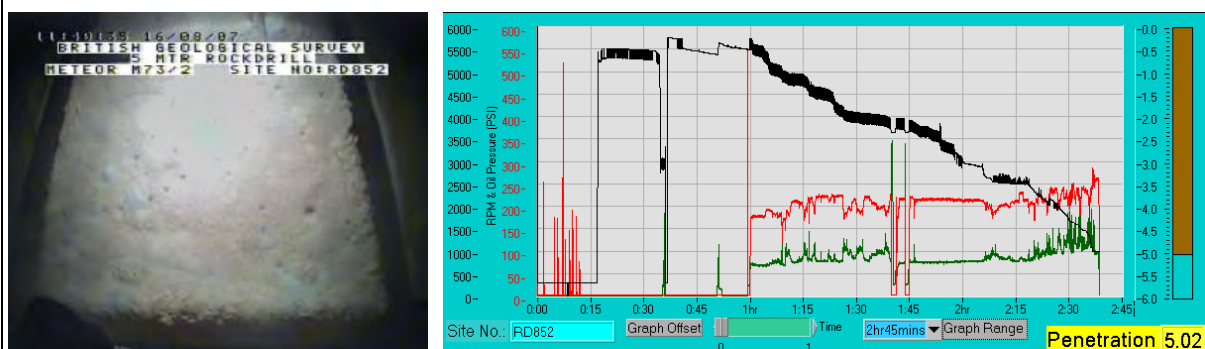
A2. Description of drilling sites

851RD



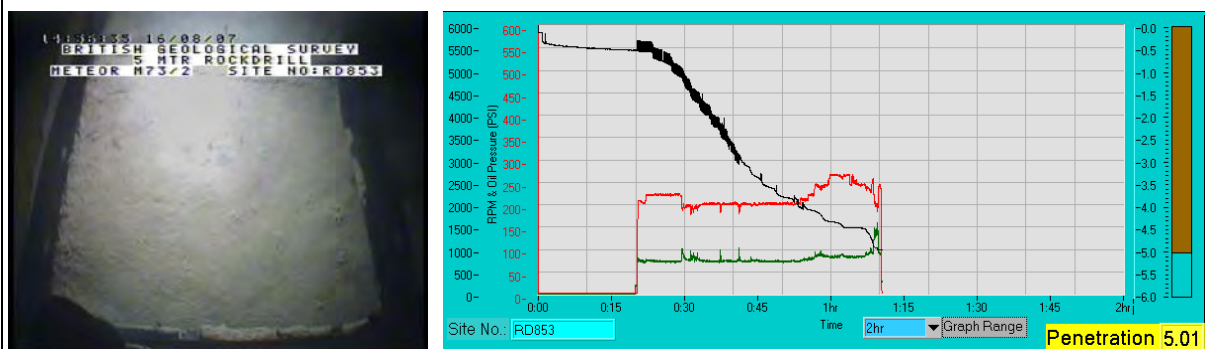
Mineralized area in the western sector of the Palinuro volcanic complex: The drill rig landed in an area characterized by a steep topography. Several large and irregularly shaped outcrops were observed during landing. The outcrops were surrounded by muddy to sandy sediment. Locally, the outcrops resembled spines and crusts. The outcrops may represent seafloor sulfides. Several unsuccessful landing attempts were made before a spot suitable for landing was found. Drilling proceeded quickly to a depth of 0.8 m. A lower penetration rate was achieved during subsequent drilling. The drill bit jammed at a final penetration of 2.30 m.

852RD

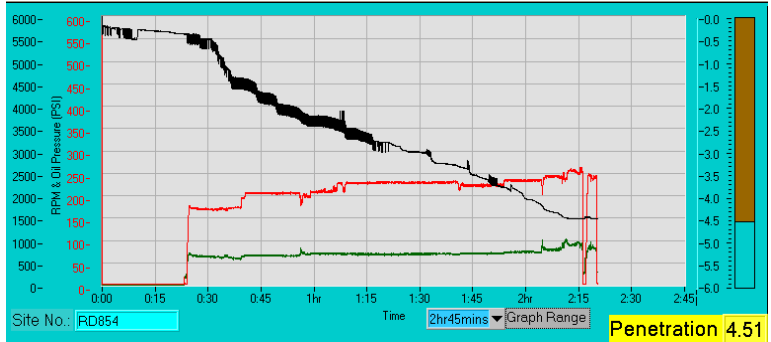


Mineralized area in the western sector of the Palinuro volcanic complex: The drill rig landed on a sedimented slope 20 m north of the previous drill site. The seafloor was covered by unconsolidated muddy to sandy sediment. Evidence for bioturbation. Impact of the drill rig caused a large sediment plume. Drilling proceeded continuously to the final penetration of 5.02 m.

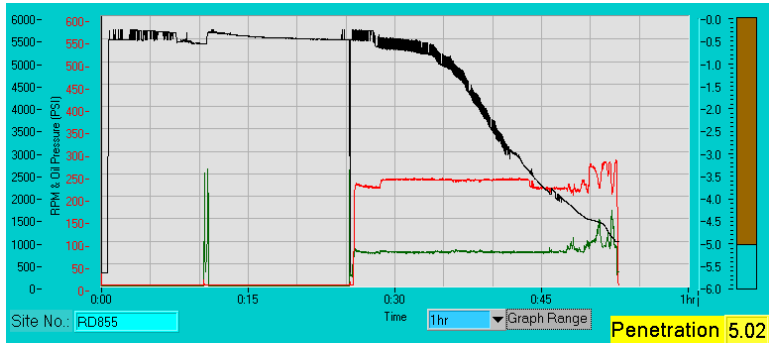
853RD



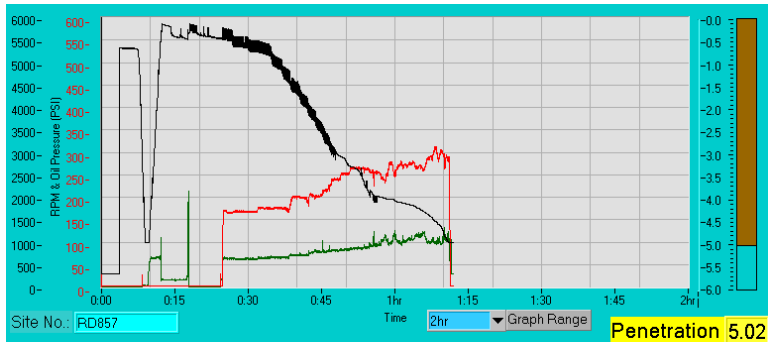
Mineralized area in the western sector of the Palinuro volcanic complex: The target site was located in a heavily sedimented area that was covered by unconsolidated muddy to sandy sediment. Evidence for bioturbation. Landing of the rig caused a sediment plume. Drilling at the site progressed continuously to the final penetration of 5.02 m.

854RD

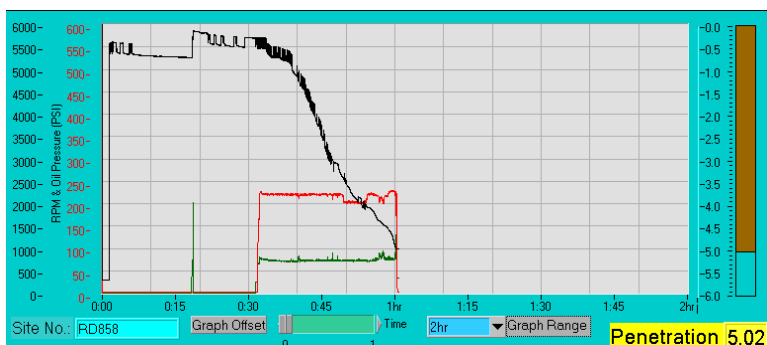
Mineralized area in the western sector of the Palinuro volcanic complex: It was attempted to land the drill rig in a heavily sedimented area. Due to the steep topography, the rig fell over. The second landing attempt was made in a similarly sedimented area. Evidence for bioturbation. Some discoloration of the muddy to sandy sediment. Impact of the drill rig caused a sediment plume. Penetration was fast to a depth of 1.4 m. Subsequent drilling proceeded at a lower rate. The drill bit was blocked at 4.51 m.

855RD

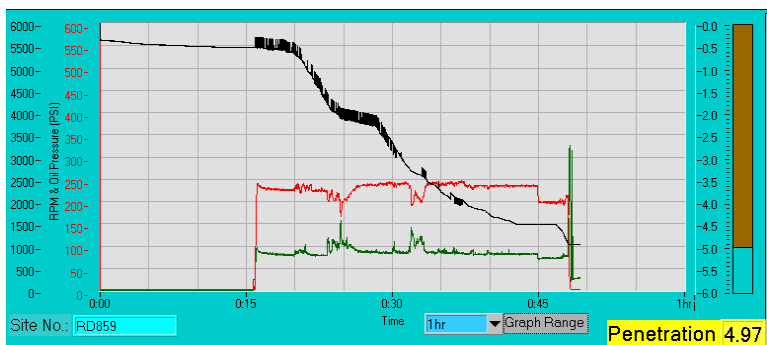
Mineralized area in the western sector of the Palinuro volcanic complex: The drill rig landed in a heavily sedimented area. Due to the steep topography, the rig fell over during the first landing attempt. The second landing attempt was successful. The seafloor was characterized by unconsolidated, muddy to sandy sediment. Evidence for bioturbation. Landing of the rig caused a small sediment plume. A final penetration of 5.02 m was achieved.

857RD

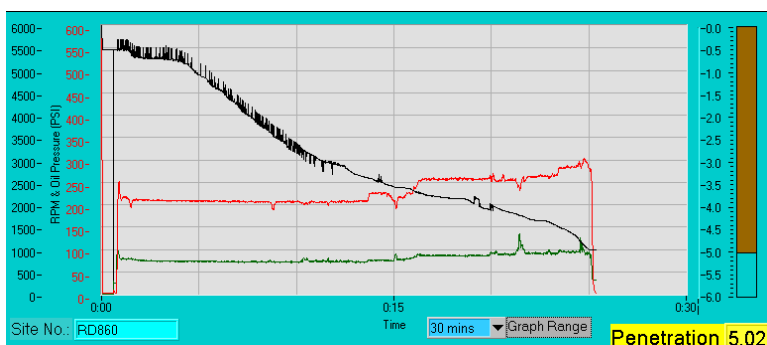
Mineralized area in the western sector of the Palinuro volcanic complex: The target area was typified by a thick cover of unconsolidated, muddy to sandy sediment. Evidence for bioturbation. Landing of the rig caused a sediment plume. A relatively fast penetration was achieved to a depth of 4.0 m. Subsequent drilling to the final penetration of 5.02 m proceeded more slowly.

858RD

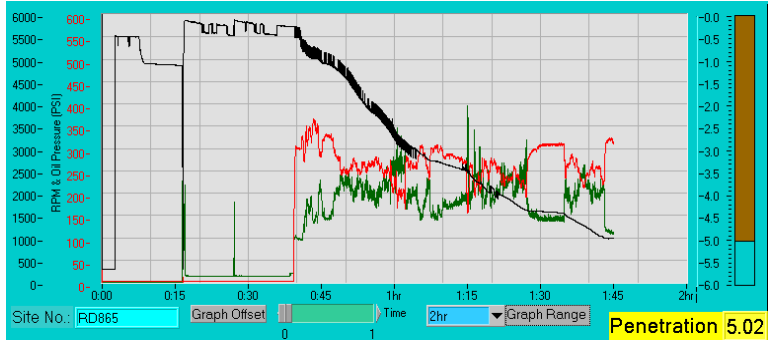
Mineralized area in the western sector of the Palinuro volcanic complex: The drill rig was placed in an area characterized by a thick sediment cover. The first landing attempt failed because the rig fell over. The second attempt of landing the rig was successful. The seafloor was covered by unconsolidated, muddy to sandy sediment. Evidence for bioturbation. Impact of the rig caused a large sediment plume. Very fast penetration to 5.02 m suggests a thick cover by unconsolidated sediment.

859RD

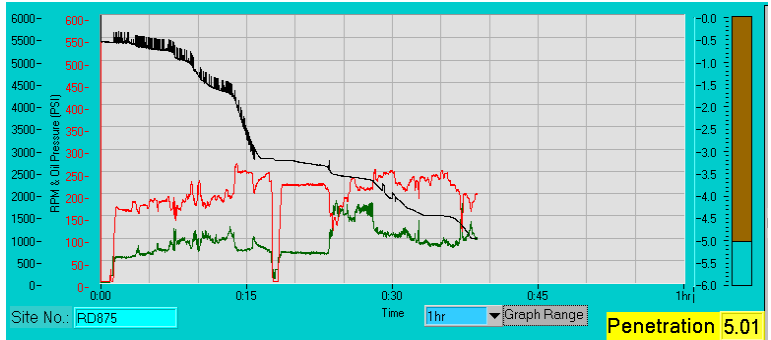
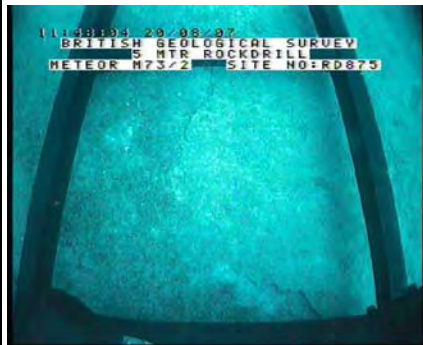
Mineralized area in the western sector of the Palinuro volcanic complex: The drill hole was placed in an area of steep topography. The drill rig fell over during a first landing attempt. The seafloor in the area was characterized by a thick cover of unconsolidated, muddy to sandy sediment. Evidence for bioturbation. The second landing attempt was successful. Impact of the rig caused a sediment plume. The drilling progress at this site was relatively fast. Only the interval between 2.0 and 2.3 m depth was drilled at a distinctly lower penetration rate. The drill was stalled at 4.52 m. A final penetration of 4.97 m was achieved.

860RD

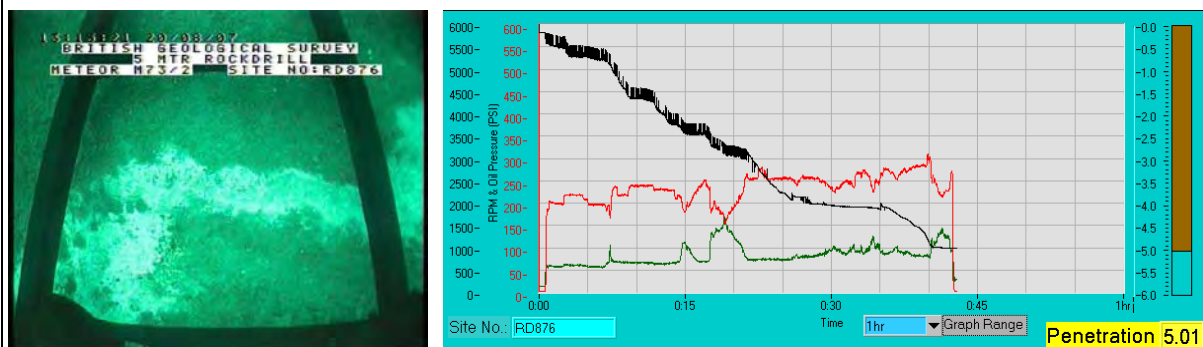
Mineralized area in the western sector of the Palinuro volcanic complex: Landing of the drill rig proved to be very difficult. Only after seven unsuccessful attempts to land the rig, a suitable landing site was found. The final landing site was characterized by a thick cover of unconsolidated, muddy to sandy sediment. Evidence for bioturbation. The impact of the rig caused a large sediment plume. Drilling at the site was fast and continuous to the final penetration of 5.02 m.

865RD

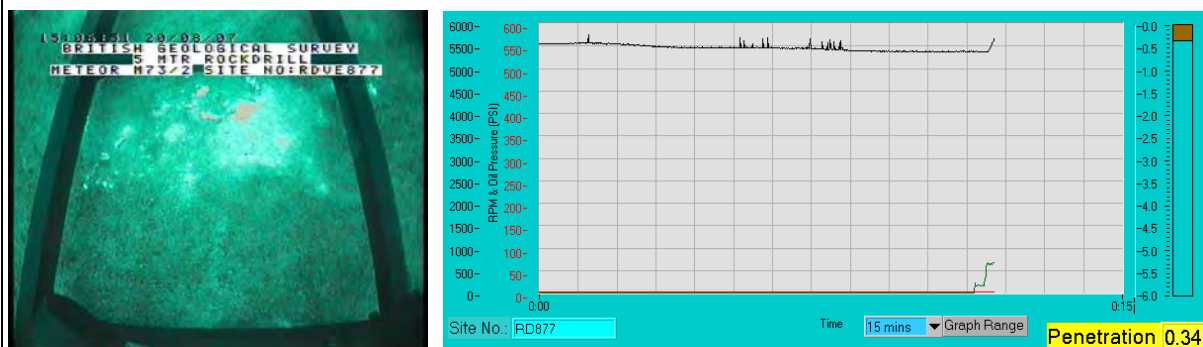
Mineralized area in the western sector of the Palinuro volcanic complex: Two unsuccessful attempts of landing the rig in an area of steep topography were made. The seafloor observed during the first landing attempt was covered by unconsolidated muddy to sandy sediment containing several large rock fragments. The final landing site was a heavily sedimented area. Evidence for bioturbation. Landing of the rig caused a large sediment plume. Drilling proceeded very quickly to a depth of 1.0 m. Subsequent drilling proceeded relatively fast, but the drilling progress decreased below 3.2 m. The final penetration was 5.02 m.

875RD

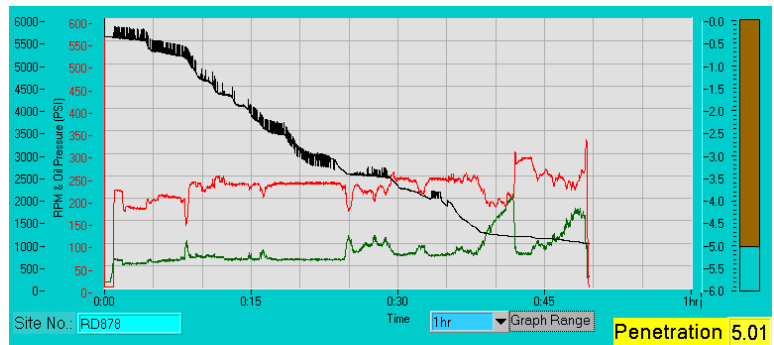
Working area north of Lisca Bianca, Panarea volcanic complex: During landing, a large, smooth and level area covered by sediment was observed. The sedimented area was surrounded by a ridge consisting of large rounded boulders. The rig landed on fine-grained, sandy to gravelly sediment. Large bacterial mats were observed during landing that mark fractures in the indurated sediment. Gas bubbling was observed from one fracture. No sediment plume observed during landing of the rig. The drilling progressed relatively slowly to a depth of 1.7 m. A higher penetration rate was achieved between 1.7 and 3.1 m. Subsequent drilling was performed at a slower rate until the final penetration of 5.02 m was reached.

876RD

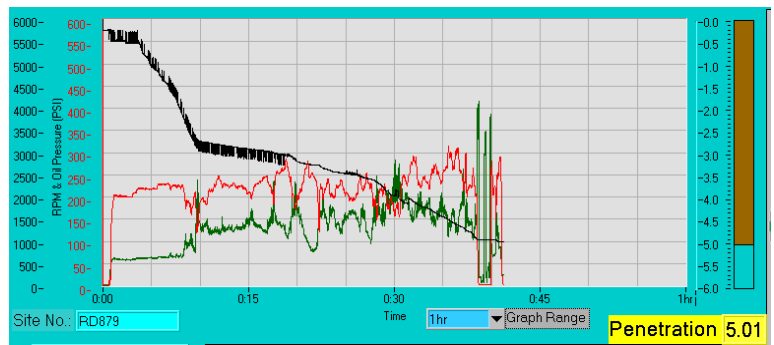
Working area north of Lisca Bianca, Panarea volcanic complex: The rig landed on a smooth and level surface. The seafloor was covered by fine-grained, sandy to gravelly sediment. Large bacterial mats. Some were dispersed during landing of the rig. Landing did not cause a sediment plume suggesting that the sediment is indurated. Drilling proceeded more or less continuously to the final penetration of 5.02 m.

877RDV

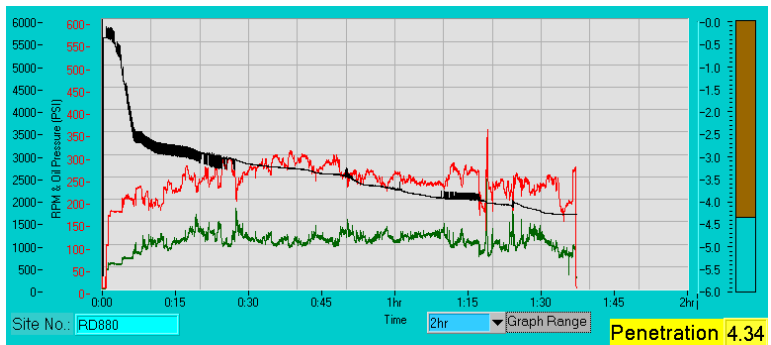
Working area north of Lisca Bianca, Panarea volcanic complex: The drill rig landed on a smooth and level surface. The seafloor was covered by fine-grained, sandy to gravelly sediment. Abundant patches of bacterial mats. The drill rig landed close to a bacterial mat that was located at a gas discharge site. Vigorous gas bubbling. Coring was conducted to a final penetration of 0.62 m.

878RD

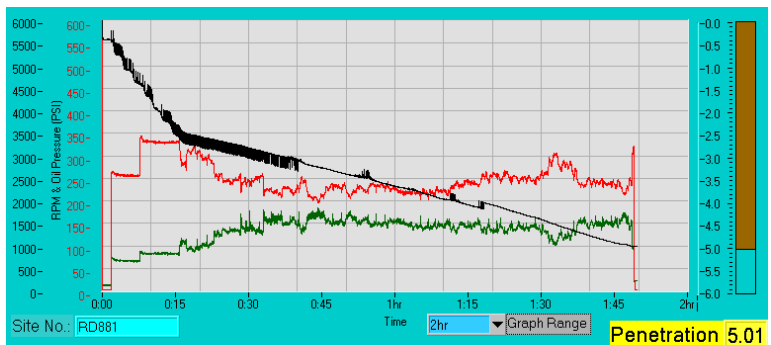
Working area north of Lisca Bianca, Panarea volcanic complex: Drilling was performed on a smooth and level surface in an area covered by fine-grained, sandy to gravelly sediment. A large bacterial mat was observed during landing that was identical to the one observed during station 876RD. The drill rig landed <1 m away from the drill hole of station 876RD. During drilling of this hole, the Posidonia subpositioning system was not working and only the ship coordinates could be determined. Based on the seafloor observations, the location of the hole 876RD was corrected. Drilling at the site proceeded more or less continuously to the final penetration of 5.02 m.

879RD

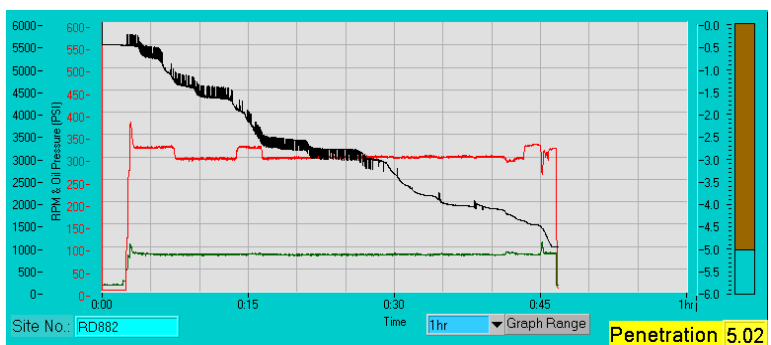
Working area north of the Secca dei Panarelli, Panarea volcanic complex: The working area was typified by a smooth and level surface. The seafloor was covered by fine-grained, sandy to gravelly sediment containing white fragments that may be shells. Evidence for bioturbation and some sediment discoloration. No sediment plume observed on landing. Rapid drilling progress was made to a depth of 2.7 m. Subsequent drilling to the final penetration of 5.02 m proceeded much slower.

880RD

Working area north of the Secca dei Panarelli, Panarea volcanic complex: The drill rig landed on a smooth and level surface. The seafloor was covered by fine-grained, sandy to gravelly sediment containing some white fragments, possibly shells. Some sediment discoloration. The footprint from a previous instrument deployment (drill hole 879RD) was observed during landing. Initially, the rig landed 1-2 m away from this hole, but subsequently moved a bit further away from the previous drill site. Landing of the rig caused a weak sediment plume. Drilling at the site proceeded quickly to a depth of 2.7 m. Subsequent drilling was performed at a slower rate. The bit was blocked at the final penetration of 4.34 m.

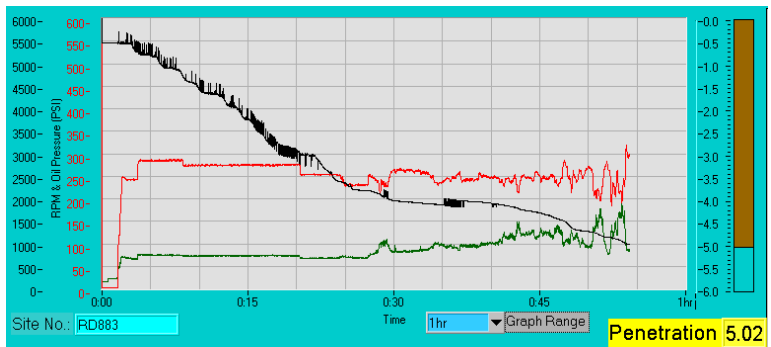
881RD

Working area north of the Secca dei Panarelli, Panarea volcanic complex: The rig landed on a smooth and level surface. The seafloor in the target area was covered by fine-grained, sandy to gravelly sediment containing white fragments that may be shells. Drilling at the site proceeded quickly to a depth of 2.5 m. Subsequent drilling to the final penetration of 5.02 m took place at a distinctly lower rate.

882RD

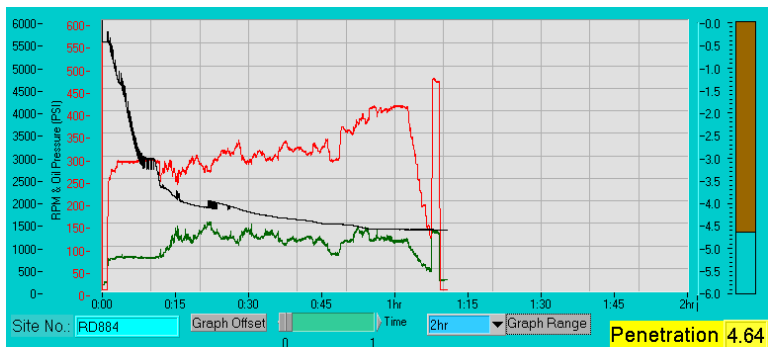
Working area north of the Secca dei Panarelli, Panarea volcanic complex: The target area was characterized by a smooth and level surface. The seafloor was covered by fine-grained, sandy to gravelly sediment. Minor sediment discoloration. Landing of the rig did not cause a sediment plume. Drilling at the site was performed to a final penetration of 5.02 m.

883RD

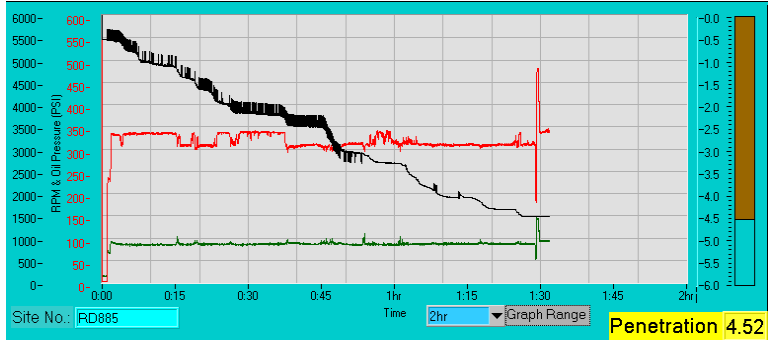


Working area north of the Secca dei Panarelli, Panarea volcanic complex: The drill rig landed on a smooth and level surface. The seafloor in the target area was covered by fine-grained, sandy to gravely sediment with evidence for bioturbation. No sediment plume was observed during landing of the rig. Drilling at the site progressed relatively continuously to the final penetration of 5.02 m.

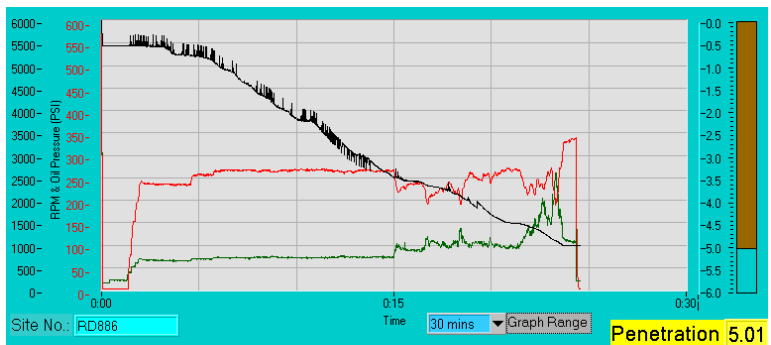
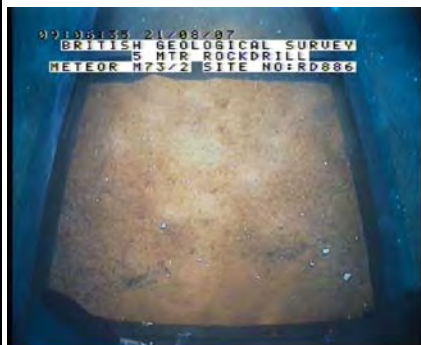
884RD



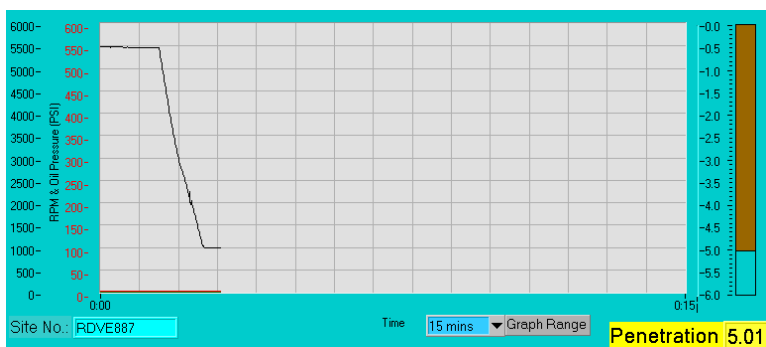
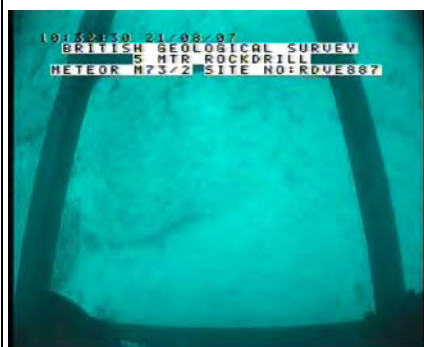
Working area north of the Secca dei Panarelli, Panarea volcanic complex: The target area was typified by a smooth and level surface. The seafloor was covered by fine-grained, sandy to gravely sediment that shows evidence for bioturbation. Intense gas bubbling was observed from one cone-shaped sediment pile. Similar pockmarks lacking gas bubbling were abundantly observed in the target area. Landing of the rig did not cause a sediment plume. Drilling at the site proceeded quickly to a depth of 3.6 m. Subsequent drilling to a depth of 4.6 m was much slower. The bit blocked at a final penetration of 4.64 m.

885RD

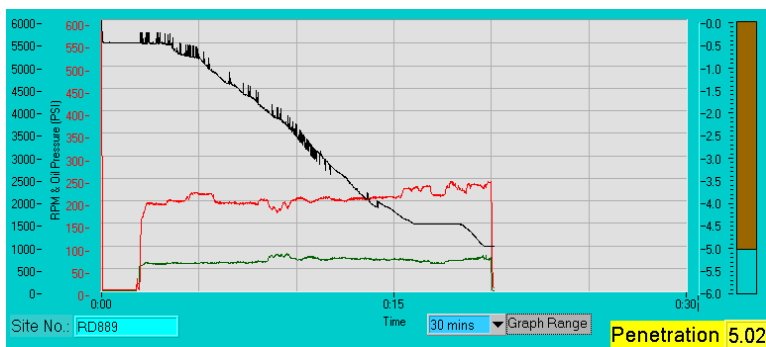
Working area north of the Secca dei Panarelli, Panarea volcanic complex: Two attempts were made to land the drill rig at the seafloor, but the topography was too steep to allow landing. Only the third attempt to land was successful. The seafloor viewed during all three attempts was covered by boulders. The boulders were subrounded to angular and typically overgrown by seafloor vegetation. The area surrounding the boulders had a conspicuous white color. On landing the drill rig, several boulders were crushed. The resulting fragments exhibited a white interior. The white material is interpreted to be identical to the intensely clay-altered andesite that was found to be wedged in the drill platform after retrieval of the instrument. Relatively intense gas bubbling was observed at the landing site. Minor sediment plume observed on landing. Drilling proceeded smoothly to a maximum penetration of 4.52 m.

886RD

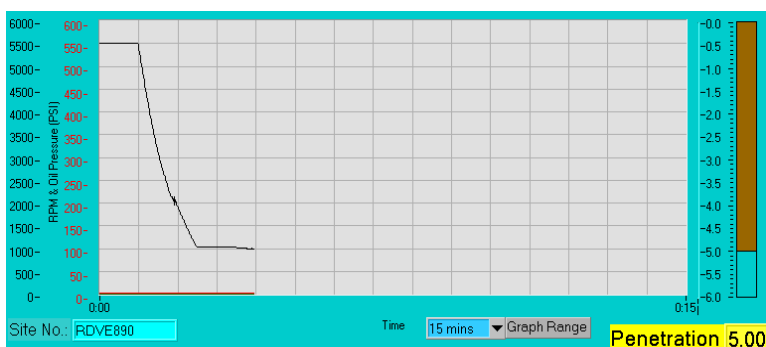
Working area north of the Secca dei Panarelli, Panarea volcanic complex: The drill rig landed in an area characterized by fine-grained, sandy to gravelly sediment containing abundant white fragments that may be shells. The sediment shows some discoloration around small cone-shaped sediment piles. These pockmarks are interpreted to be gas escape structures. A small sediment plume was caused by the landing of the rig. Drilling at the site proceeded smoothly to the final penetration of 5.02 m.

887RDV

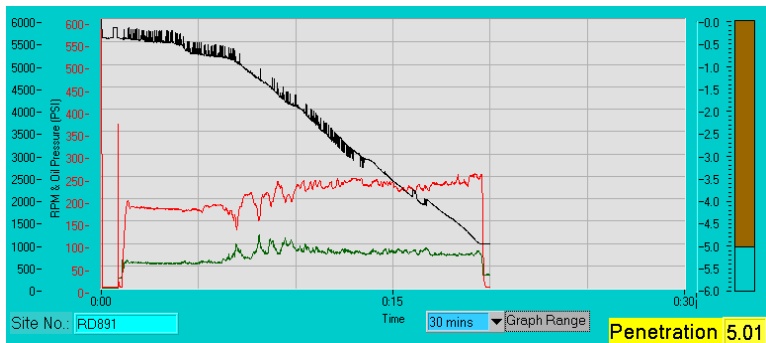
Working area north of the Secca dei Panarelli, Panarea volcanic complex: The drill rig landed on a smooth and level surface, close to several large boulders. The boulders ranged in size from about 30 to 100 cm. The surrounding sediment was fine-grained and sandy to gravelly. The legs of the drill rig landed on the boulders. Consequently, no sediment plume was observed during impact. Coring to the final penetration of 5.02 m proceeded quickly.

889RD

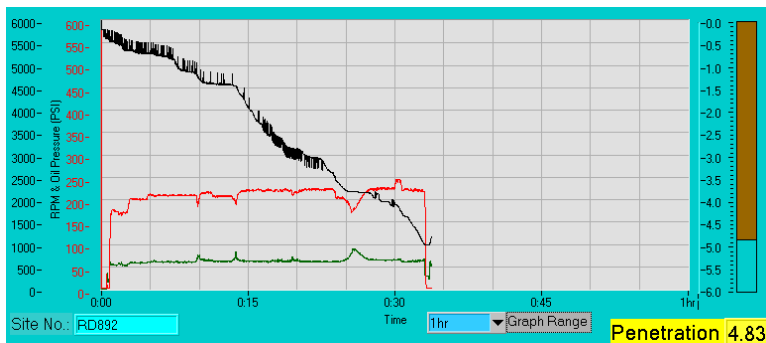
Working area north of the Secca dei Panarelli, Panarea volcanic complex: The target area was characterized by a smooth and level surface. Fine-grained, sandy to gravelly sediment with evidence for bioturbation. No sediment plume observed on landing of the rig. Drilling at the site proceeded smoothly to the final penetration of 5.02 m.

890RDV

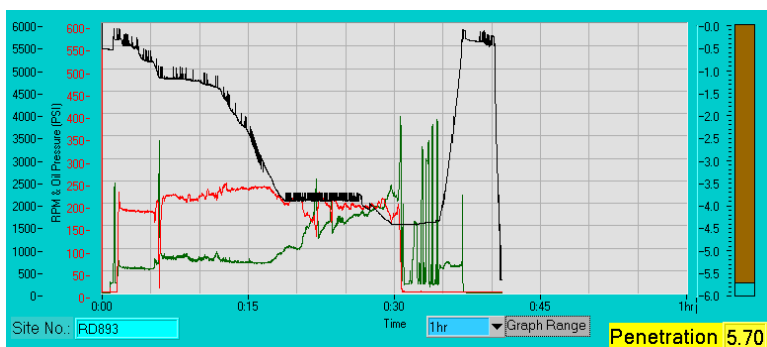
Working area north of the Secca dei Panarelli, Panarea volcanic complex: The drill rig landed at a smooth and level surface. Fine-grained sandy sediment with evidence for bioturbation. Minor sediment plume observed on landing of the rig. Coring at the site progressed quickly to the maximum penetration of 5.02 m.

891RD

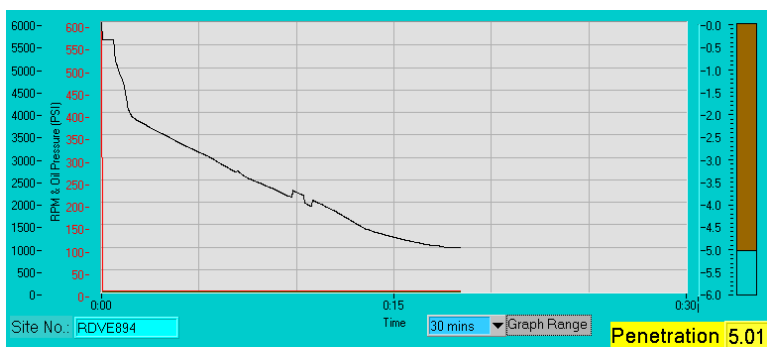
Working area north of the Secca dei Panarelli, Panarea volcanic complex: The rig landed on a level surface that was covered by boulders. The boulders were subrounded to angular and typically overgrown by seafloor vegetation. The area surrounding the boulders had a conspicuous white color. On landing the drill rig, one boulder broke open exhibiting a white interior. The white material is interpreted to be identical to the intensely clay-altered andesite recovered by drilling. Minor sediment plume observed on landing. Drilling progress at the site was slow to a depth of 0.8 m. Faster progress was made between 0.8 m and the final penetration of 5.02 m.

892RD

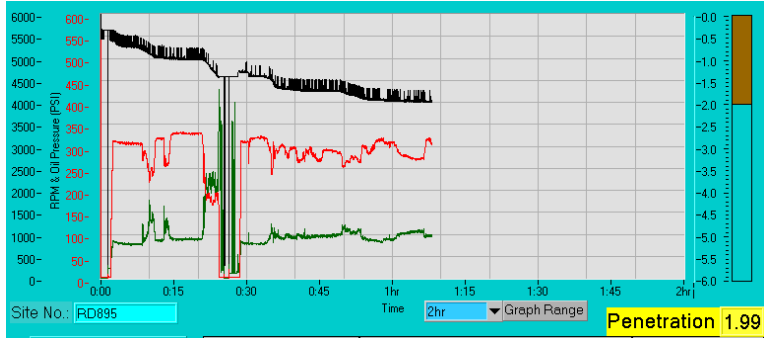
Working area north of the Secca dei Panarelli, Panarea volcanic complex: The target area was characterized by a smooth and level surface. The seafloor was covered by sandy to gravelly sediment. Evidence for bioturbation. Locally occurring pockmarks are interpreted to represent gas escape structures. No sediment plume observed during landing. Drilling at the site progressed at a relatively constant rate to the final penetration of 5.02 m.

893RD

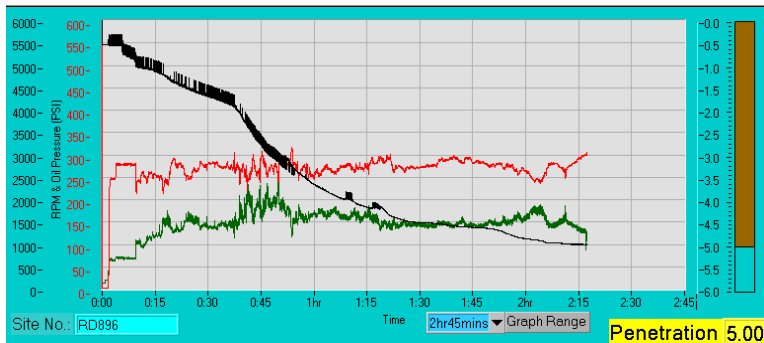
Working area north of the Secca dei Panarelli, Panarea volcanic complex: The seafloor in the target area was covered by gravelly material. Some of the coarser-grained material may be fragments of Fe oxides. Only minor sediment plume observed during landing of the rig. Drilling close to the seafloor progressed rapidly to a depth of 1.2 m. Following some slower progress, drilling proceeded quickly to a depth of 3.6 m. The drilling then slowed down. The bit was stalled at a penetration of 4.46 m.

894RDV

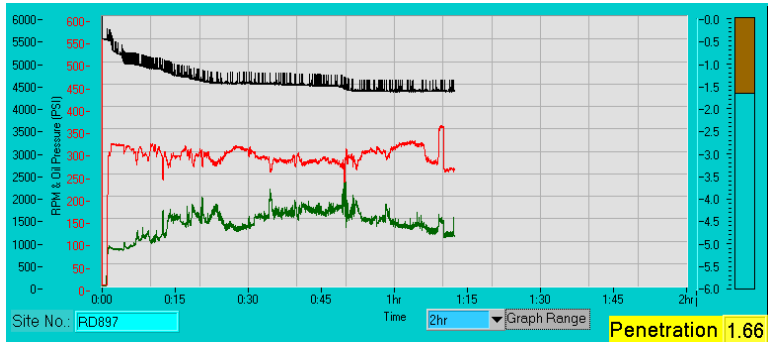
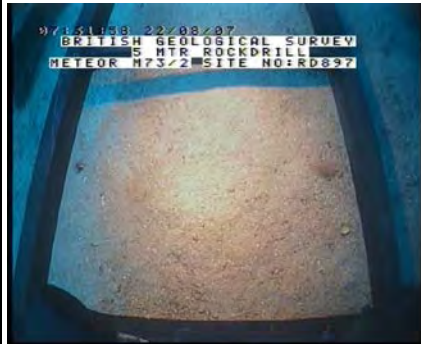
Working area north of the Secca dei Panarelli, Panarea volcanic complex: The seafloor in the target area was covered by gravelly material and up to 30 cm large, irregularly shaped crusts that may represent Fe oxides. Only minor sediment plume observed during landing of the rig. The corer quickly penetrated the substrate to a depth of 2.0 m. Coring to the final penetration of 5.00 m proceeded at a much slower rate.

895RD

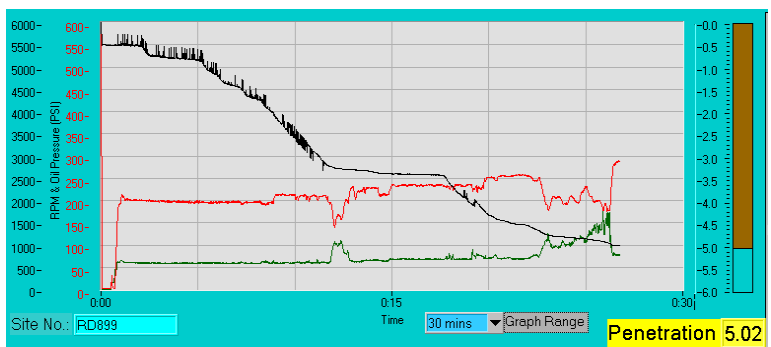
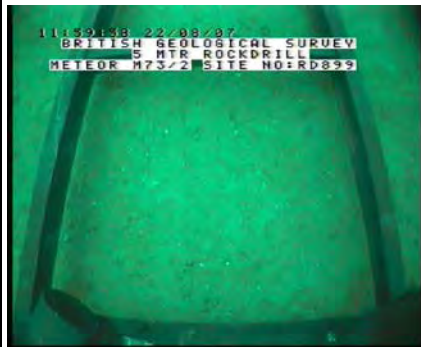
Working area northwest of Panarelli, Panarea volcanic complex: The target area was characterized by a rocky, hummocky surface of light colored lava. The rhyolite was not noticeably glassy. The lava surface appeared to be jointed or broken into blocks. Some blocks were covered by seafloor vegetation. Depressions on the lava surface were infilled by minor sediment. Abundant sea cucumbers. Landing of the rig did not cause a sediment plume. Drilling at the site progressed relatively slowly. The drill was stalled at a penetration of 1.42 m, retracted and then restarted. Coring was stopped at a final penetration of 2.00 m because no further progress could be made.

896RD

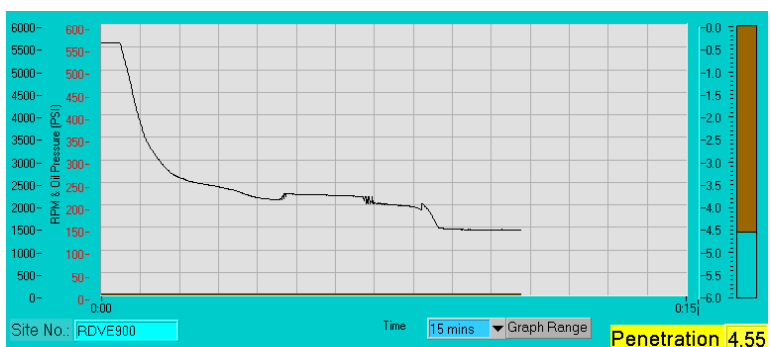
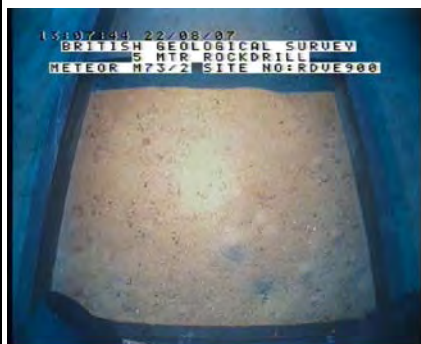
Working area northwest of Panarelli, Panarea volcanic complex: The drill rig landed on a hummocky and light colored lava surface. The felsic lava was not noticeably glassy. Possible lobe structures and joints or fractures were observed. A steep (2-3 m) lava escarpment was noted close to the landing site. Minor sediment infilling depressions on lava surface. Abundant sea cucumbers. No sediment plume observed on landing. Video observations while retracting the drill rig clearly showed that the area surrounding the drill site consisted of hummocky outcrops of felsic lava. Drilling proceeded slowly to a depth of 1.8 m. Continued drilling was initially possible at a slightly higher rate, but the rate decreases continuously as drilling proceeded to the maximum penetration of 5.00 m.

897RD

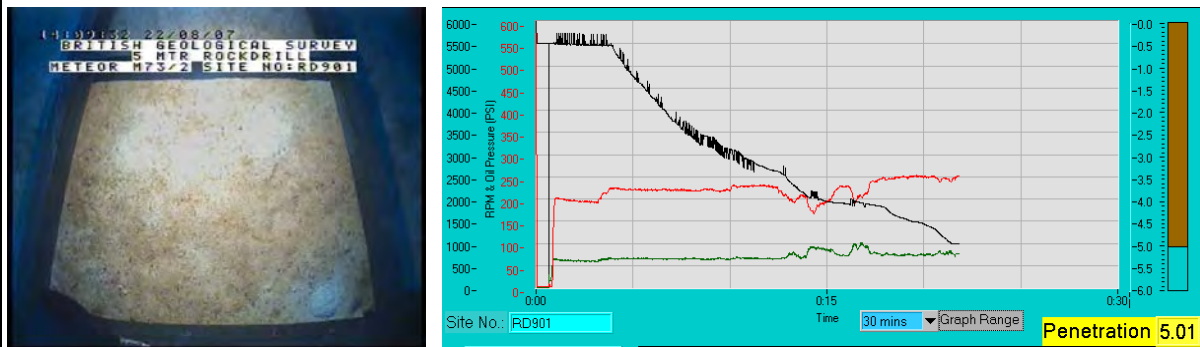
Working area northwest of Panarelli, Panarea volcanic complex: The drill rig landed on a smooth and level surface of fine-grained, sandy to gravelly sediment. Abundant angular to rounded blocks of light colored, felsic rock were observed at the seafloor during landing. These rocks are interpreted to be felsic lava blocks. No sediment plume was observed during landing of the rig. Drilling to the maximum penetration of 1.67 m progressed very slowly.

899RD

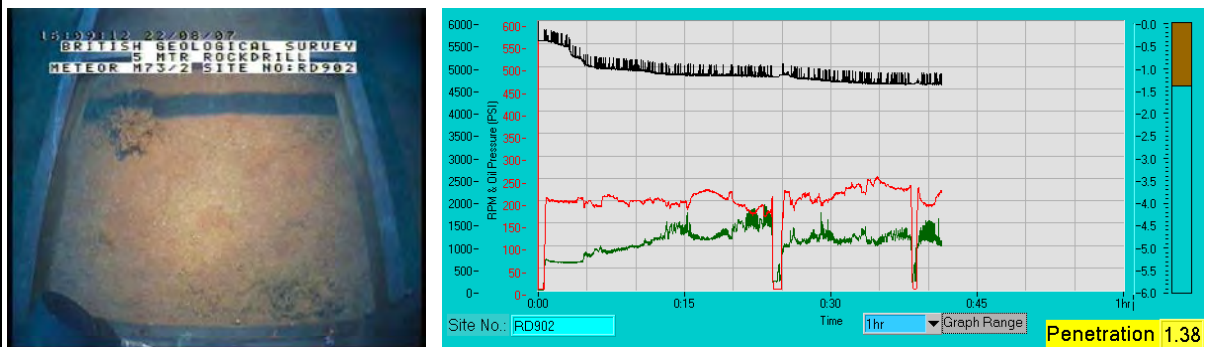
Working area north of the Secca dei Panarelli, Panarea volcanic complex: The target area was characterized by a smooth and level surface. Fine-grained, sandy to gravelly sediment with white fragments that may be shells. No sediment plume observed during landing of the rig. Drilling proceeded at a more or less constant rate from surface to a depth of 3.2 m, but was very slow between 3.2 and 3.4 m. Continued drilling to the maximum penetration of 5.01 m progressed at a moderate rate.

900RDV

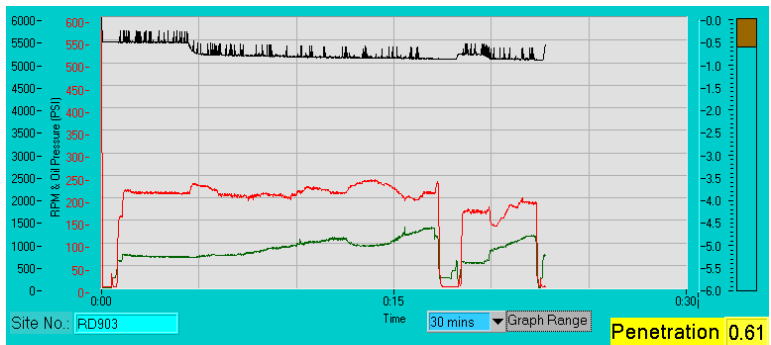
Working area north of the Secca dei Panarelli, Panarea volcanic complex: Coring was performed in an area typified by a smooth and level surface. The sediment was fine-grained and sandy, with rare white shell fragments. Abundant cone-shaped pockmarks that formed due to gas discharge. No sediment plume was observed during landing of the rig. Coring progress was fast to a depth of 3.5 m. Subsequent coring was much slower. The maximum penetration was 4.45 m.

901RD

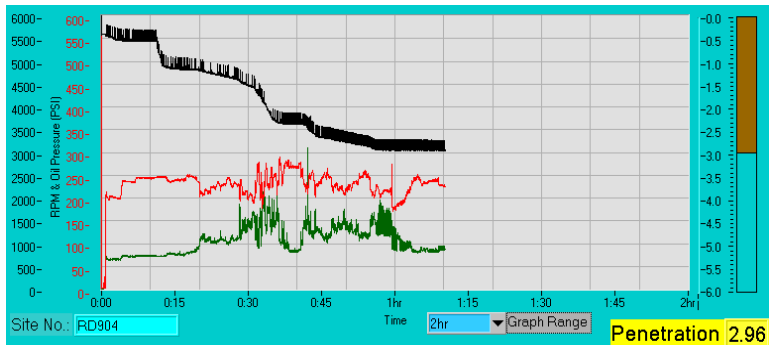
Working area north of the Secca dei Panarelli, Panarea volcanic complex: The rig landed in an area characterized by a smooth level surface. Fine-grained, sandy to gravelly sediment. Abundant pockmarks that consisted of small cone-shaped piles of sediment. Several pockmarks emanated occasional gas bubbles, with small streams of bubbles being occasionally released. No sediment plume observed when drill rig landed. The maximum penetration was 5.00 m.

902RD

Working area northwest of Panarelli, Panarea volcanic complex: The seafloor in the target area formed a slightly inclined surface that was covered by boulders. Most boulders were covered by seafloor vegetation. Individual boulders were rounded to subrounded and ranged from 10 to 50 cm in size. The infill between individual boulders consisted of fine-grained, sandy to gravelly sediment. Some boulders were covered by an unidentifiable white coating, probably bacterial mats. The ship had to move twice by 10 m because no site suitable for landing could be identified. Landing of the rig was finally conducted in a smooth and level area dominated by fine-grained and sandy sediment. No sediment plume was observed on landing. Drilling at the site progressed very slowly. The bit was blocked at a final penetration of 1.41 m.

903RD

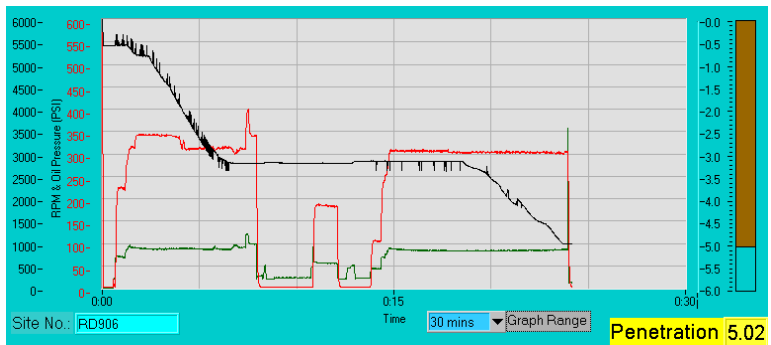
Working area northwest of Panarelli, Panarea volcanic complex: The seafloor in the target area was covered by boulders that were typically overgrown by seafloor vegetation. Individual boulders ranged in size from 10 to 50 cm and were rounded to subrounded. The infill between individual boulders consisted of fine-grained, sandy to gravelly sediment. Drilling was performed between individual boulders. No sediment plume was observed on landing. Drilling proceeded very slowly and was terminated at a final penetration of 0.93 m.

904RD

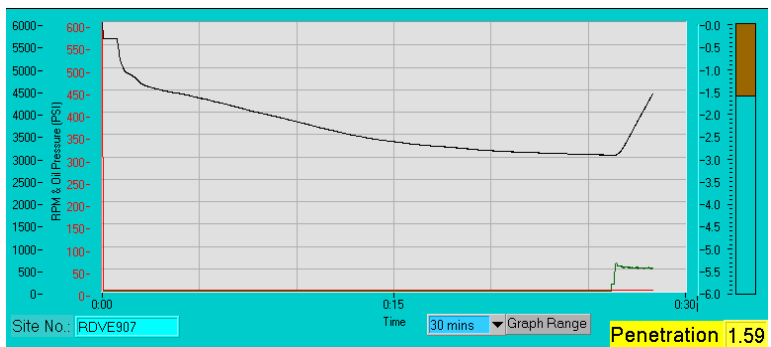
Working area northwest of Panarelli, Panarea volcanic complex: The seafloor in the target area was marked by the occurrence of large boulders that were typically covered by seafloor vegetation. Individual boulders ranged in size from 10 to 50 cm and were rounded to subrounded. The infill between individual boulders consisted of fine-grained, sandy to gravelly sediment. Very rapid drilling was possible to a depth of 1.1 m suggesting that no core was recovered from this interval. Drilling to a depth of 1.5 m progressed more slowly, followed by an interval of rapid drilling progress between 1.5 and 2.4 m. The bit was blocked at a depth of 2.96 m.

905RD

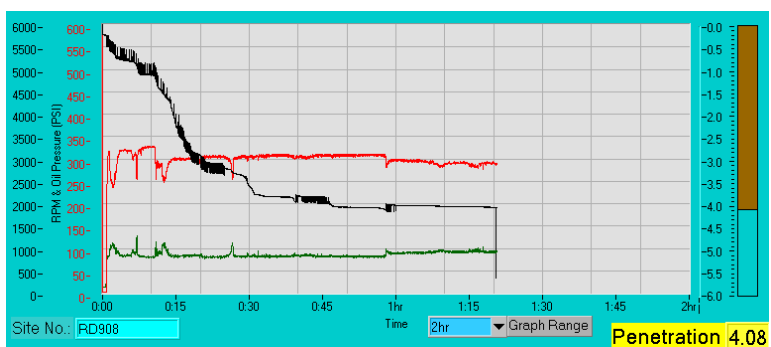
Working area north of Lisca Bianca, Panarea volcanic complex: The drill rig landed on a smooth and level surface characterized by fine-grained, sandy to gravelly sediment. Rare pockmarks representing gas escape structures were observed. No sediment plume was caused by the landing of the rig. Drilling proceeded relatively slowly. A maximum penetration of 5.02 m was reached.

906RD

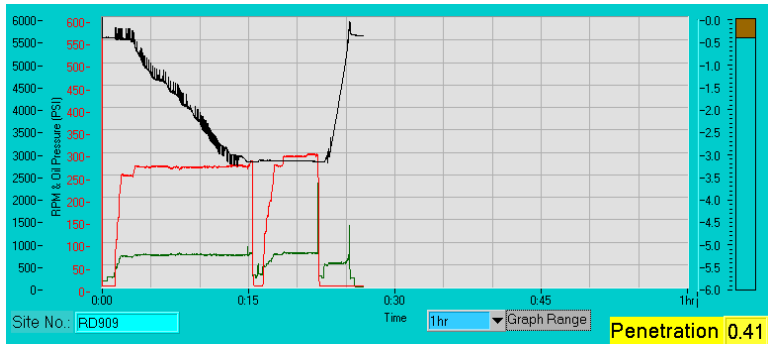
Working area north of Lisca Bianca, Panarea volcanic complex: The seafloor in the investigated area was smooth and level. The area was covered by sandy to gravely sediment. Small white shell fragments. Some seafloor vegetation. Landing of the rig did not cause a sediment plume. Drilling was relatively rapid to a depth of 3.2 m. No progress was made for some time at this depth. Further drilling proceeded relatively rapidly to a final depth of 5.02 m.

907RDV

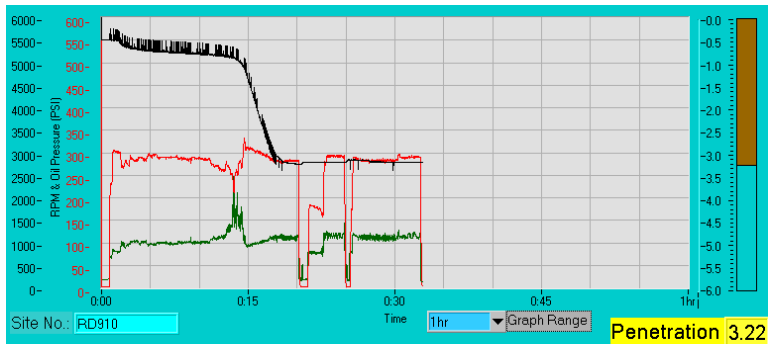
Working area north of Lisca Bianca, Panarea volcanic complex: The investigated area was typified by a smooth and level seafloor that was covered by sandy to gravely sediment. Small white shell fragments. Some seafloor vegetation. No sediment plume observed on landing. Coring to the final depth of 2.96 m progressed rapidly.

908RD

Working area north of Lisca Bianca, Panarea volcanic complex: The rig landed in an area typified by a smooth and level seafloor. Widespread bacterial mats were observed during landing. The immediate landing site was typified by fine-grained, sandy to gravely sediment. Evidence for bioturbation. Landing of the rig did not cause a significant sediment plume. Drilling proceeded relatively fast to a depth of 3.7 m. However, very slow drilling progress was made from 3.7 m to the final penetration of 4.09 m.

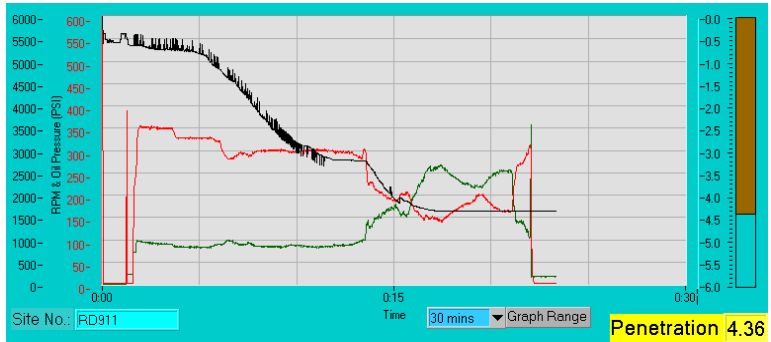
909RD

Working area north of Lisca Bianca, Panarea volcanic complex: Drill rig landed on a smooth and level seafloor that was characterized by sandy to gravelly sediment. Local evidence for bioturbation. Some pockmarks were observed that are interpreted to represent gas escape structures. Landing of the rig did not cause a sediment plume. Drilling proceeded at a more or less constant rate. The bit was blocked at a final penetration of 3.21 m.

910RD

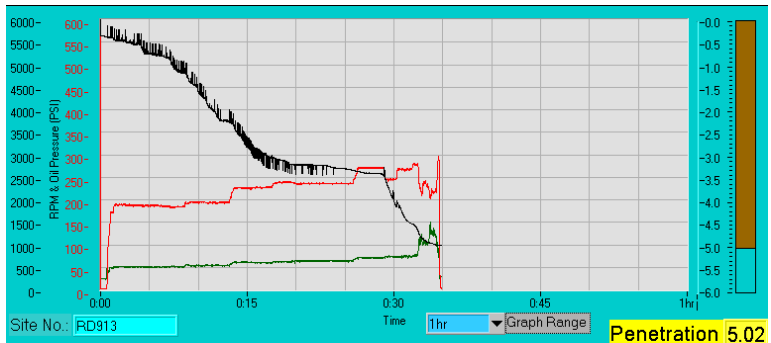
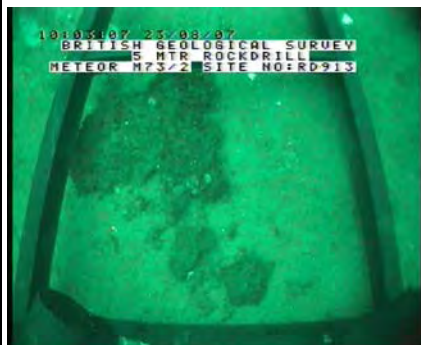
Working area north of Lisca Bianca, Panarea volcanic complex: The drill rig landed on the flank of a large outcrop of lava or indurated sediment. The outcrop was characterized by a smooth surface. Seafloor vegetation covered most of the outcrop. The fracture pattern at the surface of the outcrop suggests that it may represent a large pillow or lobe of lava. Occasional gas bubbling was observed. The outcrop was surrounded by sandy to gravelly sediment showing some evidence for bioturbation. Drilling progress was very slow to a depth of 0.7 m. However, a faster drilling rate was achieved between 0.7 and 3.1 m. The final penetration was 3.22 m.

911RD

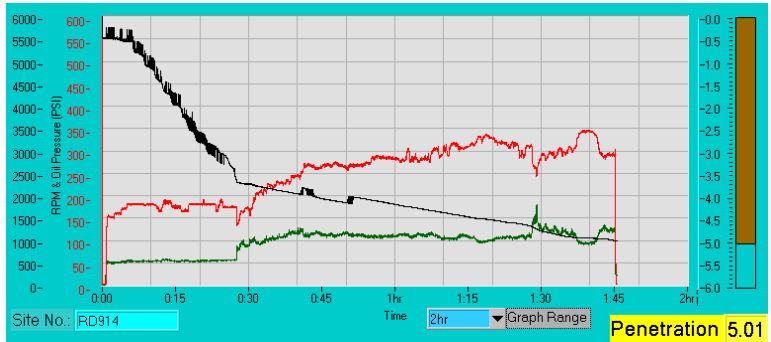


Working area north of Lisca Bianca, Panarea volcanic complex: The drill rig landed in one of the explosion craters in the working area. During lowering of the rig, a smooth and level area covered by sandy to gravelly sediment could be identified that was surrounded by a ridge of conglomerate. The seafloor within the sedimented area was typified by large patches of white and flocculent material, interpreted to be bacterial matter. The rig landed close to a several meters long fracture zone in the sediment that was surrounded by abundant bacterial matter. The landing site was also typified by the occurrence of pockmarks that represent former gas escape structures. Only a minor sediment plume was caused by the landing of the instrument. Drilling proceeded very slowly to a depth of 0.8 m. A more rapid drilling progress was made to a depth of 3.2 m. After very slow progress, fast penetration resumed to a depth of 4.3 m. The final penetration was 4.36 m.

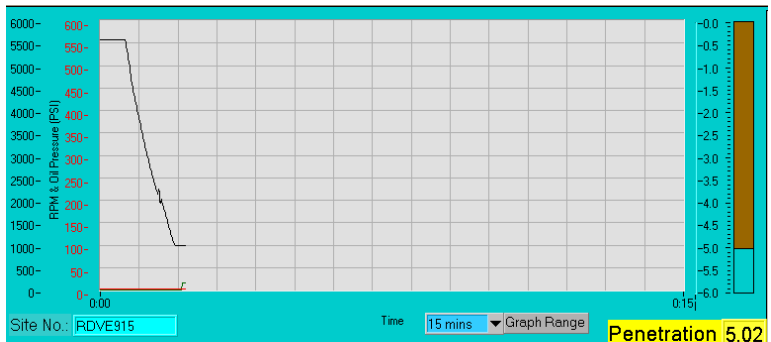
913RD



Working area north of the Secca dei Panarelli at the Panarea volcanic complex: The target area was characterized by a smooth and level surface. Fine-grained, sandy to gravelly sediment with white fragments that may be shells or hydrothermal precipitates. Meter-sized patches of indurated sediment that contained some white breccia-sized clasts. Crusts may consist of massive sulfates. Minor sediment plume observed on landing. Drilling was possible at a moderate rate to a depth of 3.2 m. Little drilling progress was made between 3.2 and 3.4 m. Following some drilling at a higher penetration rate, the bit blocked. Drilling was terminated at a final penetration of 5.02 m.

914RD

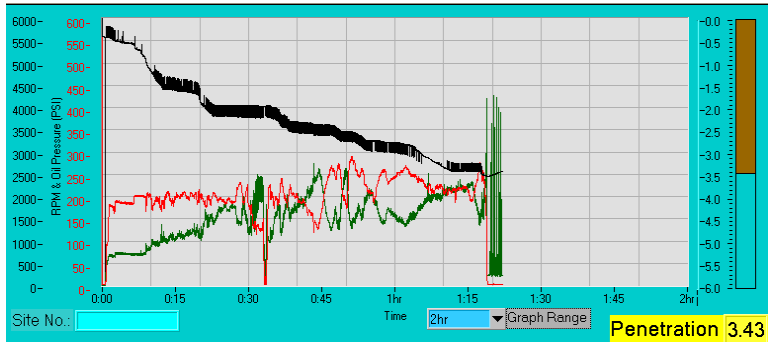
Working area north of the Secca dei Panarelli, Panarea volcanic complex: The drill landed on a smooth and level seafloor that was covered by fine-grained and sandy sediment. The seafloor was partially covered by seafloor vegetation. Locally white shell fragments. Evidence for bioturbation. Landing of the rig caused no sediment plume. CO₂ bubbling was locally observed during landing and drilling. Drilling proceeded relatively quickly from the seafloor to a depth of 3.6 m. Subsequent drilling to the final penetration of 5.01 m proceeded much slower.

915RDV

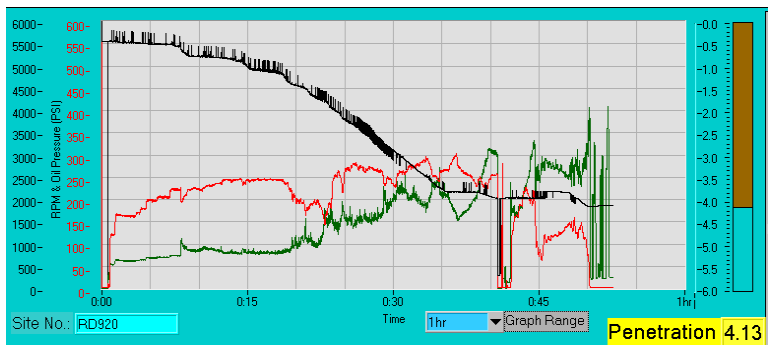
Working area north of the Secca dei Panarelli, Panarea volcanic complex: An initial landing attempt was very close to the drill site 913RD. The footprint of the drill rig was identified at the seafloor. Subsequent drilling was performed in an area characterized by a smooth and level surface that was covered by fine-grained, sandy to gravelly sediment. Minor shell fragments. The seafloor was partially covered by seafloor vegetation. Occasional evidence for bioturbation. The rig disturbed the sediment during landing and caused local CO₂ bubbling. Landing resulted only in a minor sediment plume. Coring progressed smoothly to the maximum penetration of 5.02 m.

917RD

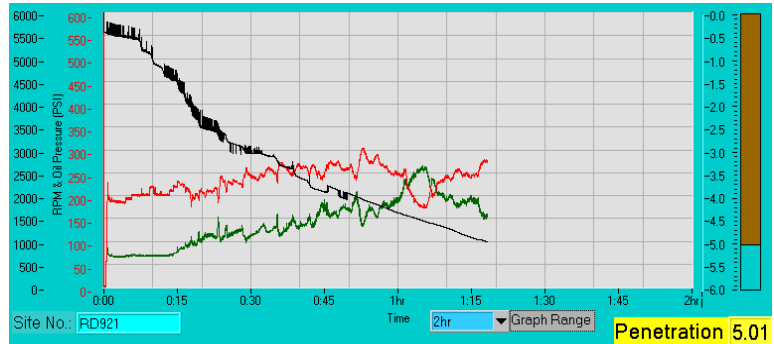
Northern working area at the Marsili volcanic complex: Eight attempts were made to land the rig, but the slope was too steep to perform drilling in the target area. Video observations during the landing attempts indicated that the seafloor in the target area was covered by Fe oxide chimney and/or mound-like structures that were festooned by bacterial communities. Impact of the drill rig caused a large sediment plume due to disintegration of the chimneys and mound-like structures. The device was recovered without drilling to repair the malfunctioning transponder.

918RD

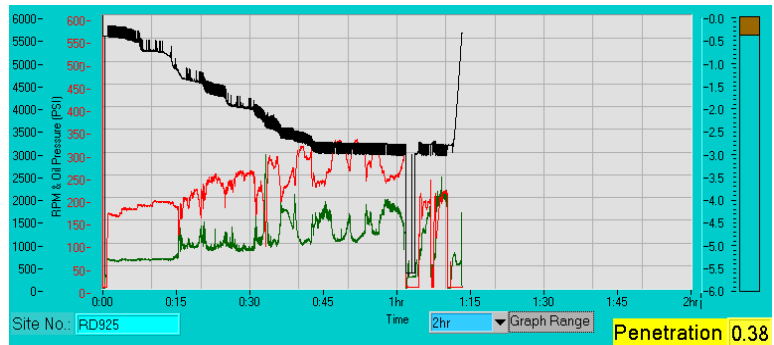
Northern working area at the Marsili volcanic complex: The first attempt of landing the drill rig failed due to the steep topography of the target area. However, the second attempt to land the drill rig was successful. The seafloor in the target area was characterized by a thick sediment cover with locally occurring bacterial communities. Small Fe oxide structures festooned by bacterial communities were observed at the final landing site. On landing, the mound-like structures broke up into larger blocks and plates. The remainder of the mound disintegrated and produced a large sediment plume. The drilling was comparably fast to a depth of 1.5 m. Drilling proceeded at a distinctly lower penetration rate to the maximum depth of 3.54 m.

920RD

Northern working area at the Marsili volcanic complex: Several attempts were made to land the rig within the field of low-temperature hydrothermal activity. During the first two attempts, the seafloor looked more degraded and sedimented and may represent an older or less active part of the vent field. No bacterial communities were observed. The sediment covering the area investigated during the third attempt appeared to be more consolidated and indurated. The sediment cracked during impact by the rig to form blocks. Some bacterial communities observed. The final landing site was located on the flank of a chimney or mound-like structure that was typified by some bacterial growth. The surface of the landing site was more rigid than those previously observed and did not break up or cause a large sediment plume. The upper part of the hole was typified by a slow drilling progress. Only after 1.1 m, drilling was possible at a faster rate. Below 3.7 m, drilling progress was again very slow and the drill bit was blocked at 4.13 m.

921RD

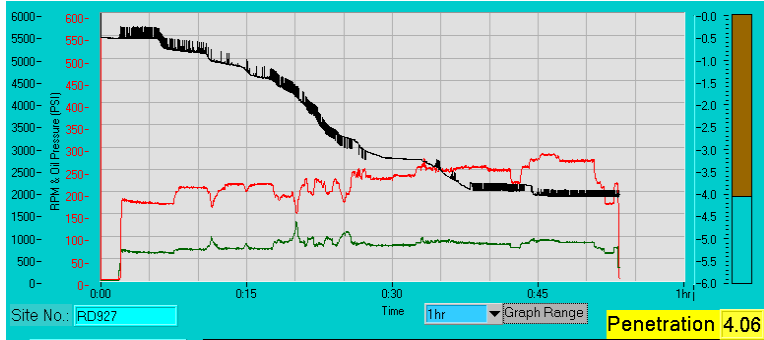
Southern working area at the Marsili volcanic complex: The landing site was typified by a relatively flat surface covered by unconsolidated sediment. Some evidence for bioturbation. Landing of the drill rig caused a weak sediment plume. Penetration was rapid to a depth of 3.0 m. Further drilling to the final penetration of 5.02 m progressed much slower.

925RD

Most westerly topographic high of the Palinuro volcanic complex: Several landing attempts were made in an area typified by large lava outcrops. The lava was locally subcropping below the muddy to sandy sediment cover. Outcrops of the lava exhibited rough surfaces or were covered by angular clasts. Topographic depressions were typically filled by sediment. Some large outcrops of the lava had steep flanks hampering successful landing of the rig. The final landing attempt was made in a more intensely sedimented area. The sediment was semi-consolidated or indurated and cracked into large blocks during impact of the rig. Drilling proceeded relatively fast to a penetration of about 3.0 m. Then, the drill bit blocked and coring was stopped at a final penetration of 3.07 m.

926RD

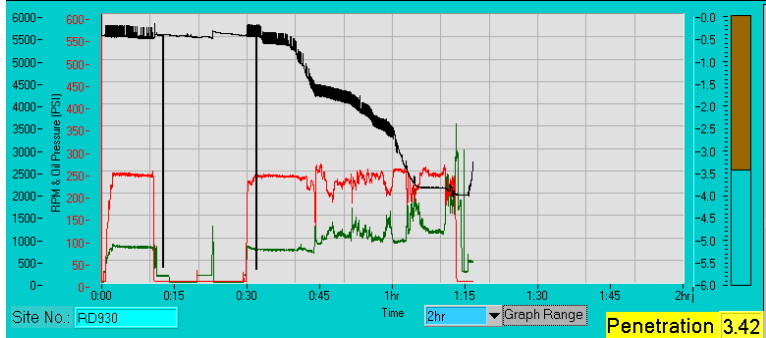
Most westerly topographic high of the Palinuro volcanic complex: Initial deployment of the instrument was marked by difficulties with the subpositioning system. After recovery of the system and fixing of the problem, the rig was lowered to the seafloor. The selected site was characterized by a thick cover of fine-grained sediment. Occasional clusters of worm burrows. The site was too steep to permit drilling. Following several unsuccessful attempts to land the rig, the site was abandoned and the drill recovered.

927RD

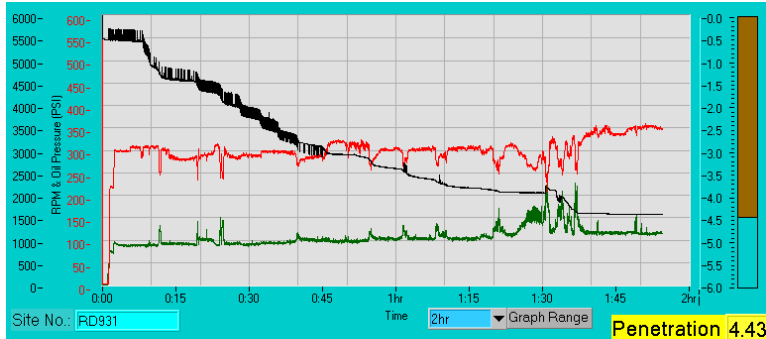
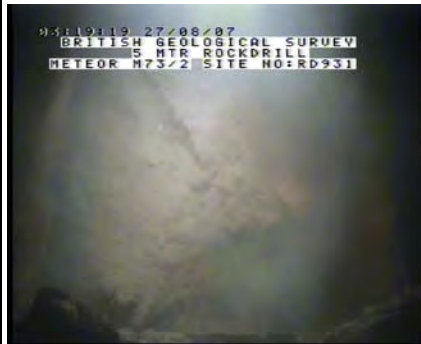
Ridge to the north of the most westerly topographic high at the Palinuro volcanic complex: Initial deployment of the instrument was aborted due to difficulties with the echo sounding system. However, the second attempt was successful. The rig landed in a relatively flat area that was covered by fine-grained sediment. Occasional clusters of worm burrows. Landing of the drill rig caused only a minor sediment plume. The legs of the drill rig did not sink in the substrate while landing. Quick penetration to a depth of 0.70 m suggesting moderately thick sediment cover. Slow drilling progress to about 3.0 m. Final penetration of 4.06 m.

928RDV

Ridge to the north of the most westerly topographic high at the Palinuro volcanic complex: The rig landed in a relatively flat area that was covered by fine-grained sediment. Occasional clusters of worm burrows. Landing of the drill rig caused only a minor sediment plume. The legs of the rig did not sink in the substrate while landing. Quick penetration to a depth of 1.2 m.

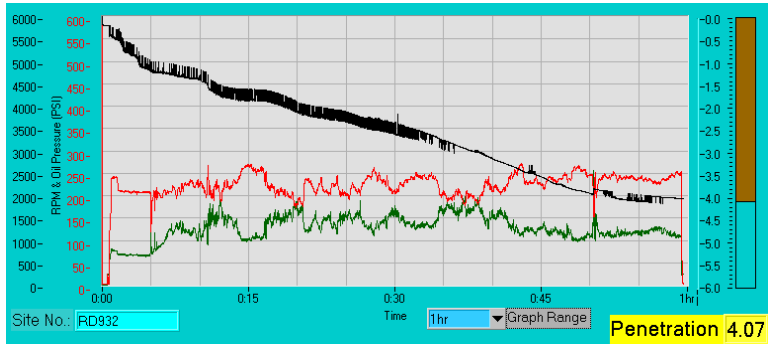
930RD

Mineralized area in the western sector of the Palinuro volcanic complex: During initial lowering to the seabed, it was noted that the echo system was malfunctioning. The first landing attempt was made in an area typified by heavy sedimentation with at least one large outcrop preventing landing due to the steep topography. The surface of the outcrop was irregularly shaped and pitted, possibly suggesting that this was an outcrop of massive sulfide. Worm burrows occur in the surrounding unconsolidated mud. The drill rig did not sink into the sediment and caused only a minor sediment plume, but started to fall over. The second landing attempt was made in a heavily sedimented area. The drill rig caused a large sediment plume during landing and sunk into the unconsolidated mud, but fell over again. During the third landing attempt, some scattered angular rocks could be seen at the heavily sedimented seabed. Abundant small conical mounds with a central burrow entrance. Landing caused a sediment plume and the leg of the drill rig sunk into the unconsolidated mud. Fast penetration for the first 1.5 m of drilling. The drilling progress was much slower between 1.5 and 2.5 m, but picked up again until stalling of the drill bit at 4.03 m.

931RD

Mineralized area in the western sector of the Palinuro volcanic complex: The drill rig landed in an area disturbed during previous drilling operation (footprint of a drill leg was visible during landing). The initial landing site was entirely covered by unconsolidated mud. Landing was not successful as the drill started to fall over and needed to be lifted again. The second landing site was nearby with the footprint of the first landing attempt still being in sight (i.e., <5 m). The final landing site was also covered by unconsolidated mud with no rocks occurring on the seafloor. Occasional worm burrows. Landing of the rig was accompanied by significant disturbance of the sediment with the rig sinking into the mud. Initial penetration was fast to a depth of about 1.5 m, followed by much slower drilling progress. Drill bit blocked at 4.43 m.

932RD



Mineralized area in the western sector of the Palinuro volcanic complex: The drill rig landed in an area disturbed during previous drilling operation (footprint of one drill leg was visible during landing). The landing site was covered by unconsolidated mud. The seafloor was covered by abundant pebble- to cobble-sized angular clasts, some of which were partially buried by the unconsolidated mud. Landing caused only a moderate sediment plume. Abundant worm burrows. Drilling progress was fast to a depth of about 1.0 m, but distinctly slower during the remainder part of the drilling operation. The drill bit blocked at 4.06 m.

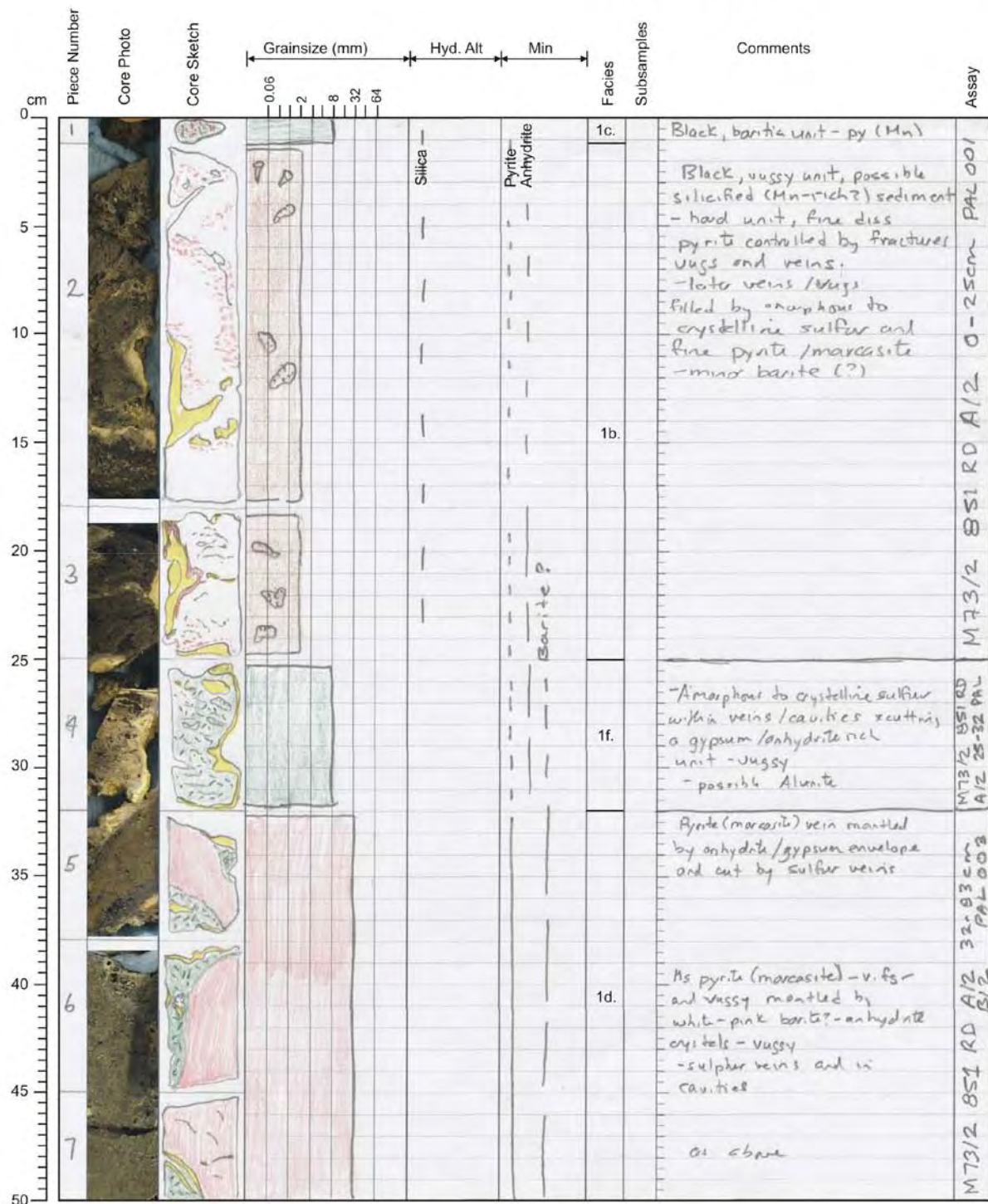
A3. Core logs

M73/2 - Station: 851 Date: Aug. 16 Time: 07:17-09:59

Lat.: 39°32.429'N Long.: 14°42.383'E Water depth: 627



- ☒ Rock core
☐ Vibro core
☐ Gravity corer



M73/2 - Station: 851 Date: Aug. 16 Time: 07:17-09:59Lat.: 39°32.429'N Long.: 14°42.383'E Water depth: 627

- ☒ Rock core
☐ Vibro core
☐ Gravity corer



cm	Piece Number	Core Photo	Core Sketch	Grainsize (mm)	Hyd. Alt	Min	Facies	Subsamples	Comments	Assay
				0.06 2 8 32 64						
50	7								as above	
55	8								Semi-massive py (marcasite) veins in a grey-bklt barite ± py groundmass cut by veinlets of sulphur - py appears to replace barite?	PAL 003
60										
65									massive, moderately vuggy pyrite cut by sulphur veins - minor remnants of barite - v. vuggy + blk (Mn)	32-83
70	9									
75										
80										
85	10								ms pyrite (vsg) + vuggy barite-anhydrite cut by sulphur vein - sulphur vein laminated at margins - vuggy xstals in open space	M73/2 851 RD A/2, B/2
90										
95	11								Vuggy blk (Mn-rich - ZnS?) with sulphate(?) - fine disseminated pyrite-marcasite in a band	B/2 83-106
100	12								as above	
	13									

M73/2 - Station: 851 Date: Aug. 16 Time: 07:17-09:59

Lat.: 39°32.429'N Long.: 14°42.383'E Water depth: 627

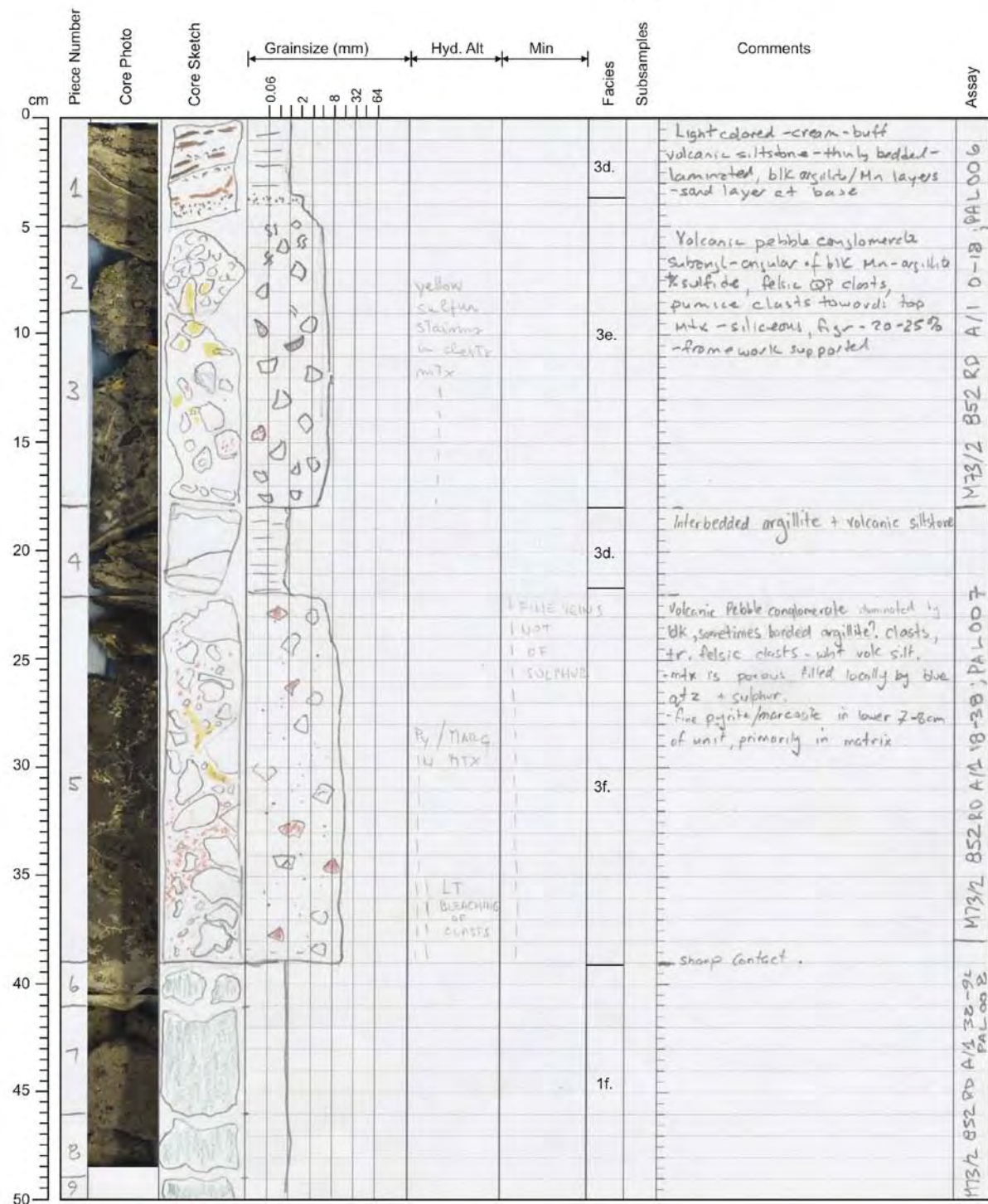
- ☒ Rock core
☐ Vibro core
☐ Gravity corer



M73/2 - Station: 852 Date: Aug. 16 Time: 10:53-13:46

Lat.: 39°32.441'N Long.: 14°42.381'E Water depth: 626

- ☒ Rock core
☐ Vibro core
☐ Gravity corer



M73/2 - Station: 852 Date: Aug. 16 Time: 10:53-13:46Lat.: 39°32.441'N Long.: 14°42.381'E Water depth: 626

- ☒ Rock core
☐ Vibro core
☐ Gravity corer

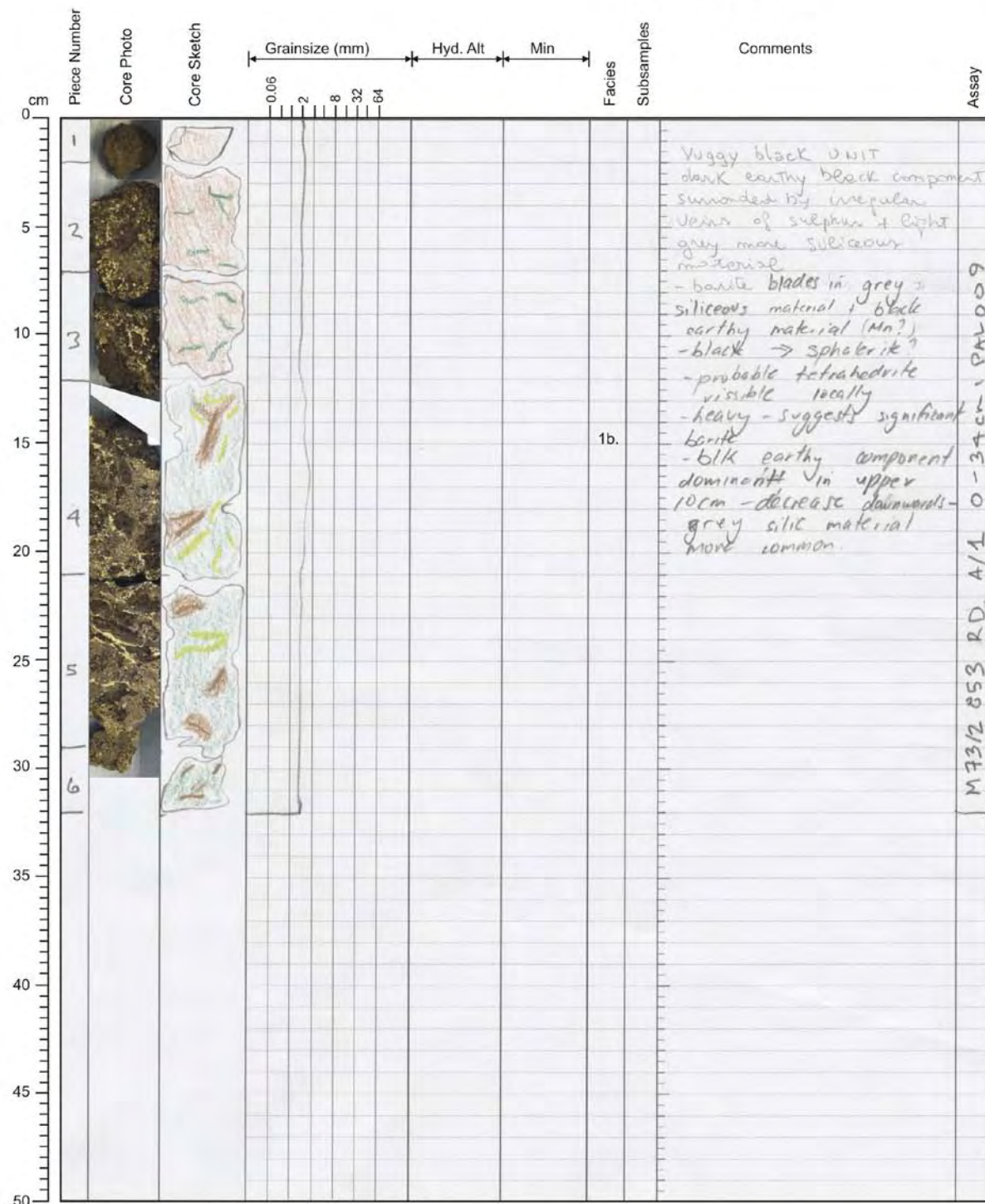


Piece Number	Core Photo	Core Sketch	Grainsize (mm)	Hyd. Alt	Min	Facies	Subsamples	Comments	Assay
cm			0.06 2 8 32 64						
50						1f.		Porous vuggy unit - distinct black colour, earthy in texture but containing bladed minerals - barite - barite(?) forms bladed network with fine pyrite/marcasite	
55								- local cavities mantled by 3-5 mm rims of ms pyrite/marc - very fine grained - possible fluid conduit - chimneys	
60								- black material may be a Zn sulphide? but no brown streak	
65								- possible tetrahedrite? red colour of silver mineral suggest ruby silver mineral.	
70									
75						1c.			
80									
85									
90									
95									
100									

PAL 008
M73/2 852 RD A1A 3B-96; PAL 008

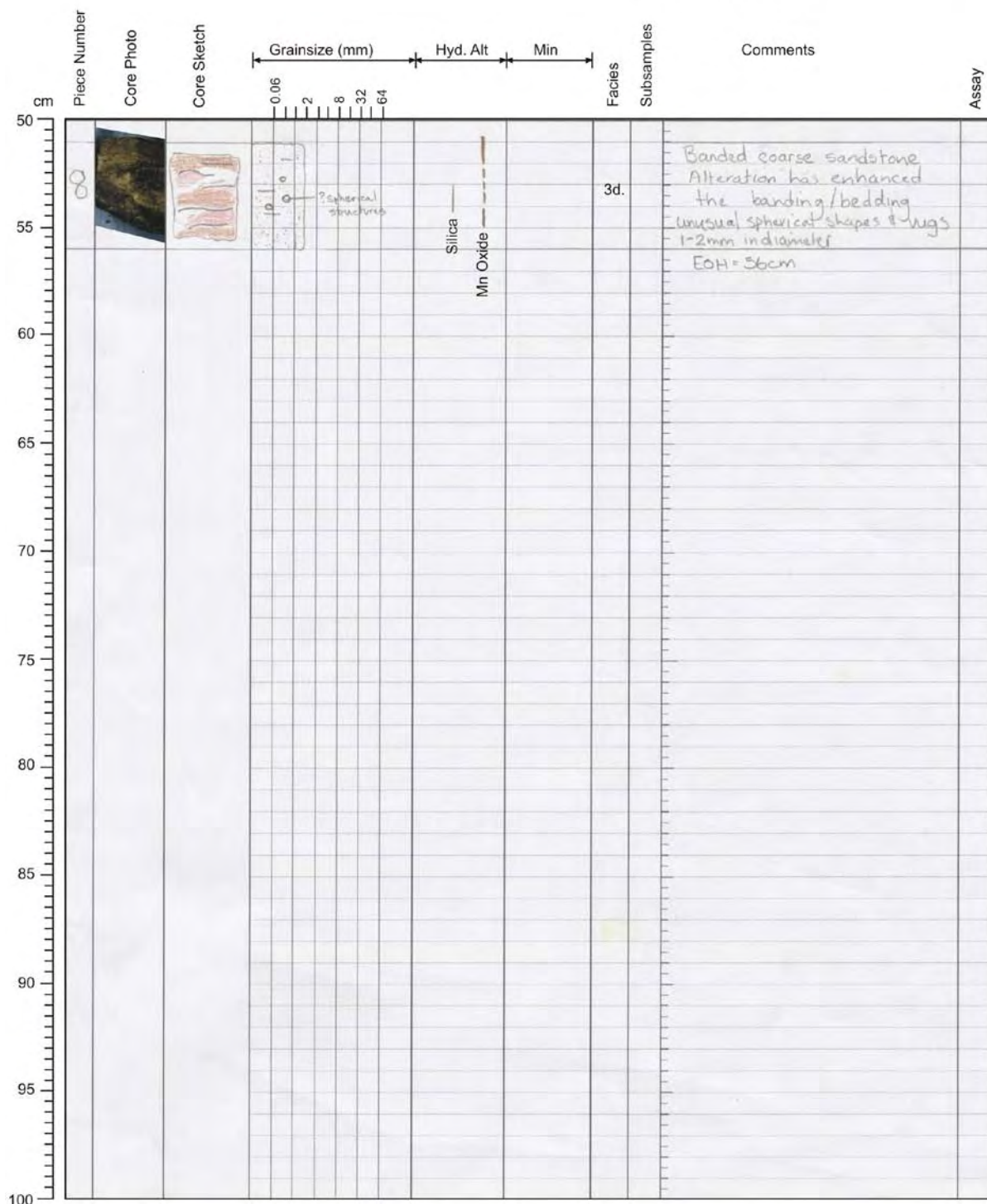
M73/2 - Station: 853 Date: Aug. 16 Time: 14:23-16:16Lat.: 39°32.439'N Long.: 14°42.403'E Water depth: 623

- ☒ Rock core
☐ Vibro core
☐ Gravity corer



M73/2 - Station: 855 Date: Aug. 16 Time: 19:48-21:11Lat.: 39°32.429'N Long.: 14°42.366'E Water depth: 620

- ☒ Rock core
☐ Vibro core
☐ Gravity corer



M73/2 - Station: 857 Date: Aug. 17 Time: 11:50-13:27Lat.: 39°32.430'N Long.: 14°42.392'E Water depth: 615

- ☒ Rock core
☐ Vibro core
☐ Gravity corer



Piece Number	Core Photo	Core Sketch	Grainsize (mm)	Hyd. Alt	Min	Facies	Subsamples	Comments	Assay
0			0.06						
1			2			Pyrite Barite Oxide	3e.	Algalite Breccia, clay Alt. volc. clasts, long tube pumice, poss. sedimentary clasts, with barite Barite network with minor pyrite nodules Mn	
2			8					Network of barite and possibly other sulphate minerals with Mn clots.	
3			32					Fine grained disseminated to dense clots of pyrite with silver sulphosalt minerals	
4			64					possible specks of chalcopyrite at 10cm and at 44cm -the unit is more sulphide dense down section.	
5									
6							1c.		
7									
8								Sulphide is less dense in this section.	

M73/2 - Station: 858 Date: Aug. 17 Time: 14:13-15:39Lat.: 39°32.446'N Long.: 14°42.393'E Water depth: 611

- ☒ Rock core
☐ Vibro core
☐ Gravity corer



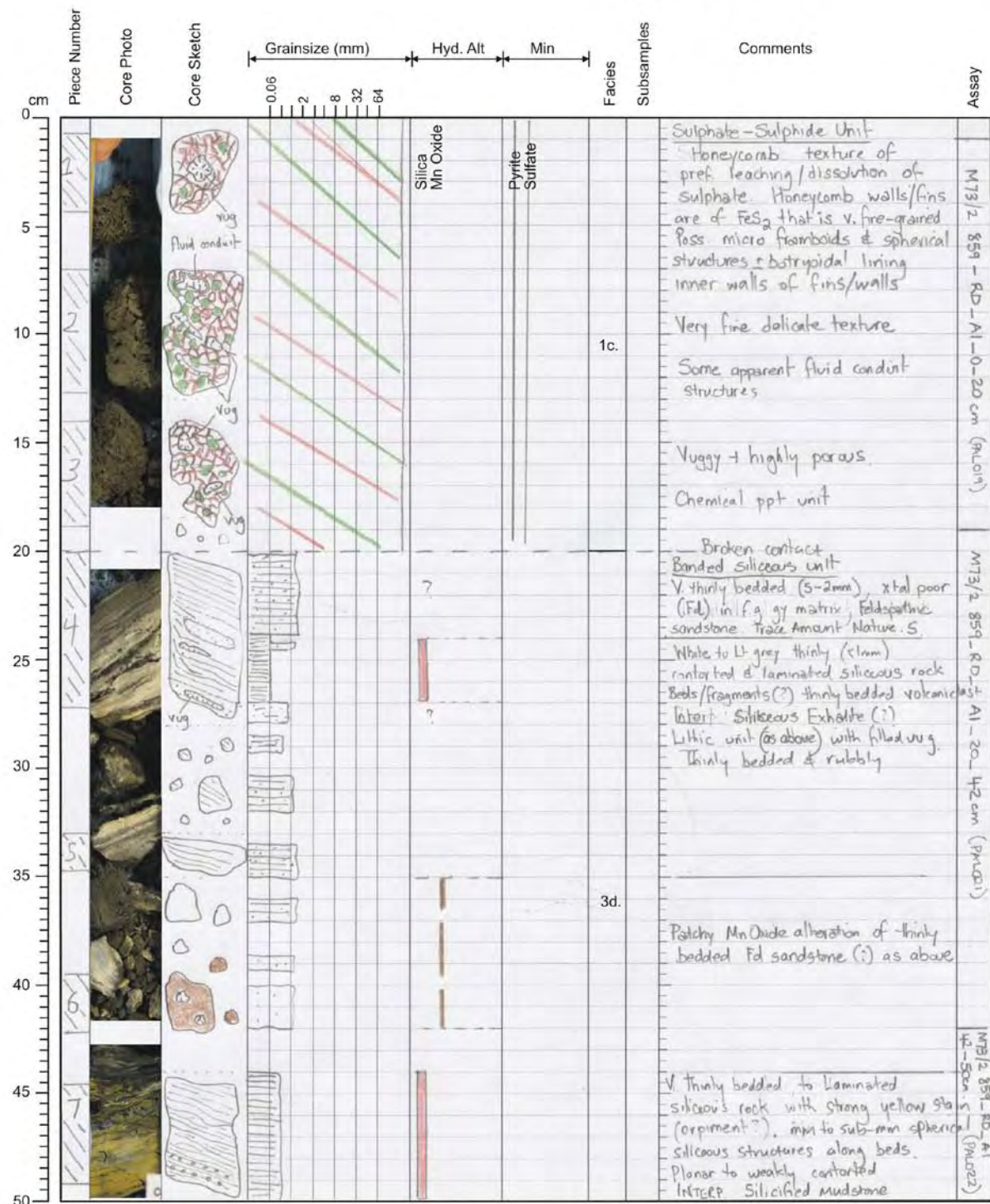
cm	Piece Number	Core Photo	Core Sketch	Grainsize (mm)				Hyd. Alt	Min	Facies	Subsamples	Comments	Assay
				0.06	2	8	32						
0	1									1e.		Py, fine-grained, minor barite as glauco crystals, some dark sulfide	M73/2 858 RD A1A 0-1cm, PAL 0VB
5													
10													
15													
20													
25													
30													
35													
40													
45													
50													

M73/2 - Station: 859 Date: Aug. 17 Time: 16:20-17:48

Lat.: 39°32.440'N Long.: 14°42.368'E Water depth: 603

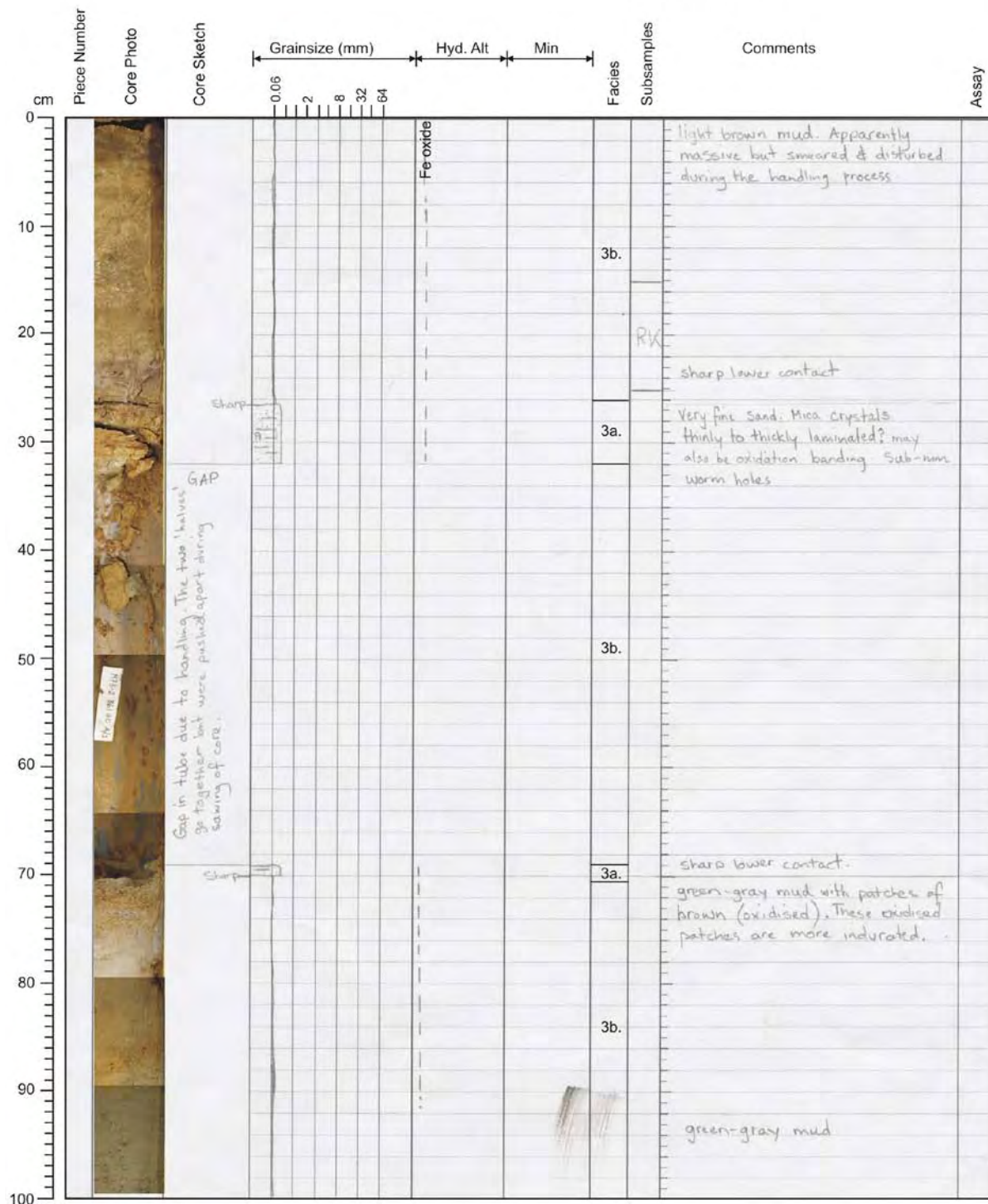


- ☒ Rock core
☐ Vibro core
☐ Gravity corer



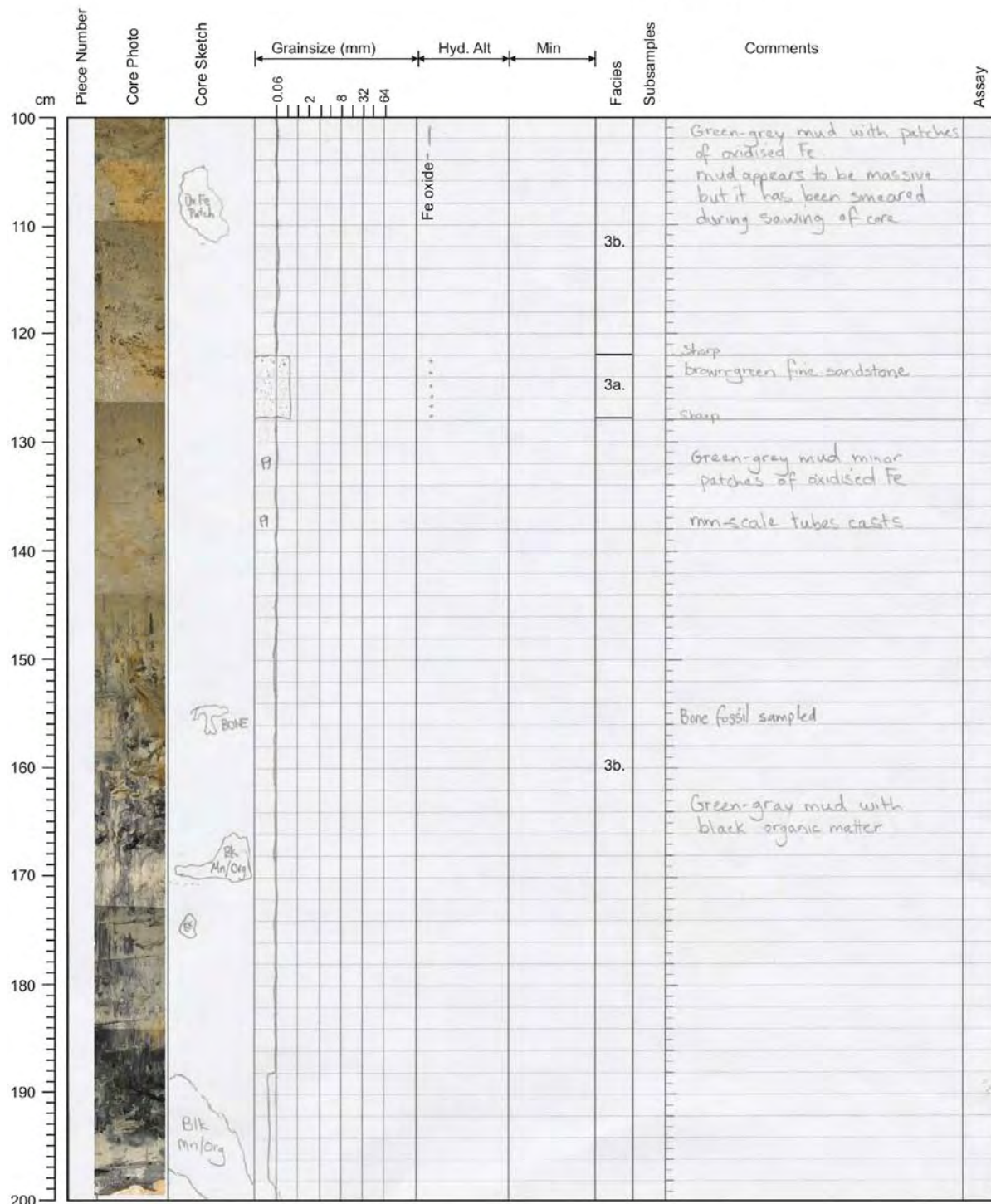
M73/2 - Station: 861 Date: Aug. 17 Time: 20:36-21:08Lat.: 39°32.354'N Long.: 14°42.444'E Water depth: 640

- ☐ Rock core
☐ Vibro core
☒ Gravity corer



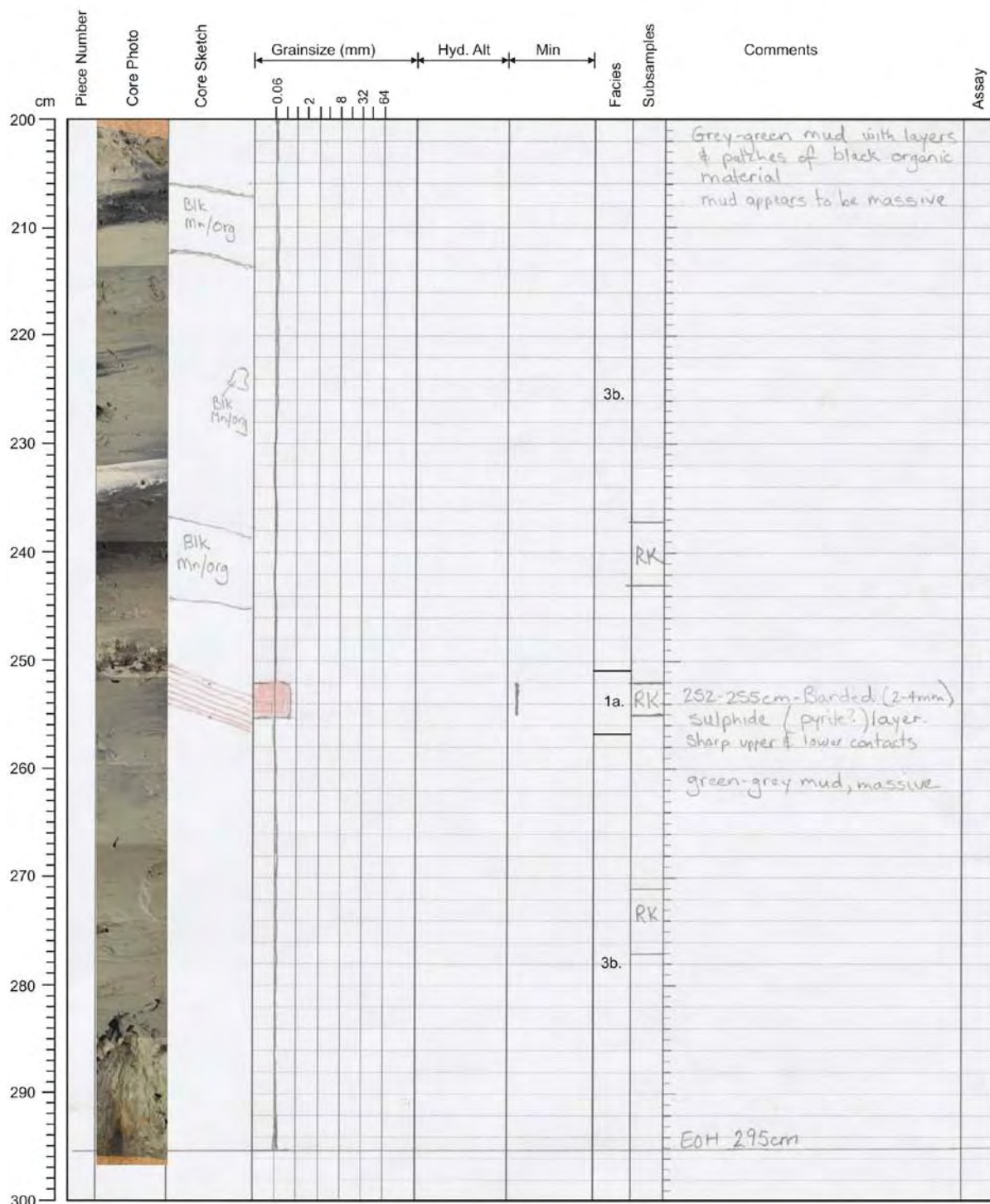
M73/2 - Station: 861 Date: Aug. 17 Time: 20:36-21:08Lat.: 39°32.354'N Long.: 14°42.444'E Water depth: 640

- ☐ Rock core
☐ Vibro core
☒ Gravity corer



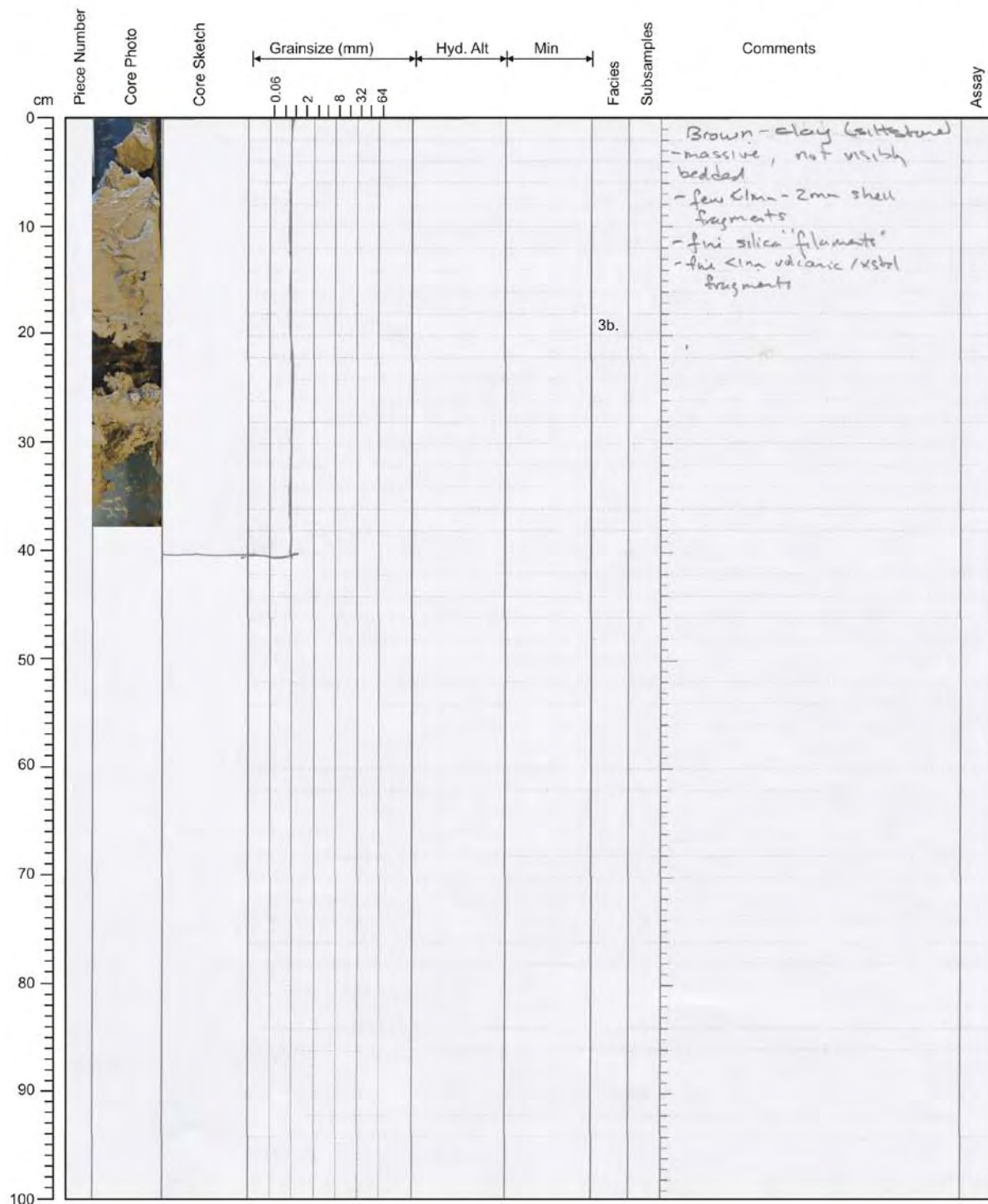
M73/2 - Station: 861 Date: Aug. 17 Time: 20:36-21:08Lat.: 39°32.354'N Long.: 14°42.444'E Water depth: 640

- ☐ Rock core
☐ Vibro core
☒ Gravity corer



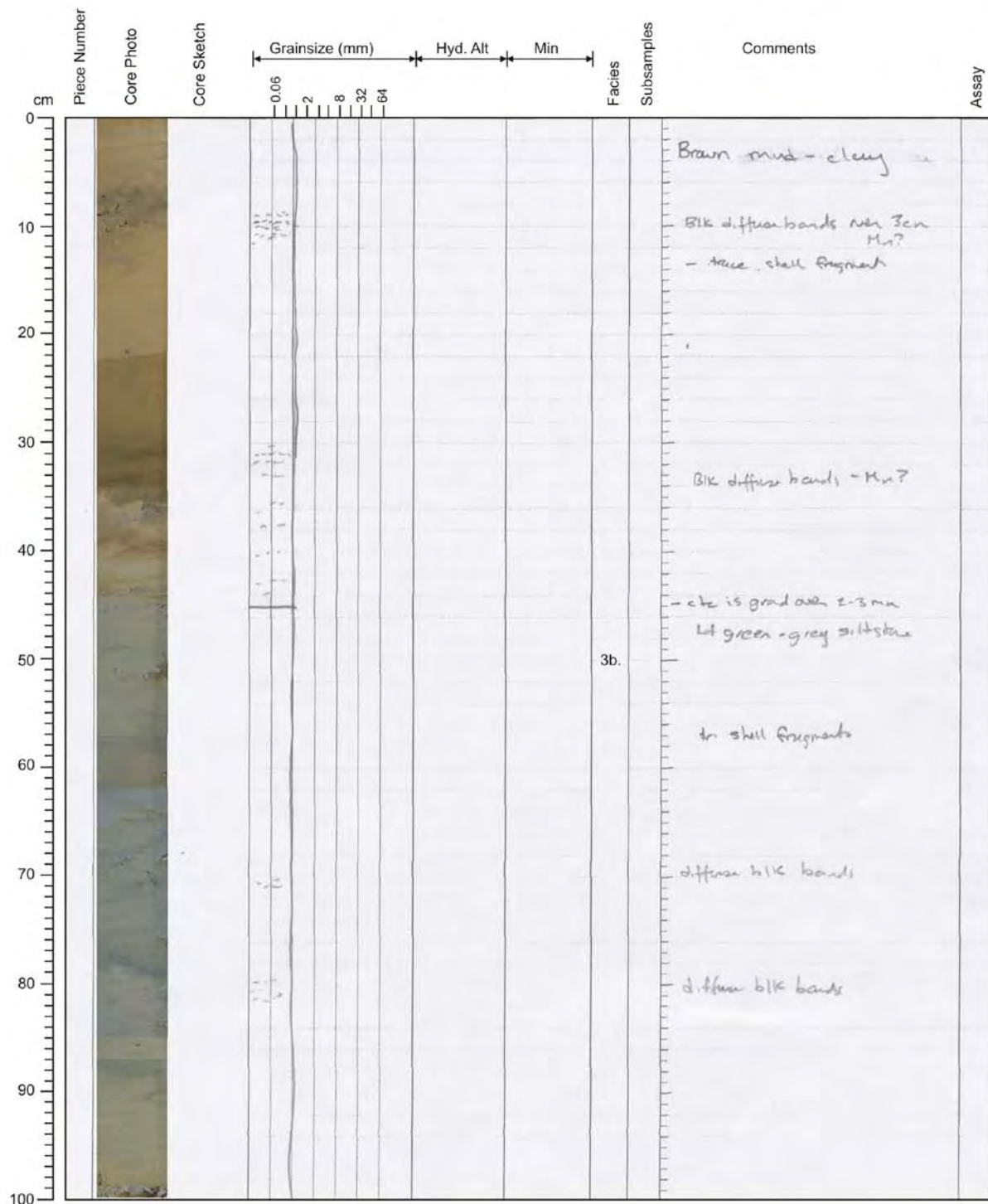
M73/2 - Station: 862 Date: Aug. 17 Time: 22:25-23:00Lat.: 39°32.504'N Long.: 14°42.300'E Water depth: 594

- ☐ Rock core
☐ Vibro core
☒ Gravity corer



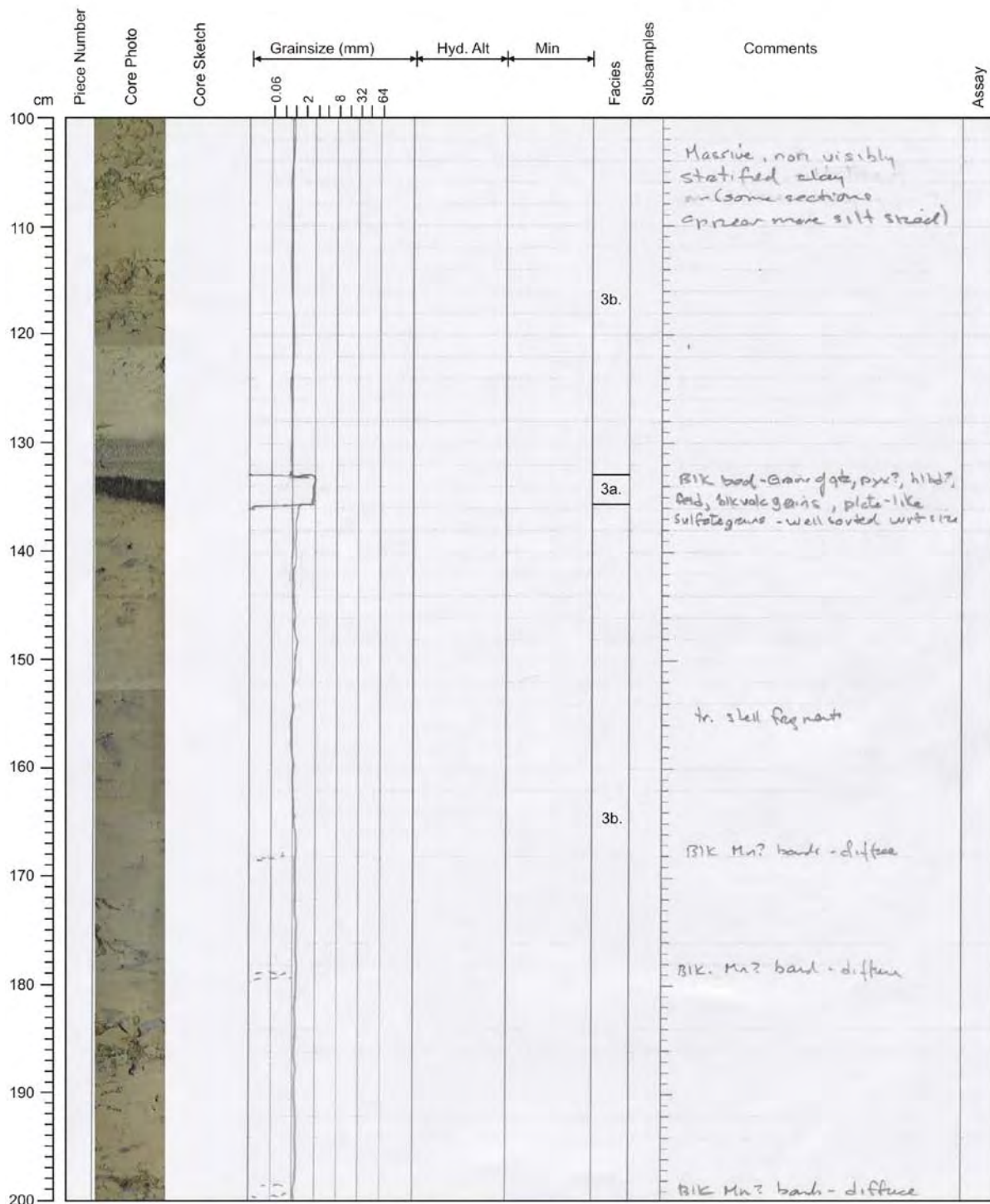
M73/2 - Station: 863 Date: Aug. 17-18 Time: 23:43-00:33Lat.: 39°31.704'N Long.: 14°40.503'E Water depth: 1071

- ☐ Rock core
☐ Vibro core
☒ Gravity corer



M73/2 - Station: 863 Date: Aug. 17-18 Time: 23:43-00:33Lat.: 39°31.704'N Long.: 14°40.503'E Water depth: 1071

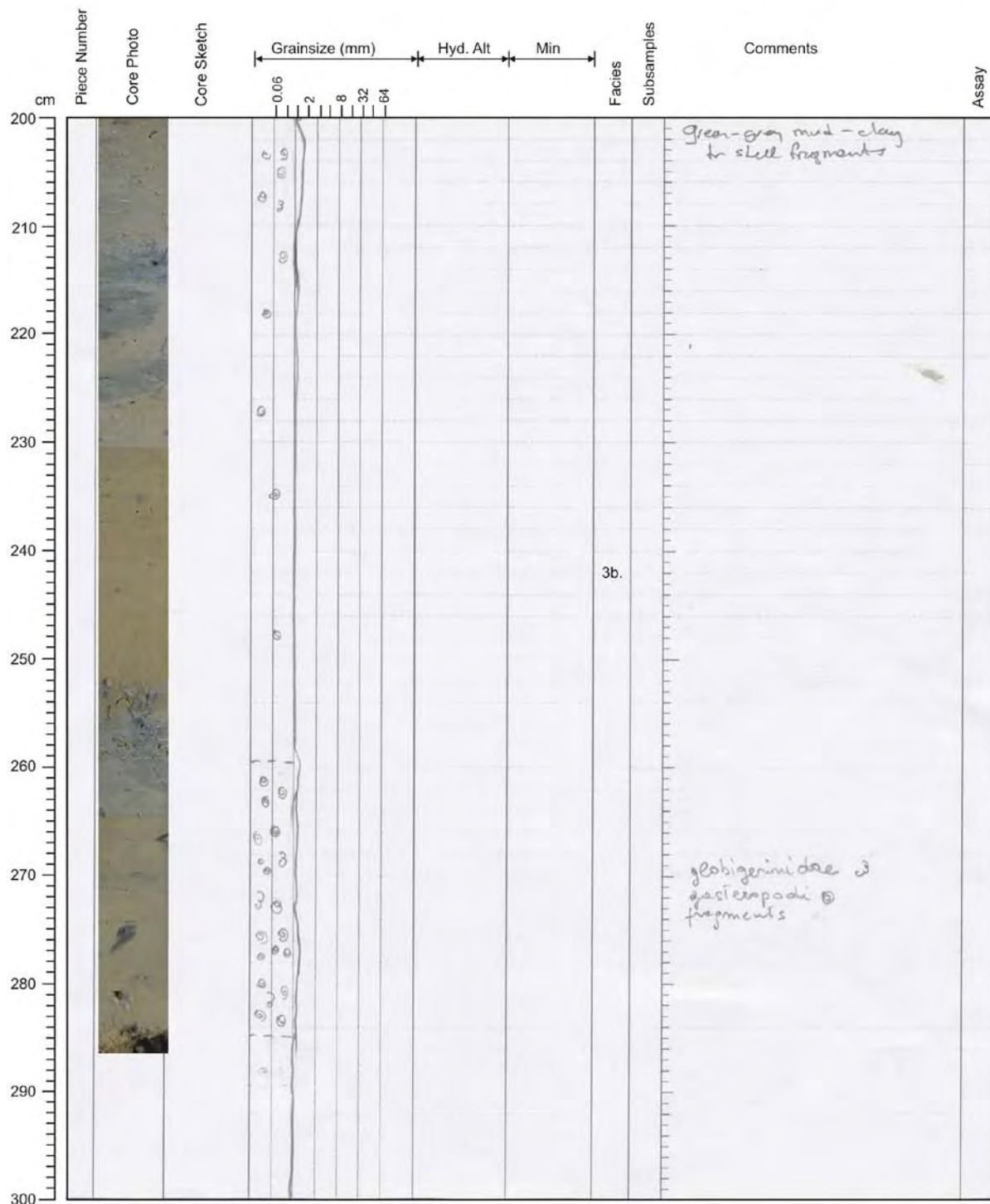
- ☐ Rock core
☐ Vibro core
☒ Gravity corer



M73/2 - Station: 863 Date: Aug. 17-18 Time: 23:43-00:33

Lat.: 39°31.704'N Long.: 14°40.503'E Water depth: 1071

- ☐ Rock core
☐ Vibro core
☒ Gravity corer



M73/2 - Station: 865 Date: Aug. 18 Time: 06:02-08:21

Lat.: 39°32.437'N Long.: 14°42.378'E Water depth: 612



- ☒ Rock core
☐ Vibro core
☐ Gravity corer



M73/2 - Station: 865 Date: Aug. 18 Time: 06:02-08:21

Lat.: 39°32.437'N Long.: 14°42.378'E Water depth: 612

- ☒ Rock core
☐ Vibro core
☐ Gravity corer



Piece Number	Core Photo	Core Sketch	Grainsize (mm)	Hyd. Alt	Min	Facies	Subsamples	Comments	Assay
			0.06 2 8 32 64						
50									
55									
60									
65									
70									
75						1c.		Barite unit with 20-25% fine disse pyrite overall, but concentrated around conduit - distinct irregular conduit lined by pyrite/marcasite and partially infilled by same with late sulphur crystals - in barite a grey metallic mineral - tetrahedrite? - marcasite/py in conduit has a botryoidal texture.	
80									
85								Pseudoclastic barite texture - remnant barite in barite-py matrix - 20-30% py - vuggy texture, py more abundant where vugs are more abundant.	
90								Vuggy textured barite unit with fine disse pyrite - 20%? - py concentrated near vugs - sulfur in cavities/vugs	
95								- fine silica in cavities at base of sample	
100									

M73/2 - Station: 865 Date: Aug. 18 Time: 06:02-08:21

Lat.: 39°32.437'N Long.: 14°42.378'E Water depth: 612

- ☒ Rock core
☐ Vibro core
☐ Gravity corer



Piece Number	Core Photo	Core Sketch	Grainsize (mm)	Hyd. Alt	Min	Facies	Subsamples	Comments	Assay
			0.06 2 8 32 64						
10								Barite unit - as above - pseudoclasts of barite - py concentrated near vugs - barite? has a pink color - anhydrite	
11								Upper part of piece is pyrite rich (+20%) within a sulfate (barite). Most of the sample consists of lighter grey sulfate - barite - that contains fine, submillimeter grey metallic mineral - tetrahedrite? with <8% pyrite that defines a "clast" within the pyrite-rich sections.	
12						1c.		Grey (faint pink) "clasts" of sulfate (barite?) containing silver-grey metallic mineral - tetrahedrite - with minor pyrite. "matrix" is a vuggy vein network of pyrite + sulphate (barite?) containing up to 15-20% (A) pyrite. Vugs lined by botryoidal pyrite (marcasite) covered by a thin "silica" film. - sulfur crystals in some vugs barite "clasts" of pyrite "matrix" are late.	M73/2 865 RD 8/6 -116-151.5 (PAL034)
13								Identical to above piece (12) - the vuggy pyrite (barite?) veins that isolate "clasts" of barite(?) contain mm to cm sized "clasts" of barite that are identical to the larger "clasts" - sulfur in vugs is late - distinct pink color of sulphide - - distinct pink color to some sulfide but "clasts" are dominantly composed of grey sulfate (barite) - heavy - vuggy texture.	
14									

M73/2 - Station: 865 Date: Aug. 18 Time: 06:02-08:21

Lat.: 39°32.437'N Long.: 14°42.378'E Water depth: 612

- ☒ Rock core
☐ Vibro core
☐ Gravity corer



Piece Number	Core Photo	Core Sketch	Grainsize (mm)	Hyd. Alt	Min	Facies	Subsamples	Comments	Assay
14			0.06 2 8 32 64					as above	
15								"Pseudoclastic facies" - blocky clasts of dominantly grey but also pink sulfide (plus pyrite + grey metallic minerals - tetrahedrite) within a pyrite-sulfide matrix. "clasts" range from 5-6 cm (t) to 2-3 mm and have sharp contacts with pyritic "ven matrix". matrix & clasts - vuggy - botryoidal py (marcasite) in cavities / vugs.	
16						1c.		- identical to piece 15 but with slightly more sulphur crystals in the vugs. - thin 1-3 mm rims of dense (massive) pyrite following margins of some of the larger vugs - some of the sulfide is "pink" in color - lower section from 180-184 contains 30-35% pyrite (vuggy).	(PAL 035) 151.5-188 RD C/6- 865 - M73/2
17								same as pieces 15+16 - pink color to some of the sulfate "clasts" - rounded "clasts" - diffuse margins with matrix.	
18								same - pink "sulfide" in vugs	
19								upper 2cm same as above	

M73/2 - Station: 865 Date: Aug. 18 Time: 06:02-08:21

Lat.: 39°32.437'N Long.: 14°42.378'E Water depth: 612

- ☒ Rock core
☐ Vibro core
☐ Gravity corer



Piece Number	Core Photo	Core Sketch	Grainsize (mm)	Hyd. Alt	Min	Facies	Subsamples	Comments	Assay
			0.06 2 8 32 64						
19								- dense, compact pyrite veins with internal vugs containing barite. - contains subhengl. clast of barite (?) up to 4cm; clast have sharp boundaries. - fossil fluid conduit - very nice! - fine-grained malachite lining same vugs - no silica in cavities - metallic	
20								- same baritic (?) unit as in pieces 15-18. - metallic Ag minerals throughout baritic "clast" - sulphur crystallized on py-malachite in cavity	
21								- ghost-like "baritic clasts" veined by dics + dense massive py vein-vein network - finer sulphate + py in mtx - minor sulphur in cavities	
22						1c.		- distinct + ghost-like baritic (?) "clasts" - vein-network of open-space sulphate cts between sulfide clasts and py-sulfate mtx.	
23								- as above	
24								- vuggy barite with larger vugs filled with sulphur crystals and Ag metallic minerals (<5%). - Fr. sharp cte with porite-barite "mtx" containing smaller sulphate clasts some of which are pink	
25								- same as lower part of piece 24	

M73/2 - Station: 865 Date: Aug. 18 Time: 06:02-08:21

Lat.: 39°32.437'N Long.: 14°42.378'E Water depth: 612

- ☒ Rock core
☐ Vibro core
☐ Gravity corer



Piece Number	Core Photo	Core Sketch	Grainsize (mm)	Hyd. Alt	Min	Facies	Subsamples	Comments	Assay
			0.06 2 8 32 64						
25						1c.		Angular-subrounded clasts of white-pink sulfate that range from 4 cm to 1 mm - sharp boundaries - mtx is a fine mixture of sulfate crystals, finer sulfate? and pyrite - mtx looks finer - sulfide/sulfate mixture - dense, heavy - barite? - mtx does not look like a vein	
26								- individual sulfate "clasts" are less common - matrix is a mixture between barite/sulfate and fine pyrite - perhaps 20-30% pyrite - From 246 m to 269 m the number + size of "sulfate clasts" decreases	
27								Gradational Boundary ↑ No visible "sulfate clast" - unit consists of a fine sulfate crystal network as above within fine pyrite intergrowth - Pyrite content increases from 250 m downward - waxy texture - later sulfur	
28						1d.		Vuggy sulfate-pyrite mixture as above - sulfate crystals in some vugs - sulfur crystals in some vugs	
29								dense mixture of dominantly pyrite with fine sulfate - white, diffuse specks - clasts of possible sulfide - coarser barite/sulfate + sulphur (lute) in vugs or adjacent to vugs	
30								- as above	
31									

M73/2 - 865 - RD - D/6 - 261-308.5 (PAL 038)

M73/2 - Station: 865 Date: Aug. 18 Time: 06:02-08:21

Lat.: 39°32.437'N Long.: 14°42.378'E Water depth: 612

- ☒ Rock core
☐ Vibro core
☐ Gravity corer



Piece Number	Core Photo	Core Sketch	Grainsize (mm)	Hyd. Alt	Min	Facies	Subsamples	Comments	Assay
cm			0.06 2 8 32 64						
300								- Pyrite-sulfate mixture as above - white specks (1mm - 2mm) may be sulfate + silica ?? - sulfur in some vugs	
305						1d.			
310								Predominately a dense fine pyrite - massive sulfide but lower right corner contains fine sulfate/silica - wussy - fine grey "sulfide" - may be pyrite in vugs	
315								As above - dense massive wussy pyrite - sulfate in vugs + white silica?	
320								Dense, massive fine pyrite with a weak fabric defined by trails of vugs - white speckled + silica?	
325								As above	
330									
335						1e.		- Dense pyrite as above cut by veins of sulfate with minor sulfur + silvery metallic mineral - tetrahedrite	
340								- Same as above - sulfate (barite veins) cut by, and contains pyrite + silver metallic mineral - sulphur in vugs	
345								- irregular vein-like silica with intergrown pyrite transecting massive pyrite - imparting a foliation or fabric	
350								Same as above	

M73/2 - Station: 865 Date: Aug. 18 Time: 06:02-08:21Lat.: 39°32.437'N Long.: 14°42.378'E Water depth: 612

- ☒ Rock core
☐ Vibro core
☐ Gravity corer



Piece Number	Core Photo	Core Sketch	Grainsize (mm)	Hyd. Alt	Min	Facies	Subsamples	Comments	Assay
350			0.06 2 8 32 64						
39									
40								As above - Dense, for massive pyrite - silica warts.	
355									
360								- lower etc is vuggy - breccia? as below in piece 41	
41								- Breccia? - subvol - rounded "clasts" of MS pyrite in an "open space" matrix of silica + sulfur - Gray sulphide with pyrite vugs - ?	
365									
370									
42								Same as piece 41	
375						1e.			
43								Same as piece 41 + 42	
380								massive dense pyrite - vuggy - upper part contains gray sulfide + pyrite as above - white specks = sulfate and or silica (amorphous?) - sulfate is vugs	
44									
385									
45								- as above, dense massive pyrite	
390									
395									
46								as above	
400									

M73/2 - Station: 865 Date: Aug. 18 Time: 06:02-08:21

Lat.: 39°32.437'N Long.: 14°42.378'E Water depth: 612

- ☒ Rock core
☐ Vibro core
☐ Gravity corer



Piece Number	Core Photo	Core Sketch	Grainsize (mm)	Hyd. Alt	Min	Facies	Subsamples	Comments	Assay
cm			0.06 2 8 32 64						
400								Massive dense pyrite - lower left corner is vuggy + possibly a breccia as above in pieces 41 + 42.	
405								-sulphide breccia plus sulphur in massive pyrite? or breccia?	
410								Upper part is a breccia as in 41 + 42. -lower section is massive, dense pyrite with specks - vugs filled by white silica?	
415									
420								dense pyrite - massive - silica spots	
425						1e.		-Sulphide breccia as in 41 + 42	
430								-sulphide breccia as in 41 + 42	
435								Sulphide breccia as in 41 + 42	
440								-sulphide breccia in upper part of piece in etc with more massive, for pyrite - etc is irregular and somewhat diffuse	
445								Massive, dense, pyrite - lower half contains specks of white silica?	
450								- Same as above in piece 55	

M73/2 - Station: 865 Date: Aug. 18 Time: 06:02-08:21Lat.: 39°32.437'N Long.: 14°42.378'E Water depth: 612

- ☒ Rock core
☐ Vibro core
☐ Gravity corer

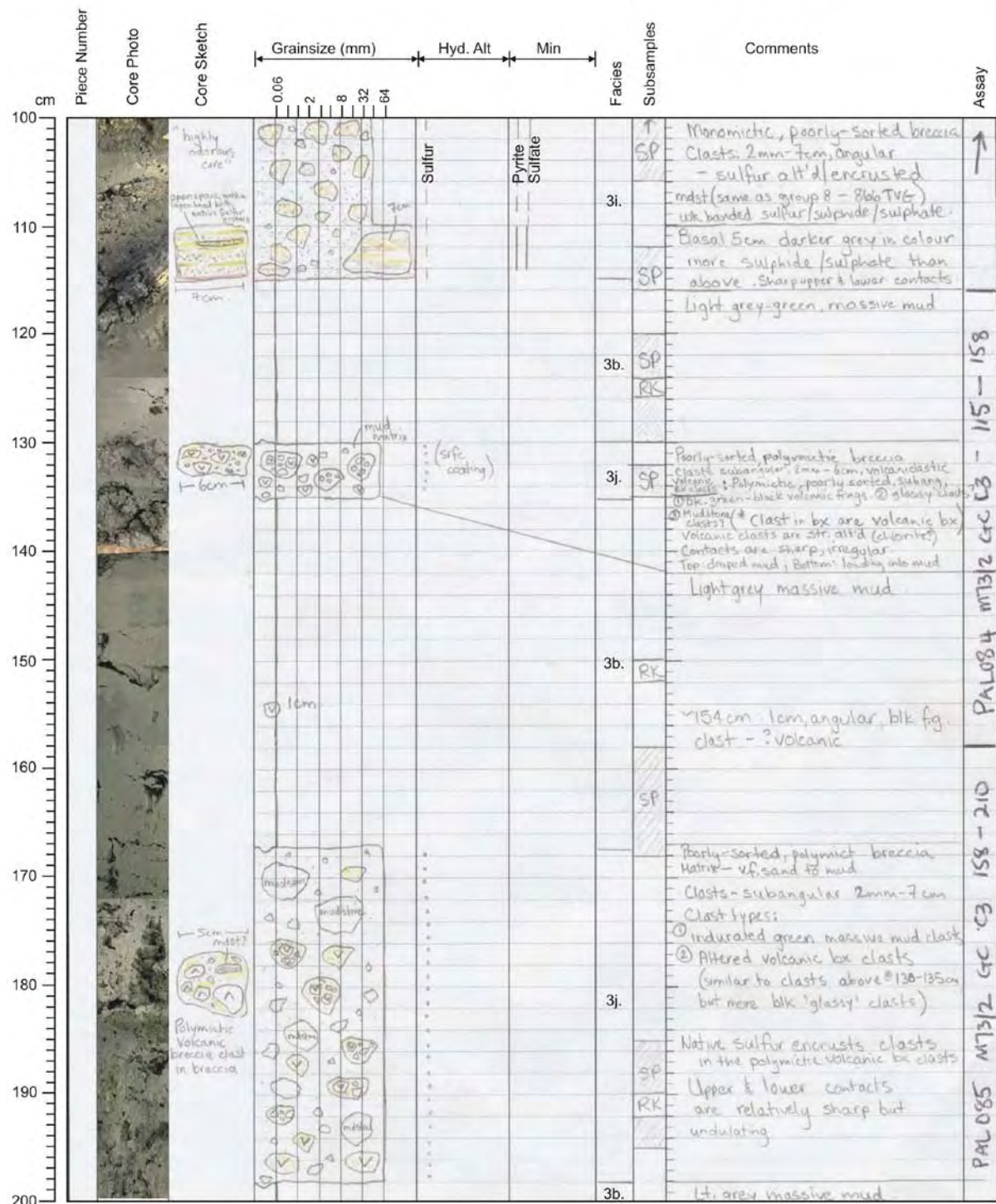


Piece Number	Core Photo	Core Sketch	Grainsize (mm)	Hyd. Alt	Min	Facies	Subsamples	Comments	Assay
cm			0.06 2 8 32 64						
450								As above, sulfate xstals in some vugs	
455								Massive dense pyrite, luggy - some vugs filled by sulfate, magenta color in white silica (amorphous?) and/or Sulphur	
460								As above in piece S7	
465									
470						1e.		As above - very coarse sulfate veins, some with sulfur xstals - grey metallic mineral possibly tetrahedrite - appears to grow on FeS pyrite + sulfate xstals in veins.	
475								Same as above in piece S9	
480									
485									
490									
495									
500									

M73/2 - Station: 871 Date: Aug. 19 Time: 14:03-14:44

Lat.: 39°32.419'N Long.: 14°42.382'E Water depth: 633


- ☐ Rock core
☐ Vibro core
☒ Gravity corer



M73/2 - Station: 871 Date: Aug. 19 Time: 14:03-14:44Lat.: 39°32.419'N Long.: 14°42.382'E Water depth: 633

- ☐ Rock core
☐ Vibro core
☒ Gravity corer

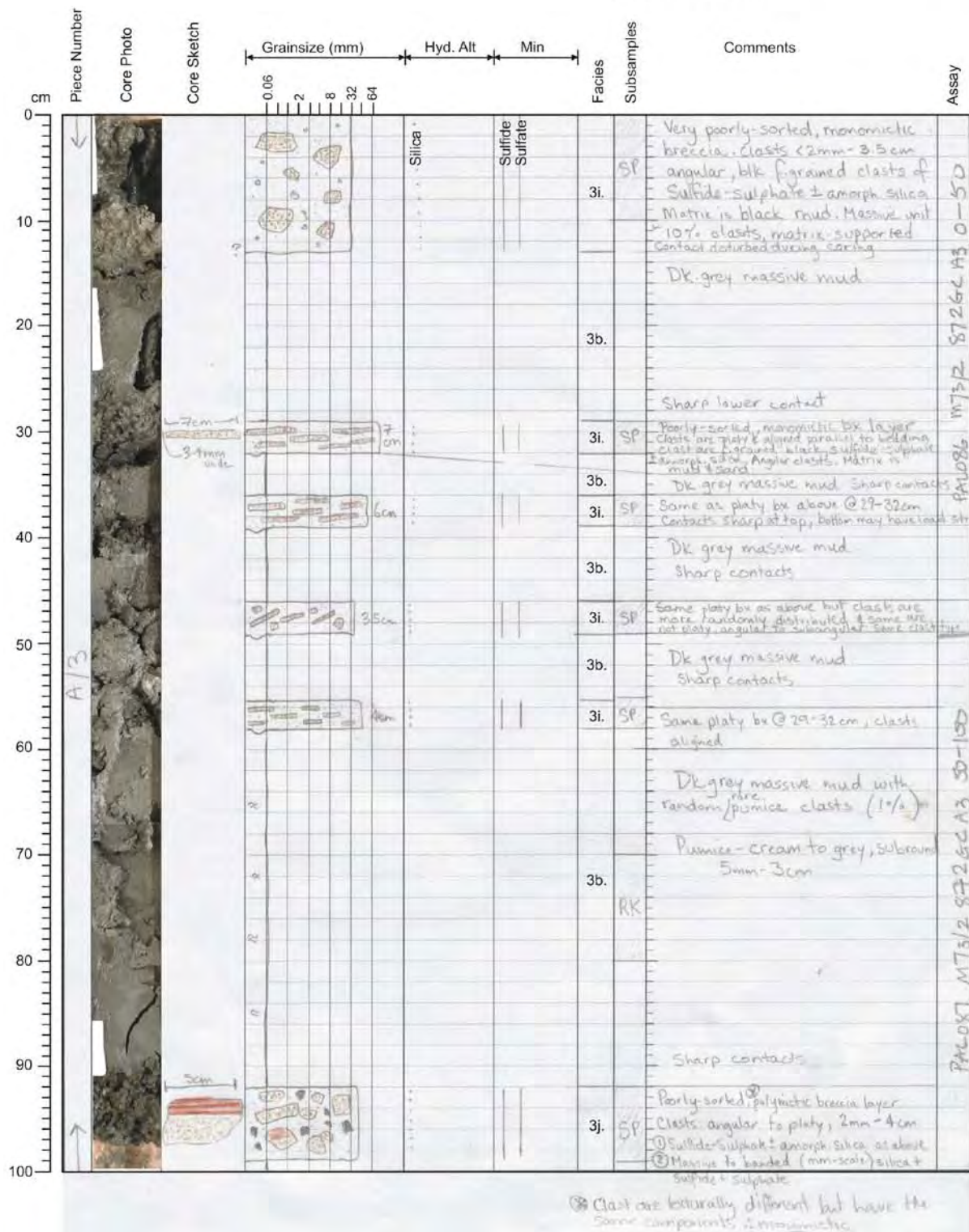


Piece Number	Core Photo	Core Sketch	Grainsize (mm)	Hyd. Alt	Min	Facies	Subsamples	Comments	Assay
			0.06 2 8 32 64						
200						3b.	SP	Lt. grey massive mud	
210								EOH=210cm	
220									
230									
240									
250									
260									
270									
280									
290									
300									

M73/2 - Station: 872 Date: Aug. 19 Time: 16:00-16:40

Lat.: 39°32.443'N Long.: 14°42.390'E Water depth: 628

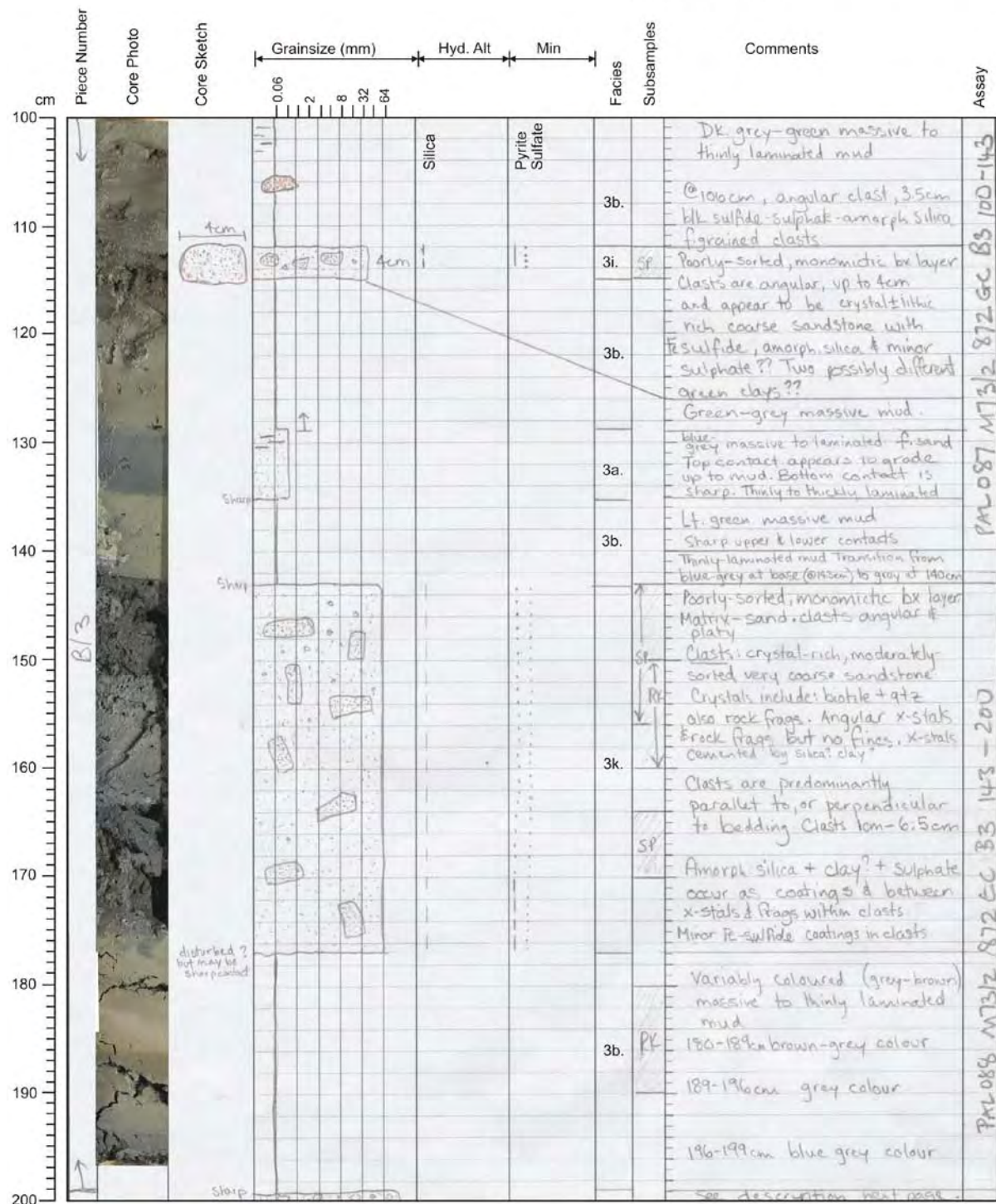
- ☐ Rock core
☐ Vibro core
☒ Gravity corer



M73/2 - Station: 872 Date: Aug. 19 Time: 16:00-16:40

Lat.: 39°32.443'N Long.: 14°42.390'E Water depth: 628

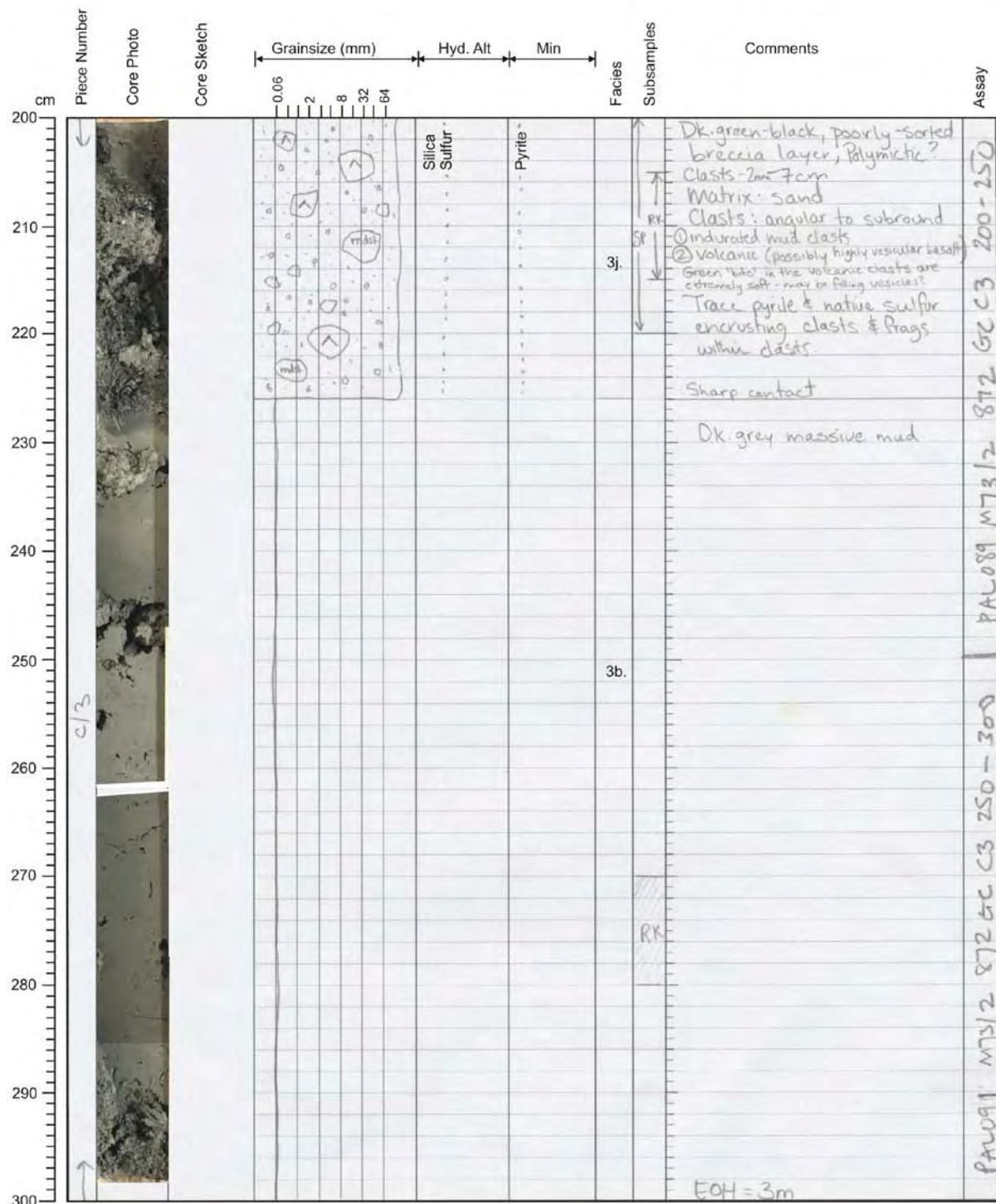
- ☐ Rock core
☐ Vibro core
☒ Gravity corer



M73/2 - Station: 872 Date: Aug. 19 Time: 16:00-16:40

Lat.: 39°32.443'N Long.: 14°42.390'E Water depth: 628

- ☐ Rock core
☐ Vibro core
☒ Gravity corer



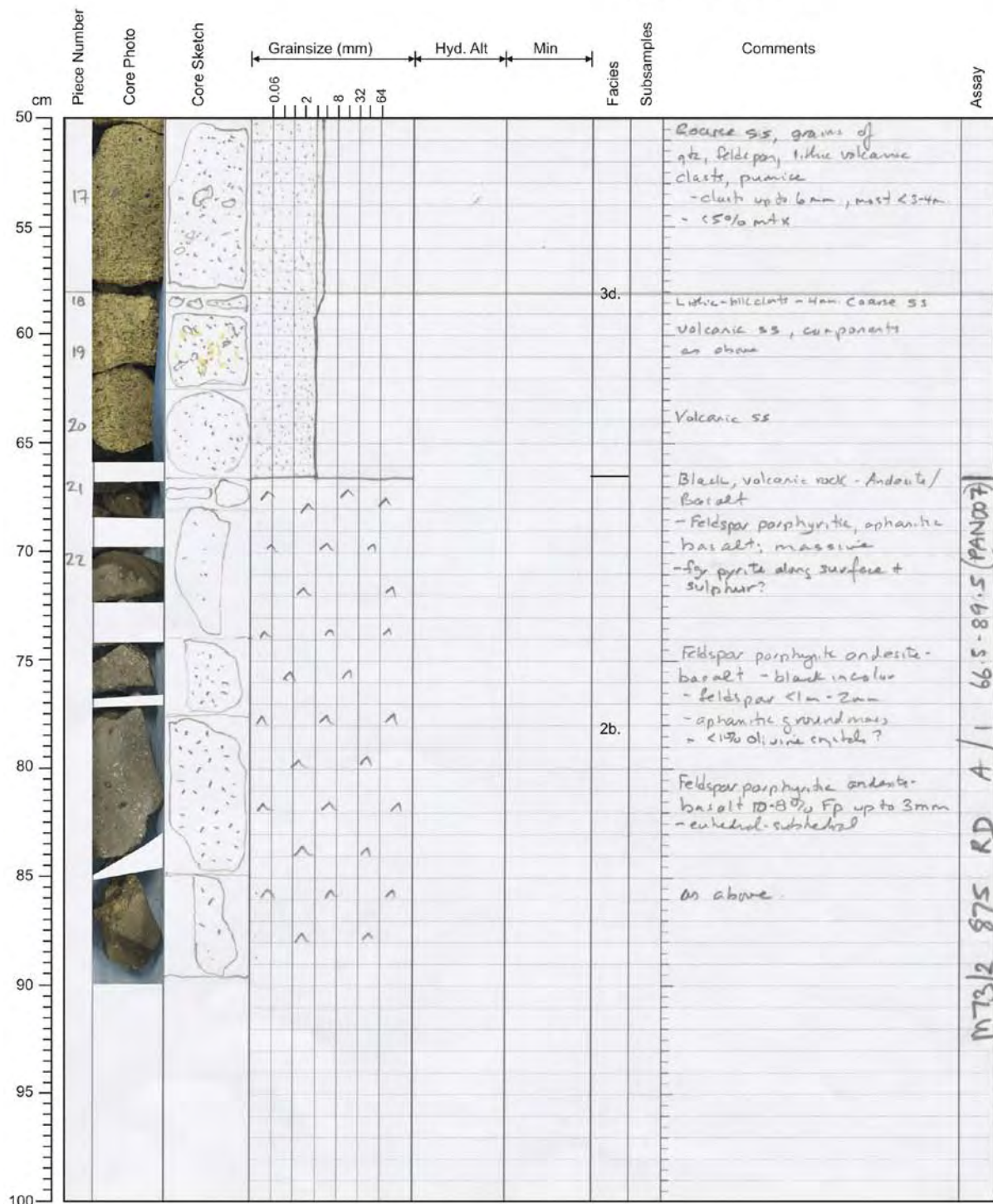
M73/2 - Station: 875 Date: Aug. 20 Time: 11:21-12:35

Lat.: 38°38.854'N Long.: 15°06.728'E Water depth: 56



2/2

- ☒ Rock core
☐ Vibro core
☐ Gravity corer



M73/2 - Station: 876 Date: Aug. 20 Time: 12:56-14:09Lat.: 38°38.848'N Long.: 15°06.719'E Water depth: 52

- ☒ Rock core
☐ Vibro core
☐ Gravity corer

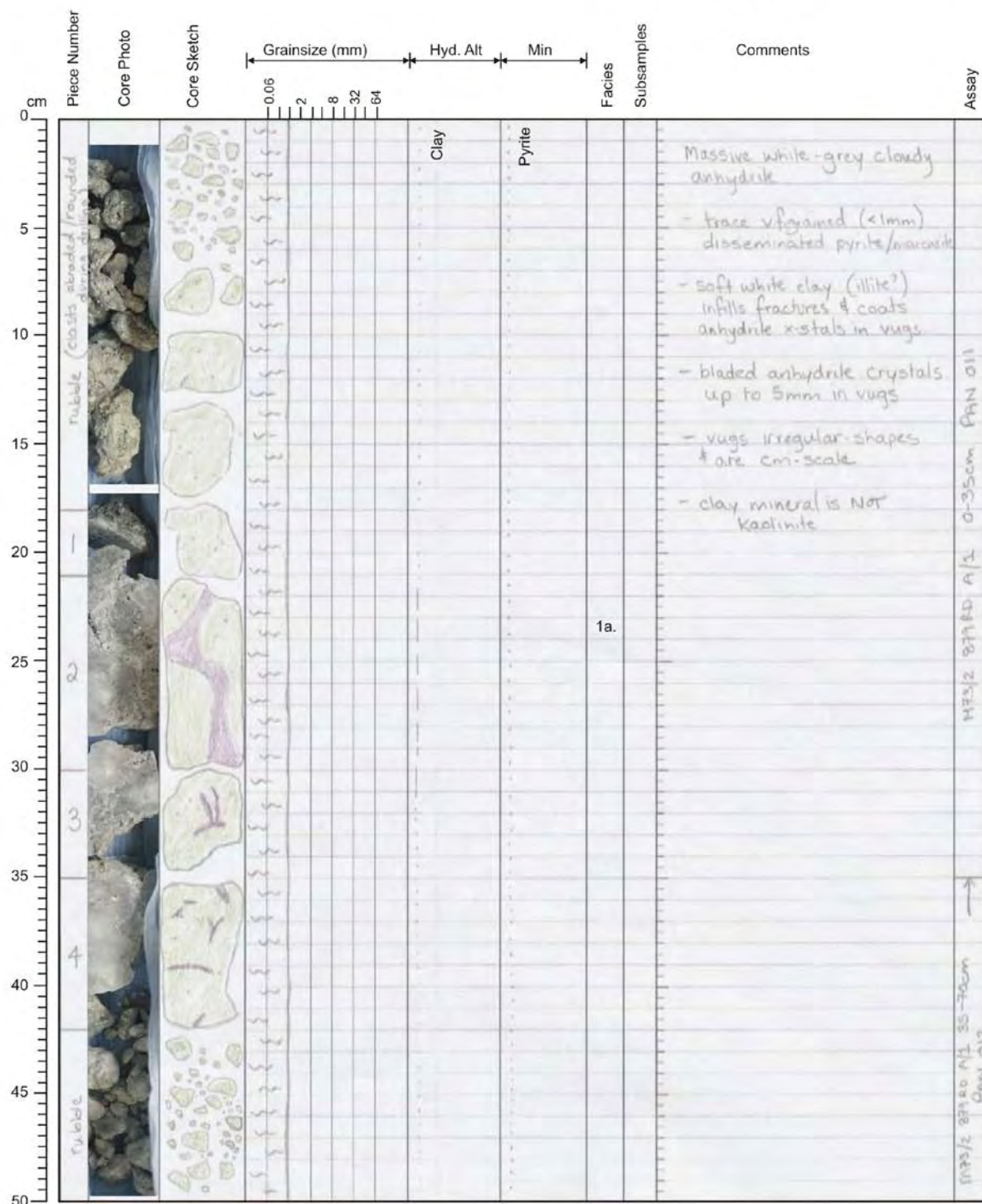


cm	Piece Number	Core Photo	Core Sketch	Grainsize (mm)					Hyd. Alt	Min	Facies	Subsamples	Comments	Assay
				0.06	2	8	32	64						
0	1												Feld porphyritic coherent Dacite - Rhyodacite	M73h 876 RD A/1
5	2										2b.		- 3-5% Fp - subhedral - aphanitic groundmass - possible xenolith of volcanoclastic - mottled appearance - py in fractures - silicified (?)	
10	3													
15														
20														
25														
30														
35														
40														
45														
50														

M73/2 - Station: 879 Date: Aug. 20 Time: 18:06-19:07

Lat.: 38°38.876'N Long.: 15°06.540'E Water depth: 54

- ☒ Rock core
☐ Vibro core
☐ Gravity corer



M73/2 - Station: 879 Date: Aug. 20 Time: 18:06-19:07Lat.: 38°38.876'N Long.: 15°06.540'E Water depth: 54

- ☒ Rock core
☐ Vibro core
☐ Gravity corer

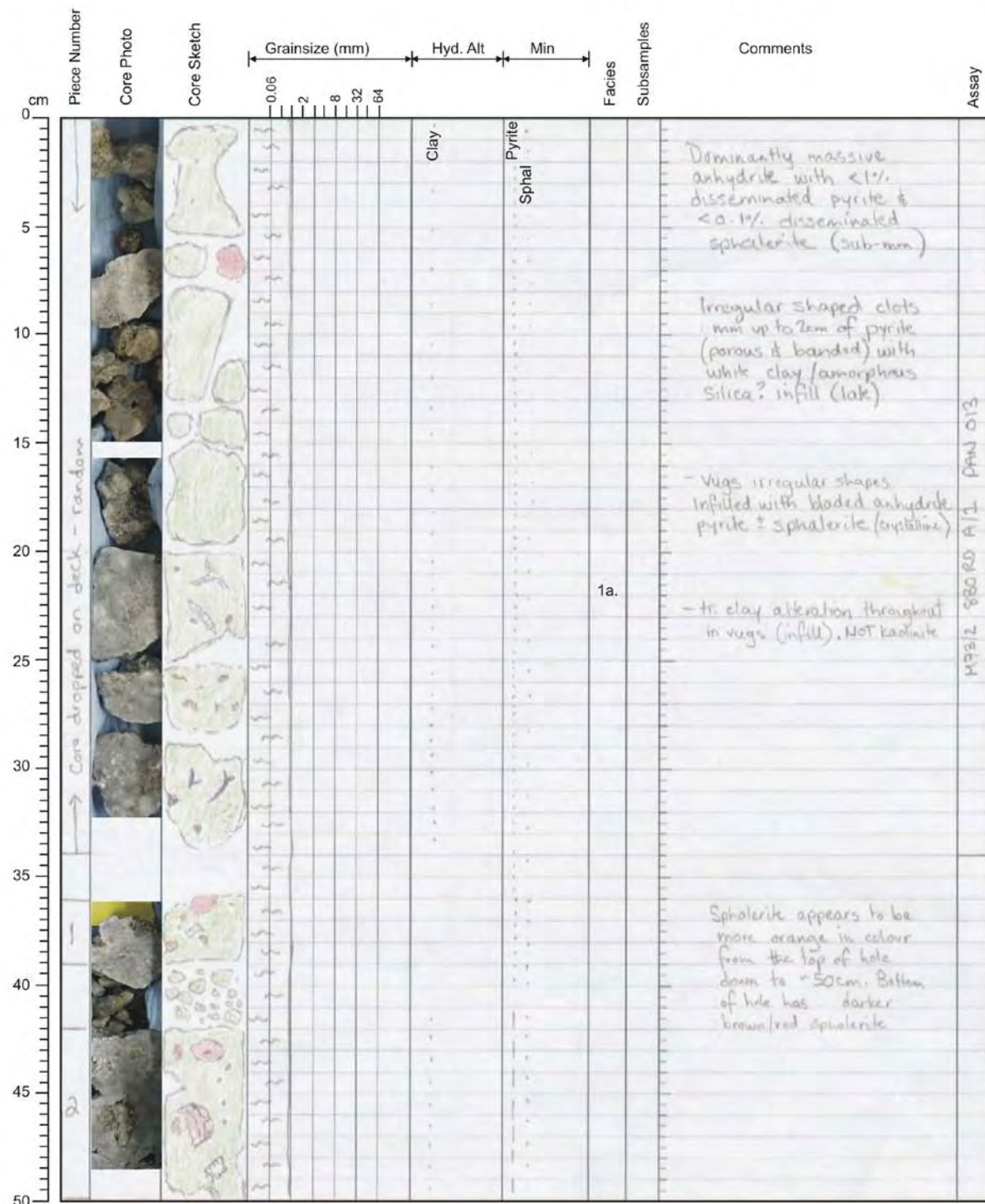


Piece Number	Core Photo	Core Sketch	Grainsize (mm)	Hyd. Alt	Min	Facies	Subsamples	Comments	Assay
50			0.06						
55			2			Clay			
60			8			Pyrite			
65			32						
70			64						
75									
80									
85									
90									
95									
100									

M73/2 - Station: 880 Date: Aug. 20 Time: 19:29-21:36

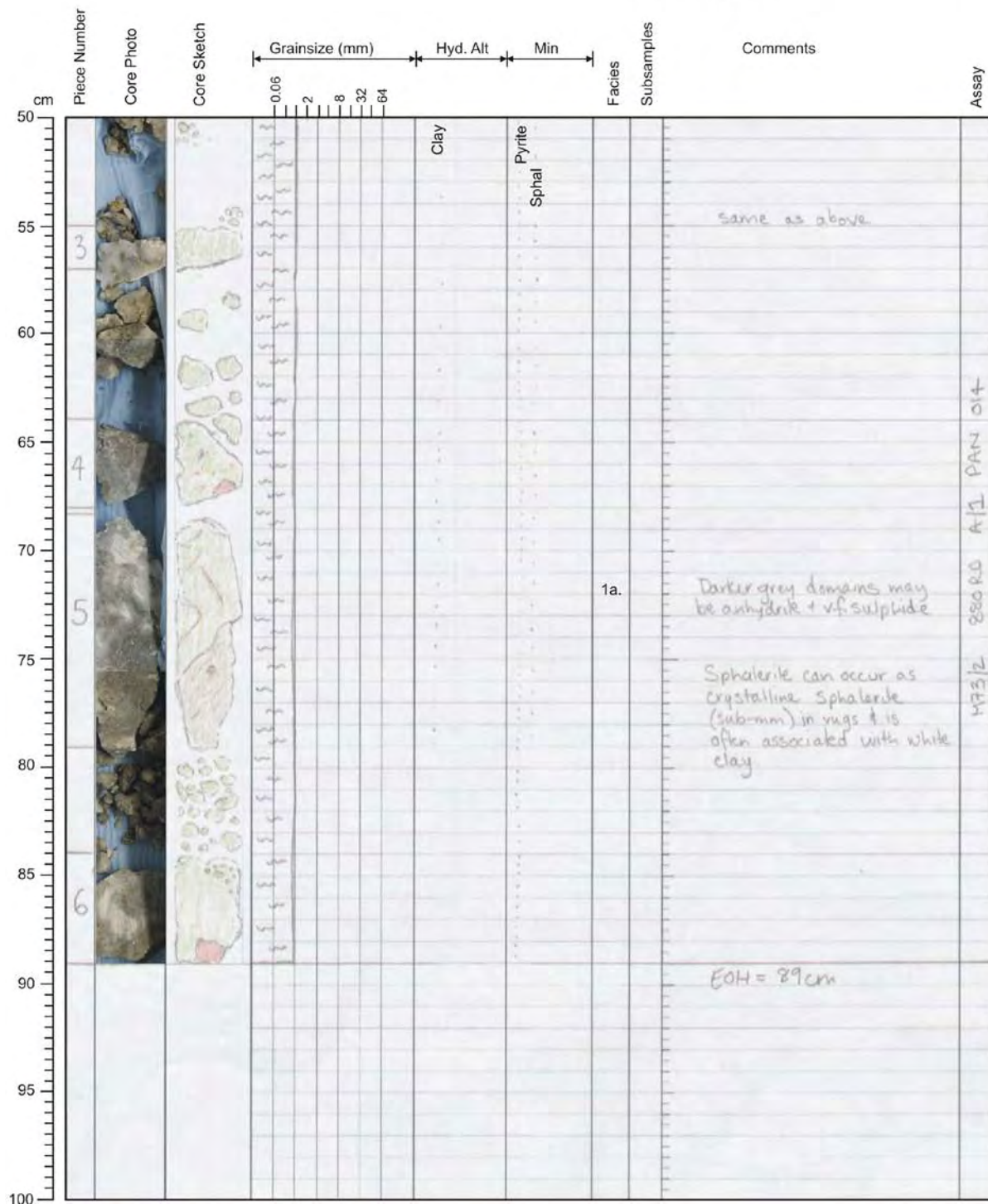
Lat.: 38°38.882'N Long.: 15°06.535'E Water depth: 55

- ☒ Rock core
☐ Vibro core
☐ Gravity corer



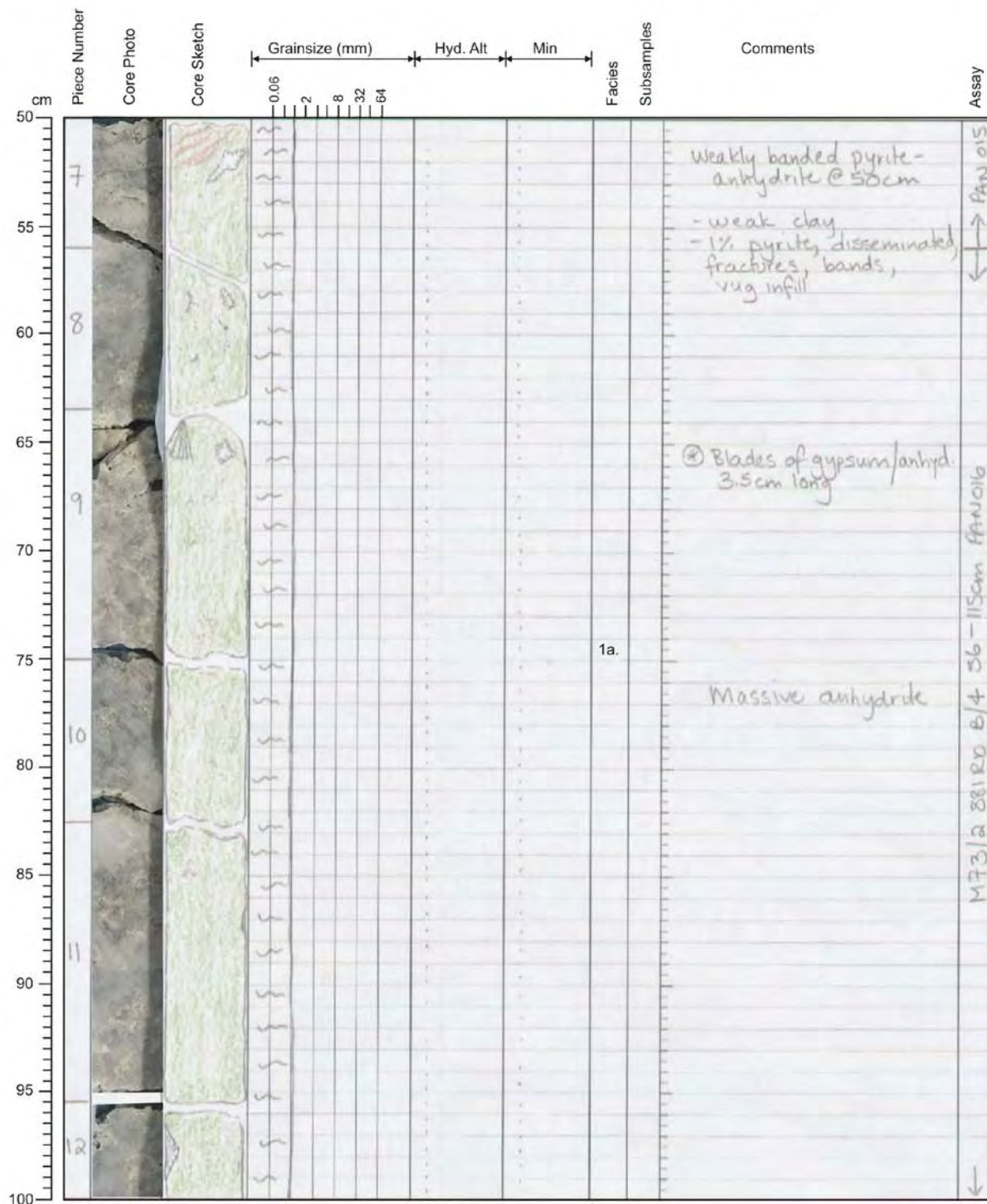
M73/2 - Station: 880 Date: Aug. 20 Time: 19:29-21:36Lat.: 38°38.882'N Long.: 15°06.535'E Water depth: 55

- ☒ Rock core
☐ Vibro core
☐ Gravity corer



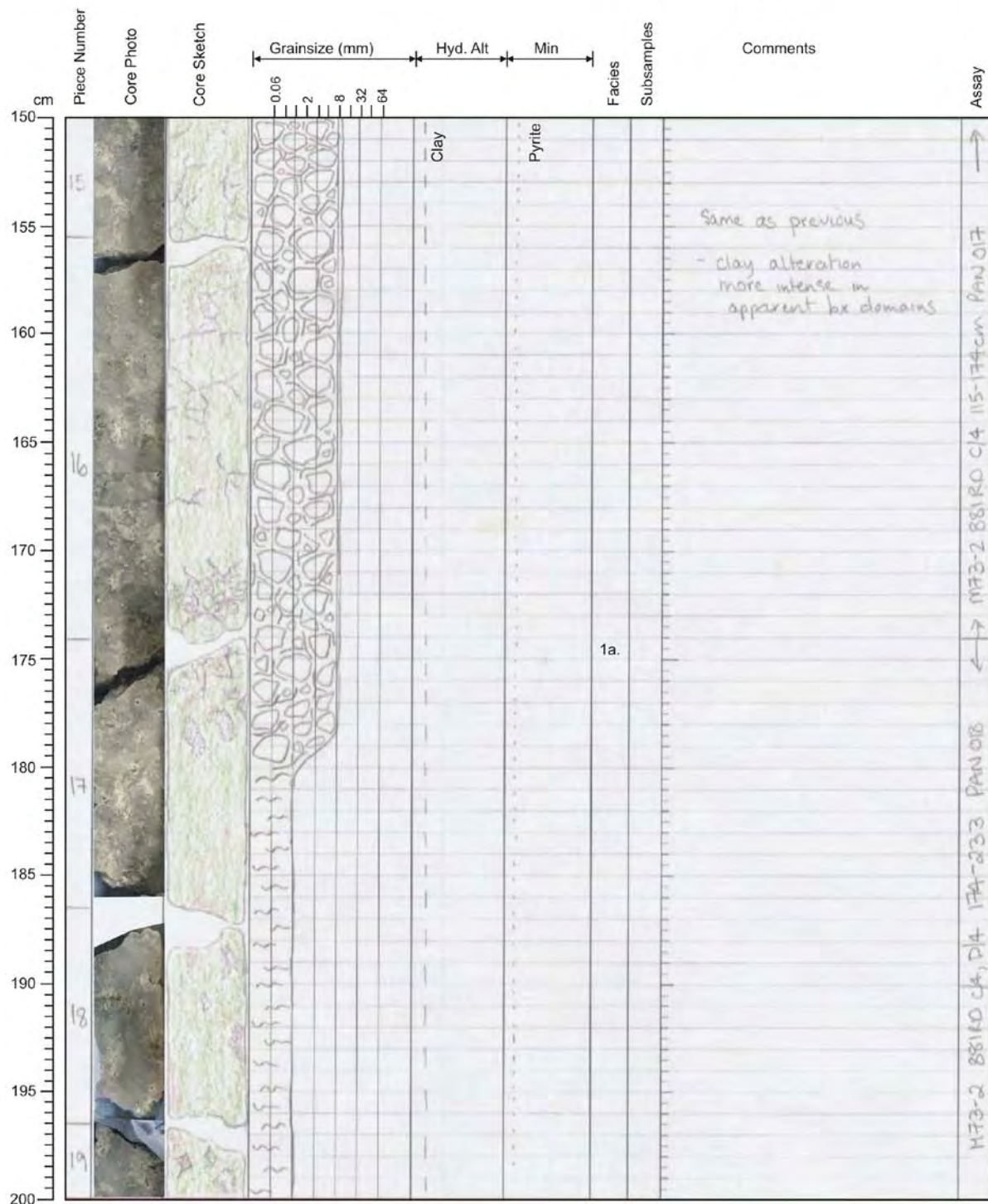
M73/2 - Station: 881 Date: Aug. 20 Time: 22:00-00:13Lat.: 38°38.893'N Long.: 15°06.522'E Water depth: 61

- ☒ Rock core
☐ Vibro core
☐ Gravity corer



M73/2 - Station: 881 Date: Aug. 20 Time: 22:00-00:13Lat.: 38°38.893'N Long.: 15°06.522'E Water depth: 61

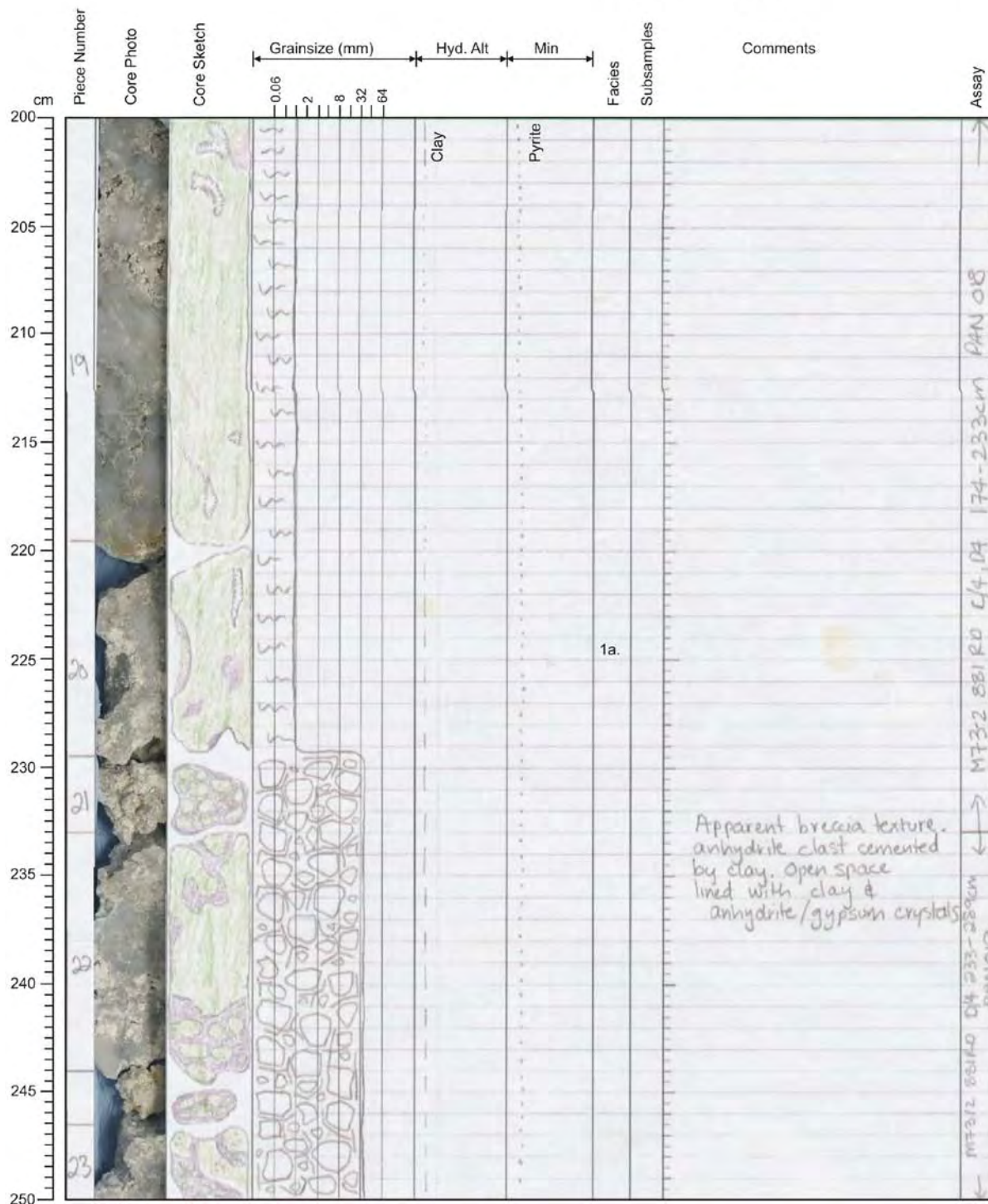
- ☒ Rock core
☐ Vibro core
☐ Gravity corer



M73/2 - Station: 881 Date: Aug. 20 Time: 22:00-00:13

Lat.: 38°38.893'N Long.: 15°06.522'E Water depth: 61

- ☒ Rock core
☐ Vibro core
☐ Gravity corer



M73/2 - Station: 881 Date: Aug. 20 Time: 22:00-00:13Lat.: 38°38.893'N Long.: 15°06.522'E Water depth: 61

- ☒ Rock core
☐ Vibro core
☐ Gravity corer



M73/2 - Station: 883 Date: Aug. 21 Time: 02:23-03:45

Lat.: 38°38.871'N Long.: 15°06.502'E Water depth: 74

- ☒ Rock core
☐ Vibro core
☐ Gravity corer



Piece Number	Core Photo	Core Sketch	Grainsize (mm)	Hyd. Alt	Min	Facies	Subsamples	Comments	Assay
			0.06 2 8 32 64						
1				Clay	Pyrite	3a.		Mud - clay - loose crystals - grains of anhydrite - grey	
2									
3								bladed anhydrite crystals - clay between crystals	
4								bladed anhydrite crystals	
5								bladed anhydrite crystals with clay between crystals - possibly some gypsum crystals (monoclinic) - recrystallized	
6								Loose aggregate of bladed anhydrite crystals	
7						1a.		- Bladed anhydrite crystals with "amorphous" soft black material between crystals - Mn? - minor clay between crystals - black material occurs between or in bands perpendicular to crystals	
8								- loose aggregate of bladed anhydrite crystals locally recrystallized to gypsum - trace to locally 10% fine dark pyrite + silver mineral possibly arsenopyrite between crystals	
9								bladed anhydrite - clay on crystal surfaces	
10								bladed anhydrite - minor clay Anhydrite grains recrystallized to gypsum - silvery sulphide + pyrite along crystal boundaries	

M73/2 - Station: 883 Date: Aug. 21 Time: 02:23-03:45Lat.: 38°38.871'N Long.: 15°06.502'E Water depth: 74

- ☒ Rock core
☐ Vibro core
☐ Gravity corer



Piece Number	Core Photo	Core Sketch	Grainsize (mm)	Hyd. Alt	Min	Facies	Subsamples	Comments	Assay
cm			0.06 2 8 32 64						
50								as above	
55						Pyrite			
60							1a.	bladed anhydrite, locally recrystallized to gypsum	
65								aggregate of loose anhydrite crystals + gypsum	
70						Sphalerite		Anhydrite crystals - minor gypsum.	
75								Pyrite, white-silver sulfide + possible sphalerite	
80									
85									
90									
95									
100									

M73/2 - Station: 884 Date: Aug. 21 Time: 04:13-05:50

Lat.: 38°38.872'N Long.: 15°06.493'E Water depth: 75

- ☒ Rock core
☐ Vibro core
☐ Gravity corer



Piece Number	Core Photo	Core Sketch	Grainsize (mm)	Hyd. Alt	Min	Facies	Subsamples	Comments	Assay
0			0.06						
1						3a.		gray-black clay-silt	
2								loose aggregate of anhydrite variably recrystallized to gypsum. - minor clay along and between gypsum/anhydrite crystals	1.5-32.5
3						1a.		Vein-like gypsum cutting anhydrite	
4								Anhydrite variably recrystallized to gypsum - vugs contain white clay mineral. - fr pyrite	
5								as above	
6								as above	
7								as above - pyrite between + inside gypsum/anhydrite crystals.	32.5-70.5
8								crystal of anhydrite	
50									

M73/2 - Station: 886 Date: Aug. 21 Time: 08:49-09:47

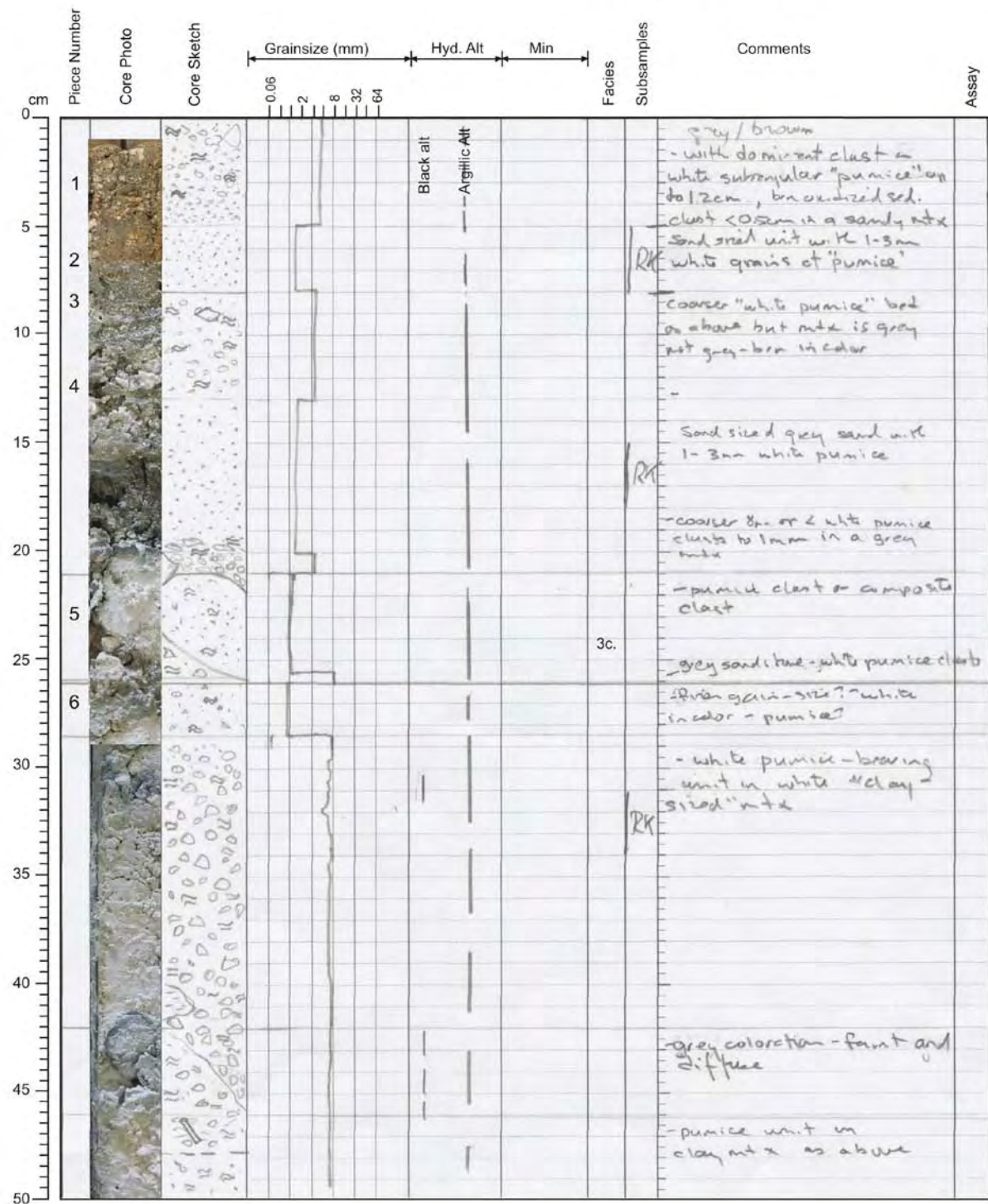
Lat.: 38°38.938'N Long.: 15°06.421'E Water depth: 81

- ☒ Rock core
☐ Vibro core
☐ Gravity corer



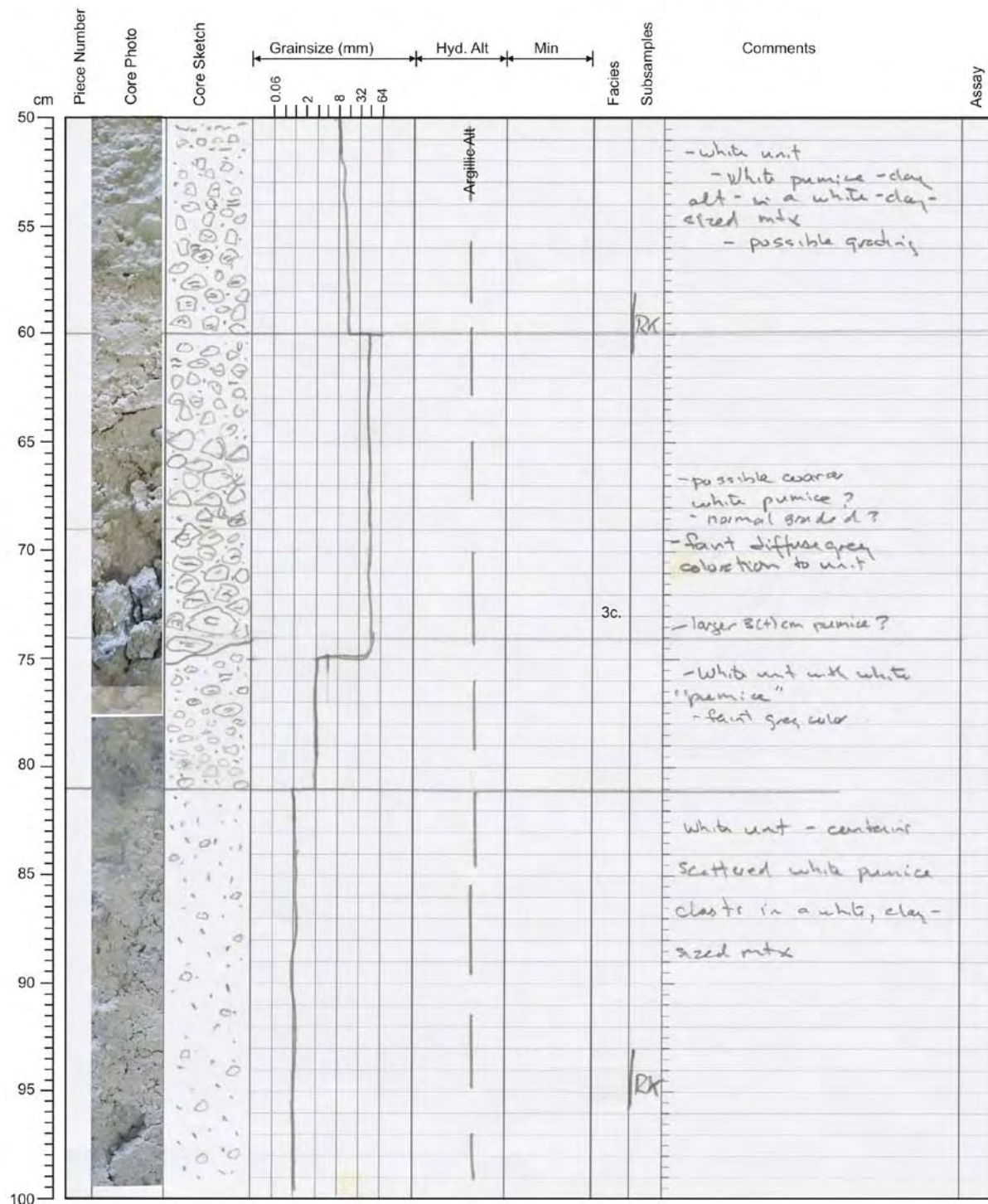
M73/2 - Station: 887 Date: Aug. 21 Time: 10:07-10:49Lat.: 38°38.930'N Long.: 15°06.448'E Water depth: 82

- ☐ Rock core
☒ Vibro core
☐ Gravity corer



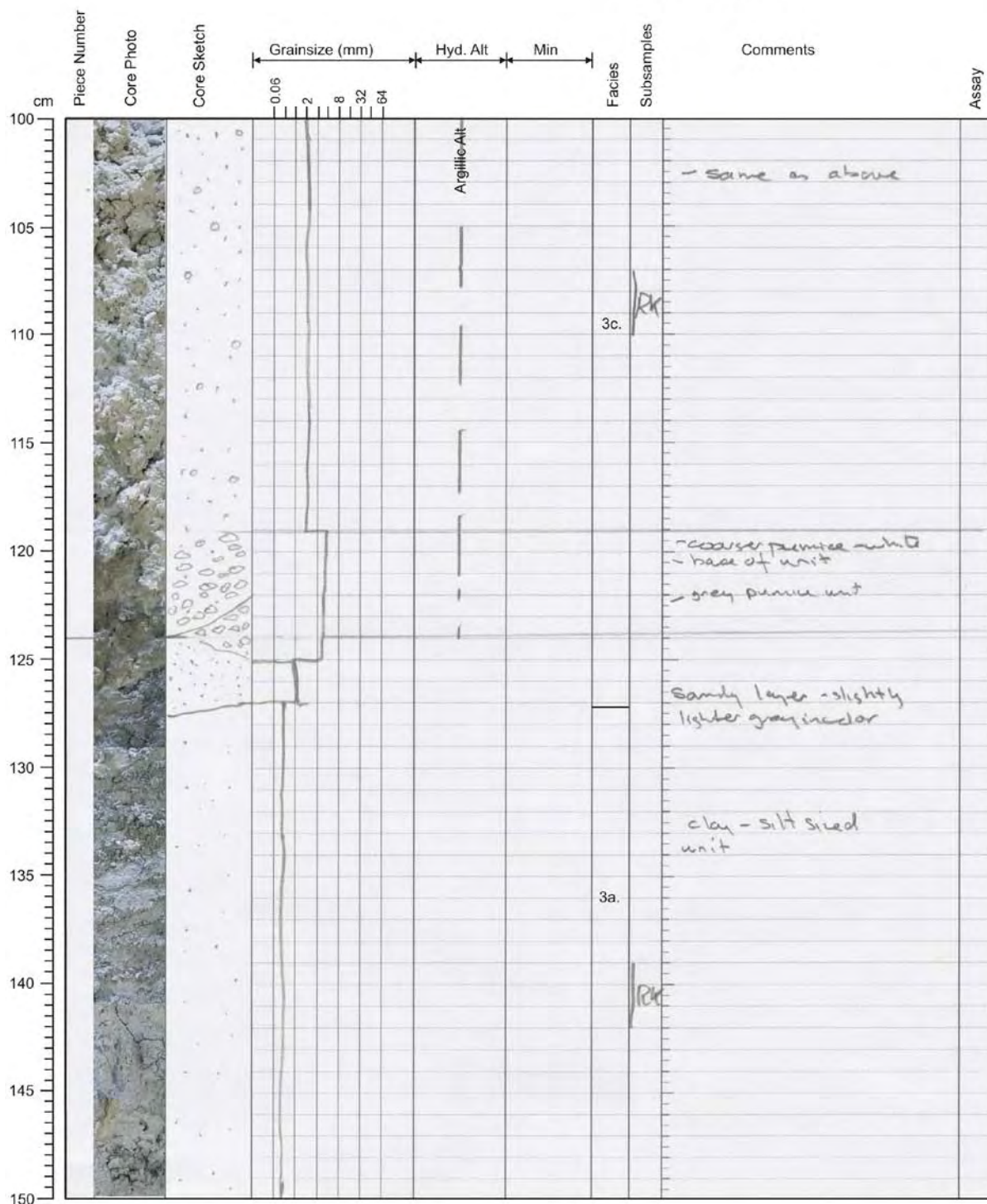
M73/2 - Station: 887 Date: Aug. 21 Time: 10:07-10:49Lat.: 38°38.930'N Long.: 15°06.448'E Water depth: 82

- ☐ Rock core
☒ Vibro core
☐ Gravity corer



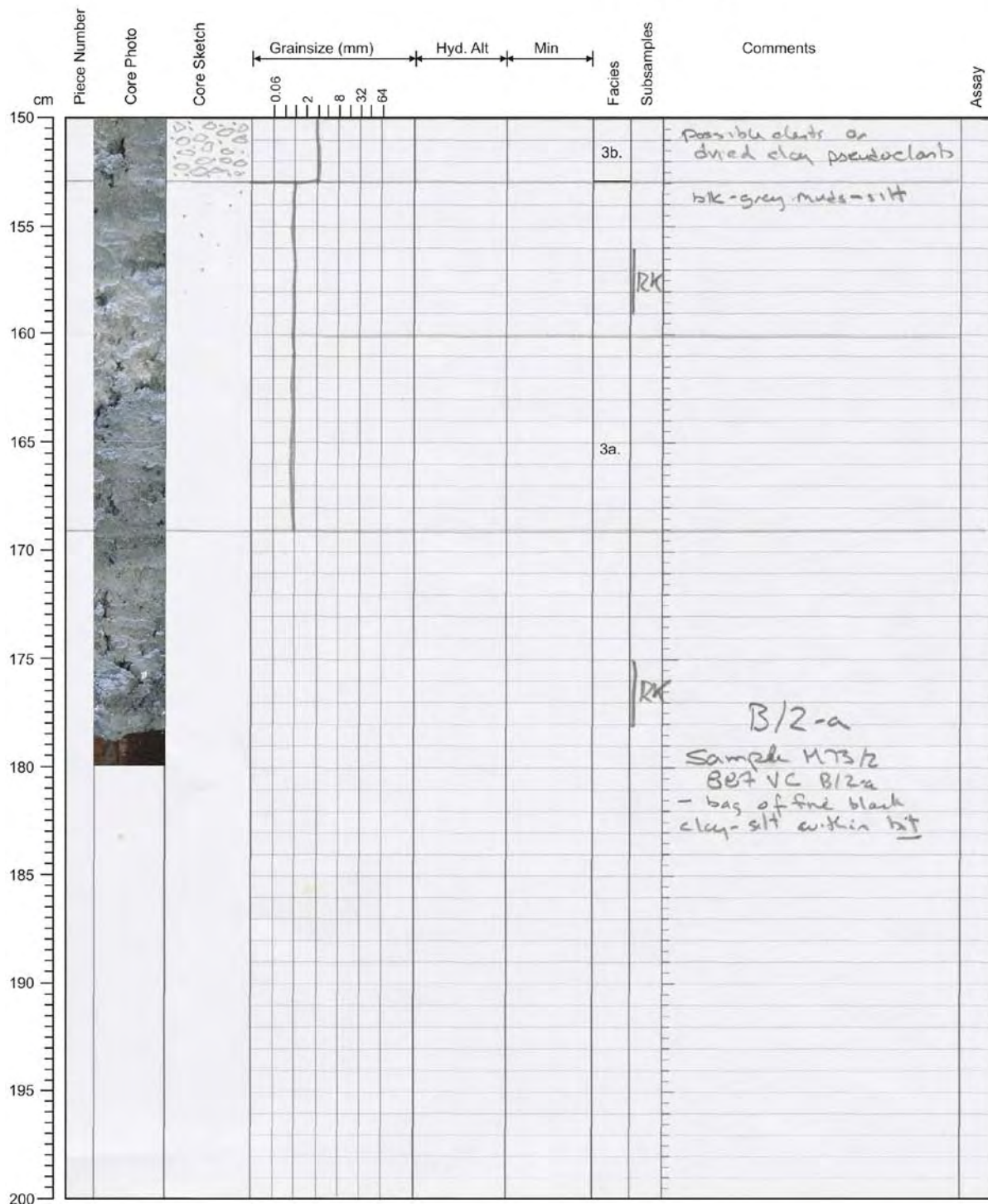
M73/2 - Station: 887 Date: Aug. 21 Time: 10:07-10:49Lat.: 38°38.930'N Long.: 15°06.448'E Water depth: 82

- ☐ Rock core
☒ Vibro core
☐ Gravity corer



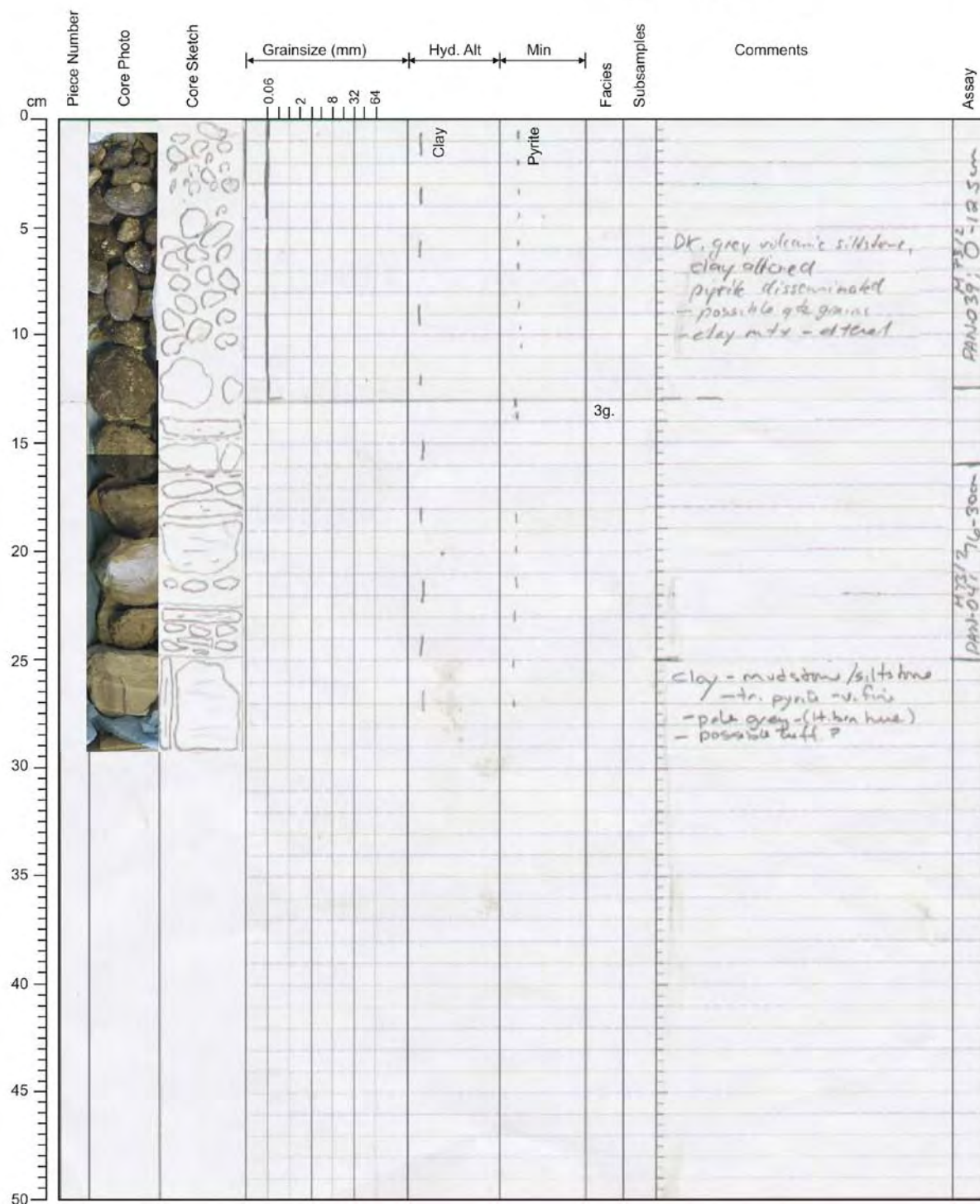
M73/2 - Station: 887 Date: Aug. 21 Time: 10:07-10:49Lat.: 38°38.930'N Long.: 15°06.448'E Water depth: 82

- ☐ Rock core
☒ Vibro core
☐ Gravity corer



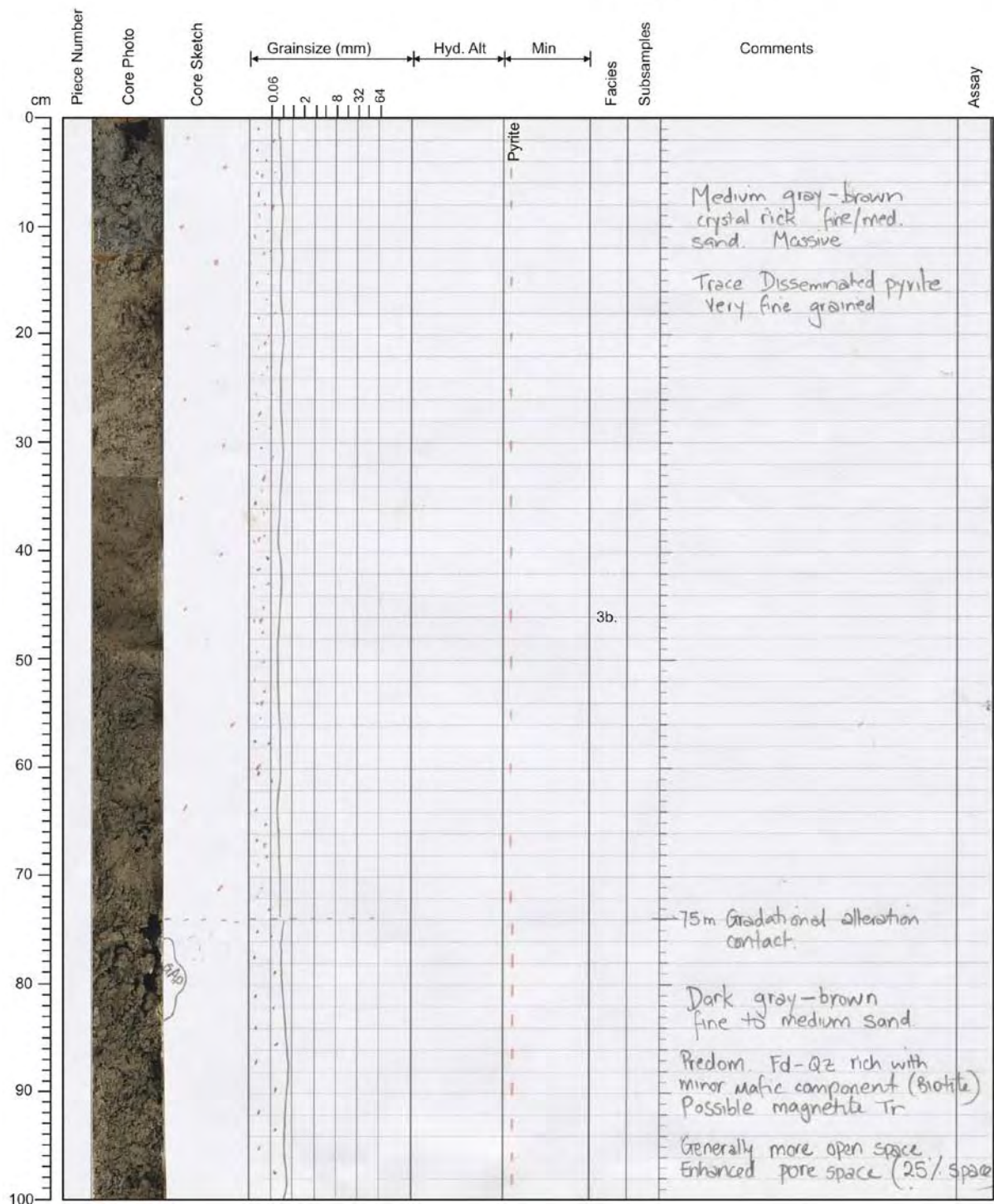
M73/2 - Station: 889 Date: Aug. 21 Time: 15:58-16:45Lat.: 38°38.953'N Long.: 15°06.419'E Water depth: 84

- ☒ Rock core
☐ Vibro core
☐ Gravity corer



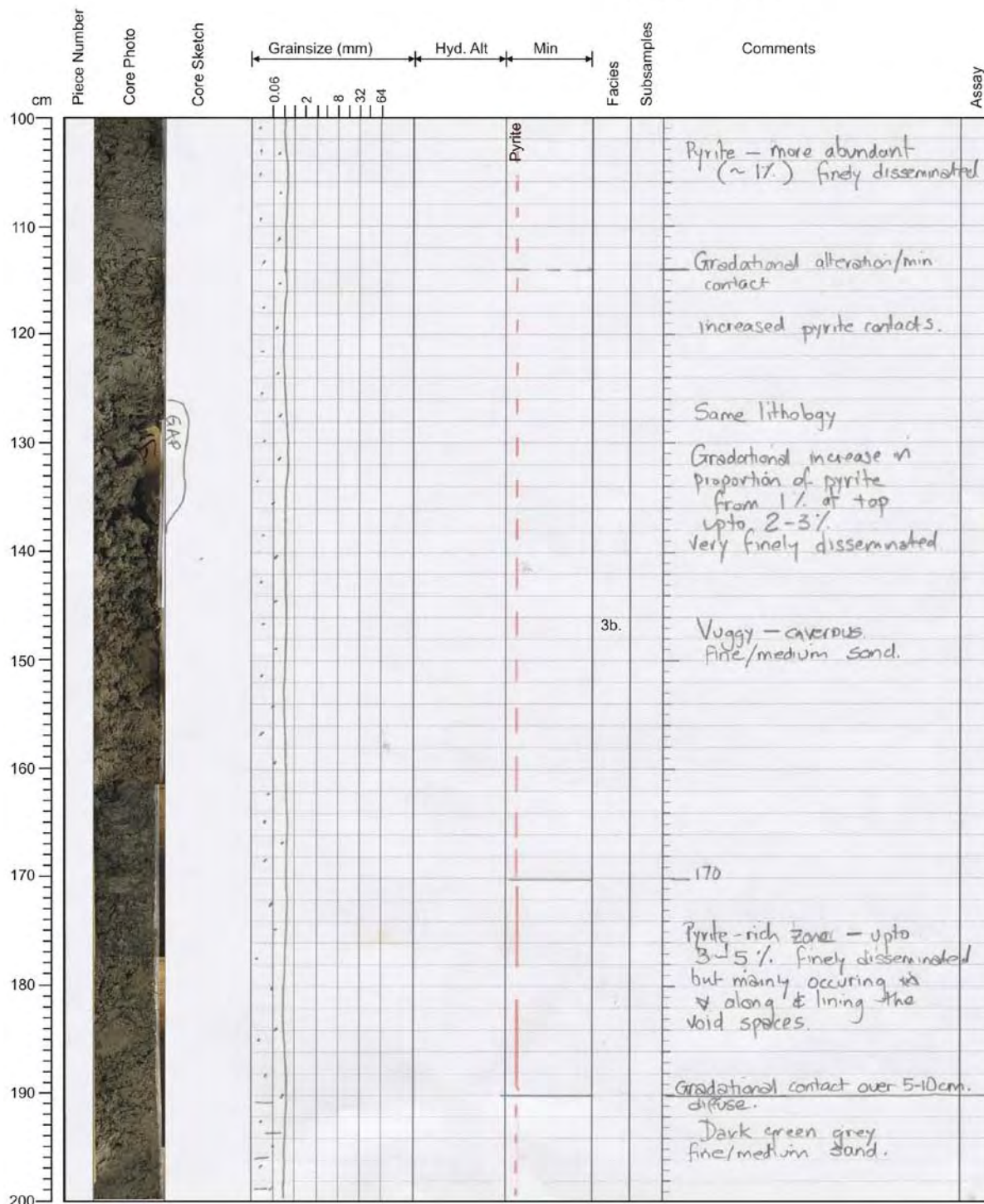
M73/2 - Station: 890 Date: Aug. 21 Time: 17:46-18:07Lat.: 38°38.949'N Long.: 15°06.407'E Water depth: 79

- ☐ Rock core
☒ Vibro core
☐ Gravity corer



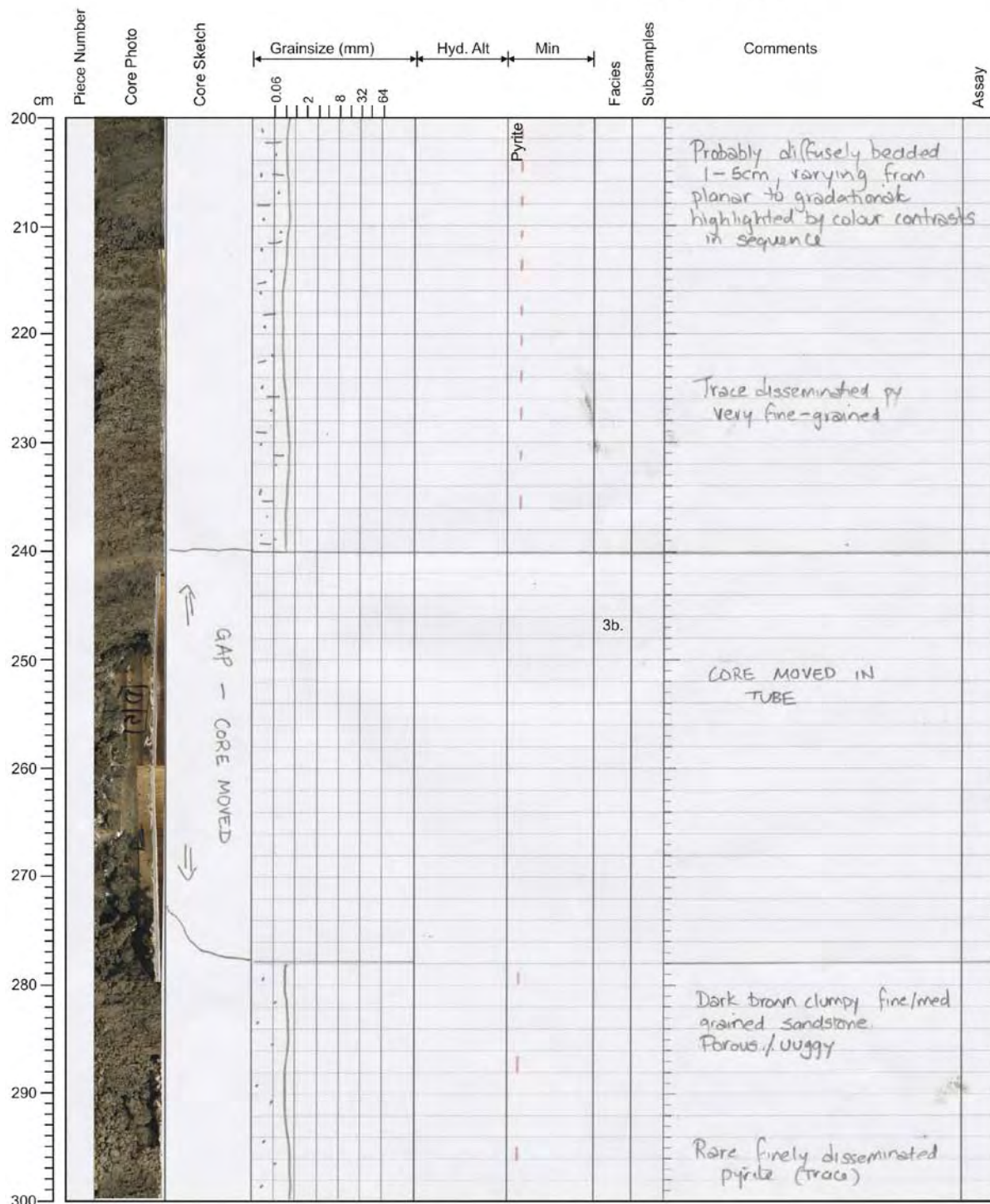
M73/2 - Station: 890 Date: Aug. 21 Time: 17:46-18:07Lat.: 38°38.949'N Long.: 15°06.407'E Water depth: 79

- ☐ Rock core
☒ Vibro core
☐ Gravity corer



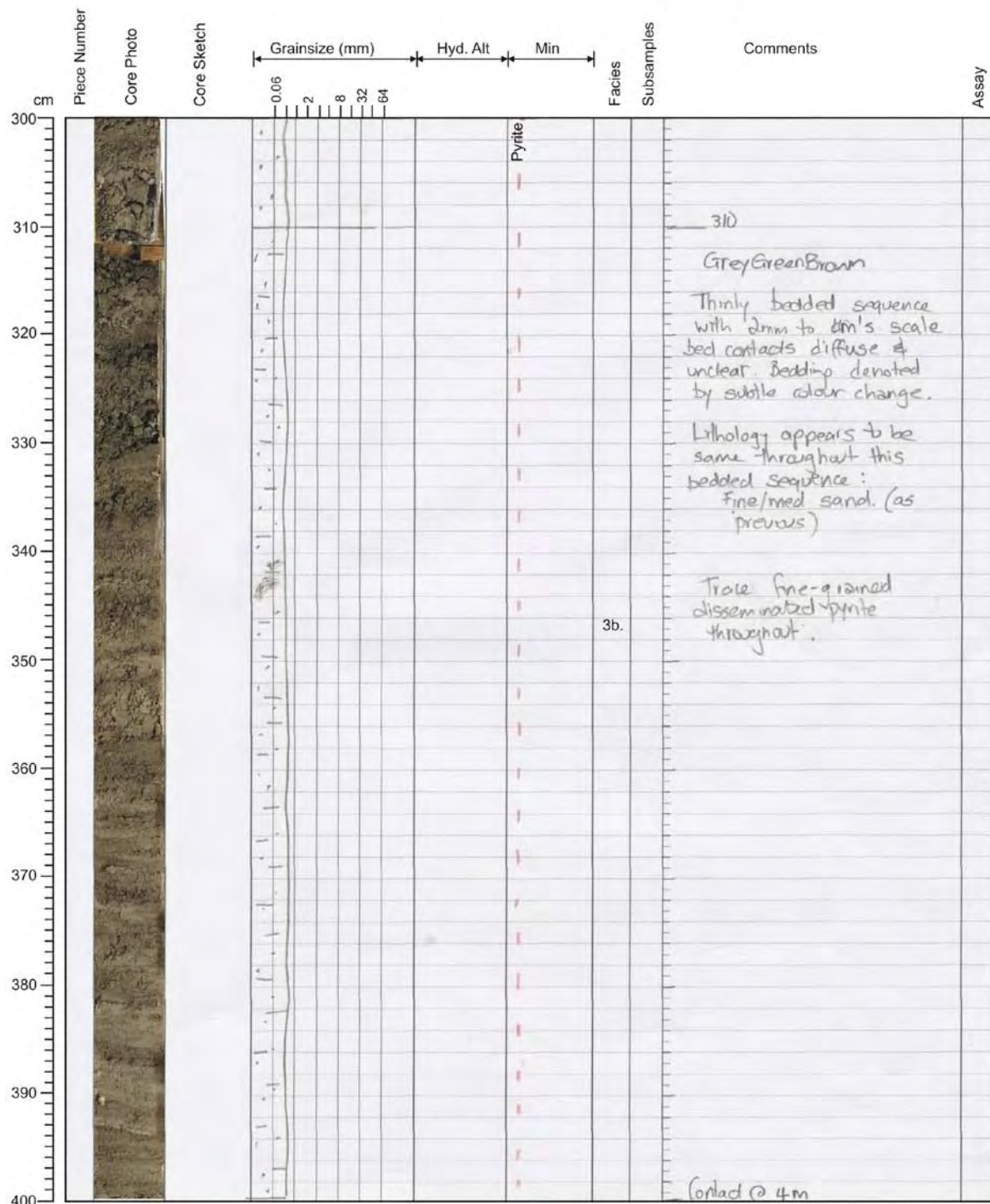
M73/2 - Station: 890 Date: Aug. 21 Time: 17:46-18:07Lat.: 38°38.949'N Long.: 15°06.407'E Water depth: 79

- ☐ Rock core
☒ Vibro core
☐ Gravity corer



M73/2 - Station: 890 Date: Aug. 21 Time: 17:46-18:07Lat.: 38°38.949'N Long.: 15°06.407'E Water depth: 79


- ☐ Rock core
☒ Vibro core
☐ Gravity corer



M73/2 - Station: 890 Date: Aug. 21 Time: 17:46-18:07Lat.: 38°38.949'N Long.: 15°06.407'E Water depth: 79

- ☐ Rock core
☒ Vibro core
☐ Gravity corer

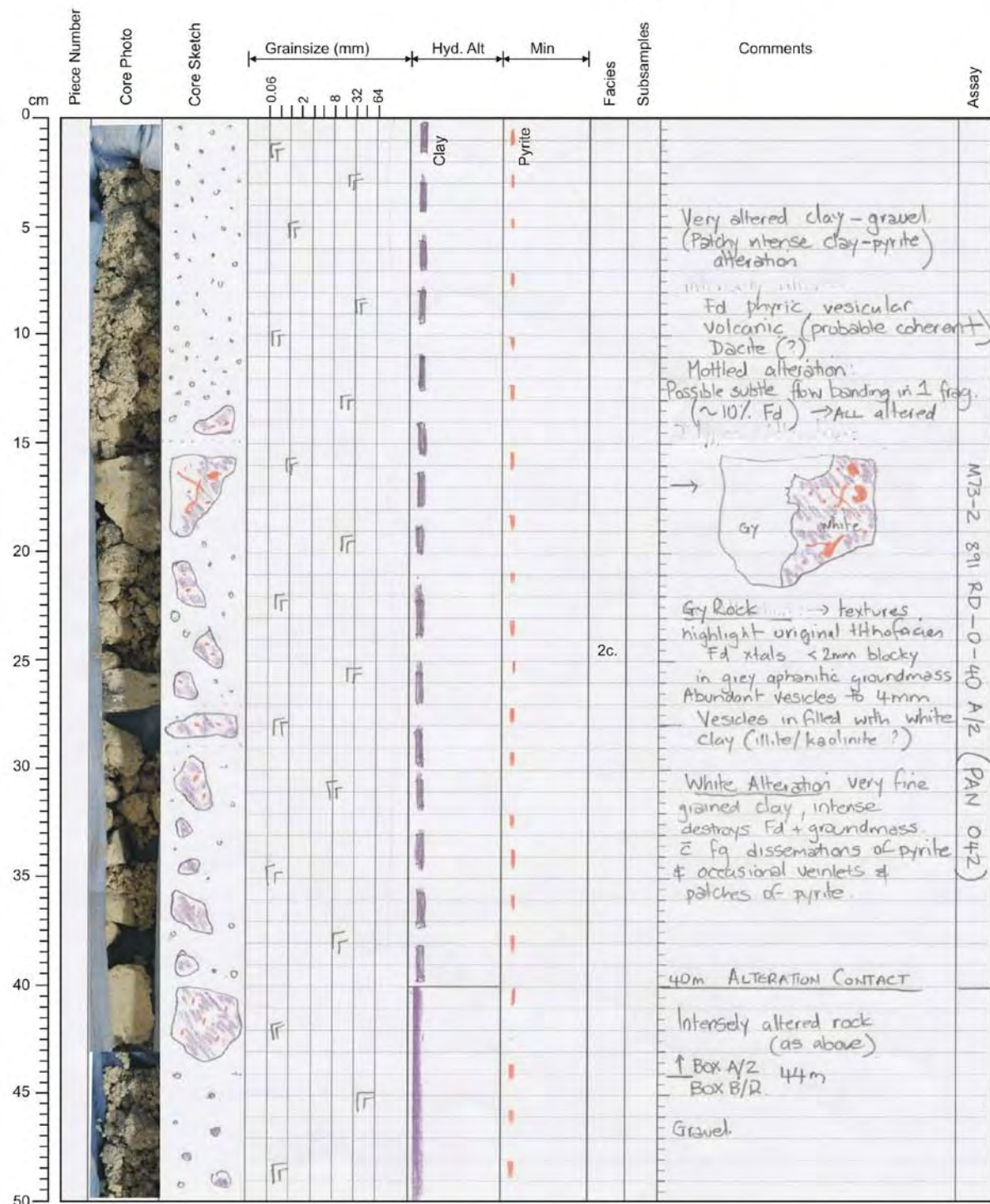


Piece Number	Core Photo	Core Sketch	Grainsize (mm)	Hyd. Alt	Min	Facies	Subsamples	Comments	Assay
cm			0.06 2 8 32 64						
400						Pyrite	3b.	Dark Brown vuggy - porous fine-medium sand. Trace pyrite. No bedding	
410		410 EOH							
420									
430									
440									
450									
460									
470									
480									
490									
500									

M73/2 - Station: 891 Date: Aug. 21 Time: 18:41-19:18

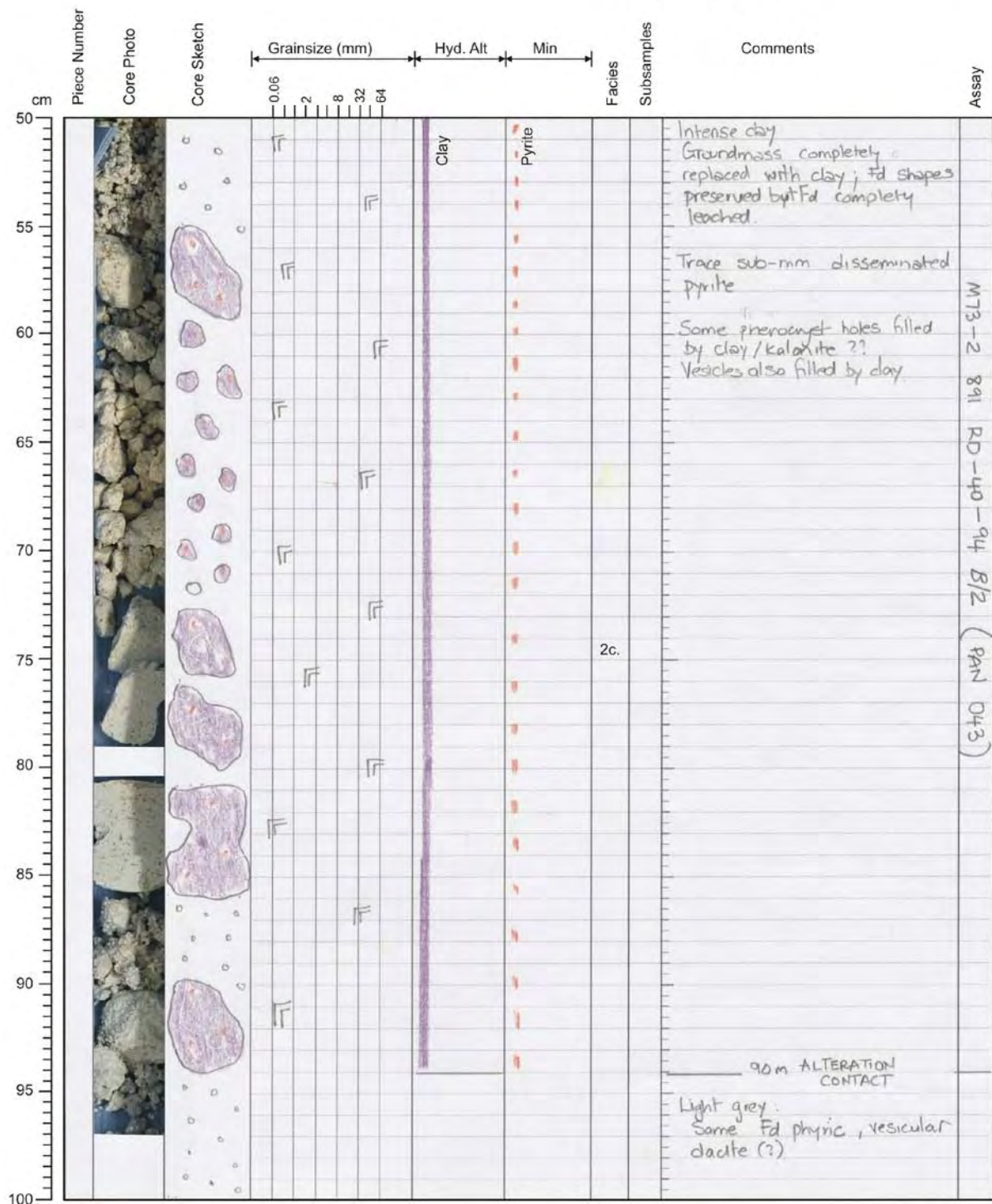
Lat.: 38°38.934'N Long.: 15°06.447'E Water depth: 80

- ☒ Rock core
☐ Vibro core
☐ Gravity corer



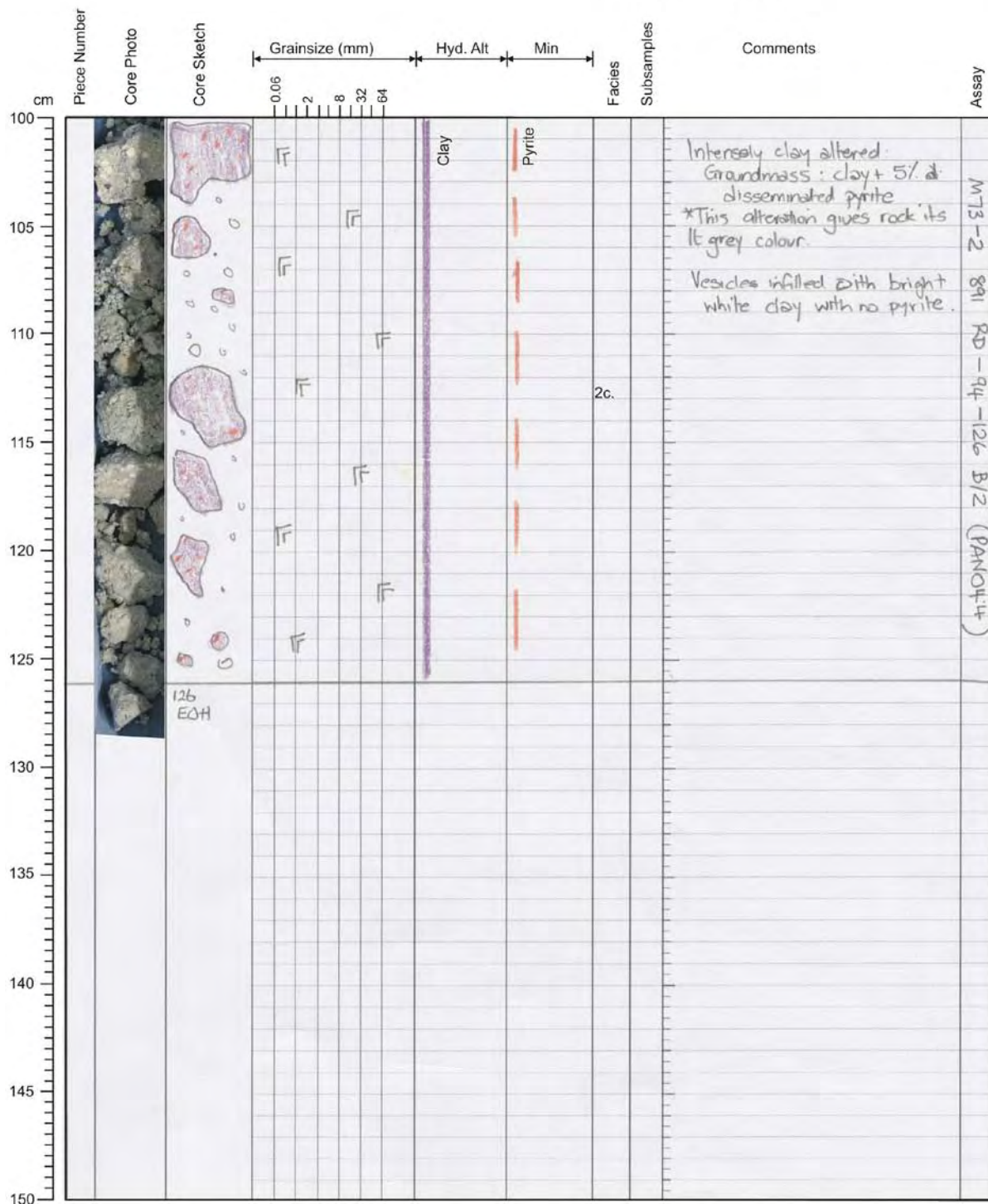
M73/2 - Station: 891 Date: Aug. 21 Time: 18:41-19:18Lat.: 38°38.934'N Long.: 15°06.447'E Water depth: 80

- ☒ Rock core
☐ Vibro core
☐ Gravity corer



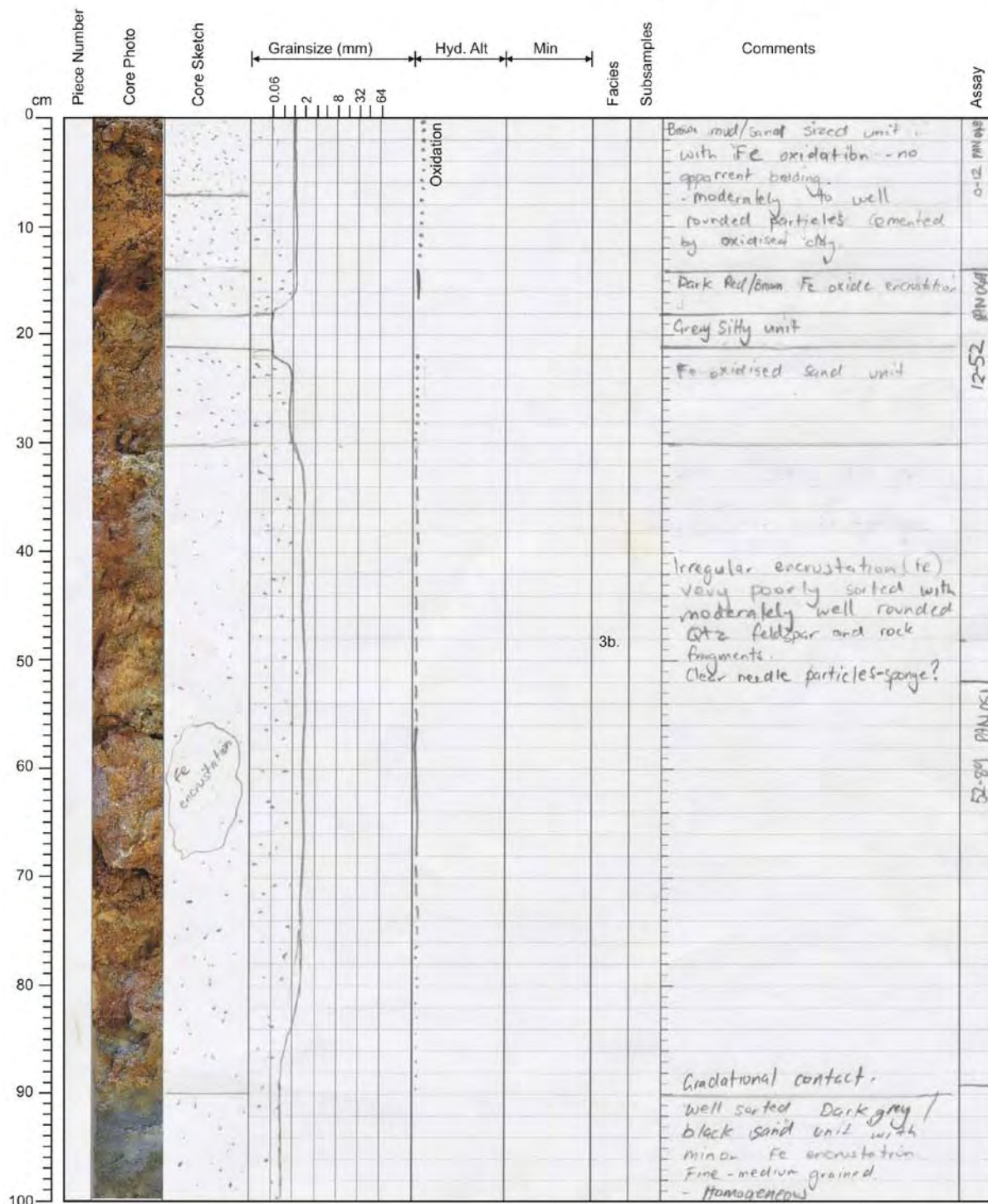
M73/2 - Station: 891 Date: Aug. 21 Time: 18:41-19:18Lat.: 38°38.934'N Long.: 15°06.447'E Water depth: 80

- ☒ Rock core
☐ Vibro core
☐ Gravity corer



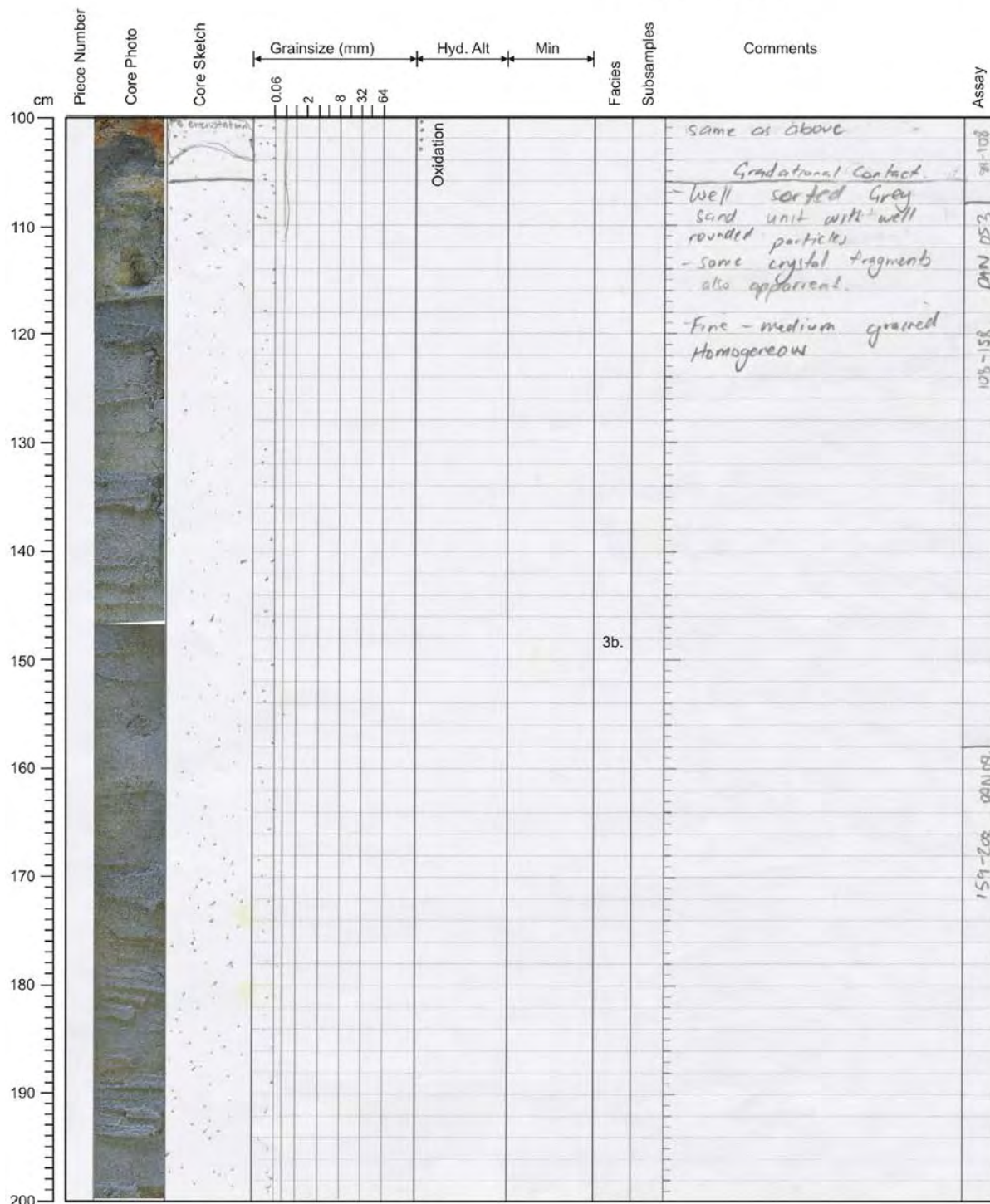
M73/2 - Station: 894 Date: Aug. 21 Time: 22:13-22:52Lat.: 38°38.934'N Long.: 15°06.361'E Water depth: 78

- ☐ Rock core
☒ Vibro core
☐ Gravity corer



M73/2 - Station: 894 Date: Aug. 21 Time: 22:13-22:52Lat.: 38°38.934'N Long.: 15°06.361'E Water depth: 78

- ☐ Rock core
☒ Vibro core
☐ Gravity corer



M73/2 - Station: 894 Date: Aug. 21 Time: 22:13-22:52Lat.: 38°38.934'N Long.: 15°06.361'E Water depth: 78

- ☐ Rock core
☒ Vibro core
☐ Gravity corer



Piece Number	Core Photo	Core Sketch	Grainsize (mm)	Hyd. Alt	Min	Facies	Subsamples	Comments	Assay
cm			0.06 2 8 32 64						
200								Same as above	
210									209 - 256- PAN 055
220									
230									
240									
250						3b.			
260									259-308 PAN 056
270									
280									
290									
300									

M73/2 - Station: 894 Date: Aug. 21 Time: 22:13-22:52Lat.: 38°38.934'N Long.: 15°06.361'E Water depth: 78

- ☐ Rock core
☒ Vibro core
☐ Gravity corer

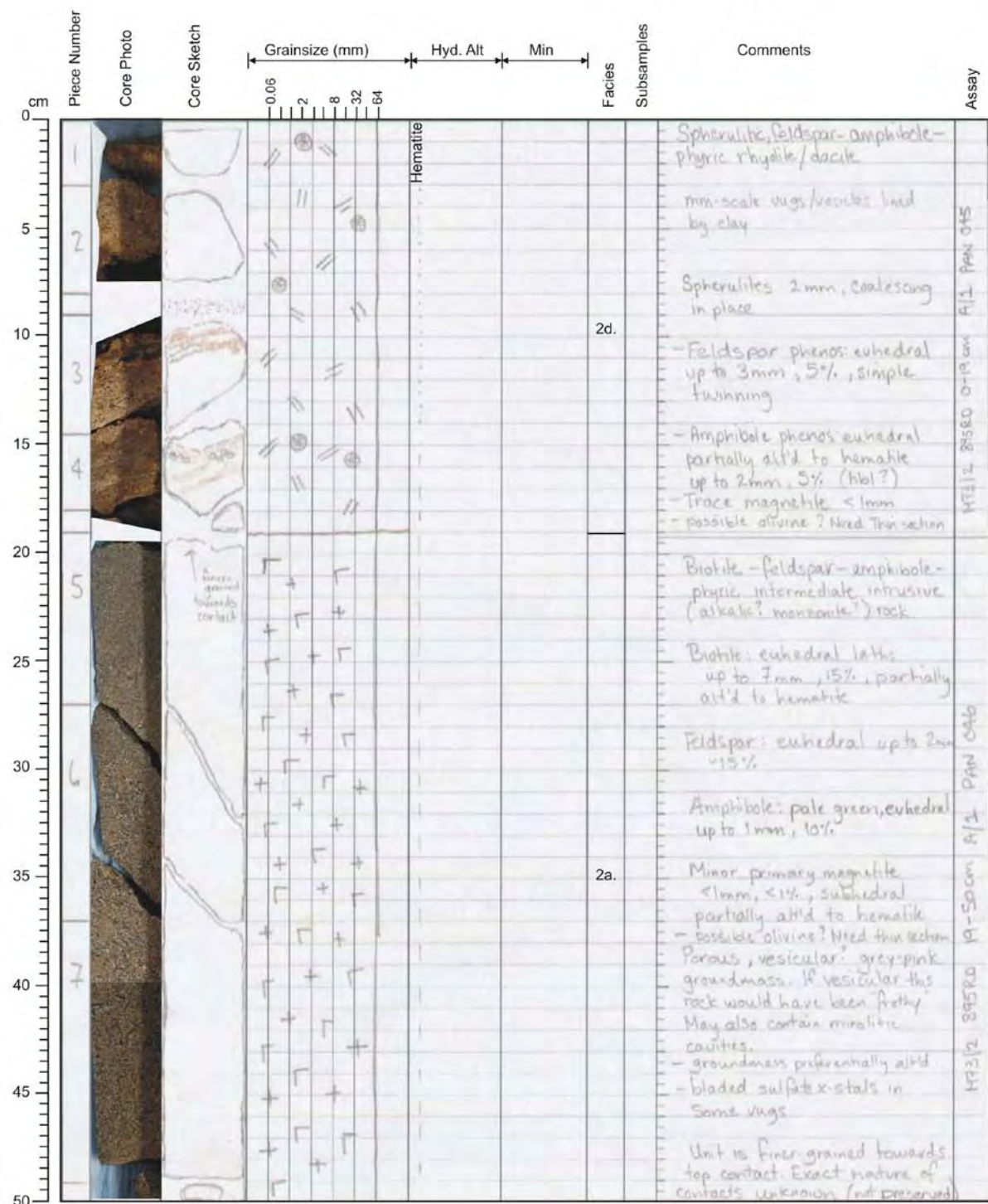


Piece Number	Core Photo	Core Sketch	Grainsize (mm)	Hyd. Alt	Min	Facies	Subsamples	Comments	Assay
cm			0.06 2 8 32 64						
300								same as above	
310								Gradational contact	
320								- Lighter grey well sorted sand unit	PAN 057
330								- Well rounded particles - crystal fragments also visible	309-358
340						3b.		- Fine to medium grained but slightly coarser than previous unit. - Still homogeneous	
350									
360									
370									358-375
380		EOH 375							
390									
400									

M73/2 - Station: 895 Date: Aug. 22 Time: 00:16-02:47

Lat.: 38°38.984'N Long.: 15°05.818'E Water depth: 61

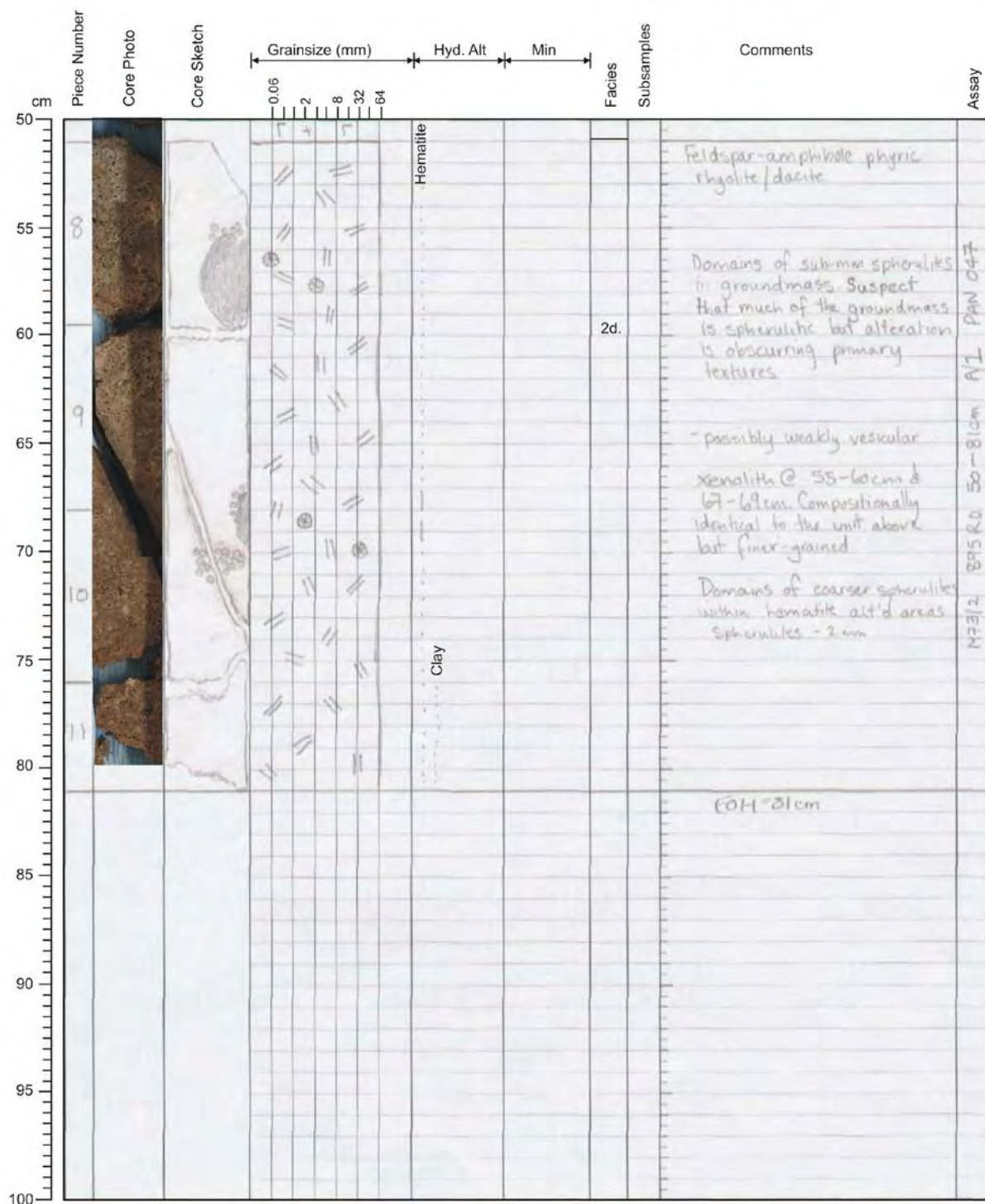
- ☒ Rock core
☐ Vibro core
☐ Gravity corer



M73/2 - Station: 895 Date: Aug. 22 Time: 00:16-02:47

Lat.: 38°38.984'N Long.: 15°05.818'E Water depth: 61

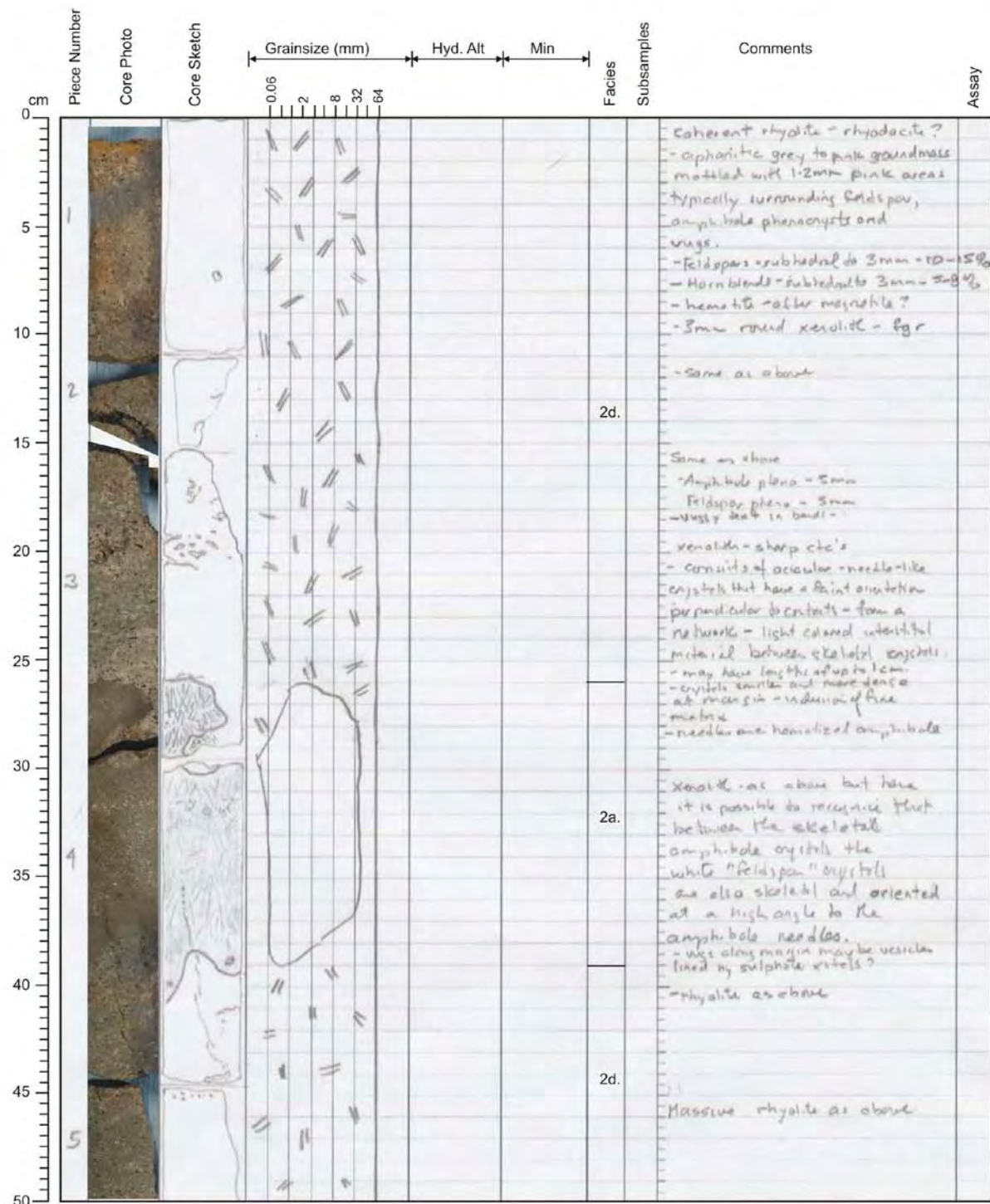
- ☒ Rock core
☐ Vibro core
☐ Gravity corer



M73/2 - Station: 896 Date: Aug. 22 Time: 03:14-06:25

Lat.: 38°39.020'N Long.: 15°05.820'E Water depth: 66

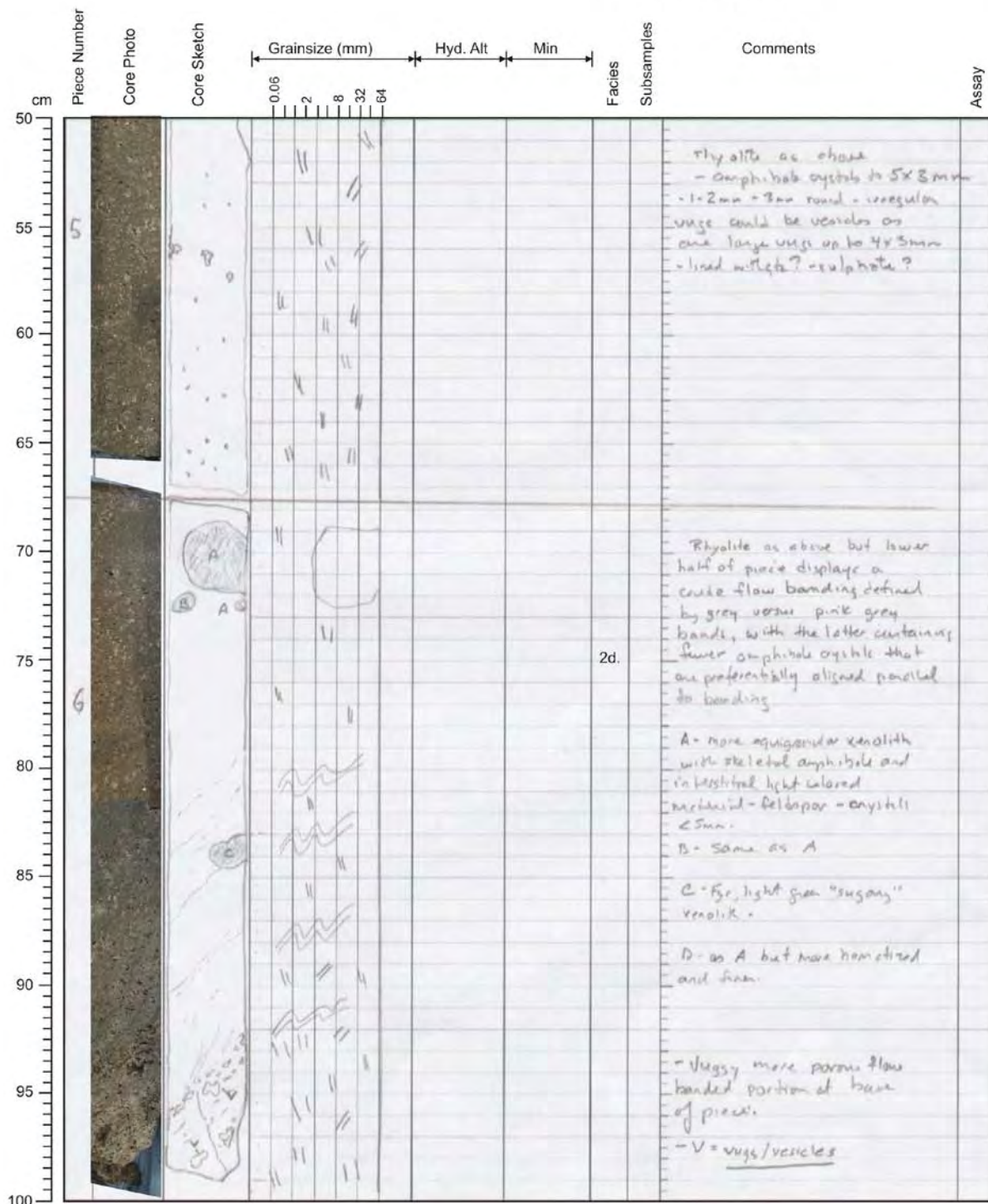
- ☒ Rock core
☐ Vibro core
☐ Gravity corer



M73/2 - Station: 896 Date: Aug. 22 Time: 03:14-06:25

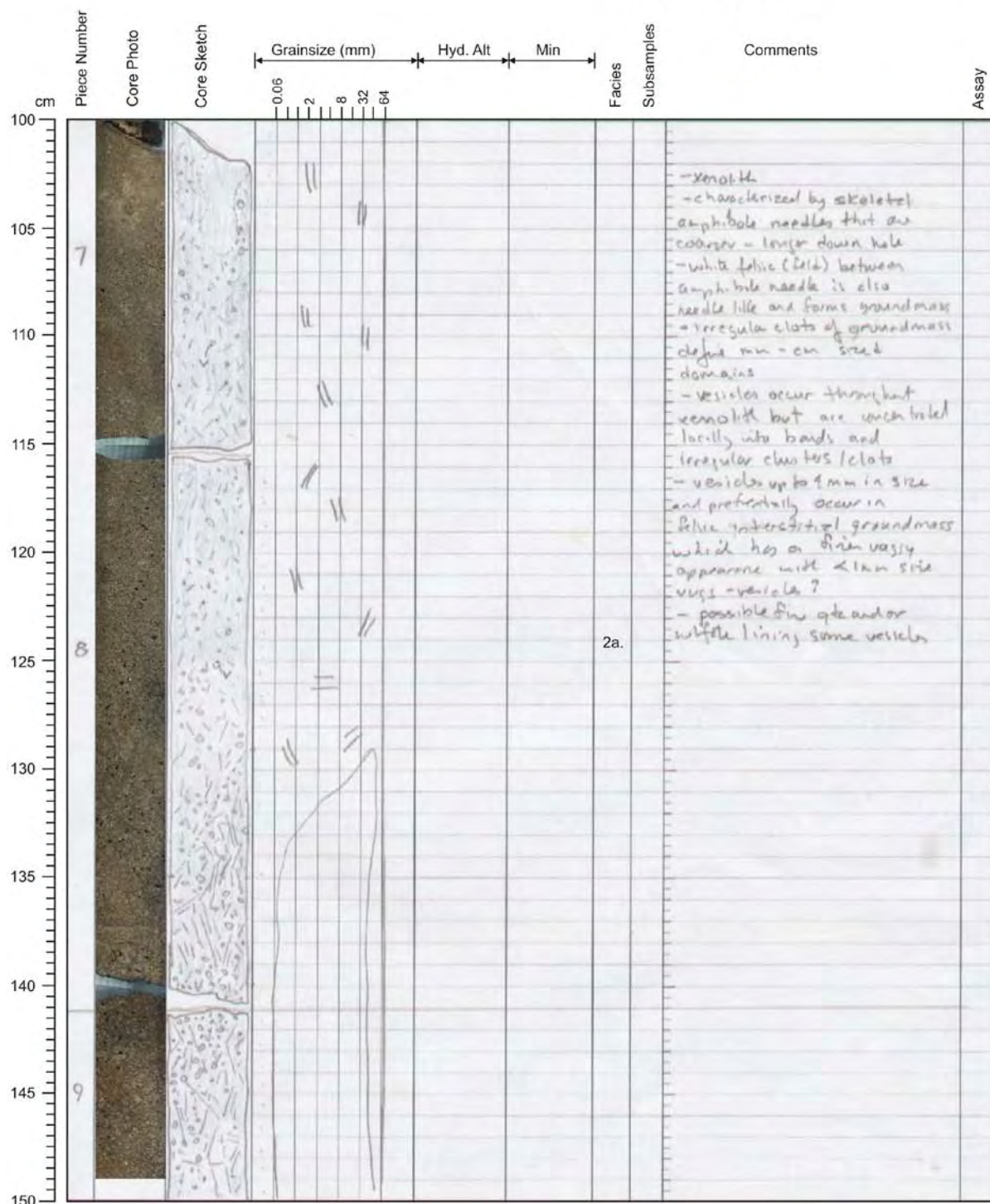
Lat.: 38°39.020'N Long.: 15°05.820'E Water depth: 66

- ☒ Rock core
☐ Vibro core
☐ Gravity corer



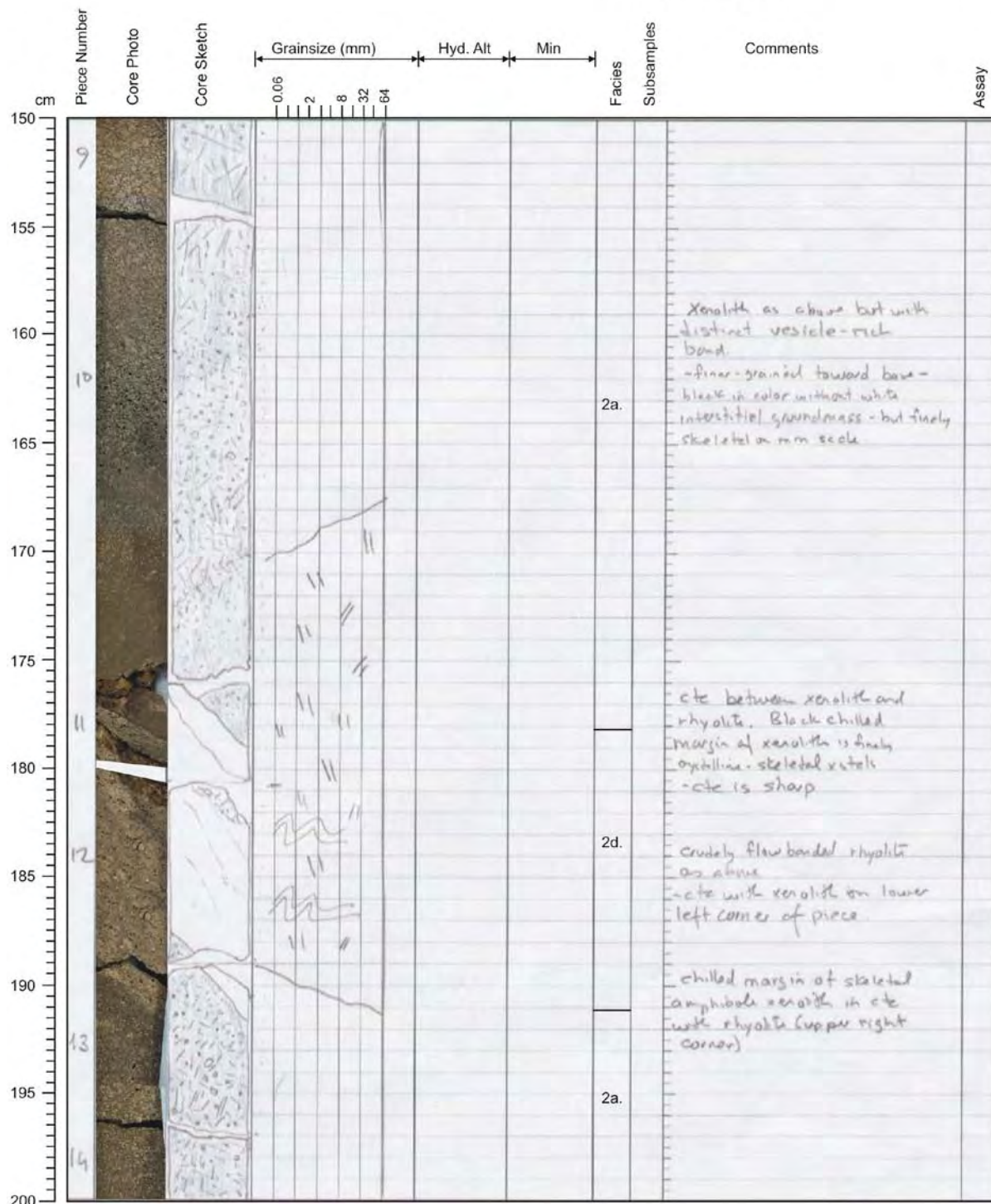
M73/2 - Station: 896 Date: Aug. 22 Time: 03:14-06:25Lat.: 38°39.020'N Long.: 15°05.820'E Water depth: 66

- ☒ Rock core
☐ Vibro core
☐ Gravity corer



M73/2 - Station: 896 Date: Aug. 22 Time: 03:14-06:25Lat.: 38°39.020'N Long.: 15°05.820'E Water depth: 66

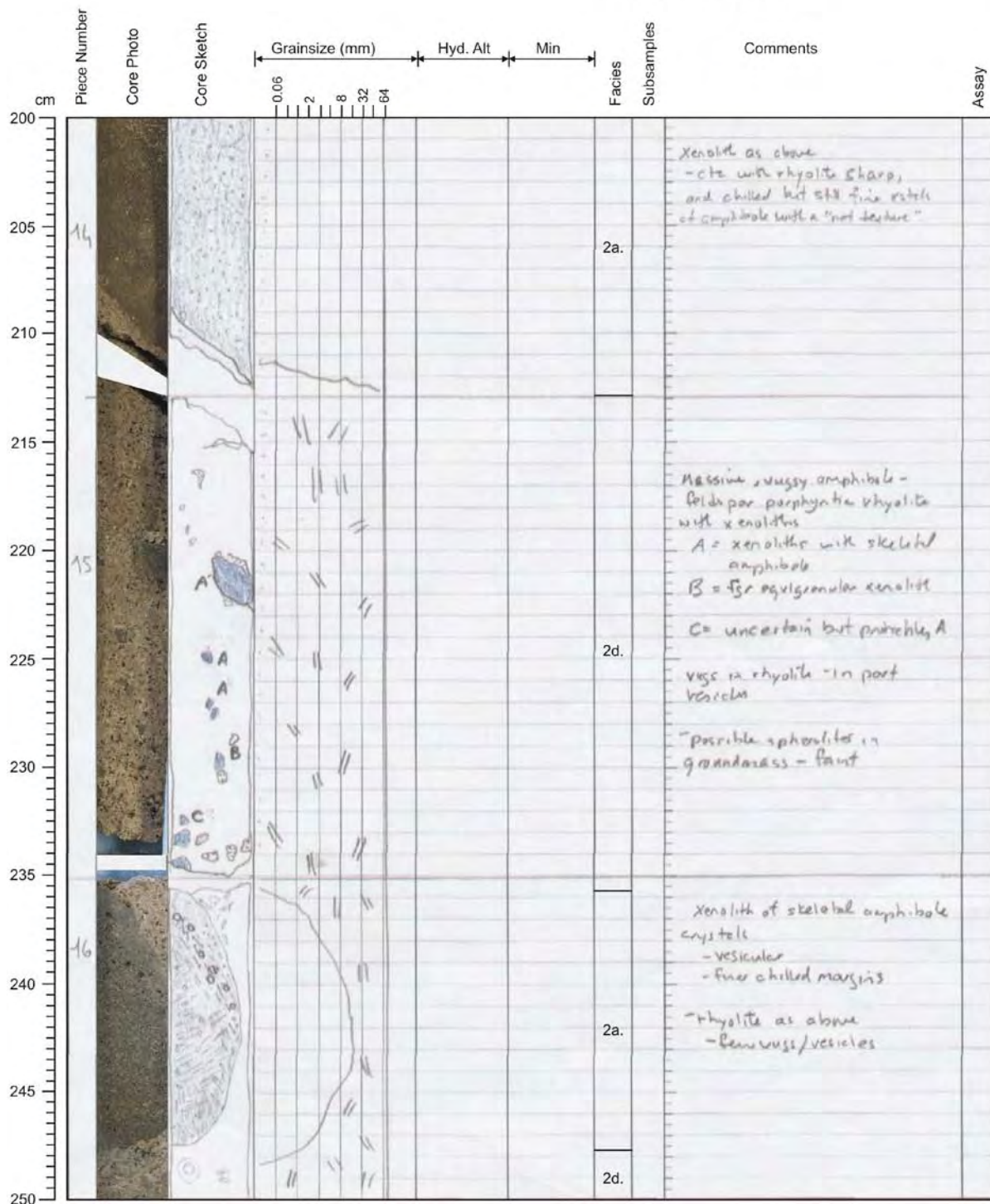
- ☒ Rock core
☐ Vibro core
☐ Gravity corer



M73/2 - Station: 896 Date: Aug. 22 Time: 03:14-06:25

Lat.: 38°39.020'N Long.: 15°05.820'E Water depth: 66

- ☒ Rock core
☐ Vibro core
☐ Gravity corer



M73/2 - Station: 896 Date: Aug. 22 Time: 03:14-06:25Lat.: 38°39.020'N Long.: 15°05.820'E Water depth: 66

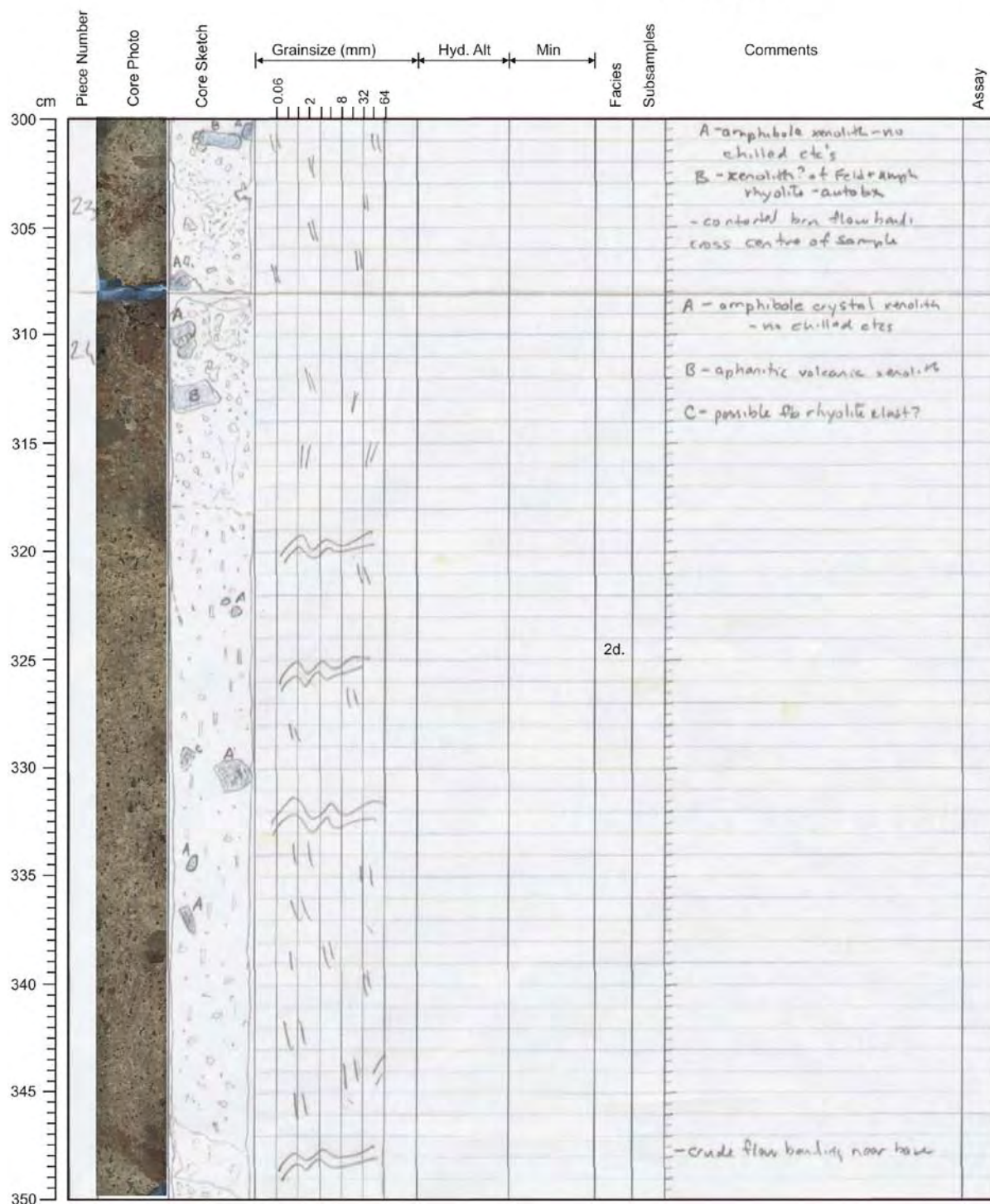
- ☒ Rock core
☐ Vibro core
☐ Gravity corer



Piece Number	Core Photo	Core Sketch	Grainsize (mm)	Hyd. Alt	Min	Facies	Subsamples	Comments	Assay
cm			0.06 2 8 32 64						
250	16							Wuggy rhyolite as above - faint flow banding	
255	17					2d.		as above - Rhyolite	
260	18							Flow banding defined by gray - pink color variation - rhyolite as above - microb. crystals? A - Equigranular xenolith - sharp cter B - large amphibole crystals - earth brown, hematitic rhyolite at base of piece	
265	19							Rhyolite as above	
270	20							- wuggy - vesicular amphibole xenolith - contacts are not visibly chilled in cte with rhyolite - vesicles here are more angular + bounded by xct. faces -	
275						2a.			
280	21							A - For xenolith - equigranular	
285									
290	22							- flow banding - brown, gray, and pink bands, - weak alignment of amphibole along + within flow bands 10% - amphibole - 5mm in size 15% - Feldspar - 4-6mm in size	
295						2d.			
300	23							- Rhyolite as above - amphibole xenolith - no chilled cte with rhyolite	

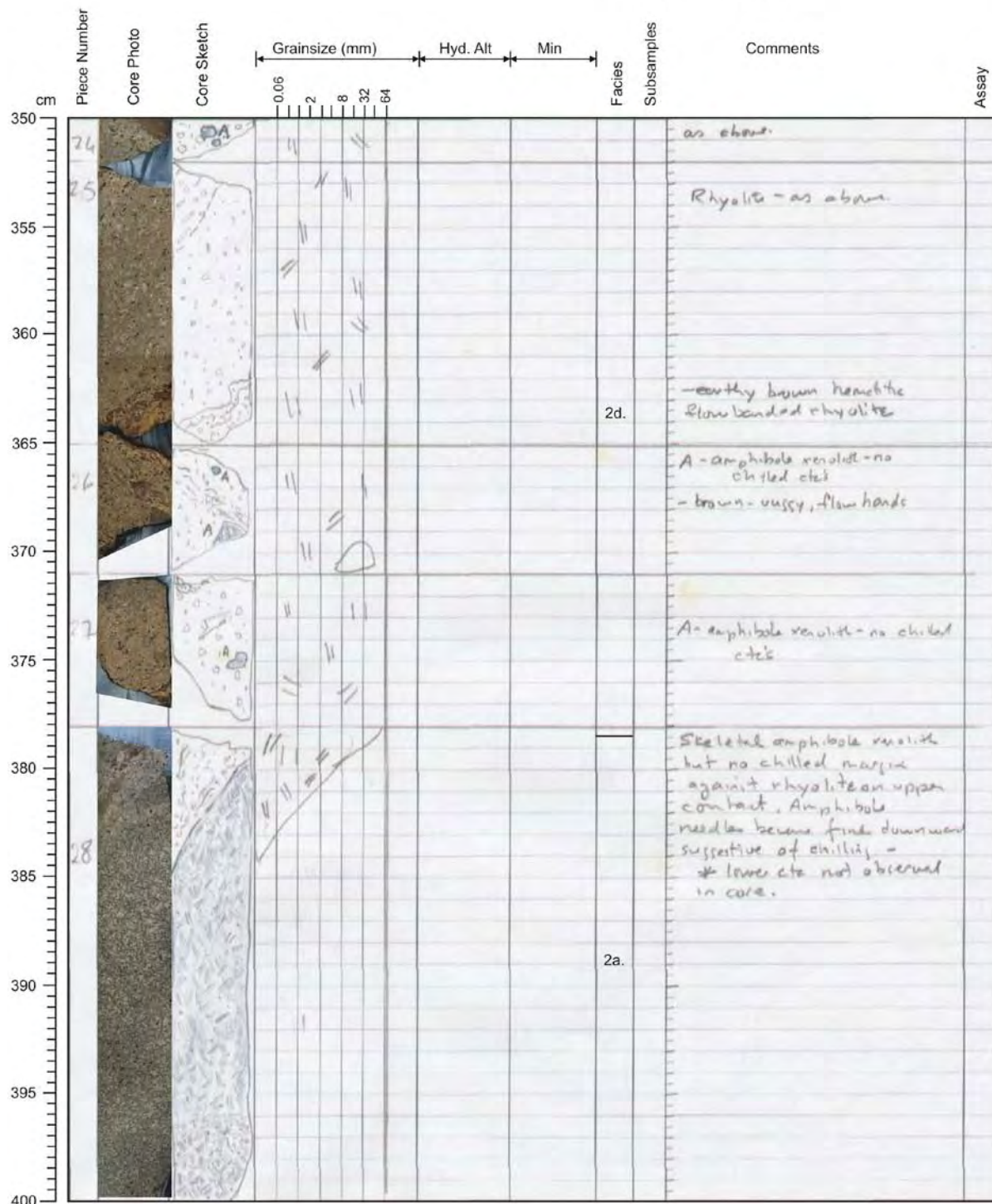
M73/2 - Station: 896 Date: Aug. 22 Time: 03:14-06:25Lat.: 38°39.020'N Long.: 15°05.820'E Water depth: 66

- ☒ Rock core
☐ Vibro core
☐ Gravity corer



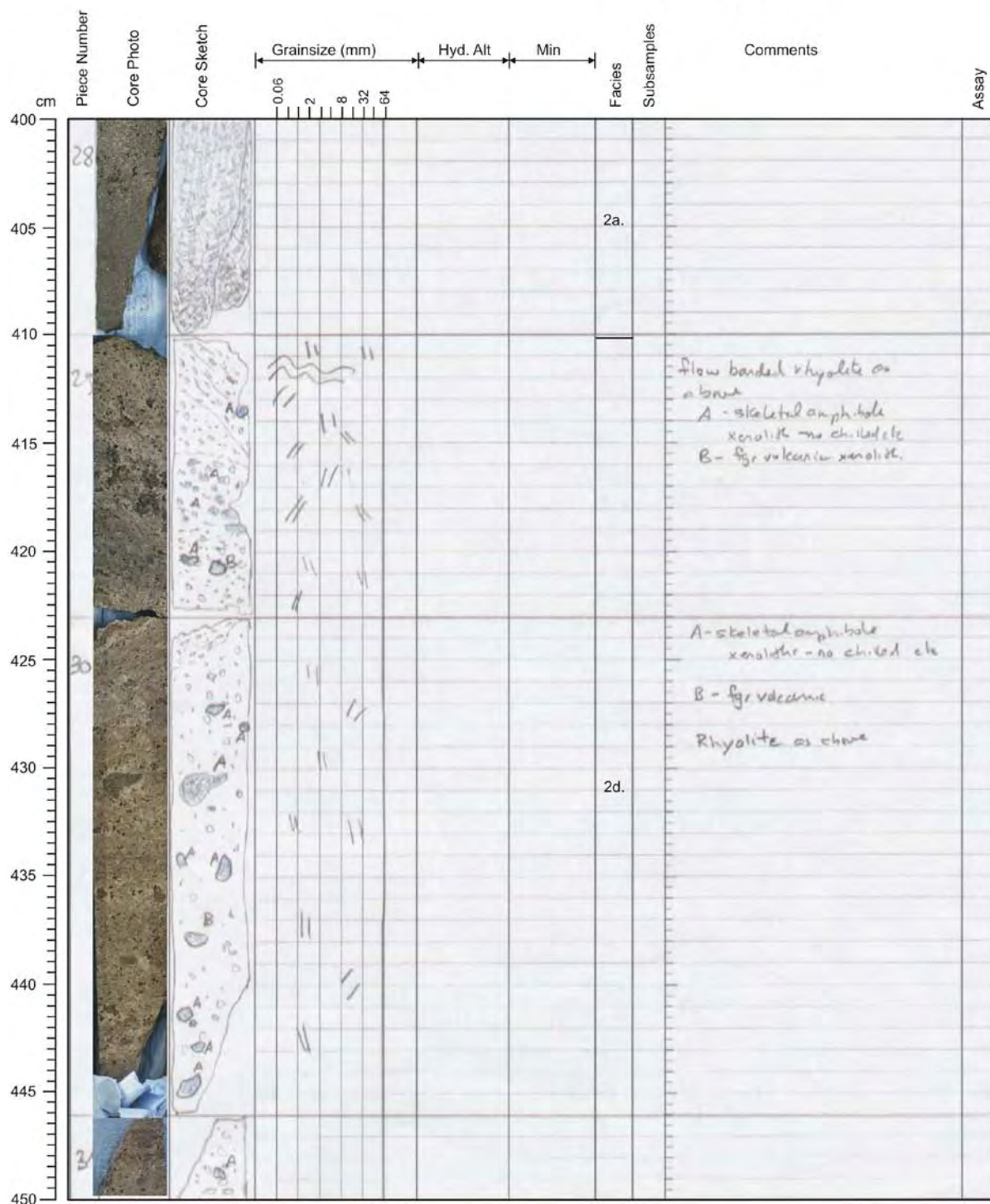
M73/2 - Station: 896 Date: Aug. 22 Time: 03:14-06:25Lat.: 38°39.020'N Long.: 15°05.820'E Water depth: 66

- ☒ Rock core
☐ Vibro core
☐ Gravity corer



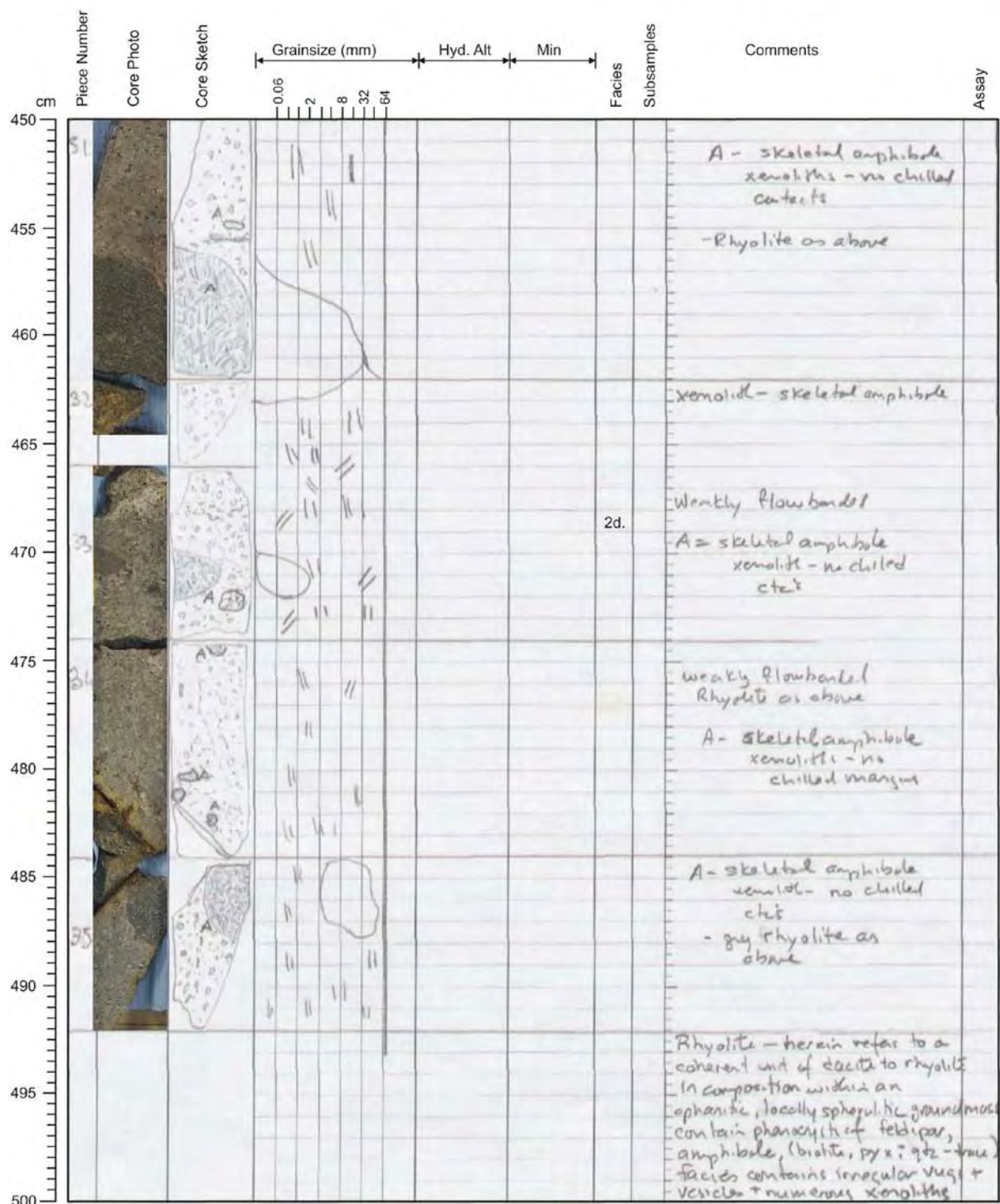
M73/2 - Station: 896 Date: Aug. 22 Time: 03:14-06:25Lat.: 38°39.020'N Long.: 15°05.820'E Water depth: 66

- ☒ Rock core
☐ Vibro core
☐ Gravity corer



M73/2 - Station: 896 Date: Aug. 22 Time: 03:14-06:25Lat.: 38°39.020'N Long.: 15°05.820'E Water depth: 66

- ☒ Rock core
☐ Vibro core
☐ Gravity corer



M73/2 - Station: 897 Date: Aug. 22 Time: 06:54-08:54Lat.: 38°39.024'N Long.: 15°05.852'E Water depth: 76

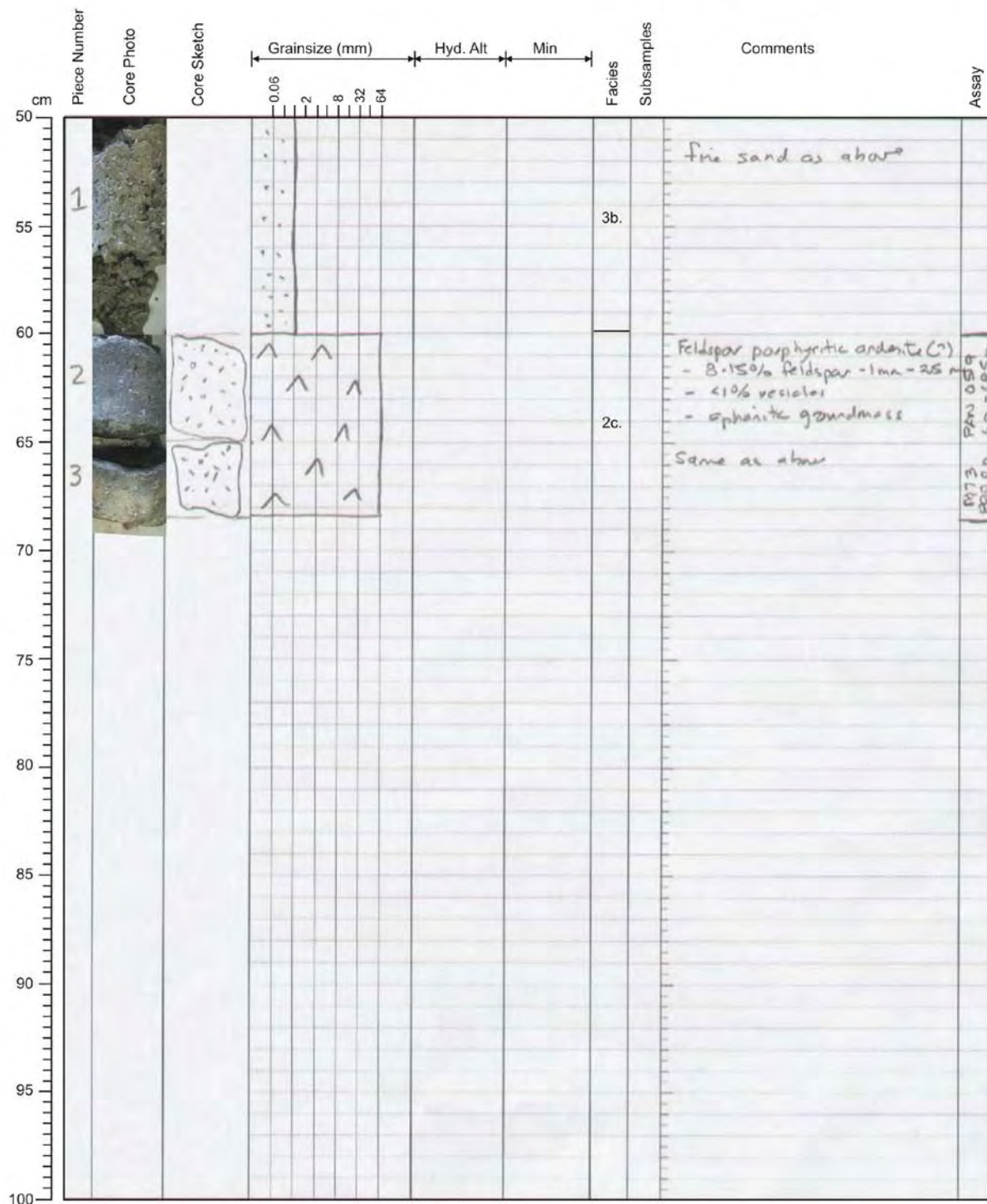
- ☒ Rock core
☐ Vibro core
☐ Gravity corer



Piece Number	Core Photo	Core Sketch	Grainsize (mm)	Hyd. Alt	Min	Facies	Subsamples	Comments	Assay
			0.06 2 8 32 64						
1								Coherent rhyolite - feldspar and amphibole phenocrysts - weak flow banding	
2							2d.	Same as above	
3								Same with Mn crust	
4								Feldspar porphyritic Andesite? Feldspar - 1-2.5mm - 8% - aphanitic groundmass	
5								Rhyolite as above	
6							2c.	Andesite as above	
7								Andesite as above	
8							2d.	Feldspar - (quartz?) porphyritic Dacite-Rhyolite - aphanitic groundmass	
9								Feldspar porphyritic andesite as above - working specimen has an orange xenolithic that may be rhyolitic	
10							2c.	Feldspar porphyritic Andesite (Dacite) as above	
11								Feldspar porphyritic Andesite - dacite as above	

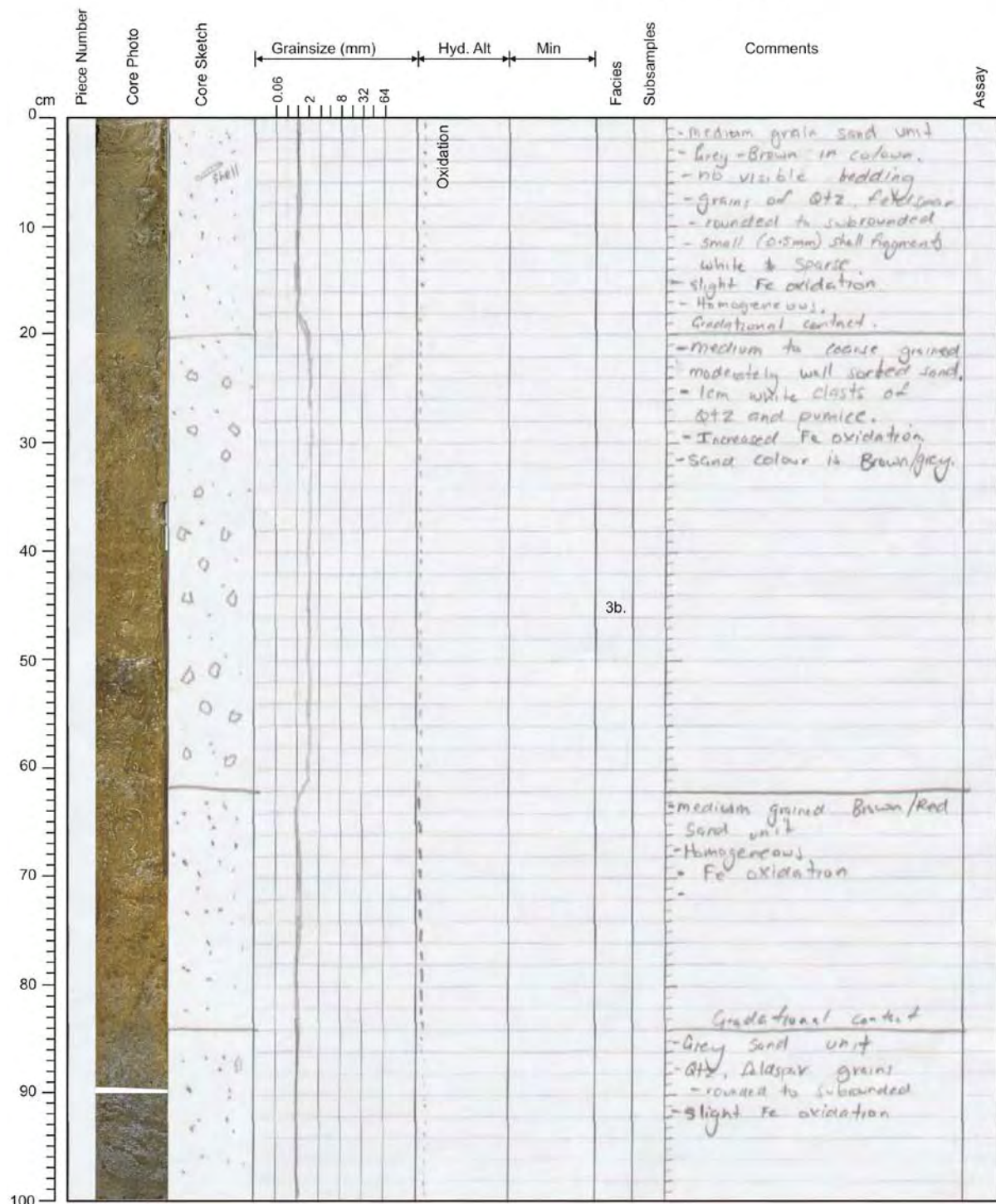
M73/2 - Station: 899 Date: Aug. 22 Time: 11:50-12:39Lat.: 38°38.979'N Long.: 15°06.432'E Water depth: 80

- ☒ Rock core
☐ Vibro core
☐ Gravity corer



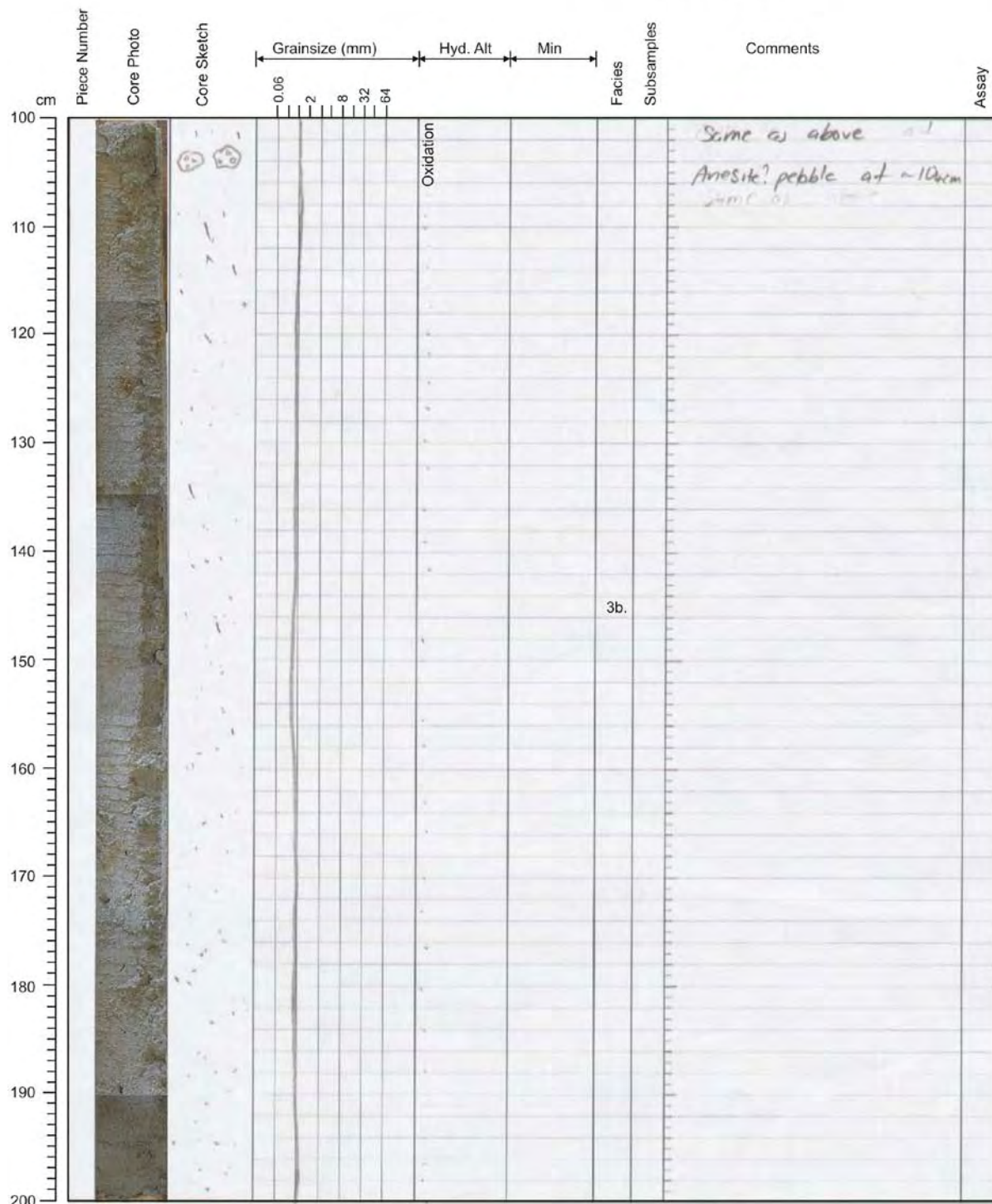
M73/2 - Station: 900 Date: Aug. 22 Time: 13:00-13:29Lat.: 38°38.999'N Long.: 15°06.398'E Water depth: 81

- ☐ Rock core
☒ Vibro core
☐ Gravity corer



M73/2 - Station: 900 Date: Aug. 22 Time: 13:00-13:29Lat.: 38°38.999'N Long.: 15°06.398'E Water depth: 81

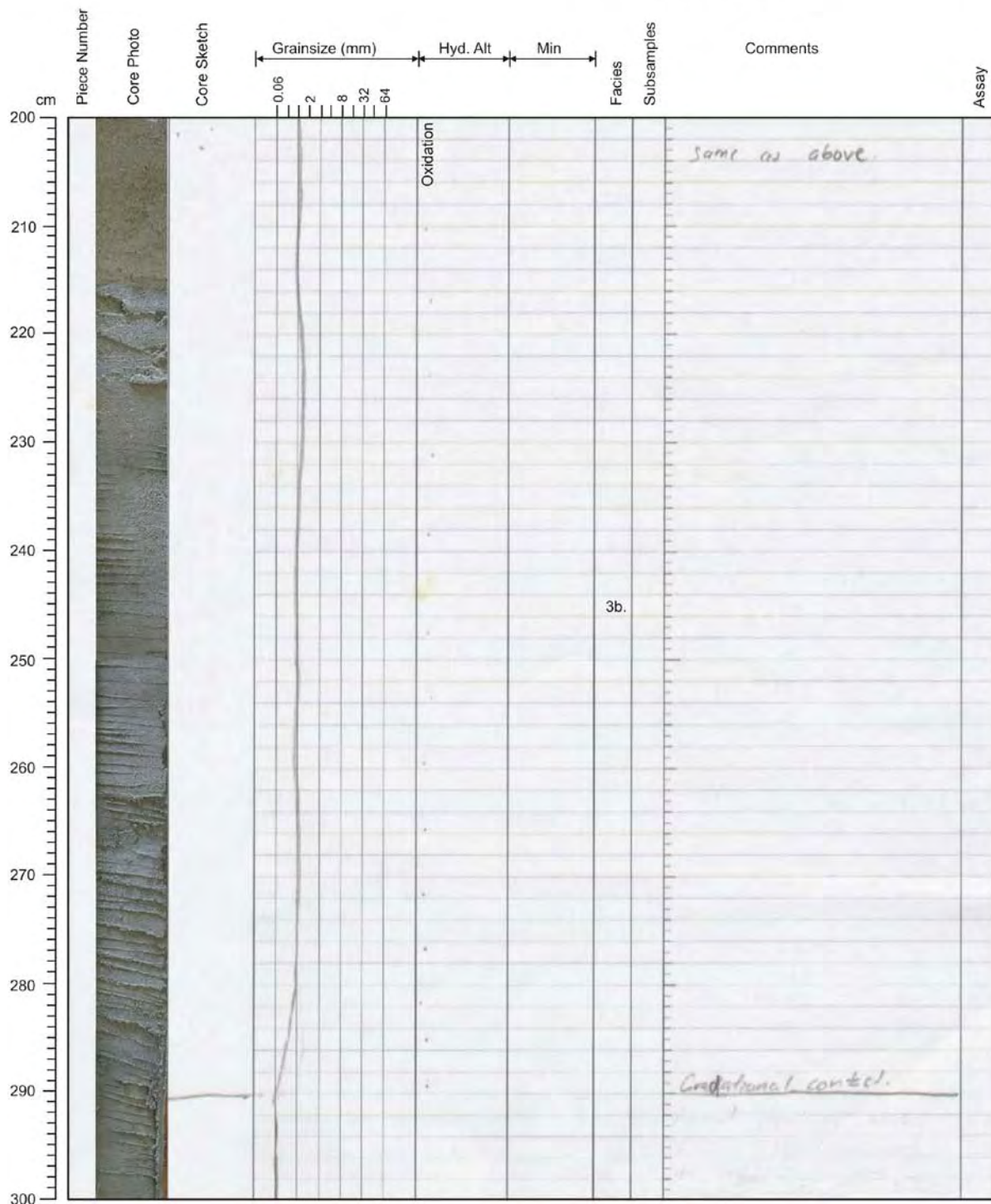
- ☐ Rock core
☒ Vibro core
☐ Gravity corer



M73/2 - Station: 900 Date: Aug. 22 Time: 13:00-13:29

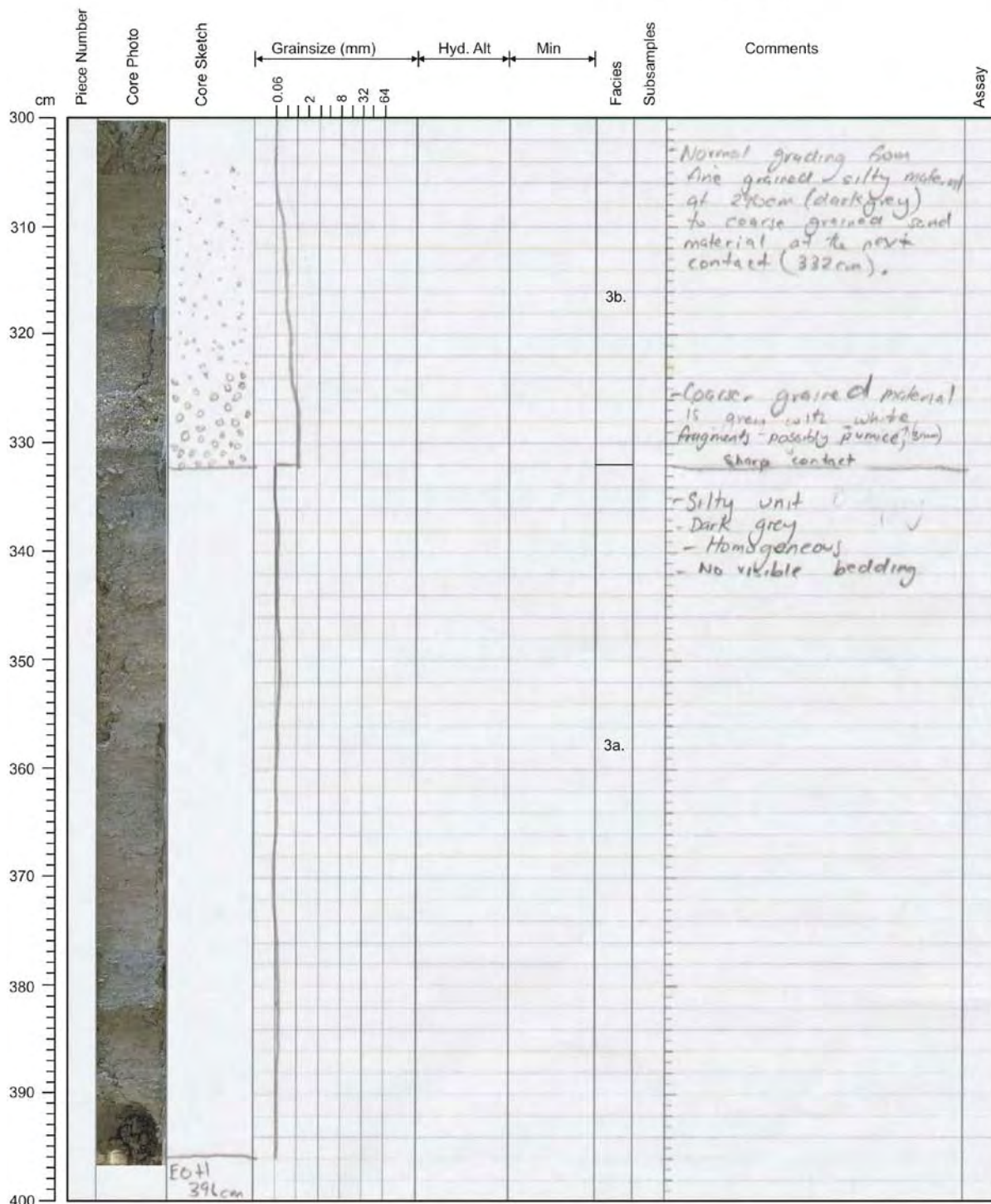
Lat.: 38°38.999'N Long.: 15°06.398'E Water depth: 81

- ☐ Rock core
☒ Vibro core
☐ Gravity corer



M73/2 - Station: 900 Date: Aug. 22 Time: 13:00-13:29Lat.: 38°38.999'N Long.: 15°06.398'E Water depth: 81

- ☐ Rock core
☒ Vibro core
☐ Gravity corer



M73/2 - Station: 902 Date: Aug. 22 Time: 15:48-16:59

Lat.: 38°38.944'N Long.: 15°05.388'E Water depth: 59

- ☒ Rock core
☐ Vibro core
☐ Gravity corer





Piece Number	Core Photo	Core Sketch	Grainsize (mm)	Hyd. Alt	Min	Facies	Subsamples	Comments	Assay
			0.06 2 8 32 64						
1								Amphibole-feldspar phyric intermediate coherent rock (dacite/andesite)	
2								Amphibole: euhedral, up to 2mm, 2% Plagioclase: euhedral, 1-2%, up to 3mm	
3								amygdales? 0.5-1mm, round to angular, infilled with blue chalcidony & white to green clay minerals, 2%. May be weathered out phenocrysts	
4								Fine-grained sugary-textured groundmass	
5						3f.		- weathered edges of feldspar on some pieces at top of hole Basal contact not exposed broken core	
6								Feldspar-phyric intermediate coherent (rhyolite/dacite) - Feldspar: subhedral, 5% 1-2mm - Amphibole: euhedral-subhedral <1% - Biotite? <<1%, euhedral - Magnetite, trace	
7								Zenoliths - x-stal-rich (same biotite-hbl-feldspar unit as seen in Zenoliths below) EDH = 38cm groundmass: fine grained interlocking feldspar laths	

M73/2 - Station: 903 Date: Aug. 22 Time: 17:13-18:20Lat.: 38°38.945'N Long.: 15°05.374'E Water depth: 60

- ☒ Rock core
☐ Vibro core
☐ Gravity corer



Piece Number	Core Photo	Core Sketch	Grainsize (mm)	Hyd. Alt	Min	Facies	Subsamples	Comments	Assay
0			0.05						
5			2					Feldspar-amphibole-phyric intermediate coherent rock	
10			8					Feldspar euhedral, 10%, 1-7mm Amphibole euhedral, 2%, 1-2mm Groundmass aphanitic EOH = 5.5cm	
15			32					weathered Fe-oxide rind on clast	
20			64					mini-size xenoliths (X-stal-mel) may be the same xenoliths as seen in previous holes (biotite-amphibole-feld-phyric)	
25									
30									
35									
40									
45									
50									

M73/2 - Station: 904 Date: Aug. 22 Time: 18:30-21:13

Lat.: 38°38.908'N Long.: 15°05.436'E Water depth: 59

- ☒ Rock core
☐ Vibro core
☐ Gravity corer



Piece Number	Core Photo	Core Sketch	Grainsize (mm)	Hyd. Alt	Min	Facies	Subsamples	Comments	Assay
0			0.06						
1			2					Boulder: Feldspar-amphibole-pyroxene phyric coherent intermediate rock	
2			8					Feldspar: euhedral, 1-2 mm, 10%, partially alt'd to illite/sericite Amphibole: euhedral, 1-4 mm, 5% Pyroxene: euhedral, 1-2 mm 1%, partially alt'd to oxide Magnetite, 1 mm, <1% Quartz? : possible phenocryst Irregular vugs/vesicles lined with & rimmed by limonite groundmass: grey, aphanitic patchy limonite/hematite alteration	
3			32					- sulfate lining vugs/vesicles - some of the vugs look like weathered out phenos - weathered outer rife to Fe-oxide - from 0-29 cm is one boulder	
4			64						
5									
6								Boulders: rounded pebbles feldspar-phyric coherent rock	
7								Boulder: lt. grey feldspar- amphibole-quartz-phyric coherent intermediate rock (dacite) Aphyric groundmass Phenocrysts euhedral, 1-2 mm Boulder: feldspar-amphibole- pyroxene-phyric coherent rock Groundmass: fine-grained crystalline possibly peritic, arcuate, spherical shape Phenocryst euhedral, Amphibole phenos up to 5 mm. Feld: 5-8% Mafics: 5%, Magnetite <1% Boulders: rounded pebbles feld-phyric coherent rock	

M73/2 - Station: 904 Date: Aug. 22 Time: 18:30-21:13

Lat.: 38°38.908'N Long.: 15°05.436'E Water depth: 59

- ☒ Rock core
☐ Vibro core
☐ Gravity corer

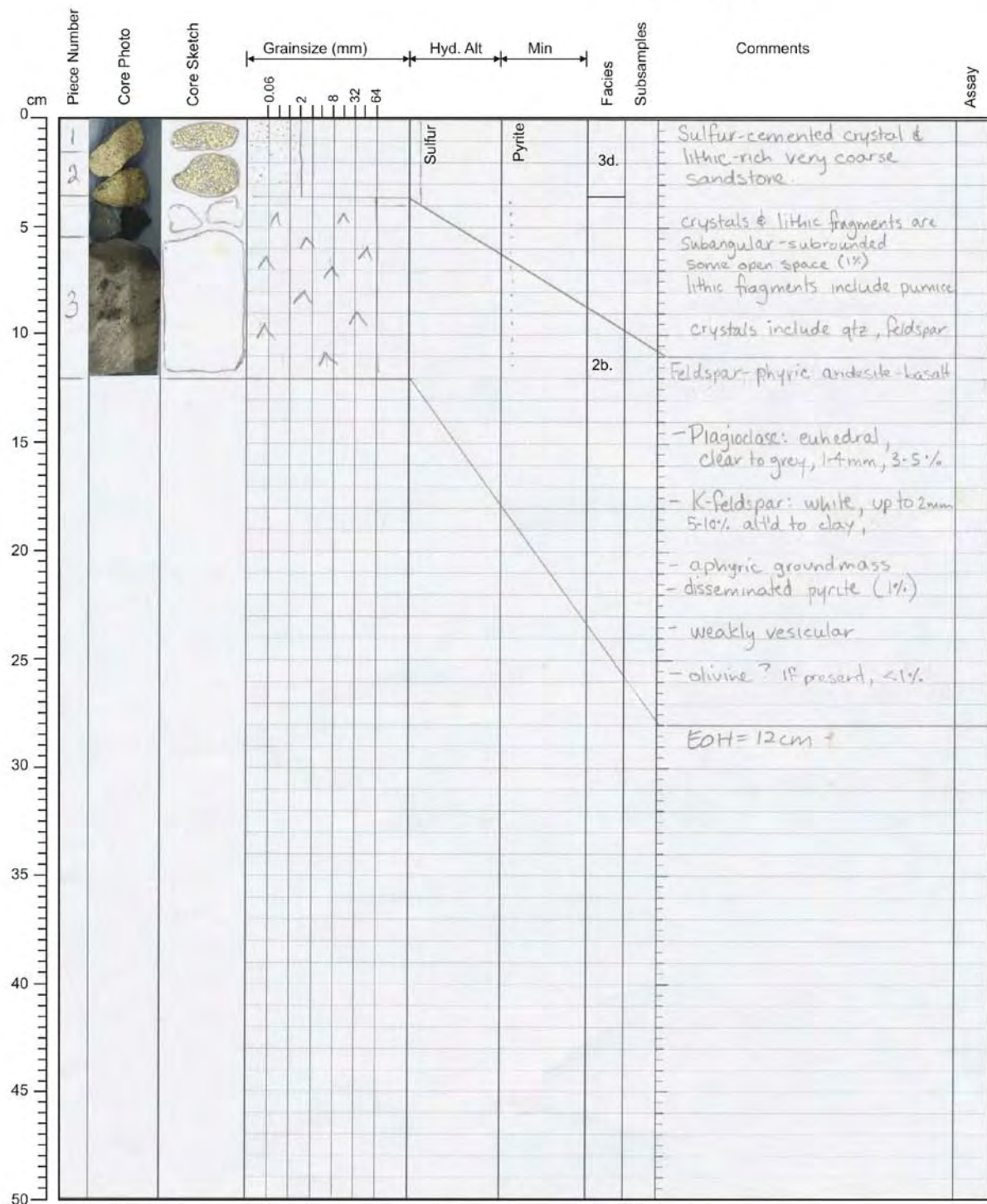


Piece Number	Core Photo	Core Sketch	Grainsize (mm)	Hyd. Alt	Min	Facies	Subsamples	Comments	Assay
cm			0.06 2 8 32 64						
50								Boulders	
55								Feldspar-amphibole-pyroxene phyric coherent rock - 2.5% total phenocrysts - possibly minor qtz - aphanitic groundmass	
60								- partial alt'n of mafic phases to Fe-oxide	
65								- some pyroxenes have a thin white rim of an unknown mineral	
70							3f.	- some vugs infilled with green clay (nontronite)	
75								- soft green clay? surface coatings	
80									
85								FOH = 85cm	
90									
95									
100									

M73/2 - Station: 908 Date: Aug. 23 Time: 01:25-03:09

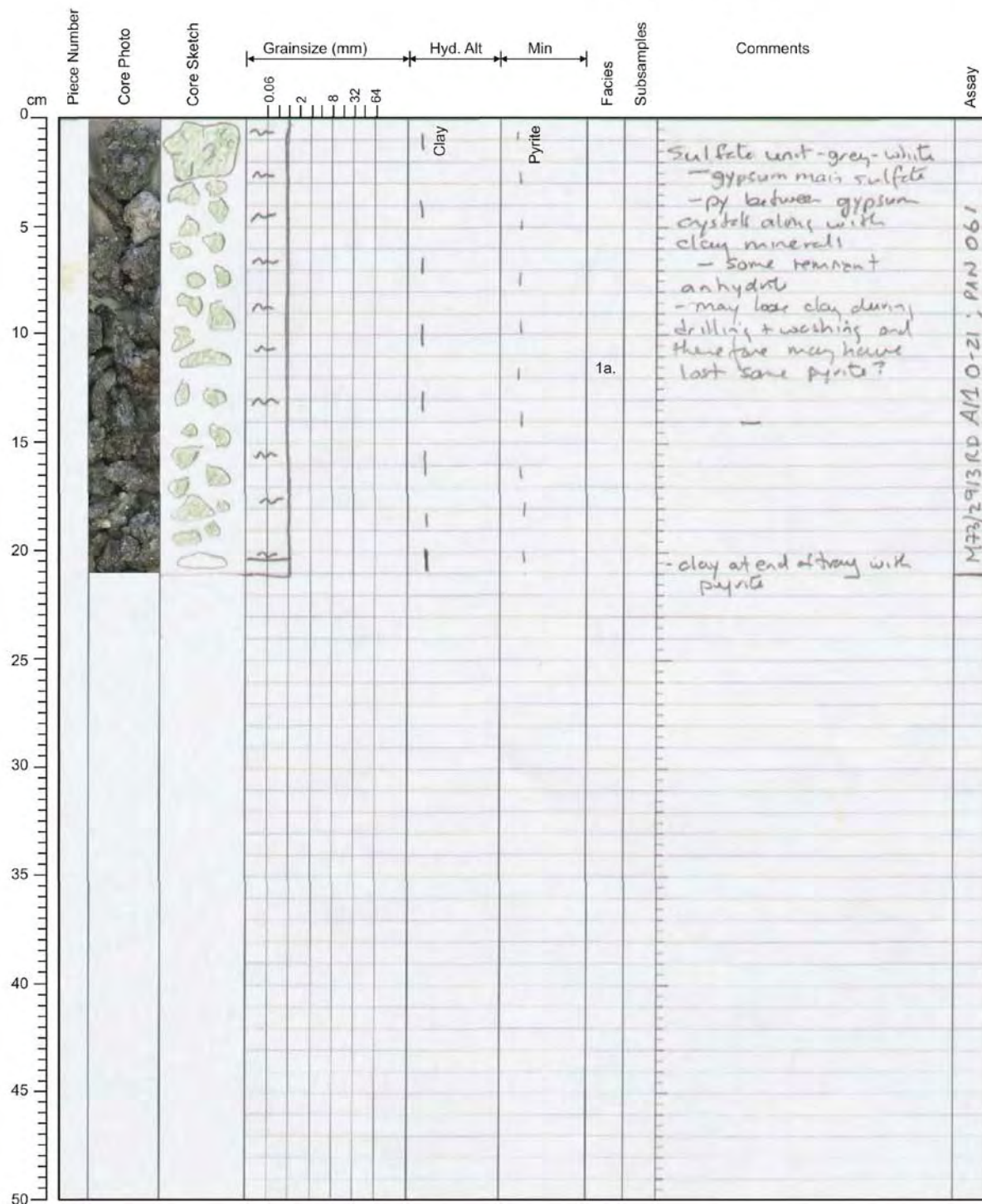
Lat.: 38°38.852'N Long.: 15°06.728'E Water depth: 63

- ☒ Rock core
☐ Vibro core
☐ Gravity corer



M73/2 - Station: 913 Date: Aug. 23 Time: 10:00-10:49Lat.: 38°38.951'N Long.: 15°06.418'E Water depth: 82

- ☒ Rock core
☐ Vibro core
☐ Gravity corer



M73/2 - Station: 914 Date: Aug. 23 Time: 11:06-13:14

Lat.: 38°38.946'N Long.: 15°06.422'E Water depth: 84

- ☒ Rock core
☐ Vibro core
☐ Gravity corer



Piece Number	Core Photo	Core Sketch	Grainsize (mm)	Hyd. Alt	Min	Facies	Subsamples	Comments	Assay
			0.06 2 8 32 64						
1				Clay	Pyrite			- mostly gypsum with minor clay between crystals - crystals rounded by dissolution? - grey-white clay - py in clay & in gypsum	PAN 062
2								- as above	O-34 on
3									
4								dominantly gypsum as above - clay + pyrite between crystals	
5								as above	
6									
7						1a.		as above as above - silvery sulfide fr.	M73/2 914 RD A12
8								as above	
9								as above	
10								as above - crystals + assemblage of yellow-silver pyrite	
11								Same as above but with distinct inclusions of massive green + grey clay - py in clay + gypsum	
12								as above - no clay inclusions	
13								as above	

M73/2 - Station: 914 Date: Aug. 23 Time: 11:06-13:14

Lat.: 38°38.946'N Long.: 15°06.422'E Water depth: 84



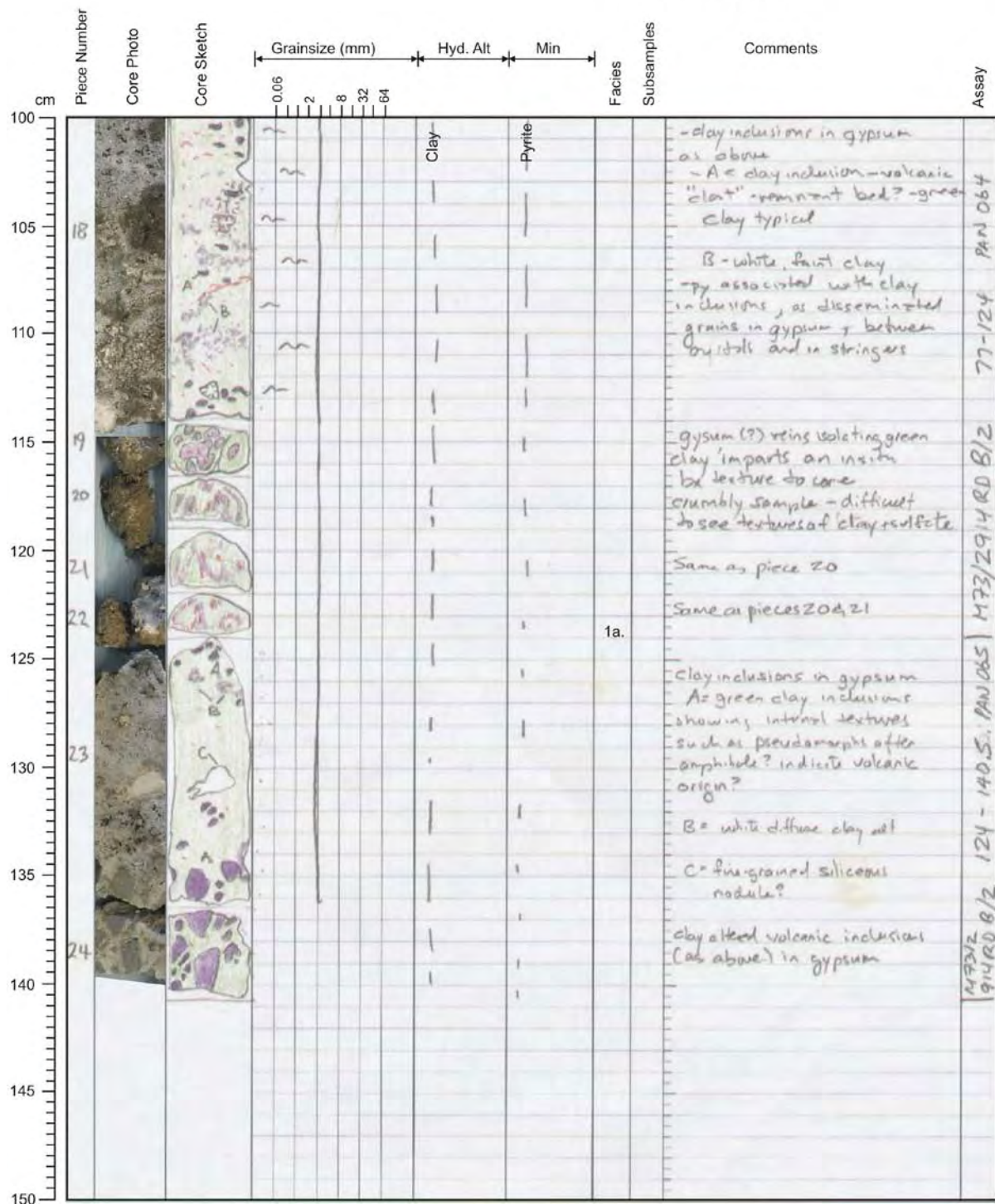
- ☒ Rock core
☐ Vibro core
☐ Gravity corer

Piece Number	Core Photo	Core Sketch	Grainsize (mm)	Hyd. Alt	Min	Facies	Subsamples	Comments	Assay
			0.06 2 8 32 64						
50									
55									
60	14							- as above, primarily gypsum. - clays range in color from white, grey, green in color, sometimes with internal structure that may suggest alteration of a rock fragment?? Other clay does not and could be rest of a fine sediment or buff?	34.77 PAU063
65									
70	15							as above	
75	16							as above	
80									
85	17							as above	
90									
95									
100	18							Clay inclusion - not gypsum - irregular inclusion, 1.5 cm to 1 mm, of predominantly green clay with occasional white clay - inclusions have pseudomorph of minerals - hornblende? Suggesting it is after a volcanic lithology - pink with clay but more concentrated in gypsum - higher pyrite content than sections above - clay inclusion - red matrix - internal text to clay inclusion suggest volcanic - py in clay but more concentrated in a between gypsum crystals	M73/2 914 RD A/2

M73/2 - Station: 914 Date: Aug. 23 Time: 11:06-13:14

Lat.: 38°38.946'N Long.: 15°06.422'E Water depth: 84

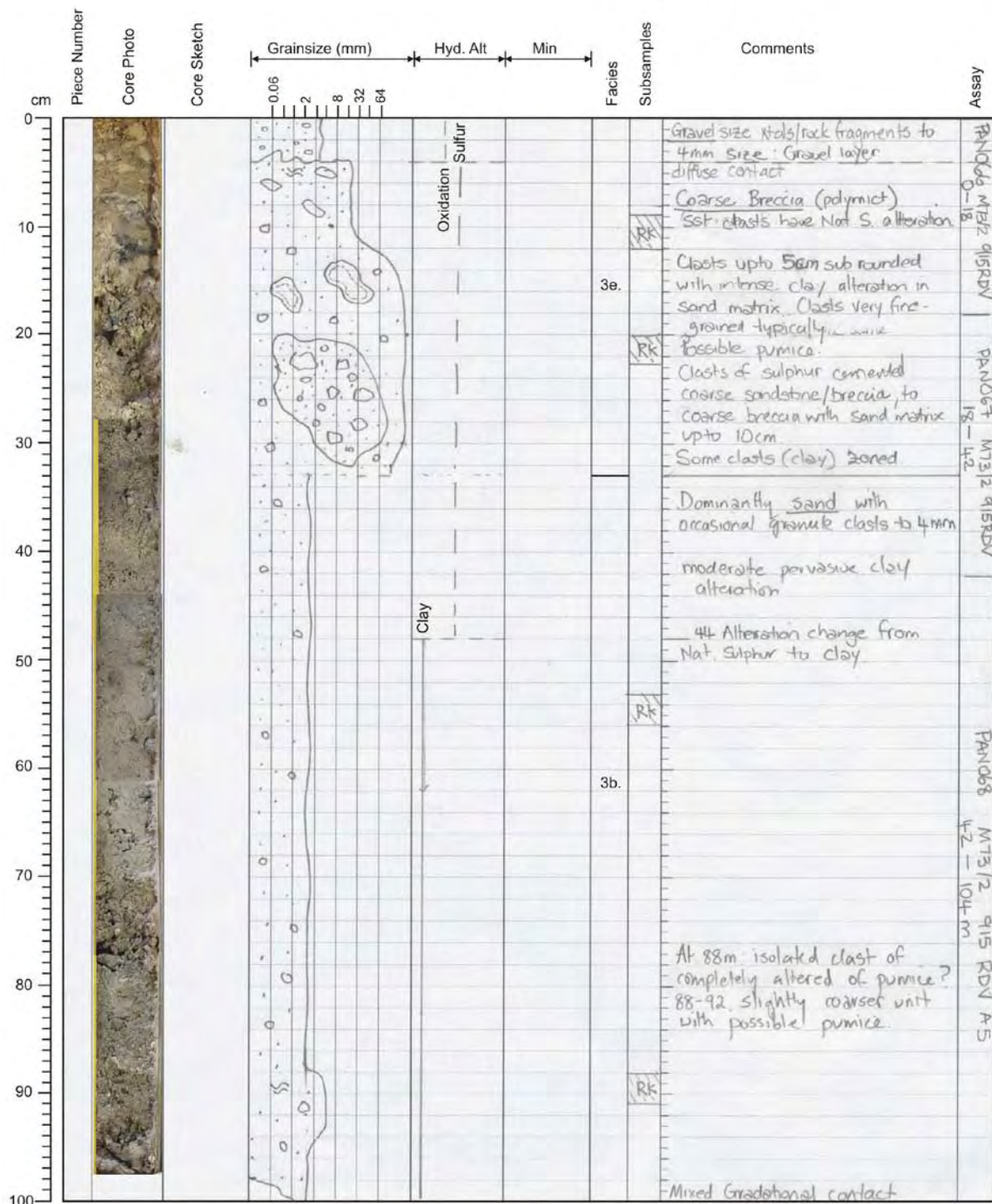
- ☒ Rock core
☐ Vibro core
☐ Gravity corer



M73/2 - Station: 915 Date: Aug. 23 Time: 13:34-14:00

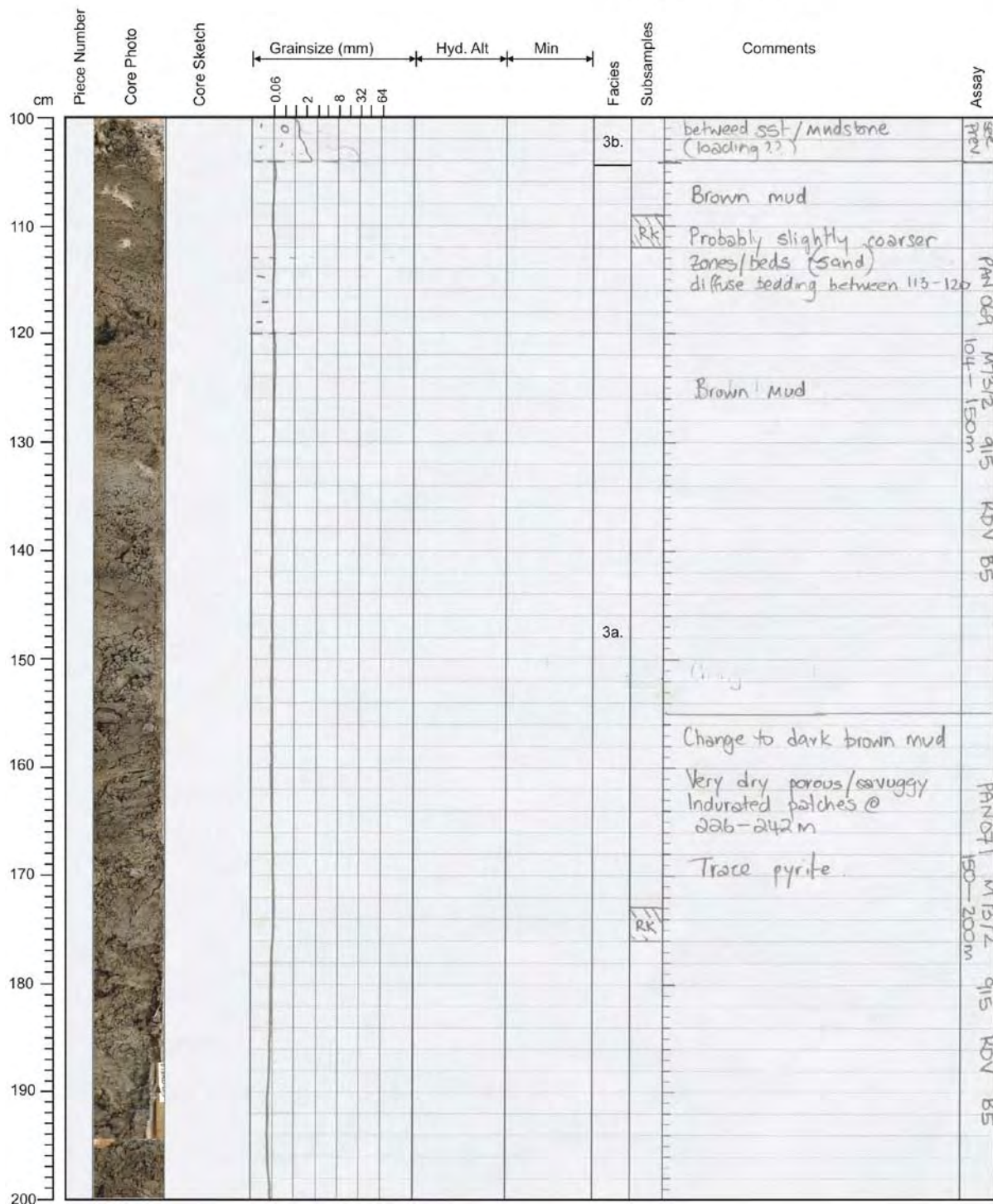
Lat.: 38°38.953'N Long.: 15°06.418'E Water depth: 82

- ☐ Rock core
☒ Vibro core
☐ Gravity corer



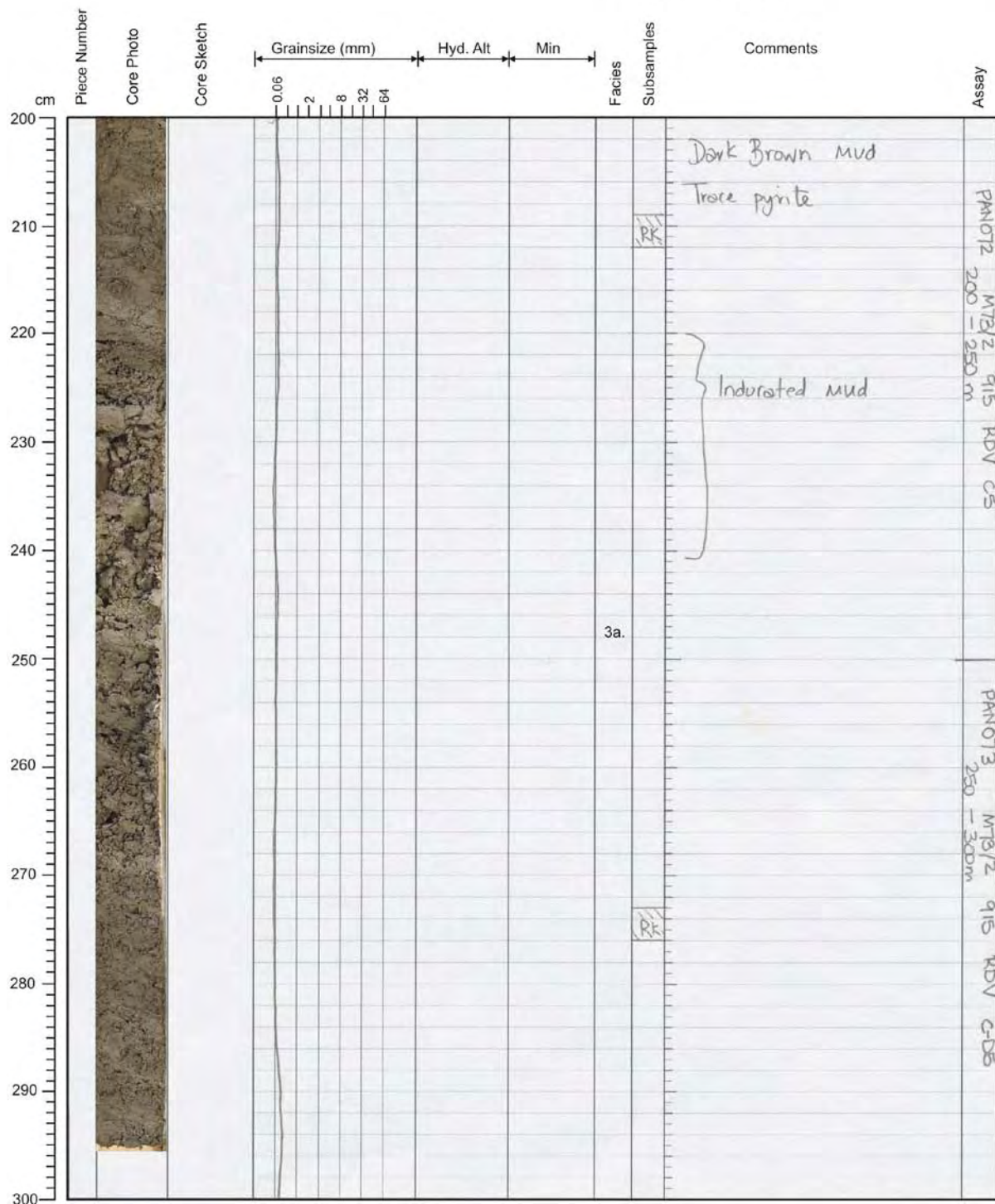
M73/2 - Station: 915 Date: Aug. 23 Time: 13:34-14:00Lat.: 38°38.953'N Long.: 15°06.418'E Water depth: 82

- ☐ Rock core
☒ Vibro core
☐ Gravity corer



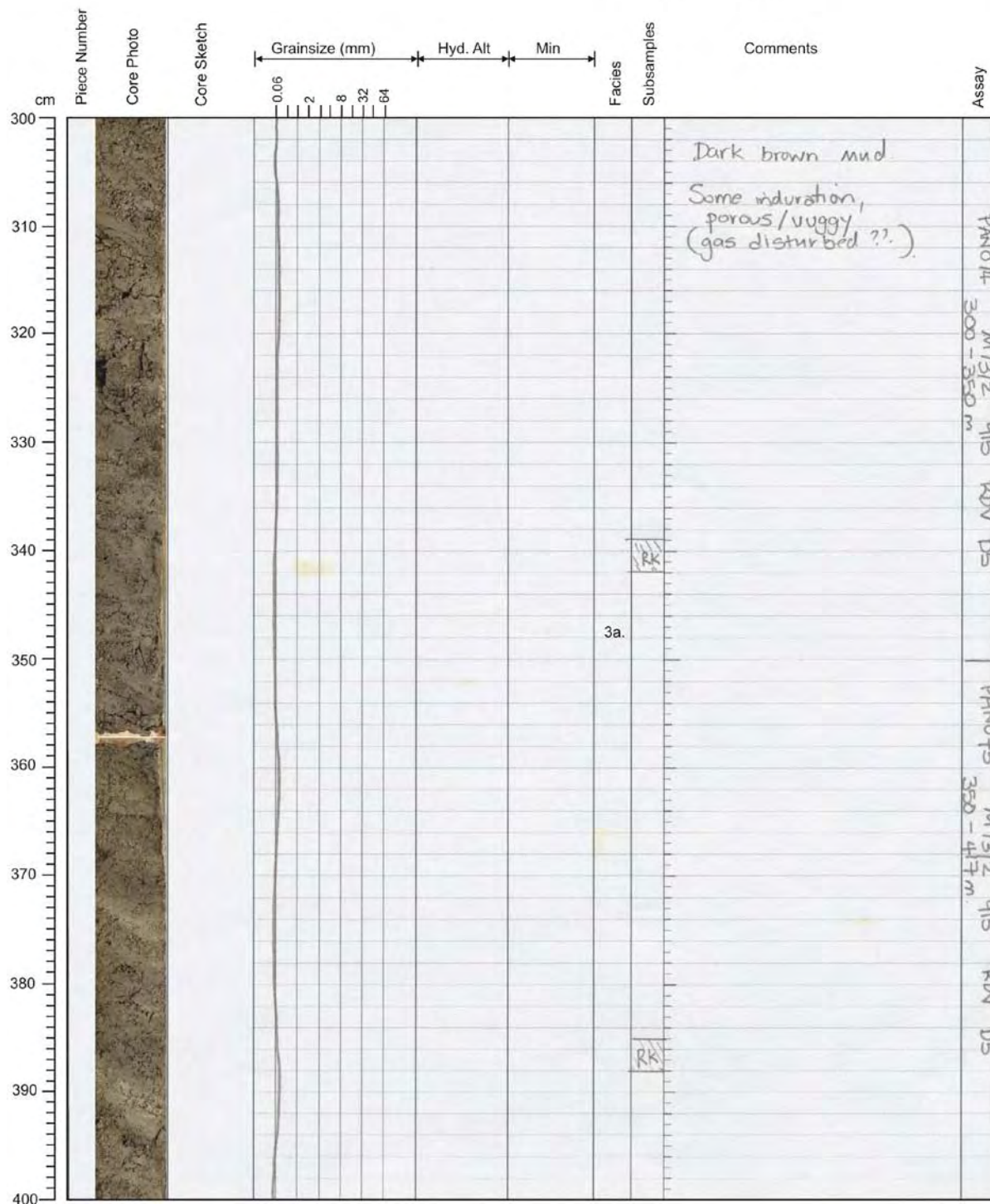
M73/2 - Station: 915 Date: Aug. 23 Time: 13:34-14:00Lat.: 38°38.953'N Long.: 15°06.418'E Water depth: 82

- ☐ Rock core
☒ Vibro core
☐ Gravity corer



M73/2 - Station: 915 Date: Aug. 23 Time: 13:34-14:00Lat.: 38°38.953'N Long.: 15°06.418'E Water depth: 82


- ☐ Rock core
☒ Vibro core
☐ Gravity corer



M73/2 - Station: 915 Date: Aug. 23 Time: 13:34-14:00Lat.: 38°38.953'N Long.: 15°06.418'E Water depth: 82

- ☐ Rock core
☒ Vibro core
☐ Gravity corer



Piece Number	Core Photo	Core Sketch	Grainsize (mm)	Hyd. Alt	Min	Facies	Subsamples	Comments	Assay
cm			0.06 2 8 32 64						
400									
410						3a.			As previous
420		47 cm EOM							
430									
440									
450									
460									
470									
480									
490									
500									

M73/2 - Station: 918 Date: Aug. 24 Time: 10:06-12:38

Lat.: 39°17.014'N Long.: 14°23.798'E Water depth: 508

- ☒ Rock core
☐ Vibro core
☐ Gravity corer



Piece Number	Core Photo	Core Sketch	Grainsize (mm)	Hyd. Alt	Min	Facies	Subsamples	Comments	Assay
			0.06 2 8 32 64						
1			✓	✓	✓			Vesicular, aphanitic, Feld porph basalt - black in color - -silica in vesicles - <10% Feld, <2mm	MARCO
2			✓	✓	✓			as above	
3			✓	✓	✓			Vesicular basalt - silica lining vesicles	
4			✓	✓	✓			minor olivine 1-2%, 1mm	
5			✓	✓	✓			as above	
6			✓	✓	✓			as above	
7			✓	✓	✓			as above	
8			✓	✓	✓			as above	
9			✓	✓	✓			as above	
10			✓	✓	✓	2a.		as above	
11			✓	✓	✓			as above	
12			✓	✓	✓			as above	
13			✓	✓	✓			as above	
14			✓	✓	✓			as above	
15			✓	✓	✓			as above	
16			✓	✓	✓			Sparsely fp - 12% <25mm Basalt vesicular silica lining some vesicles oxide crust (<1mm) on some pieces	

M73/2 - Station: 920 Date: Aug. 24 Time: 15:49-18:14

Lat.: 39°17.016'N Long.: 14°23.816'E Water depth: 513

- ☒ Rock core
☐ Vibro core
☐ Gravity corer



Piece Number	Core Photo	Core Sketch	Grainsize (mm)	Hyd. Alt	Min	Facies	Subsamples	Comments	Assay
			0.06 2 8 32 64						
1			V					Moderately vesicular plagioclase - phryic basalt	
2			V					Plagioclase - euhedral, 1-2mm 5%	
3			V					Olivine - euhedral, <1mm <1%	
4			V					Magnetite - rock is moderately magnetic but no discrete phenos therefore likely disseminated throughout groundmass	
5			V					Vesicles: round to irregular, in places elongate in one direction	
6			V			2a.		Groundmass: aphanitic, glassy with microlites	
7			V					Fe-oxide weathering on the outer surface of some pebbles	
8			V						
9			V						
10			V						
11			V						
12			V						
13			V						
50								EOH=98.5	

M73/2 - Station: 925 Date: Aug. 26 Time: 10:25-13:25

Lat.: 39°31.261'N Long.: 14°39.707'E Water depth: 635

- ☒ Rock core
☐ Vibro core
☐ Gravity corer



Piece Number	Core Photo	Core Sketch	Grainsize (mm)	Hyd. Alt	Min	Facies	Subsamples	Comments	Assay
0			0.06						
1			2					feldspar - olivine porphyritic massive aphanitic andesite-basalt - Black in colour Feldspars - 8-10% - <5mm Olivine - 1% - <2.5mm - vesicular - vesicles range up to 7mm - 3.5% - round to elongate	
2			2						
3			2					* includes a sample of clay sand that contains sand to granule-sized grains of basalt/andesite, olivine, clay altered clasts, and an intermediate amphibole porphyritic granul.	
4			2					- clay-sized mtx	
5			2					Sample 925 RD-a	
6			2						
7			2						
8			2						
30		END 29 cm							
35									
40									
45									
50									

M73/2 - Station: 927 Date: Aug. 26 Time: 16:46-19:20Lat.: 39°31.702'N Long.: 14°39.208'E Water depth: 709

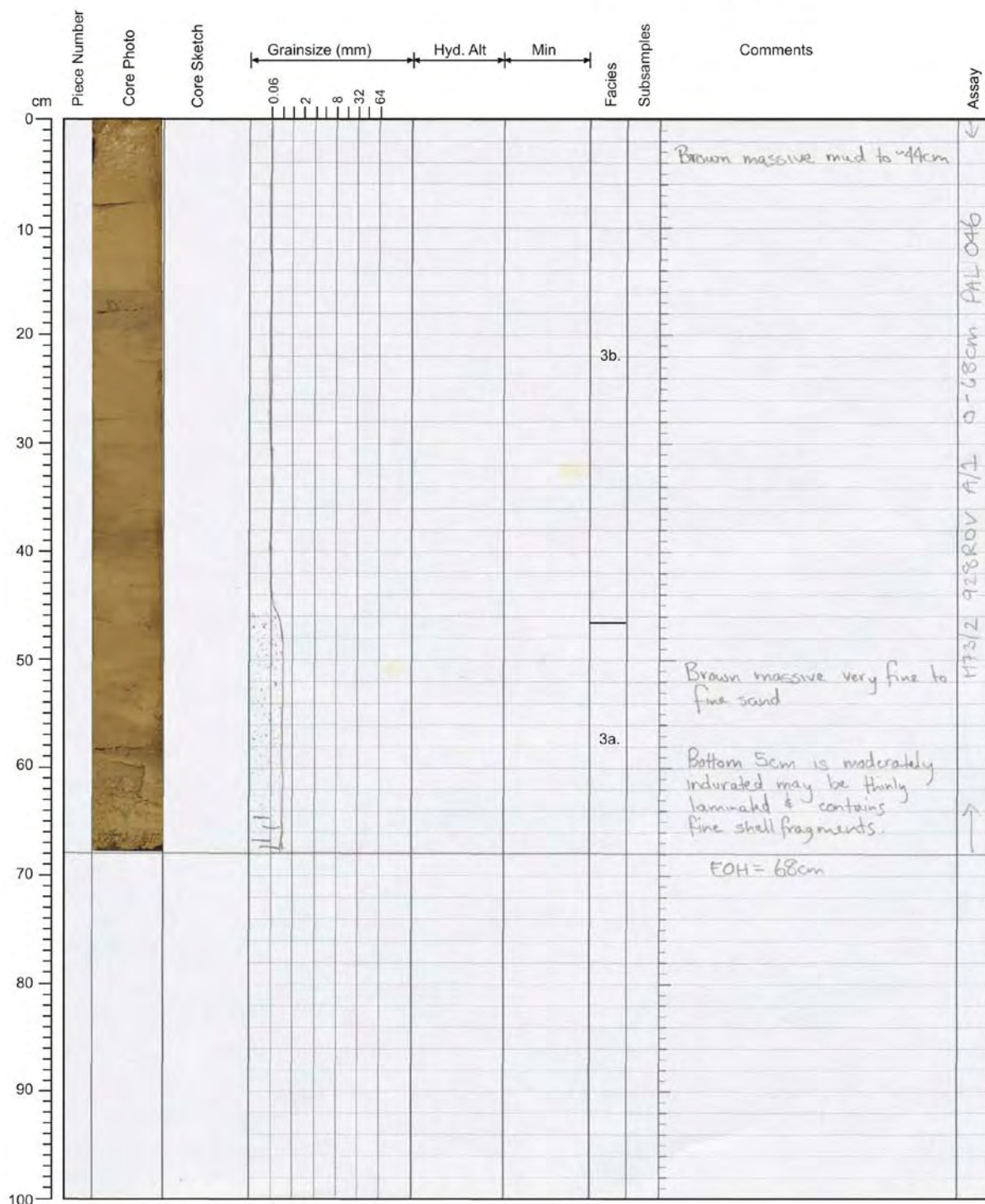
- ☒ Rock core
☐ Vibro core
☐ Gravity corer



Piece Number	Core Photo	Core Sketch	Grainsize (mm)	Hyd. Alt	Min	Facies	Subsamples	Comments	Assay
0			0.06						
5			2					Thinly-laminated very fine sand with shell fragments & rare whole shells up to 3mm - indurated Worm holes, 1mm.	
10			8					Yellow-brown crust at top of hole is Fe-oxide encrusted sand which contains a greater proportion of mafic minerals including magnetite.	
15			32					Sand is grey-brown with a few green layers near the top	
20			64					EcH = 10 cm	
25								* bottom 7 cm is unconsolidated & disrupted - apparently massive	
30									
35									
40									
45									
50									

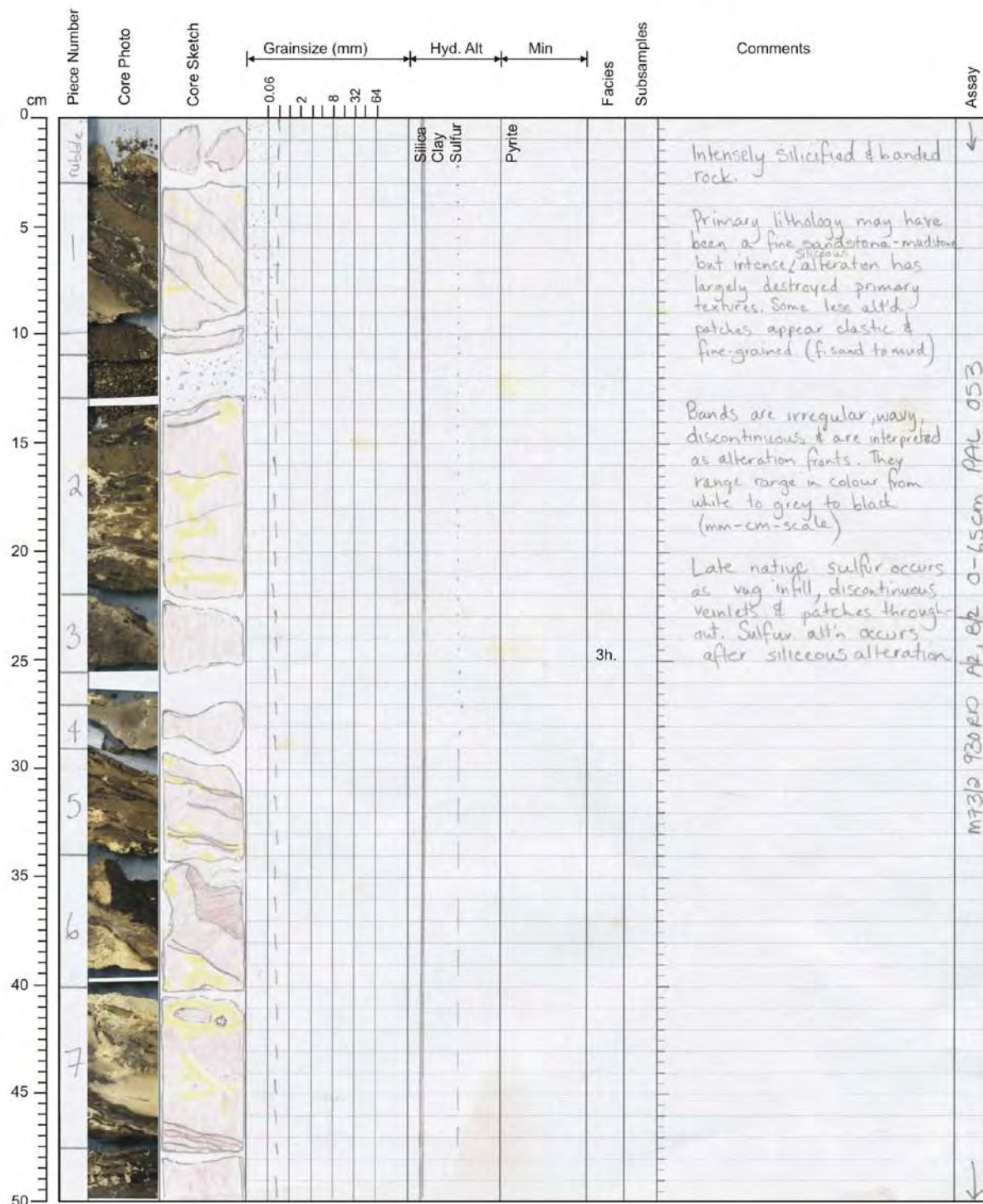
M73/2 - Station: 928 Date: Aug. 26 Time: 19:45-20:42Lat.: 39°31.695'N Long.: 14°39.201'E Water depth: 708

- ☐ Rock core
☒ Vibro core
☐ Gravity corer



M73/2 - Station: 930 Date: Aug. 26-27 Time: 23:52-02:13Lat.: 39°32.437'N Long.: 14°42.384'E Water depth: 627

- ☒ Rock core
☐ Vibro core
☐ Gravity corer



M73/2 - Station: 930 Date: Aug. 26-27 Time: 23:52-02:13Lat.: 39°32.437'N Long.: 14°42.384'E Water depth: 627

- ☒ Rock core
☐ Vibro core
☐ Gravity corer



Piece Number	Core Photo	Core Sketch	Grainsize (mm)	Hyd. Alt	Min	Facies	Subsamples	Comments	Assay
			0.06 2 8 32 64			Silica Sulfur Pyrite			
50									
55							3h.	Same as previous	
60									
65									
70							3g.	Massive, crystal & lithic-rich coarse sandstone Unaltered except for minor patchy sulfur	
75								Crystals include qtz & feldspar & minor mafic minerals	
80								Some lithic fragments pervasively altered to a green clay (up to 3%)	
85							1e.	Massive sulfide pebbles (see description below) These pebbles indicate the presence of a massive sulfide layer but context & thickness unknown	
90							3g.	Massive crystal & lithic-rich coarse sandstone (as seen above)	
95									
100									

M73/2 - Station: 930 Date: Aug. 26-27 Time: 23:52-02:13Lat.: 39°32.437'N Long.: 14°42.384'E Water depth: 627

- ☒ Rock core
☐ Vibro core
☐ Gravity corer

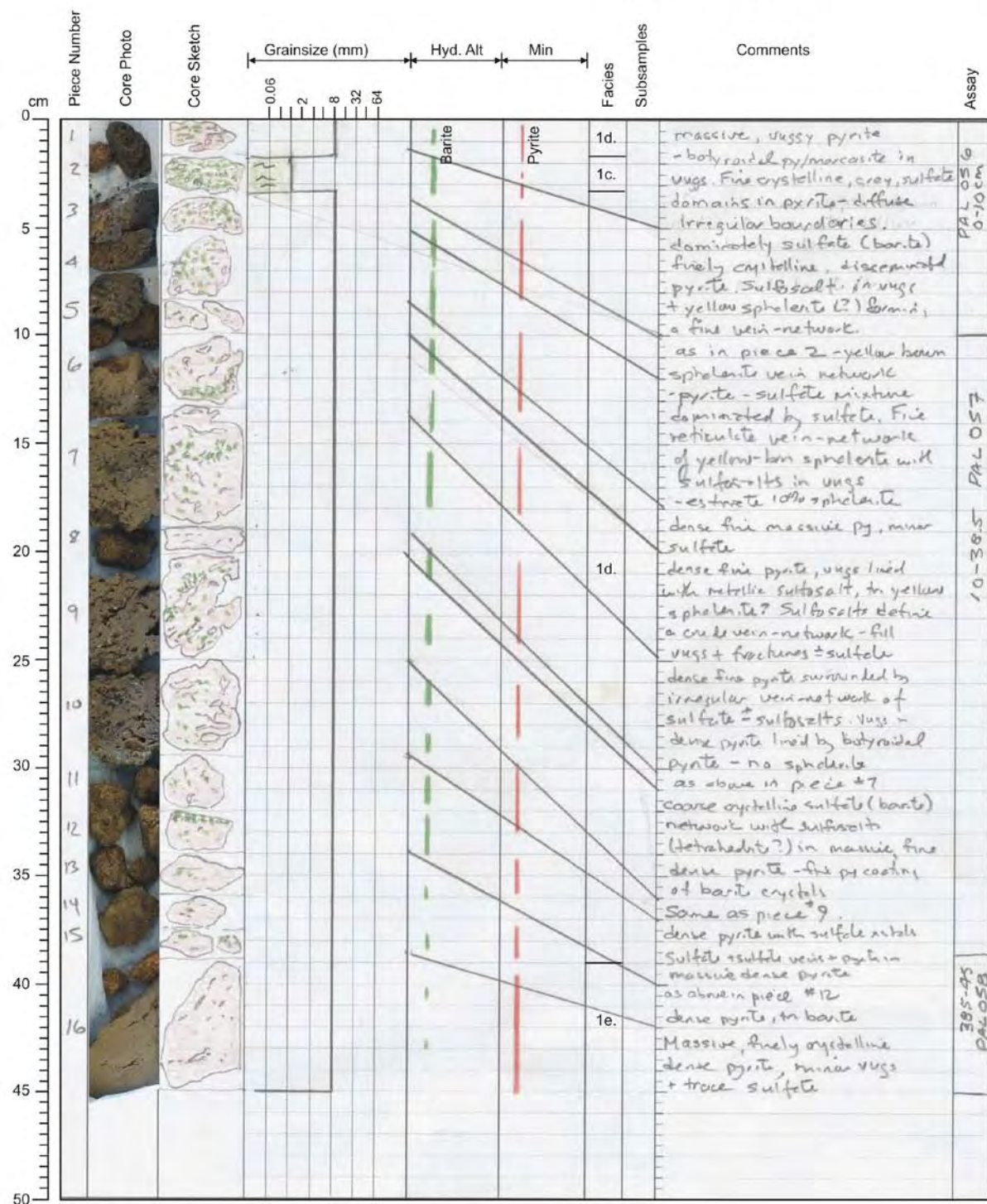


Piece Number	Core Photo	Core Sketch	Grainsize (mm)	Hyd. Alt	Min	Facies	Subsamples	Comments	Assay
cm			0.05 2 8 32 64						
100									
105								Massive sulfide 70% pyrite 28% Sulfate 2% silver coloured sulfide sulfosalt	
110						1e.		Sulfate may be a mixture of gypsum + anhydrite + barite.	
115								5-8% open space/vugs some vugs lined with cuboidal sulfate x-stals. some vugs lined with botryoidal Fe-sulfide	
120								EOH = 118cm	
125									
130									
135									
140									
145									
150									

M73/2 - Station: 931 Date: Aug. 27 Time: 02:38-05:43

Lat.: 39°32.440'N Long.: 14°42.381'E Water depth: 626

- ☒ Rock core
☐ Vibro core
☐ Gravity corer



M73/2 - Station: 932 Date: Aug. 27 Time: 06:03-07:57

Lat.: 39°32.435'N Long.: 14°42.377'E Water depth: 626

- ☒ Rock core
☐ Vibro core
☐ Gravity corer



Piece Number	Core Photo	Core Sketch	Grainsize (mm)	Hyd. Alt	Min	Facies	Subsamples	Comments	Assay
			0.06 2 8 32 64						
1				Sulfate Silica	Opiment Pyrite			Silicified, brecciated siltstone?	PAL 059
2									
3									
4						3f.		- Breccia of fine siliceous white to black siltstone, may be laminated but altered. Matrix is massive, fine-grained grey and siliceous contains some crystals (?) and finer fragments (conglomerate look in matrix) - fgr pyrite	M73/2 932 RD A15
5									
6								- grey siliceous matrix as in overlying breccia within upper 2 cm of piece surrounded by pyrite - undulating network of barite (?) plus pyrite - vuggy - network of honey sphenolite?	PAL 061
7								- sulfate network with silica in semi massive fgr vuggy pyrite - late sulfur crystals in some vugs + fractures - trace sulfur salt in some vugs	18-48
8						1d.		- as above in piece 8 - web-like network of sulfate and silica (?) within fgr vuggy pyrite - silica lines some vugs and few sulfur crystals in vugs - yellow-orange mineral (cassiterite?) in a few vugs - sphenolite - barite / orpiment? - tr. sphenolite between barite crystals in vugs	M73/2 932 RD A15
9								- as above	

M73/2 - Station: 932 Date: Aug. 27 Time: 06:03-07:57Lat.: 39°32.435'N Long.: 14°42.377'E Water depth: 626

- ☒ Rock core
☐ Vibro core
☐ Gravity corer



Piece Number	Core Photo	Core Sketch	Grainsize (mm)	Hyd. Alt	Min	Facies	Subsamples	Comments	Assay
			0.06 2 8 32 64			Sulfate Silica Pyrite			
50									
55									
60									
65									
70							1d.	upper part of piece more py - rich - fgr, dense	
75								lower part of piece more sulfate-rich - lots sulfur in vugs ± silica ± coarser barite - Sulfosalts in vugs + barite.	
80									
85									
90							1c.	Veri-network of fine pyrite in sulfate produces a pseudob texture locally	
95									
100									

M73/2 - Station: 932 Date: Aug. 27 Time: 06:03-07:57

Lat.: 39°32.435'N Long.: 14°42.377'E Water depth: 626

- ☒ Rock core
☐ Vibro core
☐ Gravity corer



Piece Number	Core Photo	Core Sketch	Grainsize (mm)	Hyd. Alt	Min	Facies	Subsamples	Comments	Assay
			0.05 2 8 32 64						
11						1c.		- sulphate-rich as above	
105						1e.		- more pyrite-rich base but with vein-net of sulfide	
110								- massive sulfide = sulfosalt + pyrite - sulphur in vugs	
115								- very sulfur-rich section - sulfur in vugs and fractures = silica	
120								- unit is a "massive sulfide" section with diss pyrite and silver colored sulfosalt	PAL 063
125						1c.		- as above - sulfur exists in irregular fractures and vugs within a sulfide-rich unit containing sulfosalts and diss pyrite	110-160
130								- irregular vein network of honey brown sphalerite	
135									
140									
145						1d.		- Sharp-walled to diffuse-walled sulfur veinlets in pyrite and sulfide - fine botryoidal pyrite-marcasite in vugs - fine sphalerite stringers - honey color sphalerite - late barite? in vugs also	M73/2 932 RD B/S; C/S
150									

M73/2 - Station: 932 Date: Aug. 27 Time: 06:03-07:57

Lat.: 39°32.435'N Long.: 14°42.377'E Water depth: 626

- ☒ Rock core
☐ Vibro core
☐ Gravity corer



Piece Number	Core Photo	Core Sketch	Grainsize (mm)	Hyd. Alt	Min	Facies	Subsamples	Comments	Assay
			0.06 2 8 32 64						
14								as above	
15								Top - intergrown barite? + sulfur (sulfosalts) - within a sulphate vein - network w/ pyrite - dense veins of massive pyrite	
16								- Dense, pyr. pyrite contains "islands" of sulfates (sulfosalts) with a fine vein-net texture and sharp - diffuse boundaries with pyrite - pseudoclasts - pyr is vuggy + contains fine vein-net of sulfates identical to the pseudoclasts of massive sulfates	160-193 PAL 064
17								pseudoclastic sulfide-sulfate "clasts" of gray, finely bladed sulfates (rounded with sharp - diffuse margins) in a pyrite or pyrite-sulfate matrix - sulfosalts in more massive sulfates + vugs - later sulfur in vugs + sulfur intergrown with sulfates	M73/2 932 RD C15
18								- Coarse sulfates (barite?) crystals forming a network with intergrown sulfur - sulfur also occurs in vugs and is crystalline - later sulfates w/ coarse sulfates?	1c.

M73/2 - Station: 932 Date: Aug. 27 Time: 06:03-07:57

Lat.: 39°32.435'N Long.: 14°42.377'E Water depth: 626

- ☒ Rock core
☐ Vibro core
☐ Gravity corer



Piece Number	Core Photo	Core Sketch	Grainsize (mm)	Hyd. Alt	Min	Facies	Subsamples	Comments	Assay
			0.06 2 8 32 64						
18						Sulfate Silica Pyrite		As above - two generations of sulfur 1) intergrown with coarse barite 2) crystalline and in vugs and fractures	
19								- similar to but with two domains - 1) fine py in barite network host this coarse bladed barite "clasts" and 2) coarse bladed barite intergrown with sulfur ± pyrite and sulfosalts. - vuggy	193-240 PAL 065
20								- network of sulfate - bladed crystals with fine disseminated pyrite ± sulfosalts - vuggy - sulfur "veins" cross-cut sulfate - diffuse boundaries	
21							1c.	In situ barite sulfate ± py ± minor sulfosalts in a vein matrix of sulfur + barite ± py "clasts" stand out because they are more finely vuggy and have a porous appearance	D/5
22								- as above in piece #21	M73/2 932 R0
23								- as above in pieces 21+22	

M73/2 - Station: 932 Date: Aug. 27 Time: 06:03-07:57

Lat.: 39°32.435'N Long.: 14°42.377'E Water depth: 626

- ☒ Rock core
☐ Vibro core
☐ Gravity corer



Piece Number	Core Photo	Core Sketch	Grainsize (mm)	Hyd. Alt	Min	Facies	Subsamples	Comments	Assay
cm			0.06 2 8 32 64						
250				Sulfate	Silica	Pyrite		pseudo breccia as above	
255									
260							1c.	pseudobreccia as above - sulfide-rich "clasts" - one highly pitted + vuggy - bladed sulfate-sulfur matrix	PAL 066
265									
270								as above	
275								vuggy pyrite (+sulfate) and coarser sulfate-sulfur as above	240-291
280								as above	
285							1d.		
290								as above - two domains 1) sulfide (py) rich + sulphate - vuggy, porous unit 2) sulfate (py, sulfosalt) rich unit, coarser bladed barite with sulfur	M73/2 932 RD D15; E15
295									
300									

A4. Description of TV-guided grab samples

Sample distribution: AB = Arnaldo De Benedetti, AE = Alessandra Esposito, AG = Anke Gardeler, ANG= Andrea Gärtner, AK = Alexander Kayser, BG = Bruce Gemmell, BW =Buyan Wan, GH = Gao-wen He, HG = Harold Gibson, KL = Klas Lackschewitz, KP = Katie Perrin, KS = Kirstie Simpson, MH = Michael Hügler, NE = Neptune Minerals, RK = Reinhard Kleeberg, SP = Sven Petersen, TM = Thomas Monecke.

Sample Group	Facies	Description	Sample distribution
M73/2-866TVG-1	Unconsolidated mud	Brownish unconsolidated mud; sampled from the upper layer of material contained in the TV-guided grab	866TVG-1: RK
M73/2-866TVG-2	Unconsolidated mud	Black unconsolidated mud; sampled from the upper layer of material contained in the TV-guided grab	866TVG-2: RK
M73/2-866TVG-3	Unconsolidated mud	Black unconsolidated mud containing fragments of banded silica-sulfide-sulfate material, mud had an in situ temperature of 52-60°C on board	866TVG-3: RK
M73/2-866TVG-4	Banded silica-sulfide-sulfate	Crudely banded silica-sulfide-sulfate layers; samples are oxidized and sample surfaces are covered by thick Fe oxide crusts; one cone-shaped banded sample that resembles a chimney structure	866TVG-4: SP 866TVG-4A: SP 866TVG-4B: SP 866TVG-4C: SP 866TVG-4D: SP 866TVG-4E: SP
M73/2-866TVG-5	Banded silica-sulfide-sulfate	Thinly (1-5 mm) banded sulfide-sulfate layers with minor gray to white silica bands; limited oxidation and surficial weathering; minor encrustation of native sulfur; sulfur locally rims open space fractures; some samples contain sharp contact between banded silica-sulfide-sulfate and vuggy sulfide-sulfate; one cone-shaped sample that resembles chimney structure; samples contain abundant casts of tubes or burrows that are 2 mm across and up to 3 cm long	866TVG-5A: NE 866TVG-5B: SP 866TVG-5C: SP 866TVG-5D: SP 866TVG-5E: SP 866TVG-5F: SP 866TVG-5H-1: AE 866TVG-5H-2: TM 866TVG-5H-3: RK 866TVG-5J-1: TM 866TVG-5J-2: KL 866TVG-5K-1: HG 866TVG-5K-2: TM 866TVG-5K-3: KS 866TVG-5K-4: AB 866TVG-5L-1: TM 866TVG-5L-2: BG 866TVG-5L-3: AB 866TVG-5M-1: TM 866TVG-5M-2: TM 866TVG-5M-3: BG 866TVG-5N: TM 866TVG-5O-1: SP 866TVG-5O-2: TM 866TVG-5O-3: SP 866TVG-5O-4: SP 866TVG-5P: BG 866TVG-5Q: NE 866TVG-5R-1: HG 866TVG-5R-2: SP 866TVG-5S: RK 866TVG-5T: HG 866TVG-5U-1: SP 866TVG-5U-2: TM 866TVG-5U-3: SP

Sample Group	Facies	Description	Sample distribution
			866TVG-5V: NE 866TVG-5W: SP
M73/2- 866TVG-6	Vuggy sulfide-sulfate	Vuggy sulfide-sulfate; clastic or pseudoclastic textures; late native sulfur veining and encrustations; some apparent breccias contain clasts of black material, possibly of altered mud or volcanic fragments; some clasts of banded silica-sulfide-sulfate	866TVG-6A: NE 866TVG-6B: SP 866TVG-6C: SP 866TVG-6D: BW 866TVG-6E: BG 866TVG-6F-1: HG 866TVG-6F-2: KL 866TVG-6F-3: SP 866TVG-6G: AB 866TVG-6H: AB 866TVG-6I: NE 866TVG-6J: SP
M73/2- 866TVG-7	Vuggy sulfide-sulfate	Vuggy sulfide-sulfate with abundant native sulfur crystals lining fractures and cavities	866TVG-7A: SP 866TVG-7B: SP 866TVG-7C: SP 866TVG-7D: SP 866TVG-7E: NE 866TVG-7F: TM 866TVG-7G: KS 866TVG-7H: KP 866TVG-7I: HG 866TVG-7J: HG 866TVG-7K: KL 866TVG-7L: GH 866TVG-7M: RK 866TVG-7N: BG 866TVG-7O: MH 866TVG-7P: ANG 866TVG-7Q: AB 866TVG-7R: AB 866TVG-7S: AB 866TVG-7T: NE 866TVG-7U: NE 866TVG-7V: KS 866TVG-7W: SP 866TVG-7X: KP 866TVG-7Y: AE 866TVG-7Z: AE 866TVG-7AA: SP 866TVG-7AB: SP 866TVG-7AC: SP
M73/2- 866TVG-8	Vuggy sulfide-sulfate	Vuggy sulfide-sulfate that is weakly layered and banded; sulfide-dominated darker bands and silica-sulfur-rich lighter bands; abundant native sulfur lining fractures and cavities	866TVG-8A: NE 866TVG-8B: SP 866TVG-8C: SP 866TVG-8D-1: HG 866TVG-8D-2: BG 866TVG-8E: BG 866TVG-8F-1: GH 866TVG-8F-2: SP 866TVG-8F-3: SP 866TVG-8G: AB 866TVG-8H: GH 866TVG-8I: KL 866TVG-8J: AB 866TVG-8K: RK 866TVG-8L: SP
M73/2-	Vuggy sulfide-	Dark colored fine-grained vuggy sulfide-	866TVG-9A: NE

Sample Group	Facies	Description	Sample distribution
866TVG-9	fide-sulfate	sulfate; massive and porous; samples comprise approximately 70% sulfide and 30% sulfate; some samples are typified by green patches, possibly scorodite	866TVG-9B: SP 866TVG-9C: RC 866TVG-9D-1: HG 866TVG-9D-2: BG 866TVG-9D-3: GH 866TVG-9D-4: SP 866TVG-9E: SP
M73/2-866TVG-10	Vuggy sulfide-sulfate	Vuggy sulfate-sulfide; two samples are cone-shaped and resemble chimneys, one sample is a delicate fossil cast, possibly from a coral	866TVG-10: SP
M73/2-867TVG-1	Unconsolidated mud	Brown to light brown unconsolidated mud	867TVG-1: RK
M73/2-867TVG-2	Bioclastic sandstone-breccia	Brown fossiliferous, bioclastic rock in a vary hard, siliceous carbonate matrix; contains relict shells, coral, and possible crystal fragments	867TVG-2A: SP 867TVG-2B: SP 867TVG-2C: SP 867TVG-2D: SP
867TVG-3	Mn-oxide	Black botryoidal Mn oxide	867TVG-3: SP
M73/2-919TVG-1	Feldspar-olivine porphyritic andesite	Black to grey black, aphanitic, sparsely feldspar and olivine porphyritic andesite; 1-5% feldspars that are <2.5mm; <1% olivine microphenocrysts that are <1 mm; elongate vesicles define flow banding; Fe oxide crust on some sample surfaces	919TVG-1A: NE 919TVG-1B: AE 919TVG-1C: HG 919TVG-1D: SP 919TVG-1E: SP 919TVG-1F: SP 919TVG-1G: SP
M73/2-919TVG-2	Fe oxide crust	Red-brown to black, Fe oxide crust; laminated; some samples have distinct chimney-like shapes; green coloration on surface of some samples	919TVG-2A: NE 919TVG-2B: BG 919TVG-2C: SP 919TVG-2D: SP 919TVG-2E: NE 919TVG-2F: SP
M73/2-919TVG-3	Fe oxide crust	Red-brown to black, Fe oxide crust; laminated; biological filaments on several samples	919TVG-3A: NE 919TVG-3B: SP 919TVG-3C: NE 919TVG-3D: SP 919TVG-3E: SP 919TVG-3F: SP
M73/2-919TVG-4	Fe oxide crust	Red-brown to black, Fe oxide crusts; laminated; green coating	919TVG-4A: NE 919TVG-4B: SP 919TVG-4C: NE 919TVG-4D: SP 919TVG-4E: SP 919TVG-4F: SP
M73/2-919TVG-5	Fe oxide crust	Red-brown to black, Fe oxide crusts; laminated; irregular and convolute forms	919TVG-5A: NE 919TVG-5B: NE 919TVG-5C: SP 919TVG-5D: RK 919TVG-5E: SP 919TVG-5F: SP
M73/2-929TVG-1	Banded silica-sulfide-sulfate	Banded silica-sulfide-sulfate consisting of 1 to 2 mm thick bands of white grey silica with minor interbeds of 1-3 mm thick tan porous, softer material; fine-grained yellow staining may be orpiment; some samples have fragmental appearance with brecciated to contorted bands and layers	929TVG-1A: NE 929TVG-1B: SP 929TVG-1C: SP 929TVG-1D: BG 929TVG-1E: TM 929TVG-1F-1: TM 929TVG-1F-2: RK 929TVG-1G: HG 929TVG-1H: SP 929TVG-1I: SP

Sample Group	Facies	Description	Sample distribution
			929TVG-K: SP 929TVG-L: SP 929TVG-M: SP 929TVG-N: SP 929TVG-O: SP 929TVG-P: SP 929TVG-Q: SP 929TVG-R: AG 929TVG-S-1: AG 929TVG-S-2: SP 929TVG-S-3: SP 929TVG-T-1: AG 929TVG-T-2: TM 929TVG-T-3: MH 929TVG-U: GH 929TVG-V: TM 929TVG-W: AK 929TVG-X: SP 929TVG-Y: SP
M73/2-929TVG-2	Banded silica-sulfide-sulfate	Banded silica-sulfide-sulfate consisting of containing 1 to 2 mm thick bands of white grey silica with minor interbeds of 1-3 mm thick tan porous, softer material; fine-grained yellow staining may be orpiment; some samples have fragmental appearance with brecciated to contorted bands and layers; coating by dark brown to black Fe and Mn oxide; intensely oxidized	929TVG-2A: NE 929TVG-2B: SP 929TVG-2C: SP 929TVG-2D: SP 929TVG-2E: SP 929TVG-2F: SP 929TVG-2G: SP 929TVG-2H: SP 929TVG-2I: SP 929TVG-2J: AG
M73/2-929TVG-3	Banded silica-sulfide-sulfate	Banded silica-sulfide-sulfate samples that are rich in silica; patches, clots and disseminations of pyrite; some samples contain minor white clay	929TVG-3A: NE 929TVG-3B: SP 929TVG-3C: SP 929TVG-3D: BG 929TVG-3E-1: HG 929TVG-3E-2: SP 929TVG-3E-3: TM 929TVG-3E-4: AG 929TVG-3F: AK 929TVG-3G-1: TM 929TVG-3G-2: SP 929TVG-3H: SP 929TVG-3I: SP 929TVG-3J: SP 929TVG-3K: SP 929TVG-3L: SP
M73/2-929TVG-4	Massive sulfate	Massive to crystalline barite; barite crystals form acicular bands that commonly reach 1 mm in width and 1 cm in lengths; some minor surface coatings by Fe oxide	929TVG-4A: NE 929TVG-4B: SP 929TVG-4C: SP 929TVG-4D: NE 929TVG-4E: TM 929TVG-4F: TM 929TVG-4H: SP 929TVG-4I: SP 929TVG-4J: SP
M73/2-929TVG-5	Massive sulfate	Massive to crystalline barite; barite crystals form acicular bands that commonly reach 1 mm in width and 1 cm in lengths; heavily oxidized; samples are coated with Fe and Mn oxide; some samples have relict corals	929TVG-5A: NE 929TVG-5B: SP 929TVG-5C: SP 929TVG-5D: SP 929TVG-5E: BG

Sample Group	Facies	Description	Sample distribution
		attached to them	929TVG-5F: KS 929TVG-5G: NE 929TVG-5H-1: AG 929TVG-5H-2: RK 929TVG-5H-3: TM 929TVG-5I: AG 929TVG-5J: AK 929TVG-5K: MH 929TVG-5L: SP
M73/2- 929TVG-6	Sandstone- siltstone	Light green crystal-rich sandstone; moderately indurated; sandstone is feldspathic, but poorly sorted; matrix contains soft grey-green clay	929TVG-6A: NE 929TVG-6B: SP
M73/2- 929TVG-7	Unconsolidated mud	Dark green unconsolidated mud	929TVG-7: SP

A5. Sample list: Clay mineralogy

Sample distribution: RK = Reinhard Kleeberg, SP = Sven Petersen.

Sample	Facies	Sample distribution
M73/2-861GC-15-25	Unconsolidated mud	RK
M73/2-861GC-237-243	Unconsolidated mud	RK
M73/2-861GC-252-255	Banded silica-sulfide-sulfate	RK
M73/2-861GC-271-277	Unconsolidated mud	RK
M73/2-871GC-0-5	Unconsolidated sand	SP
M73/2-871GC-40-50	Unconsolidated sand	SP
M73/2-871GC-60-70	Unconsolidated sand	SP
M73/2-871GC-60	Unconsolidated sand	RK
M73/2-871GC-80-90	Unconsolidated monomictic breccia of sulfide and sulfate clasts	SP
M73/2-871GC-90	Unconsolidated monomictic breccia of sulfide and sulfate clasts	RK
M73/2-871GC-96-106	Unconsolidated monomictic breccia of sulfide and sulfate clasts	SP
M73/2-871GC-112-115	Unconsolidated monomictic breccia of sulfide and sulfate clasts	SP
M73/2-871GC-120-130	Unconsolidated mud	SP
M73/2-871GC-125	Unconsolidated mud	RK
M73/2-871GC-132-135	Unconsolidated polymictic breccia of mud and volcanic clasts	SP
M73/2-871GC-150	Unconsolidated mud	RK
M73/2-871GC-158-168	Unconsolidated mud	SP
M73/2-871GC-185-195	Unconsolidated polymictic breccia of mud and volcanic clasts	SP
M73/2-871GC-190	Unconsolidated polymictic breccia of mud and volcanic clasts	RK
M73/2-871GC-200-210	Unconsolidated mud	SP
M73/2-872GC-0-10	Unconsolidated monomictic breccia of sulfide and sulfate clasts	SP
M73/2-872GC-29-32	Unconsolidated monomictic breccia of sulfide and sulfate clasts	SP
M73/2-872GC-36-39	Unconsolidated monomictic breccia of sulfide and sulfate clasts	SP
M73/2-872GC-46-49	Unconsolidated monomictic breccia of sulfide and sulfate clasts	SP
M73/2-872GC-55-58	Unconsolidated monomictic breccia of sulfide and sulfate clasts	SP
M73/2-872GC-70-80	Unconsolidated mud	RK
M73/2-872GC-92-99	Unconsolidated polymictic breccia of mud and volcanic clasts	SP
M73/2-872GC-112-115	Unconsolidated monomictic breccia of sulfide and sulfate clasts	SP
M73/2-872GC-143-156	Unconsolidated monolithic volcanic sandstone clast breccia	SP
M73/2-872GC-150-160	Unconsolidated monolithic volcanic sandstone clast breccia	RK
M73/2-872GC-164-170	Unconsolidated monolithic volcanic sandstone clast breccia	SP
M73/2-872GC-180-190	Unconsolidated mud	RK
M73/2-872GC-200-220	Unconsolidated polymictic breccia of mud and volcanic clasts	SP
M73/2-872GC-205-215	Unconsolidated polymictic breccia of mud and volcanic clasts	RK
M73/2-872GC-270-280	Unconsolidated mud	RK

Sample	Facies	Sample distribution
M73/2-887RDV-5-8	Pumice-rich sand to pebble breccia	RK
M73/2-887RDV-15-18	Pumice-rich sand to pebble breccia	RK
M73/2-887RDV-31-34	Pumice-rich sand to pebble breccia	RK
M73/2-887RDV-58-61	Pumice-rich sand to pebble breccia	RK
M73/2-887RDV-93-96	Pumice-rich sand to pebble	RK
M73/2-887RDV-107-110	Pumice-rich sand to pebble	RK
M73/2-887RDV-139-142	Unconsolidated mud	RK
M73/2-887RDV-156-159	Unconsolidated mud	RK
M73/2-887RDV-175-178	Unconsolidated mud	RK
M73/2-915RDV-9-12	Polymictic breccia with crystal-rich sandstone clasts	RK
M73/2-915RDV-20-23	Polymictic breccia with crystal-rich sandstone clasts	RK
M73/2-915RDV-53-56	Unconsolidated sand	RK
M73/2-915RDV-88-91	Unconsolidated sand	RK
M73/2-915RDV-109-112	Unconsolidated mud	RK
M73/2-915RDV-173-176	Unconsolidated mud	RK
M73/2-915RDV-209-212	Unconsolidated mud	RK
M73/2-915RDV-273-276	Unconsolidated mud	RK
M73/2-915RDV-339-342	Unconsolidated mud	RK
M73/2-915RDV-385-388	Unconsolidated mud	RK

A6. Sample list: Geochemical analysis

Sample distribution: NE = Neptune Minerals, SP = Sven Petersen, TM = Thomas Monecke.

Sample	Lab_ID	Facies	Sample Distribution
Palinuro			
M73/2-851RD-0-25	PAL001	Vuggy sulfate-sulfide; dark vuggy sulfate with black inclusions	NE
M73/2-851RD-25-32	PAL002	Massive sulfate	NE
M73/2-851RD-32-83	PAL003	Vuggy sulfide-sulfate; vuggy sulfate-sulfide; massive sulfide	NE
M73/2-851RD-83-106	PAL004	Vuggy sulfate-sulfide	NE
M73/2-851RD-106-134	PAL005	Vuggy sulfide-sulfate	NE
M73/2-852RD-0-18	PAL006	Sandstone-siltstone; polymictic breccia with pumice clasts	TM
M73/2-852RD-18-38	PAL007	Sandstone-siltstone; polymictic breccia with white and black clasts	TM
M73/2-852RD-38-96	PAL008	Massive sulfate; vuggy sulfate-sulfide	NE
M73/2-853RD-0-34	PAL009	Dark vuggy sulfate with black inclusions	NE
Reference material	PAL010		
M73/2-855RD-0-4	PAL011	Sandstone-siltstone (oxidized)	TM
M73/2-855RD-4-40	PAL012	Sandstone-siltstone	TM
M73/2-855RD-40-56	PAL013	Polymictic breccia with pumice clasts; sandstone-siltstone	TM
M73/2-857RD-0-2	PAL014	Polymictic breccia with pumice clasts	TM
M73/2-857RD-2-4	PAL015	Vuggy sulfate-sulfide	NE
M73/2-857RD-4-23	PAL016	Vuggy sulfate-sulfide	NE
M73/2-857RD-23-47	PAL017	Vuggy sulfate-sulfide	NE
M73/2-858RD-0-2	PAL018	Massive sulfide	NE
M73/2-859RD-0-20	PAL019	Vuggy sulfate-sulfide	NE
Reference material	PAL020		
M73/2-859RD-20-42	PAL021	Sandstone-siltstone	TM
M73/2-859RD-42-50	PAL022	Sandstone-siltstone (abundant sulfur)	TM
M73/2-866TVG-5A	PAL023	Banded silica-sulfide-sulfate	NE
M73/2-866TVG-6A	PAL024	Vuggy sulfide-sulfate	NE
M73/2-866TVG-7E	PAL025	Vuggy sulfide-sulfate	NE
M73/2-866TVG-8A	PAL026	Vuggy sulfide-sulfate	NE
M73/2-866TVG-9A	PAL027	Vuggy sulfide-sulfate	NE
M73/2-865RD-0-10	PAL028	Sandstone-siltstone; polymictic breccia with pumice clasts	TM
M73/2-865RD-10-18	PAL029	Sandstone-siltstone; vuggy sulfate-sulfide	NE
Reference material	PAL030		
M73/2-865RD-18-51	PAL031	Vuggy sulfate-sulfide	NE
M73/2-865RD-51-79	PAL032	Vuggy sulfate-sulfide	NE
M73/2-865RD-79-116	PAL033	Vuggy sulfate-sulfide	NE
M73/2-865RD-116-151.5	PAL034	Vuggy sulfate-sulfide	NE
M73/2-865RD-151.5-188	PAL035	Vuggy sulfate-sulfide	NE
M73/2-865RD-188-226	PAL036	Vuggy sulfate-sulfide	NE
M73/2-865RD-226-261	PAL037	Vuggy sulfate-sulfide	NE
M73/2-865RD-261-308.5	PAL038	Vuggy sulfide-sulfate	NE
M73/2-865RD-308.5-336.5	PAL039	Massive sulfide	NE
Reference material	PAL040		
M73/2-865RD-336.5-379.5	PAL041	Massive sulfide	NE
M73/2-865RD-379.5-388	PAL042	Massive sulfide	NE
M73/2-865RD-388-438	PAL043	Massive sulfide	NE
M73/2-865RD-438-484	PAL044	Massive sulfide	NE

Sample	Lab_ID	Facies	Sample Distribution
M73/2-925RD-0-29	PAL045	Feldspar-olivine porphyritic andesite	SP
M73/2-928RDV-0-68	PAL046	Unconsolidated mud; unconsolidated sand	NE
M73/2-929TVG-1A	PAL047	Banded silica-sulfide-sulfate	NE
M73/2-929TVG-2A	PAL048	Banded silica-sulfide-sulfate	NE
M73/2-929TVG-3A	PAL049	Banded silica-sulfide-sulfate	NE
Reference material	PAL050		
M73/2-929TVG-4A	PAL051	Banded silica-sulfide-sulfate	NE
M73/2-929TVG-5A	PAL052	Banded silica-sulfide-sulfate	NE
M73/2-930RD-0-65	PAL053	Mudstone-sandstone	TM
M73/2-930RD-65-100	PAL054	Crystal-rich sandstone; massive sulfide	TM
M73/2-930RD-100-118	PAL055	Massive sulfides	NE
M73/2-931RD-0-10	PAL056	Vuggy sulfide-sulfate; vuggy sulfate-sulfide	NE
M73/2-931RD-10-38.5	PAL057	Vuggy sulfide-sulfate	NE
M73/2-931RD-38.5-45	PAL058	Massive sulfide	NE
M73/2-932RD-0-18	PAL059	Polymictic breccia with white and black clasts	TM
Reference material	PAL060		
M73/2-932RD-18-48	PAL061	Vuggy sulfide-sulfate	NE
M73/2-932RD-48-110	PAL062	Vuggy sulfide-sulfate; vuggy sulfate-sulfide; with sulfides; massive sulfide	NE
M73/2-932RD-110-160	PAL063	Vuggy sulfate-sulfide; vuggy sulfide-sulfate	NE
M73/2-932RD-160-193	PAL064	Vuggy sulfide-sulfate	NE
M73/2-932RD-193-240	PAL065	Vuggy sulfate-sulfide	NE
M73/2-932RD-240-291	PAL066	Vuggy sulfate-sulfide; vuggy sulfide-sulfate	NE
M73/2-861GC-0-32	PAL067	Unconsolidated mud; unconsolidated sand	NE
M73/2-861GC-70-100	PAL068	Unconsolidated sand; unconsolidated mud	NE
M73/2-861GC-100-150	PAL069	Unconsolidated mud; unconsolidated sand	NE
Reference material	PAL070		
M73/2-861GC-150-200	PAL071	Unconsolidated mud	NE
M73/2-861GC-200-250	PAL072	Unconsolidated mud	NE
M73/2-861GC-250-295	PAL073	Unconsolidated mud; banded silica-sulfide-sulfate	NE
M73/2-862GC-0-40	PAL074	Unconsolidated mud	NE
M73/2-863GC-0-46	PAL075	Unconsolidated mud	NE
M73/2-863GC-46-100	PAL076	Unconsolidated mud	NE
M73/2-863GC-100-150	PAL077	Unconsolidated mud, unconsolidated sand	NE
M73/2-863GC-150-200	PAL078	Unconsolidated mud	NE
M73/2-863GC-200-250	PAL079	Unconsolidated mud	NE
Reference material	PAL080		
M73/2-863GC-250-280	PAL081	Unconsolidated mud	NE
M73/2-871GC-0-70	PAL082	Unconsolidated sand	NE
M73/2-871GC-70-115	PAL083	Unconsolidated monomictic breccia of sulfide and sulfate clasts	NE
M73/2-871GC-115-158	PAL084	Unconsolidated mud; unconsolidated polymictic breccia of mud and volcanic clasts	NE
M73/2-871GC-158-210	PAL085	Unconsolidated polymictic breccia of mud and volcanic clasts; unconsolidated mud;	NE

Sample	Lab_ID	Facies	Sample Distribution
M73/2-872GC-0-50	PAL086	Unconsolidated monomictic breccia of sulfide and sulfate clasts; unconsolidated mud	NE
M73/2-872GC-50-100	PAL087	Unconsolidated mud; unconsolidated monomictic breccia of sulfide and sulfate clasts; unconsolidated polymictic breccia of mud and volcanic clasts	NE
M73/2-872GC-100-143	PAL088	Unconsolidated mud; unconsolidated monomictic breccia of sulfide and sulfate clasts; unconsolidated sand	NE
M73/2-872GC-143-200	PAL089	Unconsolidated monolithic volcanic sandstone clast breccia; unconsolidated mud	NE
Reference material	PAL090		
M73/2-872GC-200-250	PAL091	Unconsolidated polymictic breccia of mud and volcanic clasts; unconsolidated mud	NE
M73/2-872GC-250-300	PAL092	Unconsolidated mud	NE
Panarea			
M73/2-875RD-0-12	PAN001	Crystal-lithic and pumice-rich sandstone to pebble conglomerate	TM
M73/2-875RD-12-14	PAN002	Crystal-lithic and pumice-rich sandstone to pebble conglomerate	TM
M73/2-875RD-14-15.5	PAN003	Crystal-lithic and pumice-rich sandstone to pebble conglomerate	TM
M73/2-875RD-15.5-18	PAN004	Crystal-lithic and pumice-rich sandstone to pebble conglomerate	TM
M73/2-875RD-18-33	PAN005	Crystal-lithic and pumice-rich sandstone to pebble conglomerate	TM
M73/2-875RD-33-66.5	PAN006	Crystal-lithic and pumice-rich sandstone to pebble conglomerate	TM
M73/2-875RD-66.5-89.5	PAN007	Feldspar-olivine porphyritic andesite	TM
M73/2-876RD-0-12	PAN008	Feldspar-olivine porphyritic andesite	TM
M73/2-878RD-7-35	PAN009	Feldspar-olivine porphyritic andesite	TM
Reference material	PAN010		
M73/2-879RD-0-35	PAN011	Massive anhydrite-gypsum	TM
M73/2-879RD-35-70	PAN012	Massive anhydrite-gypsum	TM
M73/2-880RD-0-34	PAN013	Massive anhydrite-gypsum	TM
M73/2-880RD-34-89	PAN014	Massive anhydrite-gypsum	TM
M73/2-881RD-6-56	PAN015	Massive anhydrite-gypsum	TM
M73/2-881RD-56-115	PAN016	Massive anhydrite-gypsum	TM
M73/2-881RD-115-174	PAN017	Massive anhydrite-gypsum	TM
M73/2-881RD-174-233	PAN018	Massive anhydrite-gypsum	TM
M73/2-881RD-233-289	PAN019	Massive anhydrite-gypsum	TM
Reference material	PAN020		
M73/2-883RD-2-26	PAN022	Massive anhydrite-gypsum	TM
M73/2-883RD-26-51	PAN023	Massive anhydrite-gypsum	TM
M73/2-883RD-51-69	PAN024	Massive anhydrite-gypsum	TM
M73/2-884RD-1.5-32.5	PAN025	Massive anhydrite-gypsum	TM
M73/2-884RD-32.5-70.5	PAN026	Massive anhydrite-gypsum	TM
M73/2-884RD-70.5-84	PAN027	Massive anhydrite-gypsum	TM
M73/2-886RD-0-21.5	PAN028	Massive anhydrite-gypsum	TM
M73/2-889RD-0-12.5	PAN039	Mudstone	TM
Reference material	PAN040		
M73/2-889RD-16-30	PAN041	Mudstone	TM
M73/2-891RD-0-40	PAN042	Intensely altered feldspar porphyritic andesite	TM

Sample	Lab_ID	Facies	Sample Distribution
M73/2-891RD-40-94	PAN043	Intensely altered feldspar porphyritic andesite	TM
M73/2-891RD-94-126	PAN044	Intensely altered feldspar porphyritic andesite	TM
M73/2-895RD-0-19	PAN045	Feldspar-amphibole porphyritic rhyolite	TM
M73/2-895RD-19-50	PAN046	Amphibole-biotite-feldspar porphyritic andesite	TM
M73/2-895RD-50-81	PAN047	Feldspar-amphibole porphyritic rhyolite	TM
M73/2-894RDV-0-12	PAN048	Unconsolidated sand	TM
M73/2-894RDV-12-52	PAN049	Unconsolidated sand	TM
Reference material	PAN050		
M73/2-894RDV-52-89	PAN051	Unconsolidated sand	TM
M73/2-894RDV-89-108	PAN052	Unconsolidated sand	TM
M73/2-894RDV-108-158	PAN053	Unconsolidated sand	TM
M73/2-894RDV-159-208	PAN054	Unconsolidated sand	TM
M73/2-894RDV-209-258	PAN055	Unconsolidated sand	TM
M73/2-894RDV-259-308	PAN056	Unconsolidated sand	TM
M73/2-894RDV-309-358	PAN057	Unconsolidated sand	TM
M73/2-894RDV-358-375	PAN058	Unconsolidated sand	TM
M73/2-899RD-60-68.5	PAN059	Feldspar porphyritic andesite	TM
Reference material	PAN060		
M73/2-913RD-0-21	PAN061	Massive anhydrite-gypsum	TM
M73/2-914RD-0-34	PAN062	Massive anhydrite-gypsum	TM
M73/2-914RD-34-77	PAN063	Massive anhydrite-gypsum	TM
M73/2-914RD-77-124	PAN064	Massive anhydrite-gypsum	TM
M73/2-914RD-124-140.5	PAN065	Massive anhydrite-gypsum	TM
M73/2-915RD-0-18	PAN066	Polymictic breccia with crystal-rich sandstone clasts	TM
M73/2-915RD-18-42	PAN067	Polymictic breccia with crystal-rich sandstone clasts, unconsolidated sand	TM
M73/2-915RD-42-104	PAN068	Unconsolidated sand	TM
M73/2-915RD-104-150	PAN069	Unconsolidated mud	TM
Reference material	PAN070		
M73/2-915RD-150-200	PAN071	Unconsolidated mud	TM
M73/2-915RD-200-250	PAN072	Unconsolidated mud	TM
M73/2-915RD-250-300	PAN073	Unconsolidated mud	TM
M73/2-915RD-300-350	PAN074	Unconsolidated mud	TM
M73/2-915RD-350-417	PAN075	Unconsolidated mud	TM
Marsili			
M73/2-918RD-0-32	MAR001	Feldspar-olivine porphyritic andesite	TM
M73/2-919TVG-1A	MAR002	Feldspar-olivine porphyritic andesite	NE
M73/2-919TVG-2A	MAR003	Fe oxide crust	NE
M73/2-919TVG-3A	MAR004	Fe oxide crust	NE
M73/2-919TVG-4A	MAR005	Fe oxide crust	NE
M73/2-919TVG-5A	MAR006	Fe oxide crust	NE

A7. Sample list: Petrographic analysis

Sample distribution: AB = Arnaldo De Benedetti.

Sample	Facies	Sample Distribution
Panarea		
M73/2-875RD-79-81	Feldspar-olivine porphyritic andesite	AB
M73/2-878RD-23-27	Feldspar-olivine porphyritic andesite	AB
M73/2-887RDV-30-35	Pumice-rich sand to pebble breccia	AB
M73/2-887RDV-57-62	Pumice-rich sand to pebble breccia	AB
M73/2-887RDV-92-97	Pumice-rich sand to pebble breccia	AB
M73/2-887RDV-105-110	Pumice-rich sand to pebble breccia	AB
M73/2-895RD-29-34	Amphibole-biotite-feldspar porphyritic andesite	AB
M73/2-895RD-39-45	Amphibole-biotite-feldspar porphyritic andesite	AB
M73/2-895RD-62-67	Feldspar-amphibole porphyritic rhyolite	AB
M73/2-896RD-4-9	Feldspar-amphibole porphyritic rhyolite	AB
M73/2-896RD-21-25	Feldspar-amphibole porphyritic rhyolite	AB
M73/2-896RD-31-34	Amphibole-biotite-feldspar porphyritic andesite	AB
M73/2-896RD-39-42	Amphibole-biotite-feldspar porphyritic andesite	AB
M73/2-896RD-52-58	Feldspar-amphibole porphyritic rhyolite	AB
M73/2-896RD-71-76	Feldspar-amphibole porphyritic rhyolite with xenoliths of amphibole-biotite-feldspar porphyritic andesite	AB
M73/2-896RD-79-84	Feldspar-amphibole porphyritic rhyolite	AB
M73/2-896RD-84-90	Feldspar-amphibole porphyritic rhyolite	AB
M73/2-896RD-106-109	Amphibole-biotite-feldspar porphyritic andesite	AB
M73/2-896RD-146-149	Amphibole-biotite-feldspar porphyritic andesite	AB
M73/2-896RD-171-175	Amphibole-biotite-feldspar porphyritic andesite	AB
M73/2-896RD-184-189	Feldspar-amphibole porphyritic rhyolite	AB
M73/2-896RD-203-206	Amphibole-biotite-feldspar porphyritic andesite	AB
M73/2-896RD-220-224	Feldspar-amphibole porphyritic rhyolite	AB
M73/2-896RD-320-324	Feldspar-amphibole porphyritic rhyolite	AB
M73/2-896RD-398-402	Amphibole-biotite-feldspar porphyritic andesite	AB
M73/2-896RD-449-454	Feldspar-amphibole porphyritic rhyolite	AB
M73/2-897RD-34-41	Feldspar porphyritic andesite	AB

A8. Sample list: Pore water geochemistry

Abbreviations: IC = ion chromatography, EC = electrical conductivity, Eh = redox potential.

Sample	pH	Eh (mV)	EC (mS/cm)	Speciation	ICP-MS	IC
Palinuro						
M73/2-861GC-25	7.25	297	57.5	-	X	X
M73/2-861GC-45	-	-	-	-	-	-
M73/2-861GC-85	7.59	316	57.7	-	X	X
M73/2-861GC-105	7.36	150	58.6	-	X	X
M73/2-861GC-125	7.38	182	58.6	-	X	X
M73/2-861GC-145	7.25	132	57.9	-	X	X
M73/2-861GC-165	7.34	197	55.4	-	X	X
M73/2-861GC-185	-	-	58.0	-	-	-
M73/2-861GC-205	7.24	175	58.1	-	-	-
M73/2-861GC-225	7.01	164	58.0	-	X	X
M73/2-861GC-245	7.04	185	58.9	-	-	-
M73/2-861GC-265	7.20	321	-	-	-	-
M73/2-862GC-10				-	-	-
M73/2-862GC-20				-	-	-
M73/2-862GC-30				-	-	-
M73/2-862GC-40				-	-	-
M73/2-862GC-50				-	X	-
M73/2-862GC-60				-	-	-
M73/2-863GC-10	7.66	420	61.1	-	X	X
M73/2-863GC-30	7.51	426	57.8	-	X	X
M73/2-863GC-50	7.61	394	59.9	-	X	X
M73/2-863GC-90	7.53	323	58.0	-	X	X
M73/2-863GC-130	7.64	370	57.7	-	X	X
M73/2-863GC-150	7.62	351	61.0	-	X	X
M73/2-863GC-170	7.65	317	57.5	-	-	-
M73/2-863GC-190	7.78	370	57.3	-	X	X
M73/2-863GC-210	7.76	339	56.5	-	-	-
M73/2-863GC-230	7.67	388	57.9	-	-	-
M73/2-863GC-250	7.72	391	59.3	-	X	X
M73/2-863GC-270	7.66	388	57.5	-	-	-
M73/2-863GC-290	7.03	-		-	-	-
M73/2-871GC-0	7.59	189	63.8	-	-	-
M73/2-871GC-20	6.98	-	60.5	-	-	-
M73/2-871GC-40	6.92	-		-	-	-
M73/2-871GC-60	6.24	42	58.8	X	X	X
M73/2-871GC-80	7.17	-159	68.5	X	X	X
M73/2-871GC-100	6.90	-146	70.6	-	-	-
M73/2-871GC-120	6.91	-	0.0	-	-	-
M73/2-871GC-140	7.10	-108	67.5	-	-	-
M73/2-871GC-160				-	-	-
M73/2-871GC-180				-	-	-
M73/2-871GC-200				-	-	-
M73/2-872GC-10	7.35	86	58.6	X	X	-
M73/2-872GC-30	7.67	119	57.6	X	-	-
M73/2-872GC-50	6.84	190	58.2	X	X	X
M73/2-872GC-70	7.37	183	58.6	X	-	-
M73/2-872GC-90	6.46	31	58.8	X	X	X
M73/2-872GC-110	6.10	-75	60.0	X	X	X

Sample	pH	Eh (mV)	EC (mS/cm)	Speciation	ICP-MS	IC
M73/2-872GC-130	6.41	-111	60.2	X	X	X
M73/2-872GC-150	6.64	-	58.7	-	-	-
M73/2-872GC-170	6.60	-143	66.5	X	X	X
M73/2-872GC-190	6.79	-	66.9	-	-	-
M73/2-872GC-210	6.84	-138	68.5	-	-	-
M73/2-872GC-230	-	-	-	-	-	-
M73/2-872GC-250	7.01	-162	68.5	-	-	-
M73/2-872GC-270	7.08	-	-	-	-	-
M73/2-928RDV-10	7.30	394	56.4	-	X	-
M73/2-928RDV-20	7.53	308	59.1	X	-	X
M73/2-928RDV-30	7.47	307	57.0	-	X	X
M73/2-928RDV-40	7.71	329	57.0	X	-	-
M73/2-928RDV-50	7.65	312	57.3	-	X	X
M73/2-928RDV-60	7.68	345	55.8	X	-	-
Panarea						
M73/2-887RDV-30	5.32	187	57.7	X	X	X
M73/2-887RDV-50	5.47	152	59.3	X	X	X
M73/2-887RDV-70	5.41	135	59.0	X	X	X
M73/2-887RDV-90	5.75	137	62.9	X	X	X
M73/2-887RDV-110	6.00	240	61.0	-	-	-
M73/2-887RDV-130	5.72	149	63.1	X	X	X
M73/2-887RDV-150	6.05	-	-	-	X	X
M73/2-887RDV-170	6.99	267	73.4	-	-	-
M73/2-887RDV-190	6.55	293	74.2	X	X	-
M73/2-890RDV-10	7.20	-	58.5	-	-	-
M73/2-890RDV-40	6.73	391	-	X	X	-
M73/2-890RDV-60	6.58	281	-	X	-	-
M73/2-890RDV-80	-	-	-	-	-	-
M73/2-890RDV-100	7.08	-	56.6	X	-	-
M73/2-890RDV-130	-	-	-	-	-	-
M73/2-890RDV-170	7.11	295	-	X	-	-
M73/2-890RDV-200	7.16	-	59.8	X	X	-
M73/2-890RDV-230	6.93	-	-	-	-	-
M73/2-890RDV-250	6.97	337	56.4	-	-	-
M73/2-890RDV-290	6.79	-	-	-	-	-
M73/2-890RDV-310	-	-	-	-	-	-
M73/2-890RDV-350	7.08	-	-	X	-	-
M73/2-890RDV-380	6.81	-	43.9	-	-	-
M73/2-890RDV-410	6.88	-	-	-	-	-
M73/2-894RDV-5	5.67	419	56.9	-	X	X
M73/2-894RDV-45	5.80	249	56.6	-	X	X
M73/2-894RDV-85	5.80	255	57.0	-	X	X
M73/2-894RDV-125	6.18	207	57.1	-	X	-
M73/2-894RDV-155	6.83	118	-	-	-	-
M73/2-894RDV-185	6.17	208	57.0	-	X	X
M73/2-894RDV-225	5.90	-	-	-	-	-
M73/2-894RDV-255	6.73	150	57.2	-	-	-
M73/2-894RDV-285	6.19	234	57.3	-	X	X
M73/2-894RDV-305	6.62	-	57.0	-	-	-
M73/2-894RDV-345	6.56	-	-	-	-	-
M73/2-894RDV-365	6.16	195	57.0	-	X	X
M73/2-907RDV-5	5.57	308	59.6	-	X	X
M73/2-907RDV-25	5.35	271	59.5	X	X	X

Sample	pH	Eh (mV)	EC (mS/cm)	Speciation	ICP-MS	IC
M73/2-907RDV-45	5.76	287	60.7	X	X	X
M73/2-907RDV-65	6.06	293	60.9	X	X	X
M73/2-907RDV-85	6.32	-	-	-	X	-
M73/2-907RDV-105	5.69	218	61.5	X	X	X
M73/2-907RDV-125	5.70	259	61.4	-	X	X
M73/2-907RDV-145	5.74	261	61.4	x	X	X
M73/2-907RDV-165	5.72	189	61.2	-	X	X
M73/2-907RDV-185	5.75	241	61.8	X	X	X
M73/2-915RDV-10	5.98	293	57.7	-	X	-
M73/2-915RDV-25	5.30	211	57.5	X	X	X
M73/2-915RDV-45	5.62	193	58.1	X	X	X
M73/2-915RDV-65	5.57	219	57.5	X	X	X
M73/2-915RDV-85	5.71	199	58.0	X	X	X
M73/2-915RDV-125	-	-	-	-	X	-
M73/2-915RDV-165	6.88	-	-	-	-	-
M73/2-915RDV-205	6.78	-	59.0	-	-	-
M73/2-915RDV-245	6.47	345	60.0	-	-	-
M73/2-915RDV-285	6.38	310	60.9	X	X	X
M73/2-915RDV-325	6.93	-	56.3	-	-	-
M73/2-915RDV-355	-	-	-	-	-	-
M73/2-915RDV-375	7.00	-	57.0	-	-	-
M73/2-915RDV-395	6.77	-	63.6	-	-	-
M73/2-915RDV-415	6.76	-	62.2	-	-	-

	Speciation	ICP-MS	IC
Palinuro	13	27	22
Panarea	23	33	26
Total	36	60	48

A9. Sample list: Sulfur geochemistry

Sample	H ₂ S (μmol/l)	MBB	Sediment sample
Palinuro			
M73/2-861GC-45	0	X	-
M73/2-861GC-105	0	X	-
M73/2-861GC-125	0	X	-
M73/2-861GC-145	0	X	-
M73/2-861GC-165	0	X	-
M73/2-861GC-185	0	X	-
M73/2-861GC-205	0.70	X	-
M73/2-861GC-225	0.62	X	-
M73/2-861GC-245	3.69	X	-
M73/2-861GC-265	2.89	X	-
M73/2-862GC-40	0	X	-
M73/2-863GC-10	0	X	-
M73/2-863GC-30	0	X	-
M73/2-863GC-50	0	X	-
M73/2-863GC-90	0	X	-
M73/2-863GC-130	0	X	-
M73/2-863GC-150	0	X	-
M73/2-863GC-170	0	X	-
M73/2-863GC-190	0	X	-
M73/2-863GC-210	0	X	-
M73/2-863GC-230	0	X	-
M73/2-863GC-250	0	X	-
M73/2-863GC-270	0	X	-
M73/2-871GC-0	0	X	X
M73/2-871GC-20	0	X	X
M73/2-871GC-40	0	X	X
M73/2-871GC-60	6.65	X	X
M73/2-871GC-70	-	-	X
M73/2-871GC-80	507.27	X	-
M73/2-871GC-100	537.13	X	X
M73/2-871GC-120	523.58	X	X
M73/2-871GC-140	534.62	X	X
M73/2-871GC-160	443.05	X	X
M73/2-871GC-180	530.60	X	X
M73/2-871GC-200	-	-	X
M73/2-872GC-25	-	-	X
M73/2-872GC-30	0	X	-
M73/2-872GC-50	0	X	X
M73/2-872GC-70	0	X	-
M73/2-872GC-90	0	X	X
M73/2-872GC-110	88.34	X	X
M73/2-872GC-130	329.66	X	X
M73/2-872GC-150	405.68	X	-
M73/2-872GC-170	-	-	X
M73/2-872GC-180	-	-	X
M73/2-872GC-190	513.80	X	X
M73/2-872GC-210	207.50	-	-
M73/2-872GC-220	-	-	X
M73/2-872GC-230	465.88	X	X
M73/2-872GC-240	-	-	X

Sample	H ₂ S (μmol/l)	MBB	Sediment sample
M73/2-872GC-250	-	-	X
M73/2-872GC-270	508.53	X	-
M73/2-872GC-290	-	-	X
Panarea			
M73/2-887RDV-30	2.41	X	-
M73/2-887RDV-35	-	-	X
M73/2-887RDV-50	3.01	X	-
M73/2-887RDV-70	3.87	X	X
M73/2-887RDV-90	0.78	X	-
M73/2-887RDV-100	-	-	X
M73/2-887RDV-110	0.76	X	-
M73/2-887RDV-130	2.81	X	-
M73/2-887RDV-150	2.84	X	-
M73/2-887RDV-170	-	-	X
M73/2-887RDV-190	0	X	X
M73/2-890RDV-10	0	X	-
M73/2-890RDV-40	0.23	X	-
M73/2-890RDV-60	13.55	X	-
M73/2-890RDV-80	0	-	-
M73/2-890RDV-130	0	-	-
M73/2-890RDV-170	8.41	X	-
M73/2-890RDV-180	-	-	X
M73/2-890RDV-200	1.73	X	-
M73/2-890RDV-230	0	X	-
M73/2-890RDV-250	0	X	-
M73/2-890RDV-295	-	X	-
M73/2-890RDV-310	0	-	-
M73/2-890RDV-350	8.76	X	-
M73/2-894RDV-5	0	X	-
M73/2-894RDV-55	0	X	-
M73/2-894RDV-85	0	-	-
M73/2-894RDV-125	0	X	-
M73/2-894RDV-185	0	X	-
M73/2-894RDV-225	0	-	-
M73/2-894RDV-255	0	X	-
M73/2-894RDV-285	0	X	-
M73/2-894RDV-305	0	X	-
M73/2-894RDV-335	0	X	-
M73/2-894RDV-365	0	X	-
M73/2-907RDV-5	0	X	-
M73/2-907RDV-45	0	X	-
M73/2-907RDV-65	0	X	-
M73/2-907RDV-85	0	X	-
M73/2-907RDV-105	0.16	X	-
M73/2-907RDV-125	0	X	-
M73/2-907RDV-145	0	X	-
M73/2-907RDV-165	0.43	X	-
M73/2-907RDV-185	0	X	-
M73/2-915RDV-10	0.83	-	-
M73/2-915RDV-25	5.67	-	-
M73/2-915RDV-45	5.15	-	X
M73/2-915RDV-65	3.49	-	-
M73/2-915RDV-85	4.07	-	X

Sample	H ₂ S (μ mol/l)	MBB	Sediment sample
M73/2-915RDV-135	-	-	X
M73/2-915RDV-245	0	-	X
M73/2-915RDV-285	0	-	-
M73/2-915RDV-325	0	-	-
M73/2-915RDV-395	0	-	-
M73/2-915RDV-405	-	-	X
M73/2-915RDV-415	0	-	-

A10. Sample list: Microbiology

Station	Comment	DNA	FISH	REM	GBZ	DMSO	Gly	4°C	Cult.
Palinuro									
Surface seawater	Sampled on August 16, 2007	X	X						
851RD	28 cm	X	X	X		X		X	X
852RD	Top, bottom	X	X					X	
855RD	Top	X	X					X	
861GC	5 cm, 88 cm, 190 cm, 230 cm, 240 cm, 250 cm	X	X	X		X	X	X	X
863GC	5 cm, 45 cm, 125 cm, 135 cm	X	X	X		X	X	X	X
865RD	Top	X							
866TVG	Mud and crusts	X	X	X	X	X	X	X	X
866TVG	Shrimps	Frozen and conserved in ethanol							
871GC	5 cm, 150 cm, 175 cm, 190 cm, 270 cm	X	X	X		X	X	X	X
872GC	130 cm, 150 cm, 190 cm, 210 cm, 235 cm	X	X	X		X	X	X	
926RD	Background sediment								
928RDV	20 cm, 65 cm, 75 cm								
929TVG	Sediment								
Panarea									
Surface seawater	Sampled on August 20, 2007	X	X						
875RD	Top								
877RDV	0-5 cm								
885RD	top	X	X			X		X	
887RDV	0-2 cm, 10 cm, 38 cm, 45 cm, 75 cm, 165 cm	X	X	X	X	X	X	X	X
890RDV	5 cm, 165 cm, 385 cm								
891RD	Top	X	X					X	
894RDV	5 cm, 30 cm, 90 cm, 130 cm	X	X	X		X	X	X	
900RDV	0-4 cm, 5 cm, 50 cm, 85 cm, 330 cm	X	X	X		X	X	x	
907RDV	0-4 cm, 20 cm, 35 cm	X	X	X		X	X	X	
907RDV	Fish	Conserved in ethanol							
914RDV	Bottom	X	X						
915RDV	30 cm	X	X	X		X			
Marsili									
917RD	Fe oxide crusts	X	X	X		X			
919TVG	Fe oxide crusts	X	X	X		X			
919TVG	Fe oxide mud	X	X	X					
919TVG	Yellowish mud	X	X	X					

IFM-GEOMAR Reports

No.	Title
1	RV Sonne Fahrtbericht / Cruise Report SO 176 & 179 MERAMEX I & II (Merapi Amphibious Experiment) 18.05.-01.06.04 & 16.09.-07.10.04. Ed. by Heidrun Kopp & Ernst R. Flueh, 2004, 206 pp. In English
2	RV Sonne Fahrtbericht / Cruise Report SO 181 TIPTEQ (from The Incoming Plate to mega Thrust EarthQuakes) 06.12.2004.-26.02.2005. Ed. by Ernst R. Flueh & Ingo Grevemeyer, 2005, 533 pp. In English
3	RV Poseidon Fahrtbericht / Cruise Report POS 316 Carbonate Mounds and Aphotic Corals in the NE-Atlantic 03.08.-17.08.2004. Ed. by Olaf Pfannkuche & Christine Utecht, 2005, 64 pp. In English
4	RV Sonne Fahrtbericht / Cruise Report SO 177 - (Sino-German Cooperative Project, South China Sea: Distribution, Formation and Effect of Methane & Gas Hydrate on the Environment) 02.06.-20.07.2004. Ed. by Erwin Suess, Yongyang Huang, Nengyou Wu, Xiqiu Han & Xin Su, 2005, 154 pp. In English and Chinese
5	RV Sonne Fahrtbericht / Cruise Report SO 186 – GITEWS (German Indonesian Tsunami Early Warning System 28.10.-13.1.2005 & 15.11.-28.11.2005 & 07.01.-20.01.2006. Ed. by Ernst R. Flueh, Tilo Schoene & Wilhelm Weinrebe, 2006, 169 pp. In English
6	RV Sonne Fahrtbericht / Cruise Report SO 186 -3 – SeaCause II, 26.02.-16.03.2006. Ed. by Heidrun Kopp & Ernst R. Flueh, 2006, 174 pp. In English
7	RV Meteor, Fahrtbericht / Cruise Report M67/1 CHILE-MARGIN-SURVEY 20.02.-13.03.2006. Ed. by Wilhelm Weinrebe und Silke Schenk, 2006, 112 pp. In English
8	RV Sonne Fahrtbericht / Cruise Report SO 190 - SINDBAD (Seismic and Geoacoustic Investigations Along The Sunda-Banda Arc Transition) 10.11.2006 - 24.12.2006. Ed. by Heidrun Kopp & Ernst R. Flueh, 2006, 193 pp. In English
9	RV Sonne Fahrtbericht / Cruise Report SO 191 - New Vents "Puaretanga Hou" 11.01. - 23.03.2007. Ed. by Jörg Bialas, Jens Greinert, Peter Linke, Olaf Pfannkuche, 2007, 190 pp. In English

No.	Title
10	FS ALKOR Fahrtbericht / Cruise Report AL 275 - Geobiological investigations and sampling of aphotic coral reef ecosystems in the NE-Skagerrak, 24.03. - 30.03.2006, Eds.: Andres Rüggeberg & Armin Form, 39 pp. In English
11	FS Sonne / Fahrtbericht / Cruise Report SO 192-1: MANGO: Marine Geoscientific Investigations on the Input and Output of the Kermadec Subduction Zone, 24.03. - 22.04.2007, Ernst Flüh & Heidrun Kopp, 127 pp. In English
12	FS Maria S. Merian / Fahrtbericht / Cruise Report MSM 04-2: Seismic Wide-Angle Profiles, Fort-de-France – Fort-de-France, 03.01. - 19.01.2007, Ed.: Ernst Flüh, 45 pp. In English
13	FS Sonne / Fahrtbericht / Cruise Report SO 193: MANIHIKI Temporal, Spatial, and Tectonic Evolution of Oceanic Plateaus, Suva/Fiji – Apia/Samoa 19.05. - 30.06.2007, Eds.: Reinhard Werner and Folkmar Hauff, 201 pp. In English
14	FS Sonne / Fahrtbericht / Cruise Report SO195: TOTAL TONGA Thrust earthquake Asperity at Louisville Ridge, Suva/Fiji – Suva/Fiji 07.01. - 16.02.2008, Eds.: Ingo Grevemeyer & Ernst R. Flüh, 106 pp. In English
15	RV Poseidon Fahrtbericht / Cruise Report P362-2: West Nile Delta Mud Volcanoes, Piräus – Heraklion 09.02. - 25.02.2008, Ed.: Thomas Feseker, 63 pp. In English
16	RV Poseidon Fahrtbericht / Cruise Report P347: Mauritanian Upwelling and Mixing Process Study (MUMP), Las-Palmas - Las Palmas, 18.01. - 05.02.2007, Ed.: Marcus Dengler et al., 34 pp. In English
17	FS Maria S. Merian Fahrtbericht / Cruise Report MSM 04-1: Meridional Overturning Variability Experiment (MOVE 2006), Fort de France – Fort de France, 02.12. - 21.12.2006, Ed.: Thomas J. Müller, 41 pp. In English
18	FS Poseidon Fahrtbericht /Cruise Report P348: SOPRAN: Mauritanian Upwelling Study 2007, Las Palmas - Las Palmas, 08.02. - 26.02.2007, Ed.: Hermann W. Bange, 42 pp. In English
19	R/V L'ATALANTE Fahrtbericht / Cruise Report IFM-GEOMAR-4: Circulation and Oxygen Distribution in the Tropical Atlantic, Mindelo/Cape Verde - Mindelo/Cape Verde, 23.02. - 15. 03.2008, Ed.: Peter Brandt, 65 pp. In English
20	RRS JAMES COOK Fahrtbericht / Cruise Report JC23-A & B: CHILE-MARGIN-SURVEY, OFEG Barter Cruise with SFB 574, 03.03.-25.03. 2008 Valparaiso – Valparaiso, 26.03.-18.04.2008 Valparaiso - Valparaiso, Eds.: Ernst Flüh & Jörg Bialas, 242 pp. In English

No.	Title
21	FS Poseidon Fahrtbericht / Cruise Report P340 – TYMAS "Tyrrhenische Massivsulfide", Messina – Messina, 06.07.-17.07.2006, Eds.: Sven Petersen and Thomas Monecke, 77 pp. In English
22	RV Atalante Fahrtbericht / Cruise Report HYDROMAR V (replacement of cruise MSM06/2), Toulon, France - Recife, Brazil, 04.12.2007 - 02.01.2008, Ed.: Sven Petersen, 103 pp. In English
23	RV Atalante Fahrtbericht / Cruise Report MARSUED IV (replacement of MSM06/3), Recife, Brazil - Dakar, Senegal, 07.01. - 31.01.2008, Ed.: Colin Devey, 126 pp. In English
24	RV Poseidon Fahrtbericht / Cruise Report P376 ABYSS Test, Las Palmas - Las Palmas, 10.11. - 03.12.2008, Eds.: Colin Devey and Sven Petersen, 36 pp, In English
25	RV SONNE Fahrtbericht / Cruise Report SO 199 CHRISP Christmas Island Seamount Province and the Investigator Ridge: Age and Causes of Intraplate Volcanism and Geodynamic Evolution of the south-eastern Indian Ocean, Merak/Indonesia – Singapore, 02.08.2008 - 22.09.2008, Eds.: Reinhard Werner, Folkmar Hauff and Kaj Hoernle, 210 pp. In English
26	RV POSEIDON Fahrtbericht / Cruise Report P350: Internal wave and mixing processes studied by contemporaneous hydrographic, current, and seismic measurements, Funchal – Lissabon, 26.04.-10.05.2007 Ed.: Gerd Krahnemann, 32 pp. In English
27	RV PELAGIA Fahrtbericht / Cruise Report Cruise 64PE298: West Nile Delta Project Cruise - WND-3, Heraklion - Port Said, 07.11.-25.11.2008, Eds.: Jörg Bialas & Warner Brueckmann, 64 pp. In English
28	FS POSEIDON Fahrtbericht / Cruise Report P379/1: Vulkanismus im Karibik-Kanaren-Korridor (ViKKi), Las Palmas – Mindelo, 25.01.-12.02.2009, Ed.: Svend Duggen, 74 pp. In English
29	FS POSEIDON Fahrtbericht / Cruise Report P379/2: Mid-Atlantic-Researcher Ridge Volcanism (MARRVi), Mindelo- Fort-de-France, 15.02.-08.03.2009 Ed.: Svend Duggen, 80 pp. In English



Das Leibniz-Institut für Meereswissenschaften
ist ein Institut der Wissenschaftsgemeinschaft
Gottfried Wilhelm Leibniz (WGL)

The Leibniz-Institute of Marine Sciences is a
member of the Leibniz Association
(Wissenschaftsgemeinschaft Gottfried
Wilhelm Leibniz).

Leibniz-Institut für Meereswissenschaften / Leibniz-Institute of Marine Sciences

IFM-GEOMAR
Dienstgebäude Westufer / West Shore Building
Düsternbrooker Weg 20
D-24105 Kiel
Germany

Leibniz-Institut für Meereswissenschaften / Leibniz-Institute of Marine Sciences

IFM-GEOMAR
Dienstgebäude Ostufer / East Shore Building
Wischhofstr. 1-3
D-24148 Kiel
Germany

Tel.: ++49 431 600-0
Fax: ++49 431 600-2805
www.ifm-geomar.de